




ADVERTIMENT. L'accés als continguts d'aquesta tesi queda condicionat a l'acceptació de les condicions d'ús establertes per la següent llicència Creative Commons:  http://cat.creativecommons.org/?page_id=184

ADVERTENCIA. El acceso a los contenidos de esta tesis queda condicionado a la aceptación de las condiciones de uso establecidas por la siguiente licencia Creative Commons:  <http://es.creativecommons.org/blog/licencias/>

WARNING. The access to the contents of this doctoral thesis it is limited to the acceptance of the use conditions set by the following Creative Commons license:  <https://creativecommons.org/licenses/?lang=en>

Stress-induced neuronal activation in the medial prefrontal cortex

**Identification,
molecular profiling
and manipulation
of stressor-specific neuronal
populations**

Patricia Molina Molina

Institut de Neurociències

Departament de Biologia Cel·lular, Fisiologia i Immunologia

Unitat de Fisiologia Animal

Facultat de Biociències

DIRECTORES

ANTONIO ARMARIO GARCÍA

Institut de Neurociències

**Departament de Biologia Cel·lular, Fisiologia
i Immunologia**

Unitat de Fisiologia Animal
Facultat de Biociències

RAÛL ANDERO GALÍ

Institut de Neurociències

**Departament de Psicobiologia
i de Metodologia de les Ciències de la Salut**

Unitat de Psicobiologia
Facultat de Psicologia



Stress-induced neuronal activation in the medial prefrontal cortex

Identification, molecular profiling and manipulation of stressor-specific neuronal populations

Patricia Molina Molina
2022

Memoria de tesis doctoral presentada por Patricia Molina Molina para optar al grado de Doctora en Neurociencias por la Universidad Autònoma de Barcelona.

Este trabajo ha sido realizado bajo la dirección de:

Doctor Antonio Armario García, Instituto de Neurociencias, Departamento de Biología Celular, Fisiología e Inmunología de la Universidad Autònoma de Barcelona.

Doctor Raül Andero Gali, Instituto de Neurociencias, Departamento de Psicobiología y Metodología de las Ciencias de la Salud de la Universidad Autònoma de Barcelona.

DIRECTOR Y TUTOR

ANTONIO ARMARIO GARCÍA

DIRECTOR

RAÛL ANDERO GALI

DOCTORANDA

PATRICIA MOLINA MOLINA

The present thesis has received funding from the following entities:

Ministerio de Ciencia e Innovación/Ministerio de Economía y Competitividad

SAF2017-017-83430-R

Ministerio de Ciencia e Innovación (PID2020-118844RB-IO

PID2020-118844RB-I00

Generalitat de Catalunya

SGR2017-457

During this PhD thesis, Patricia Molina Molina was recipient of a FPU grant (FPU16/05416) from Ministerio de Educación, Cultura y Deporte.

Abstract

Stress exposure has been associated with the development of psychiatric disorders, but its consequences are strongly dependent on the characteristics of the stressors. However, little is known about how stressor particularities (e.g. nature or intensity) affect their brain processing. The medial prefrontal cortex (mPFC) plays a role in the regulation of behavioural and neuroendocrine responses to stressors, but experimental data are controversial. Hence, the main objectives of this thesis have been to identify in the mPFC stressor-specific neuronal populations and describe their molecular profile as well as manipulate these neuronal populations in order to elucidate their role in the regulation of the stress response. Experiments were conducted in adult male Sprague-Dawley rats.

To identify potential stressor-specific mPFC neurons, we first characterised the dynamics of expression of *c-fos* intronic and mature transcripts by double in situ hybridisation fluorescence. We combined a single or double exposure to stress (inescapable footshock, IS and immobilisation, IMO) with appropriate times to identify neurons activated only by the last stressor (intronic+), only activated by the first stressor (mature+) and those activated by both (intronic+, mature+). Colocalization analyses revealed that IMO and IS recruit a high number of overlapping neurons and a relatively low number of stressor-specific neurons, which could presumably be the most important ones to determine the differential behavioural and physiological consequences of the two stressors.

We further compared the molecular profile of neurons of the prelimbic cortex (PL) activated in response to different stressors by using the PhosphoRiboTRAP approach, which consists on the immunoprecipitation of the phosphorylated ribosomal protein S6, a marker of neuronal activation, and subsequent sequencing analysis of the mRNA associated with the ribosomes (translatome). Translatomic profiling of activated neurons in response to restraint (RES), IMO or IS showed numerous genes differentially expressed versus basal conditions, and a substantial proportion of them was shared by the three stressors. The overall molecular profile of IMO and RES was strikingly similar despite they have different stress intensities, whereas that of IS markedly differed from the other two stressors, indicating a major contribution of the particular nature of the stressor. Our data suggest a potential stressor-specific molecular signature in the PL.

Finally, we designed a viral vector expressing either the excitatory or inhibitory DREADD under the control of the *c-fos* promoter (activity-dependent) to either reactivate or inhibit, respectively, stress-activated PL

neurons. Exposure to stress (IS) significantly increased viral vector levels 4h later compared to basal conditions, thereby validating our approach. IS-exposed animals showed a reduced activity and exploration in novel environments and modest effects on coping strategies in the forced swim test (FST). PL neuronal reactivation did not affect behavioural consequences of IS in activity or exploration, but increased passive coping strategies in the FST and interfered with consolidation of fear memory. PL neuronal inactivation did not show marked behavioural effects, except for increased exploratory activity in stress-naïve rats. At the hormonal level, PL neuronal re-activation significantly reduced corticosterone response to the behavioural tests both in stress-naïve and IS animals, with an opposite pattern after neuronal inhibition. Therefore, although neuronal manipulation at the behavioural level showed very modest effects, our results point towards a tonic inhibitory role of PL neurons in modulating the corticosterone response to emotional stress.

Together, our findings demonstrate the existence of stressor-specific neuronal populations in the mPFC, provide key insights into the differences between stressors with regard to the molecular profile of activated neurons in the PL, and suggest a possible implication of these neurons in the behavioural and hormonal stress response.

Resumen

La exposición a estrés se ha asociado al desarrollo de enfermedades psiquiátricas, aunque sus consecuencias dependen considerablemente de las características de los estímulos estresantes. No obstante, apenas conocemos cómo las particularidades de los estímulos estresantes (v.g. naturaleza o intensidad) afectan a su procesamiento cerebral. La corteza prefrontal medial (mPFC) participa en la regulación de las respuestas conductuales y neuroendocrinas a estrés, pero los datos experimentales son contradictorios. Por ello, los principales objetivos de esta tesis han sido identificar en mPFC poblaciones neuronales específicas de distintos estímulos estresantes y su perfil molecular, así como manipularlas para estudiar su papel. Los experimentos se han realizado en ratas macho *Sprague-Dawley* adultas.

Para identificar neuronas potencialmente específicas de cada estímulo estresante, caracterizamos primero la dinámica de expresión de los transcritos intrónico y maduro de *c-fos* usando doble hibridación in situ fluorescente. Combinamos una exposición única o exposición a dos estímulos (choque inescapable, IS e inmovilización, IMO) con tiempos apropiados para identificar neuronas únicamente activadas por el último estímulo (intrónico+), por el primero (maduro+), o por ambos (intrónico+, maduro+). Los análisis de colocalización demostraron que IMO e IS reclutan un gran número de neuronas comunes y un relativo bajo número de neuronas específicas de estímulo, presumiblemente las más importantes para determinar las distintas consecuencias de los dos estímulos.

Comparamos posteriormente los perfiles moleculares de las neuronas de la corteza prelímbica (PL) activadas tras diferentes estímulos estresantes mediante la técnica de PhosphoRiboTRAP, consistente en la inmunoprecipitación de la proteína ribosomal S6 fosforilada (un marcador de activación neuronal) y la consiguiente secuenciación del ARNm asociado a los ribosomas (*traductoma*). El estudio del *traductoma* en respuesta a restricción de movimiento (RES), IMO o IS mostró un gran número de genes diferencialmente expresados en comparación con la condición basal, así como una gran proporción de genes compartidos por los distintos estímulos. El perfil molecular general de IMO y RES fue altamente similar, a pesar de sus diferencias en intensidad, pero claramente diferente de IS, indicando una importante contribución de la naturaleza particular de los estímulos. Nuestros datos sugieren una posible huella molecular específica de cada estímulo estresante en PL.

Finalmente, diseñamos un vector viral en el que la expresión del receptor DREADD activador o inhibidor estaba controlada por el promotor de *c-fos* (dependiente de actividad), para posteriormente reactivar o inhibir,

respectivamente, las neuronas de PL previamente activadas por estrés. La exposición a IS incrementó la expresión del vector viral 4 h más tarde, validando así nuestra aproximación. Los animales expuestos a IS mostraron una reducción de la actividad y la exploración en ambientes nuevos y un modesto impacto sobre el afrontamiento en la natación forzada. La reactivación de las neuronas de PL no afectó al impacto de IS en actividad o exploración, pero incrementó el afrontamiento pasivo en el test de natación forzada e interfirió con la consolidación de la memoria del miedo. La inactivación de las neuronas de PL no tuvo efectos salvo un incremento de la exploración en ratas no expuestas a IS. A nivel hormonal, la reactivación neuronal redujo la respuesta de corticosterona a las pruebas conductuales tanto en animales controles como expuestos a IS, con una tendencia opuesta tras la inhibición neuronal. Por consiguiente, la manipulación neuronal mostró efectos muy modestos a nivel conductual, pero apuntó a una función inhibidora tónica sobre la respuesta de corticosterona al estrés emocional.

En conjunto, nuestros resultados demuestran la existencia de poblaciones neuronales específicas de estímulo estresante en mPFC, aportan información relevante sobre las diferencias entre estímulos respecto al perfil molecular de neuronas activadas en PL y sugieren su posible implicación en la respuesta conductual y hormonal a estímulos estresantes.

Index

Abbreviations.....	11
Introduction.....	13
1. Stress concept	14
2. Stress response and HPA axis	19
2.1. The hypothalamic-pituitary-adrenal axis	19
2.1. Processing of stressors in the brain	23
3. Prefrontal cortex and the stress response.....	30
3.1. Medial prefrontal cortex structure	31
3.2. Medial prefrontal cortex functions	32
3.3. Medial prefrontal cortex connectivity.....	33
3.4. Effects of stress in the medial prefrontal cortex.....	35
3.5. Role of the medial prefrontal cortex in the stress response	37
4. Immediate early genes and neuronal activation	51
4.1. <i>c-fos</i> as a marker of neuronal activation	51
4.2. <i>c-fos</i> contribution to the field of stress.....	55
4.3. Temporal dynamics of <i>c-fos</i> expression	57
4.4. Use of <i>c-fos</i> for the study of activated neuronal ensembles.....	58
5. Technologies for the study of stress-activated neuronal ensembles.....	61
5.1. Neuronal manipulation based on activity-dependent promoters.....	61
5.2. Transcriptomic / Translatomic profiling of activated neurons	66
Materials and methods.....	71
1. Animals	72
2. General procedures	72
2.1. Animal housing and handling	72
2.2. Blood samples collection.....	72
2.3. Recording and analyses of behavioural tests.....	73
3. Stress paradigms and behavioural tests	73
3.1. Immobilisation (IMO).....	73
3.2. Inescapable footshock (IS).....	73
3.3. Restraint (RES)	74
3.4. Open field (OF).....	74
3.5. Hole Board (HB).....	75
3.6. Forced Swim Test (FST).....	76
4. Biochemical analysis	77
5. Perfusion and histological processing	77
5.1. Perfusion.....	77

5.2. Brain sectioning	78
6. Fluorescent in situ hybridisation (FISH)	78
6.1. Probes generation.....	78
6.2. In situ hybridisation assay (ISH).....	79
6.3. Image acquisition and quantification.....	81
7. Immunofluorescence	83
7.1. Immunostaining protocols.....	83
7.2. Image acquisition and quantification.....	84
8. Viral vector generation and delivery.....	86
8.1. Viral vectors design	86
8.2. Viral vector production	87
Table 5. Components of the transfection solution.	87
Table 6. Reagents and volumes used for SYBR Green RT-PCR reaction.....	88
8.3. Viral vector delivery: stereotaxic surgery.....	89
8.4. Histological verification of viral vector injections.....	89
9. Drugs.....	90
10. PhosphoRiboTRAP and RNA- sequencing	90
10.1. Stimuli and brain dissection.....	90
10.2. Coupling beads with pS6 antibody	91
10.3. Homogenisation	91
10.4. Immunoprecipitation	92
10.5. RNA purification and sequencing	93
10.6. qRT-PCR analyses.....	94
10.7. Bioinformatic analysis of RNA-seq data.....	94
10.8. Statistical analysis	95
Chapter 1: Identification of neuronal ensembles activated specifically by different emotional stressors in the mPFC	97
1. Introduction	98
2. Temporal dynamics of <i>c-fos</i> RNA expression after IMO exposure	100
2.1. Experimental design.....	100
2.2. Results	101
3. Specificity of neuronal activation in response to IMO and IS in the mPFC	108
3.1. Experimental design.....	108
3.2. Results	109
Chapter 2: Molecular profiling of neurons activated in response to emotional stressors differing in intensity and nature in the PL	126
1. Introduction	127
2. S6 phosphorylation after different times of IMO and different emotional stressors.....	128

2.1. Experimental design	128
2.2. Results	129
3. Colocalization between pS6 and c-Fos after IMO exposure	132
3.1. Experimental design	132
3.2. Results	132
4. PhosphoRiboTRAP: translomic profiling of PL neurons activated after acute exposure to different emotional stressors	134
4.1. Experimental design	134
4.2. Results	136
Chapter 3: Chemogenetic manipulation of stress-activated neurons in the PL	146
1. Introduction	147
2. Design and validation of expression of AAV1-pfos:hM3Dq:mCherry	149
2.1. Experimental design	149
2.2. Results	149
3. Design and validation of AAV9-pfos(Int+Ex):hM3Dq: mCherry:PEST... ..	150
3.1. Experimental design	150
3.2. Behavioural consequences of inescapable footshock exposure	154
3.3. Re-activation of stress-activated neurons in the PL	156
3.4. Inhibition of stress-activated neurons in the PL	163
Discussion	169
1. Identification of neuronal ensembles activated in response to IMO and IS in the mPFC	170
1.1. Temporal dynamics of <i>c-fos</i> expression after exposure to IMO	170
1.2. Analysis of the number of activated neurons and intensity of signal	172
1.3. Validation of the experimental design	173
1.4. Study of neuronal ensembles specifically activated by emotional stressors in the mPFC	175
1.5. Important methodological considerations	180
2. Molecular profiling of cells activated by different emotional stressors in the PL cortex	181
2.1. Characterisation of pS6 expression after exposure to stress and colocalization with c-Fos	181
2.2. Translomic profiling of PL activated cells after exposure to different stressors	183
2.3. Important considerations	186
3. Behavioural and hormonal consequences of manipulating stress-activated neurons in the PL cortex	187
3.1. Design and validation of an IEG-based viral vector for manipulating stress-activated neurons	188
3.2. Short-term behavioural consequences of IS exposure in general activity and exploratory behaviour	190

3.3. Consequences of IS stress and PL neuronal manipulation in locomotor and exploratory activity	192
3.4. Consequences of IS stress and PL neuronal manipulation in grooming behaviour	194
3.5. Consequences of IS stress and PL neuronal manipulation in coping strategies.....	195
3.6. Consequences of PL neuronal manipulation after IS exposure in contextual fear memory	196
3.7. Modulation of HPA response to emotional stressors by PL neuronal manipulation.....	197
3.8. Important considerations.....	199
3.9. Future directions	202
Conclusions.....	204
Bibliography	207

Abbreviations

5-HT: 5-hydroxytryptamine or serotonin	DHM: dorsomedial hypothalamus
A: adrenaline	DIG: digoxigenin
AAV: adeno-associated viral vector	dlPFC: dorsolateral prefrontal cortex
ACC: anterior cingulate cortex	dmPFC: dorsomedial prefrontal cortex
ACTH: adrenocorticotrophic hormone	DMSO: dimethyl sulfoxide
AP-1: activator protein 1	Dox: doxycycline
Arc: activity-regulated cytoskeleton-associated	DREADD: designer receptors exclusively
ARE: AU-rich element	activated by designer drugs
AU: arbitrary units	DRD1: dopamine receptor D1
AVP: arginine vasopressin	DRD2: dopamine receptor D2
BAS: basal	DRN: dorsal raphe nucleus
BLA: basolateral amygdala	DTT: dithiothreitol
BNST: bed nucleus of the stria terminalis	EC: entorhinal cortex
BSA: bovine serum albumin	EGFP: enhanced green fluorescent protein
CA: closed arms	EPM: elevated plus maze
CaMK: calcium-calmodulin dependent kinase	E-SARE: enhanced synaptic activity-responsive
CaMKK: calcium-calmodulin dependent kinase	element
kinase	EYFP: enhanced yellow fluorescent protein
cAMP: cyclic adenosine monophosphate	FC: fear conditioning
catFISH: Cellular compartment analysis of	FDR: false discovery rate
temporal activity by fluorescence in situ	FISH: fluorescent in situ hybridisation
hybridization	Fl: fluorescein
Ca/CRE: Ca ²⁺ /cAMP response element	FST: forced swim test
CeA: central nucleus of the amygdala	GABA: gamma-aminobutyric acid
CFC: contextual fear conditioning	GAD67: glutamic acid decarboxylase, 67 kDa
ChR2: channelrhodopsin-2	isoform
CK1: casein kinase 1	GAS: general adaptation syndrome
CNO: clozapine N-oxide	GC: glucocorticoids
CNS: central nervous system	GFAP: glial fibrillary acidic protein
CORT: corticosterone	GFP: green fluorescent protein
CREB: cAMP response element-binding	GR: glucocorticoid receptor
CREERT ² : tamoxifen-dependent	GzLM: generalised lineal model
Cre	recombinase
CRH: corticotropin-releasing hormone	HB: hole board
CRHR1: CRH receptor 1	HBSS: Hanks Balanced Salt Solution
CRHR2: CRH receptor 2	HDAC: histone deacetylases
CRS: chronic restraint stress	HEK293T: human embryonic kidney cells 293T
Ctrl: control	HF: hippocampal formation
CTS: controllable stress	hnRNA: heteronuclear RNA
CUS: chronic unpredictable stress	HPA: hypothalamic-pituitary-adrenal
DA: dopamine	IC: insular cortex
DAPK: death-associated protein kinase	IEG: immediate early gene
DBS: deep brain stimulation	IF: immunofluorescence
dcPVN: dorsal cap of the paraventricular nucleus	IL: infralimbic cortex
of the hypothalamus	IL-1β: interleukin 1β
DEPC: diethyl pyrocarbonate	IntDen: integrated density
dFISH: double fluorescent in situ hybridization	i.p.: intraperitoneal administration
	IP: immunoprecipitation

IMO: immobilisation on board
 IRES: internal ribosome entry site
 IS: inescapable footshock
 ISH: in situ hybridisation
 ITI: inter-trial interval
 KPBS: potassium phosphate-buffered saline
 LC: locus coeruleus
 LE: Long Evans
 LH: learned helplessness
 LHb: lateral habenula
 LS: lateral septum
 LSv: lateral septum ventral
 LV: lentiviral vector
 MAPK: mitogen-activated protein kinase
 MeA: medial amygdala
 mPFC: medial prefrontal cortex
 mPOA: medial preoptic area
 mPVN: magnocellular paraventricular nucleus of the hypothalamus
 mpdPVN: medial parvocellular dorsal paraventricular nucleus of the hypothalamus
 mpvPVN: medial parvocellular ventral paraventricular nucleus of the hypothalamus
 MR: mineralocorticoid receptor
 MRN: median raphe nucleus
 mRNA: mature RNA
 mTOR: mammalian target of rapamycin
 NA: noradrenaline
 NAc: nucleus accumbens
 NDS: normal donkey serum
 NE: novel environment
 NFS: novelty feeding suppression
 NRS: normal rabbit serum
 NTS: nucleus of the solitary tract
 OA: open arms
 OF: open field
 PAG: periaqueductal gray matter
 PBN: parabrachial nucleus
 PCA: principal component analysis
 PFA: paraformaldehyde
 PFC: prefrontal cortex
 PI3K: phosphatidylinositol-3-kinase
 PKA: protein kinase A
 PKC: protein kinase C
 PKG: protein kinase G
 PL: prelimbic cortex
 POD: peroxidase
 POMC: proopiomelanocortin
 PP-1: protein phosphatase 1
 PrCm: medial precentral area
 pS6: phosphorylated ribosomal protein S6
 PV: parvalbumin
 PVTh: paraventricular nucleus of the thalamus
 PVN: paraventricular nucleus of the hypothalamus
 RAM: robust activity marking
 RES: restraint
 RIA: radioimmunoassay
 RNA-seq: RNA sequencing
 ROI: region of interest
 RSK: p90 ribosomal S6 kinase
 RT-PCR: reverse transcription polymerase chain reaction
 S6K1: ribosomal S6 kinase 1
 SARE: synaptic activity-responsive element
 SD: Sprague Dawley
 SEM: standard error of the mean
 siRNA: small interfering RNA
 SMA: sympatho-medullo-adrenal axis
 smPVN: submagnocellular paraventricular nucleus of the hypothalamus
 SON: supraoptic nucleus
 SPB: shock probe burying
 SRE: serum response element
 SRF: serum response factor
 SSC: sodium saline citrate
 SST: somatostatin
 STD: standard deviation
 TAM: tamoxifen
 TEA: triethanolamine
 TRAP: translating ribosome affinity purification
 TST: tail suspension test
 tTA: tetracycline-controlled transactivator
 UTS: uncontrollable stress
 vGluT1: vesicular glutamate transporter 1
 VIP: vasoactive intestinal polypeptide
 vmPFC: ventromedial prefrontal cortex
 vSUB: ventral subiculum
 VTA: ventral tegmental area

Introduction

1. Stress concept

Stress is highly present in our modern society and our daily lives. It has been dubbed by many as the “Health Epidemic of the 21st Century” (see revision by Fink, 2016), and thousands of research articles have been published about stress and stress-related pathologies. Despite this, it has been extremely difficult to reach a consensus in the scientific community on a precise definition of stress.

Historically, the term “stress” was first used in physics of elastic materials. Stress refers to the mutual actions which occur in a body to which a system of forces is applied, whereas strain refers to the resulting internal distortion of the object (revised in Levine, 2005). The term “stress” was later borrowed by the endocrinologist Hans Selye, one of the most influential scientific figures in the stress field. In fact, the foundations for the modern theories of stress were laid by him and Walter B Cannon.

At the beginning of the 20th century, the physiologist Walter B Cannon coined the term homeostasis (from the Greek “hómoios” similar and “stásis” standing still or steady) to describe the coordinated physiological processes which maintain most of the steady states in the organism (Cannon, 1929). His studies were based on the concept developed earlier, at the end of the 19th century, by Claude Bernard: the “milieu intérieur”. Bernard described how complex living organisms maintain constant the internal environment bathing cells – or the “milieu intérieur” – by continual compensatory changes of bodily functions, which is the condition of free, independent life (cited in Holmes, 1986). Cannon extended Claude Bernard’s concept of the internal environment and described homeostasis as the physiological mechanisms that enable organisms to adapt to challenges and maintain several critical variables, such as blood pressure, core temperature, and glycemia, within a narrow range despite changes in the environment. He emphasized the role of the sympathetic nervous system and the adrenal medulla (sympatho-medullo-adrenal system, SMA) as a crucial mechanism to restore homeostasis and enhance survival. Furthermore, he coined the widely used term “fight-or-flight” response to describe the animals’ behavioural and endocrine responses to threats (Cannon, 1929).

The endocrinologist Hans Selye deserves much of the credit for introducing the term “stress” in a biological context in the 20th century and highly popularizing the stress theory in the scientific community. He observed that patients with different illnesses shared many “non-specific symptoms” that were a common response to different stimuli experienced by the body. Apart from these clinical observations, he performed experiments with

laboratory rats exposed to a variety of noxious stimuli and observed that they also experienced these common effects. These effects included the development of a characteristic triad consisting of adrenal enlargement, involution of the thymic gland and other lymphatic structures, and gastrointestinal ulceration. Based on this, he defined stress as “the nonspecific response of the body to any demand upon it”. With “nonspecific response”, he meant that exposure to any noxious agent would result in similar symptomatology, regardless of the nature of the agent or stimulus. In 1936, he published a report in *Nature* in which he referred to this symptom picture as the “general adaptation syndrome (GAS)”, which was composed of three phases: an alarm reaction, a resistance stage and a final phase of exhaustion. During the alarm phase, the body reacts to the agent by activating different emergency response systems, including the SMA axis. If stress exposure continues and the organism can effectively adapt, the resistance phase develops. Finally, if there is prolonged exposure to the stressor, this may eventually result in exhaustion and eventually the development of pathology (Selye, 1936).

Selye demonstrated that these symptoms were associated with the activation of the hypothalamic-pituitary-adrenal (HPA) axis and the secretion of glucocorticoids by the adrenal cortex. In contrast to Cannon, who focused on the adrenal medulla and the sympathetic response, Selye emphasized the HPA axis as the key effector of the stress response and the adrenal cortex as the principal organ. Furthermore, he went one step further by highlighting the dual role of the HPA axis, essential to resistance and adaptation to challenges, but also being responsible for the development of pathological conditions. Indeed, Selye’s original concept that prolonged stress can lead to disease is widely accepted nowadays. Moreover, while Cannon referred to stress in terms of the stimuli which elicited a response, Selye defined stress usually in terms of the response (e.g. adrenal hypertrophy, thymicolymphatic involution). This ambiguous use gave rise to considerable confusion in the field and Selye was forced to create a neologism, “stressor”, to refer to the causative agent, and retain stress for the resulting condition. The current terminology distinguishes between the stimulus or agent (stressor), the state generated in the organism (stress) and the response or reaction of the organism (stress response) (Armario, 2006b).

The theoretical foundations established by Selye and Cannon have been substantially elaborated over the years. Despite the undeniable influence of Selye’s work in the field of stress, his theory soon became the subject of considerable criticism. The criticism was mainly directed at the assumption of the nonspecific stress response. In the 1970s, working with primates, Mason (Mason, 1975) noted that common cortisol response to various

stressors differing in nature (e.g. restraint in chairs, cold, heat, haemorrhage) shared emotional disturbances and that this could be the reason of the similar stress response. However, cortisol response to surgery can be observed under anaesthesia, thus precluding emotional experience (Lilly, 1994). It is then clear that physical stressors can activate the stress response regardless of conscious mechanisms and emotional activation.

Returning to the lack of specificity of Selye's theory, Pácak and Palkovits also carried out a series of experiments in which they showed that different stressors (mainly physical stressors) specifically activated different regions of the brain (Pacák and Palkovits, 2001) suggesting that the response pattern to stressors of different nature was heterogeneous. In addition, they also showed that different physical stressors exhibited different neuroendocrine profiles. This lack of specificity of the stress response has been a central matter of discussion for physiologists. Chrousos and Gold (1992) modified Selye's theory of non-specificity by posing the idea that although the physiological and behavioural response to threatened homeostasis can be specific to the stressor, when the threat to homeostasis exceeds a certain threshold, any stressor would elicit the nonspecific "stress syndrome". In this regard, the current consideration is that two different physiological responses are elicited by physical stressors (Armario, 2006a): (i) a specific response to the stimulus, not related to its stressful properties, and (ii) a non-specific response, which is common to all stressors. Hence, the physiological response would be the sum of the specific and non-specific responses to a challenge.

The concept of homeostasis proved to be limited in describing the functioning of the physiological mechanisms used to adapt to external perturbations. Physiological parameters fluctuate within certain ranges, which can be further modulated by oscillating circadian and ultradian rhythms or even seasonal changes. The classical concept of homeostasis implied strict stability, depending on fixed set-point mechanisms and constant signals, and for this reason, it was not considered ideal for describing stress responses. Bruce McEwen revised this term and introduced a more flexible concept in the field of stress: allostasis (McEwen and Stellar, 1993). This concept had been originally coined by Sterling and Eyer to refer to the ability to maintain the stability of the internal milieu through change (Sterling and Eyer, 1988). Allostasis involves the action of different factors (e.g. hormones) which continuously change to maintain the stability of physiological variables by predicting the need to meet anticipated demands, thereby allowing adaptation of the organism to external perturbations. Upon exposure to a stressor, allostatic responses are triggered to adapt to the situation, but if the allostatic response is either prolonged in

time, inadequate, excessive or overstimulated by repeated stressors, the cost of reinstating stability might become too high, a condition termed allostatic load. Remarkably, long-term allostatic load can lead to the development of pathological conditions (McEwen, 1998).

The original conceptualization of stress by Selye was mainly based on the influence of agents which directly threaten homeostasis, and it seemed to ignore the cognitive processing of information and the influence of the psychological factors. However, subsequent work of different scientists emphasized the importance of psychological stressors. Nowadays there is plenty of evidence unambiguously supporting that psychological factors are crucial for determining the stress response. In this regard, the contribution of Weiss in the early seventies was crucial. Weiss demonstrated in a series of experiments in rats using a well-validated stress paradigm of electric shock that the stress response (e.g. measured by stomach ulceration) could be modified depending on the degree to which the shock could be predicted and the shock duration and/or intensity could be controlled (Weiss, 1972). S. Levine is another researcher who has also substantially contributed to the integration of psychological factors in the stress concept. Levine emphasizes that stress should be considered as a process that includes the stimulus and the behavioural and physiological output, but also the perceptual, higher-level cortical processing of this information (Levine, 2005).

In line with this, Richard Lazarus (1993) also remarked that the cognitive processing of stressful situations (appraisal) and the underlying psychological mechanisms are crucial to determine how individuals face challenging situations and to modulate the consequences of exposure to stressors. He proposed that the stress response is elicited when an individual perceives that the demands of an environmental stimulus are greater than their ability to meet these demands. In other words, when the challenge surpasses the coping strategies of individuals. According to his theory, situations would only be considered stressful if they are perceived as threatening and uncontrollable by the individual. Depending on the behaviour adopted to face a particular situation, classically two types of coping strategies have been considered in animals: active coping (or proactive strategy), focused on directly facing the aversive situation, and passive coping (or reactive strategy), centred in escaping or avoiding the situation (Koolhaas et al., 1999). More recently, Koolhaas and colleagues (2011) went beyond and proposed that stress must be defined in terms of cognitive perception of controllability and/or predictability that is expressed in a physiological and behavioural response. Indeed, they claim that the conceptualisation should be extended to consider stressors only if they are

uncontrollable and/or unpredictable. This fact remarks the importance that is given at present to cognitive and perceptual aspects of stress.

Hopefully, this review of the historical evolution of the concept of stress has provided a picture of the complexity of this composite, multidimensional concept. All existing definitions include some components separately, however, finding a proper and integrated definition of the term still challenges researchers at present. One of the definitions that our research group considers the most adequate to contextualize our study in a proper theoretical framework is the one proposed by Vigas: "Stress is the response of the organism, evolved in the course of the phylogeny, to agents actually or symbolically endangering its integrity and that cannot be solved with the normal homeostatic mechanisms" (Vigas, 1980). A fundamental aspect of this definition is that it encompasses both stimuli which directly compromise homeostasis (systemic stressors) and those which represent a potential but not actual threat to the organism (emotional stressors).

Systemic (or physical) stressors represent a direct challenge to homeostasis and they are recognized by somatic or visceral sensory pathways. Haemorrhage, hypoxia or infection are examples of these types of stressors. Conversely, emotional (or psychogenic) stressors represent a potential rather than a direct threat to homeostatic mechanisms and therefore, the stress response elicited is considered anticipatory and preparative rather than reactive. They are interpreted by exteroceptive sensory modalities and integrated by cognitive and affective information processing systems in the central nervous system (CNS). These stressors include exposure to unknown environments, predator odour and social defeat (Herman and Cullinan, 1997; Herman et al., 2003). Commonly employed laboratory stressors, such as immobilization, forced swim or electric footshocks may be included in a third category, mixed stressors, as they have both physical and emotional components in different proportions. However, the pattern of brain activation induced by these stressors (e.g. induction of immediate early genes (IEG) such as *c-fos*) is highly similar to that of purely emotional stressors, such as a novel environment (Pacák and Palkovits, 2001). This strongly suggests that they have a main emotional component and therefore, they can be considered predominantly emotional stressors (herein referred to as emotional stressors).

2. Stress response and HPA axis

Exposure to a stressor triggers a wide range of physiological and behavioural changes which are designed to face dangerous or potentially dangerous situations and aimed at reinstating homeostasis, thereby increasing the probability of survival of the individual. Importantly, effective stress responses imply both that the response is rapidly activated when needed and efficiently turned off after cessation of the stressor (for a review see Ulrich-Lai and Herman, 2009). The two most important and best-characterised systems activated in response to stress in all vertebrates are the HPA and the SMA axes.

The SMA is rapidly activated in response to stress and leads to the release of the catecholamines adrenaline (A) and noradrenaline (NA) from the adrenal medulla, although 70% of the total NA released into plasma comes from sympathetic nerve endings. A and NA act on diverse target organs and modulate many physiological processes, enabling the organism to deal with the immediate challenge. Hence, the SMA can rapidly induce changes in the cardiovascular system, increasing heart rate and blood pressure. Moreover, it also induces changes in energy mobilisation, including increases in the metabolic rate and glycogen breakdown, and hence increased glucose levels. Importantly, it is a very transient response that is rapidly terminated due to the extremely short half-life of catecholamines in blood (e.g. 2.5 min for NA) and the compensatory action of the parasympathetic nervous system (Kvetnansky et al., 2009).

The activation of the HPA axis culminates in the secretion of glucocorticoids (GC) into the bloodstream by the adrenal cortex. GC act at multiple levels and modulate many physiological functions, with the main objectives of mobilising bodily energy resources to successfully face the challenge, particularly if prolonged in time, and to prepare the organism for future stressors (Munck et al., 1984; Sapolsky et al., 2000). Remarkably, excessive or dysregulated activation of the HPA axis has been associated with the pathological consequences of stressor exposure, both physiological (e.g. lipid metabolism, immunodepression) and psychiatric (depression, schizophrenia). For this reason, the HPA axis has been one of the best characterised neuroendocrine systems (Armario, 2006a) and a key topic in the field of stress.

2.1. The hypothalamic-pituitary-adrenal axis

The information from stressful stimuli converges at the paraventricular nucleus of the hypothalamus (PVN), the key brain region involved in the control of the HPA axis. This nucleus is functionally complex and

participates in the regulation of both neuroendocrine and vegetative functions. Based on morphological, cytological and functional criteria, it can be subdivided into different regions: (1) magnocellular (mPVN), (2) dorsal cap (dcPVN), (3) medial parvocellular (mpPVN), which in turn can be subdivided into ventral (mpvPVN) and dorsal (mpdPVN), and (4) submagnocellular (smPVN) (Herman et al., 2003; Armario, 2006a). The magnocellular region comprises neurons that synthesize arginine vasopressin (AVP) and oxytocin and project to the neurohypophysis to release these peptides into the bloodstream. The dcPVN, mpvPVN and smPVN contain neurons that synthesize corticotropin-releasing hormone (CRH) and other peptides. This in turn is involved in the regulation of the autonomic response to stress through their projections to the brainstem. Finally, the parvocellular neurons of the mpdPVN are responsible for activating the HPA axis. These neurons synthesize CRH and AVP and, through their axonal projections to the median eminence, they release these hormones into the portal circulation, which then reach the adenohypophysis (or anterior pituitary gland). There, CRH induces the synthesis and release of the adrenocorticotrophic hormone (ACTH) by corticotrophic cells into the systemic circulation. Although CRH is the major ACTH secretagogue, AVP acts synergistically with CRH to promote ACTH release. Subsequently, ACTH travels through systemic circulation and acts in the zone fasciculata of the adrenal cortex to promote the synthesis and secretion of glucocorticoids (GC) (primarily cortisol in humans and corticosterone in rodents) (Swanson and Sawchenko, 1983; Antoni, 1986). GC regulate a myriad of physiological functions in multiple target tissues, including metabolism, immune function, cardiovascular function, growth, reproduction, and cognition (Sapolsky et al., 2000) (**Figure 1**).

Broadly, GC functions have been categorised into two main classes: modulating actions, which alter the response of the organism to a stressor and preparative actions, which adjust the response of the organism to subsequent stressors or promote adaptation to a chronic stressor. Modulating actions can in turn be classified into permissive, suppressive and stimulating (Munck et al., 1984; Sapolsky et al., 2000). Briefly, permissive actions are mediated by GCs present before the stressor and prime the mechanisms that the organism needs to respond to stress. These actions take place independently of the stress-induced increase in GC concentrations, thereby optimizing the immediate response, such as the increase in heart rate. Suppressive actions and stimulating actions are dependent on the stress-induced rise in GC levels and occur one hour or more after stressor onset. These delayed GC actions are crucial either for preventing the negative consequences of a prolonged stress response (e.g. inhibiting the immune and inflammatory responses and the HPA axis

response itself through feedback mechanisms) (suppressive) or for enhancing the effects of other hormones released during the initial phase of the stress response (stimulating) (Sapolsky et al., 2000).

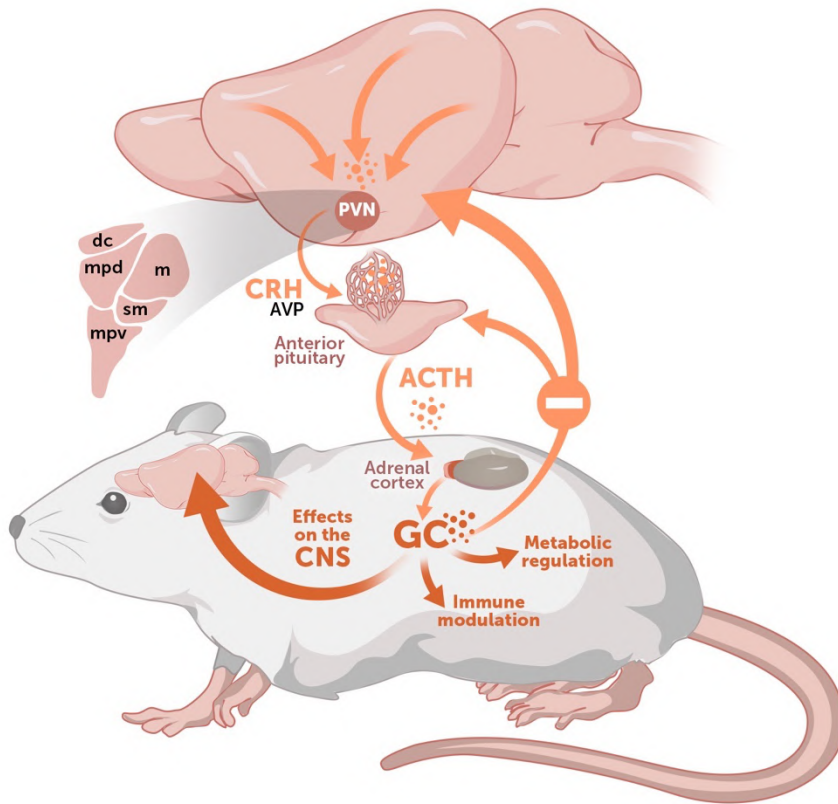


Figure 1. Mechanisms of HPA axis activation and functions.

Exposure to a stressor induces activation of hypophysiotropic neurons located in the dorsomedial parvocellular region of the paraventricular nucleus of the hypothalamus (mpdPVN). These neurons synthesize corticotropin-releasing hormone (CRH) and vasopressin (AVP) and, in response to stress, these hypothalamic factors are released into the hypophysial portal vessels that access the anterior pituitary gland. They then act on the corticotrope cells of the anterior pituitary and induce the release of the adrenocorticotrophic hormone (ACTH) into the systemic circulation. The main target for circulating ACTH is the adrenal cortex, where it stimulates the synthesis and secretion of glucocorticoids (GC; corticosterone in rats and mice and predominantly cortisol in humans and other mammals). GC regulate a myriad of physiological functions, including metabolic and immune regulation. Furthermore, one of the main effects of GC is to regulate HPA axis activity by negative feedback mechanisms acting at different levels, such as the anterior pituitary, the PVN and other extrahypothalamic regions. *Abbreviations general scheme: ACTH, adrenocorticotrophic hormone; CRH, corticotropin-releasing hormone; GC, glucocorticoid; PVN, paraventricular nucleus of the hypothalamus. Abbreviations schematic drawing of the PVN: dc, dorsal cap; m, magnocellular; mpd, medial parvocellular dorsal; mpv, medial parvocellular ventral; sm, submagnocellular.*

CRH and CRH receptors

CRH is the principal member of a family of neuropeptides which includes urocortin 1, 2 and 3. These bind to two receptors: CRHR1 and CRHR2 (which has two variants: CRHR2 α and CRHR2 β). Many studies have indicated a crucial role of this family in the modulation of the stress response. CRH has a high affinity for CRHR1, a G-coupled receptor found in anterior pituitary corticotrope cells, and a low affinity for the G-coupled receptor CRHR2. CRH triggers the HPA axis response through its binding to CRHR1, which is widely distributed through the SNC, including areas involved in stress-processing such as the medial prefrontal cortex (mPFC), lateral septum (LS), hippocampal formation (HF), central amygdala (CeA) and various brainstem nuclei (Bale and Vale, 2004; Aguilera, 2012). This extrahypothalamic expression has been suggested to play an important role in the behavioural and autonomic responses to stress (Bale and Vale, 2004). In contrast, CRHR2 expression is more restricted through the SNC, being located mainly in the LS, HF, dorsal raphe nucleus (DRN) and hypothalamus. Whereas CRHR1 has been classically associated with the activation of the behavioural and HPA response to stress, CRHR2 has been related to a reduced response (Korosi and Baram, 2008). However, a recent study by Anthony et al. (2014) has challenged this view by showing that activation of CRHR2 neurons located in the LS increases mpdPVN activation and induces anxiogenic behaviours.

Glucocorticoid receptors

GCs exert their genomic actions through binding to two receptor subtypes: the mineralocorticoid receptors (MR) and the glucocorticoid receptors (GR), which are distributed in many organs, including the brain. MR have a high affinity for GC (10-fold higher than GR) and hence, they are usually extensively bound to GC in basal conditions. Conversely, GR are only activated after high levels of GC are reached, such as in response to stress or during the peak of the circadian rhythm.

MR and GR show a distinct distribution in the CNS (Reul and De Kloet, 1986; De Kloet et al., 2005). Whereas the GR have a ubiquitous distribution in the brain, being widely present in important areas for stressor processing, such as the mPFC, HF, amygdala, LS and bed nucleus of the stria terminalis (BNST), MR have a much more restricted expression: they are mainly expressed in the HF, and to a less extent, in the mPFC and the amygdala.

GC can mediate their functions through genomic and non-genomic pathways. Their classic genomic actions are exerted through binding to GR or MR, which act as ligand-activated transcription factors and hence, upon binding of the GC, translocate to the cell nucleus where they induce broad

changes in gene transcription. However, there is also evidence for non-genomic effects of GC, which occur within minutes after the increase in circulating GCs and seem to depend on receptors of the cell membrane, although their precise nature and the molecular underlying mechanisms are still not fully understood (Groeneweg et al., 2012).

Negative feedback on the HPA axis

Although GCs have a major function in restoring stress-induced homeostatic alterations, if prolonged in time, their effects can be detrimental. Therefore, appropriate and strict control of GC concentration is key for the organism. In this regard, GC exert negative feedback at multiple levels of the HPA axis, including the pituitary gland, the PVN and other extrahypothalamic regions, by inhibiting effector CRH neurons and ACTH release, thereby constraining HPA activation (for a review see Armario, 2006a; Myers et al., 2012). These distributed feedback mechanisms offer multiple sites for fine adjustment of HPA axis output depending on the demands of the situation. The negative feedback mechanisms have been classically divided into slow and fast feedback. It has been classically considered that rapid feedback starts immediately after GC release and depends on the rate of increase in GC levels, terminating once GC levels are stabilised, although this topic is currently being reconsidered (see Osterlund et al., 2016). This time frame is too fast to be mediated by genomic effects and thus, it is believed to rely on non-genomic receptors. There is evidence suggesting that it could be mediated by both a reduced glutamatergic input into the mpdPVN through endocannabinoid signalling and potentiation of GABAergic input through nitric oxide. The slow feedback is mediated by genomic GR and MR and involves the inhibition of the transcription of CRH, AVP and POMC (proopiomelanocortin) genes, which in turn would suppress HPA axis activation (Keller-Wood and Dallman, 1984; Watts, 2005 and for a review see Myers et al., 2012).

2.1. Processing of stressors in the brain

Stressor-related information from different sensory systems reaches the brain and it results in the activation of several brain areas which orchestrate the wide range of physiological and behavioural changes elicited in response to stress (**Figure 2**). The current knowledge we have about the processing of stressors in the CNS has been gained mainly through two approaches: (1) detection of activated neurons by the use of immediate early genes (IEGs), such as the neuronal marker *c-fos*, which will be discussed in detail in Section 4, and (2) lesion or inactivation studies of particular brain areas.

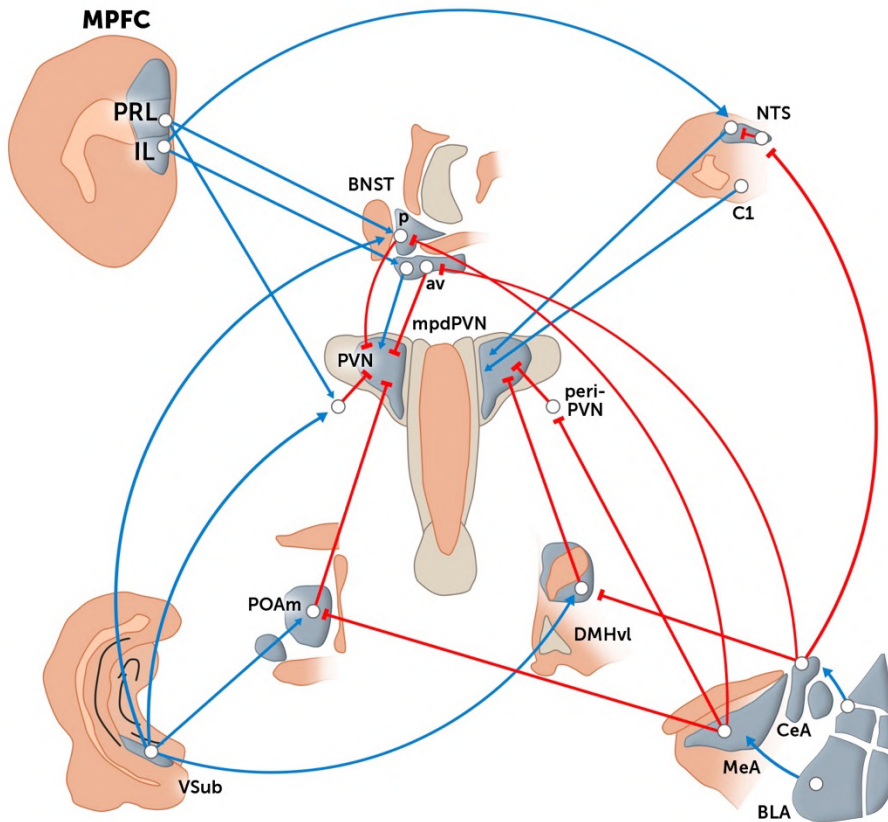


Figure 2. Neural mechanisms of stress integration.

Blue lines represent excitatory projections whereas red lines represent inhibitory projections. The medial prefrontal cortex (mPFC) projects through the prelimbic (PL) and infralimbic (IL) cortices, which have different projection patterns to areas involved in the modulation of HPA axis response. The PL sends excitatory projections to the peri-PVN (paraventricular nucleus of the hypothalamus) region and the posterior subdivision of the bed nucleus of the stria terminalis (BNST), which send GABAergic projections to the medial parvocellular dorsal division of the PVN (mpdPVN). Conversely, the IL projects to the nucleus of the solitary tract (NST) and the antero-ventral subdivision of the BNST, which send excitatory projections to the mpdPVN. The hippocampal formation (HF) sends excitatory projections through the ventral subiculum (vSUB) to several subcortical regions, including the posterior BNST, the peri-PVN region, the medial preoptic area (mPOA) and the dorsomedial hypothalamus (DMH), which send GABAergic projections to the mpdPVN. The central nucleus of the amygdala (CeA) sends GABAergic projections to the anteroventral subdivision of the BNST and the DMH. Moreover, GABAergic neurons of the CeA also project to GABAergic interneurons of the NTS, thereby causing disinhibition of the NTS projections to the mpdPVN. The medial nucleus of the amygdala (MeA) sends inhibitory projections to GABAergic regions with direct projections to the PVN, such as the posterior division of the BNST, the mPOA and the peri-PVN region, thereby causing trans-synaptic disinhibition. Finally, the basolateral nucleus of the amygdala (BLA) modulates HPA axis activity through its glutamatergic projections to the CeA and MeA (adapted from Ulrich-Lai and Herman, 2009 and Herman et al., 2016).

Based mainly on IEGs lesioning studies, it has been determined that the stress-regulatory circuits activated by a particular stressor are dependent on the nature of the stimulus (Herman and Cullinan, 1997; Pacák and Palkovits, 2001). Systemic stressors such as haemorrhage or infection, which represent a direct challenge to homeostasis, require a rapid activation of the HPA axis. For this reason, most of the brain areas involved in their processing send direct projections to the PVN, bypassing the need for cognitive processing. By contrast, emotional stressors, of anticipatory nature, require more complex higher-order processing and hence they activate telencephalic regions, such as the mPFC and the amygdala. These regions do not project directly to the PVN but instead send projections to intermediate relays (Herman and Cullinan, 1997). Therefore, from the explanation above it can be established that regardless of the nature of stressors, a common characteristic of their brain processing is that their information always converges at the PVN. For this reason, the PVN is considered the key centre for the integration of stimulatory and inhibitory signals that regulate the HPA axis response.

Direct projections to the PVN

The PVN receives direct projections from numerous hypothalamic nuclei but a restricted number of extra-hypothalamic brain regions. In general, these direct PVN-projecting neurons are located in regions that receive first- or second-order inputs from visceral afferents, somatic nociceptors or humoral sensory pathways. Hence, most of these PVN-projecting neurons are perfectly suited to elicit fast and reflexive activation of the HPA axis, as required by systemic stimuli (for a review see Herman et al., 2003). The activation of the HPA axis mediated by systemic stressors involves fundamentally the brainstem, the circumventricular organs and the hypothalamus (Herman et al., 2003; Ulrich-Lai and Herman, 2009; Myers et al., 2017a).

The brainstem receives information about major homeostatic perturbations, such as blood loss and visceral or somatic pain and hence, it has been postulated to mediate reflexive responses to systemic stressors. The A2/C2 region or nucleus of the solitary tract (NTS) and the A1/C1 region or ventrolateral medulla (VLM) send noradrenergic and adrenergic projections directly to the PVN and are the main pathway for direct activation of the HPA response. Moreover, the dorsal and median raphe nucleus (DRN and MRN, respectively) send serotonergic fibres to the PVN and surrounding regions, which mainly have an excitatory effect on HPA axis activation. Furthermore, the periaqueductal grey matter (PAG) is also involved in the regulation of autonomic and behavioural stress

responses (e.g. active vs passive coping strategies) as well as the regulation of the HPA axis. Its role in HPA axis regulation seems to be mediated by direct glutamatergic projections to the PVN (Herman et al., 2003).

The circumventricular organs, such as the subfornical organ and the organum vasculosum of the lamina terminalis lack the blood-brain barrier, so they can effectively detect volume and osmotic blood changes in the organism (e.g. electrolyte balance and blood pressure) and project directly to the PVN to stimulate HPA axis activity when there is an alteration in these physiological parameters (Herman et al., 2003; Ulrich-Lai and Herman, 2009). Moreover, the information related to the energy balance of the organism is conveyed to the PVN by direct projections from the arcuate nucleus, which contains neurons that sense glucose, leptin and insulin levels (Woods et al., 1998).

Moreover, the PVN is heavily innervated by GABAergic neurons from the peri-PVN region, which provide a substantial tonic inhibition and in turn, they are targeted by different limbic areas such as the mPFC, the HF and the amygdala, thereby providing an important relay site to translate limbic information into modulation of the HPA response. Additionally, the PVN also receives massive input from other hypothalamic structures, such as the dorsomedial nucleus of the hypothalamus (DMH) and the medial preoptic area (mPOA), which send both GABAergic and glutamatergic projections to the PVN and therefore, depending on the balance between the two types of projections, they can either inhibit or activate the HPA axis (Roland and Sawchenko, 1993; Herman et al., 2003). Apart from being important in regulating the HPA response, the DMH also participates in the cardiovascular response to emotional stressors (Fontes et al., 2011).

Finally, a key telencephalic structure that sends abundant direct projections to the PVN is the BNST, which contains mainly GABAergic neurons and is one of the main relay stations of the corticolimbic circuit to the PVN (Cullinan et al., 1993; Dong and Swanson, 2004). The BNST is anatomically highly complex and the different subdivisions may play a very different role in regulating HPA activity. In this line, lesion to the posterior BNST enhances ACTH and corticosterone secretion after restraint, as well as c-fos and Crh expression in the PVN (Herman et al., 1994; Choi et al., 2007). This region receives glutamatergic projections from the ventral subiculum (vSUB) and infralimbic (IL) and prelimbic (PL) cortices, and GABAergic projections from the medial amygdala (MeA) (Cullinan et al., 1993; Canteras et al., 1995; Vertes, 2004), supporting the idea that this subdivision mainly inhibits the PVN. Conversely, lesions to the anterior division of the BNST inhibit HPA axis responses to acute psychogenic stress, which suggests an excitatory role for this region (Choi et al., 2007).

Indirect projections to the PVN

The regulation of emotional stress responses is controlled in a top-down manner by the integrated activation of different corticolimbic areas, such as the mPFC, the HF and the amygdala. These structures have little direct inputs into the PVN, but rather rely on a trans-synaptic mechanism of communication through intermediate synaptic relays (for a review see (Herman et al., 2003, 2005). Studies have shown that most of the relay neurons between the limbic system and PVN neurons are GABAergic, thereby representing an opportunity for tuning HPA axis activity through adjustment of the PVN inhibitory tone.

There is substantial evidence for the role of the HF in stress inhibition, both in rodent models and humans. Accordingly, the drive of hippocampal output neurons primarily inhibits HPA axis activation in response to stress, whereas lesions to this region increase reactivity to emotional or psychogenic (but not systemic) stressors (Herman et al., 1998). Herman and colleagues have shown that the regulation of the HPA axis response is mainly mediated by the vSUB, the main hippocampal output pathway. In this regard, lesions in the vSUB increase *Crh* expression levels in the PVN and enhance HPA axis response to restraint stress, without having effects on basal corticosterone secretion. Moreover, these lesions prolong HPA axis response following restraint or novelty, but not after ether inhalation (Herman et al., 1998; Mueller et al., 2004), collectively providing evidence that this modulatory function is specific to the stressor modality. Neuronal tracing studies indicate that glutamatergic neurons of the vSUB synapse into GABAergic neurons located in different PVN-projecting nuclei, such as the peri-PVN area, the posterior BNST, the DMH and other hypothalamic structures (Herman et al., 2005; Jankord and Herman, 2008). Therefore, this by-synaptic connection would translate the excitatory hippocampal output into inhibition of the PVN. Moreover, the vSUB also innervates several limbic forebrain structures (Herman and Mueller, 2006), indicating a more complex role in the regulation of stress response. Classically, the HF has also been postulated as an important site of feedback for GC inhibition of the HPA axis. It presents high levels of GR and MR and hence, it is well endowed for detecting a wide range of circulating GC levels and modulating negative feedback inhibition of the HPA axis (Reul and De Kloet, 1986; Jacobson and Sapolsky, 1991).

Another structure that participates in the regulation of the stress response is the amygdala. In this case, the existing literature suggests that the role of this brain region in HPA axis modulation is mainly excitatory. The principal output neurons related to this process are located in the medial (MeA) and central nuclei of the amygdala (CeA) and are predominantly GABAergic.

Both subdivisions are important for driving HPA axis responses, but studies indicate that they play a different role depending on the type of stressor. Thus, the MeA is activated by stressors such as restraint or forced swim, but not by systemic stimuli such as haemorrhage or administration of interleukin 1 beta (IL-1 β), whereas the latter stressors mainly activate the CeA (Dayas et al., 2001). Similar to the HF, the amygdala does not have direct projections to the PVN. Therefore, activation of the HPA axis by these nuclei is mediated by GABAergic output neurons which synapse onto GABAergic neurons of intermediate structures which in turn project directly to the PVN (Herman et al., 2003; Jankord and Herman, 2008). This circuit triggers trans-synaptic disinhibition, resulting in a net activation of the HPA axis response. The MeA projects to the posterior and medial divisions of the BNST, the mPOA and the peri-PVN region. Conversely, the CeA sends projections to the anterior and lateral divisions of the BNST, the DMH and the NTS (Herman et al., 2003; Jankord and Herman, 2008; Ulrich-Lai and Herman, 2009). Regarding other amygdala subdivisions, the basolateral amygdala (BLA) mainly sends glutamatergic projections to the CeA and MeA and thus, its role in regulating the HPA axis may be mediated in part by the coordination of the output from these two subdivisions (Jankord and Herman, 2008). However, the BLA also projects to the anterodorsal BNST and other nuclei which in turn project to the PVN, suggesting that it may interact with the PVN independently of the CeA and MeA. The role of the BLA in the regulation of the stress response is not clear. It has been proposed to participate in the response to emotional stressors, although lesions in this area do not appear to affect HPA response to acute stressors (Feldman et al., 1994). Instead, it seems that it is related to enhancing the HPA axis response to novel stressors after exposure to chronic stress (Bhatnagar et al., 2004).

The mPFC has been pointed out as a key centre for the processing of stressful information and the coordination of stress response (revised by McKlveen et al., 2015). Nevertheless, its role in the modulation of the HPA axis is very complex, which is one of the main reasons why we have focused on this brain region in this doctoral thesis. Based mainly on its differential connectivity with other brain areas, the PFC can be subdivided into the prelimbic cortex (PL) and the infralimbic cortex (IL) (Ongur and Price, 2000), which will be described in more detail in Section 3 of the introduction. Briefly, some studies suggest that the distinct subdivisions of the mPFC may differentially modulate the stress response, although other studies do not support this view. On the one hand, lesion studies in the rat PL have shown increased Crh mRNA levels in the PVN and increased HPA response after emotional stressors, without altering the response to systemic stressors (Diorio et al., 1993; Figueiredo et al., 2003; Radley et al., 2006).

Conversely, acute activation of the PL inhibits HPA response to emotional stressors (Jones et al., 2011). The role of the IL is less clear, in that lesions in this brain region seem to not affect the HPA axis response following exposure to emotional stressors (Radley et al., 2006), suggesting that this region does not inhibit the HPA axis response to emotional stimuli. Nevertheless, this topic will be discussed in further detail in the following section. Anatomical studies in rats have failed to demonstrate direct connections from the mPFC to the PVN (Hurley et al., 1991; Vertes, 2004), consistent with a trans-synaptic mechanism of action. The PL modulates the HPA axis response through glutamatergic projections to the posterior BNST, the paraventricular nucleus of the thalamus (PVTh) and the peri-PVN, thereby activating GABAergic neurons in these relay areas, which in turn inhibit the PVN. In contrast, the IL sends glutamatergic projections to the anterior BNST, the CeA, the NTS, the DMH and the lateral hypothalamus (LH; for a review see Herman et al., 2005; Ulrich-Lai and Herman, 2009). In summary, although the existing data is not consistent, the studies point towards a distinct role of the two mPFC subdivisions in the regulation of stress response.

Another brain region that participates in stressor processing and modulation of HPA axis response is the LS, especially its ventral region (LSv). Although the exact role of the LSv in stress response is not yet fully understood, it has been classically associated with an inhibitory influence on the HPA axis response to acute emotional stressors (Singewald et al., 2011). However, more recently an excitatory role has been proposed (Anthony et al., 2014). Most LS neurons are GABAergic and they do not project directly to the PVN but innervate the peri-PVN region and other hypothalamic relays such as the mPOA, the anterior hypothalamus and the LH. Notably, these PVN-projecting regions contain both glutamatergic and GABAergic neurons, ideally positioning the LS to either inhibit or activate the HPA axis response (for a review see Herman et al., 2003; Myers et al., 2014). Lesion studies in the LS have shown enhanced plasma ACTH and corticosterone levels and increased c-fos expression in the PVN in response to forced swim as well as more passive coping in this test. Interestingly, administration of a 5-HT_{1A} receptor antagonist in the LS enhances and prolongs stress-induced ACTH and corticosterone levels, while the administration of an antagonist reduces HPA axis activity and promotes more active coping strategies, suggesting that the role of the LS in the HPA axis response to stress is mediated at least in part by serotonergic receptors (Singewald et al., 2011). Moreover, tracing studies have shown that the inhibitory influence of the LS may be mediated by LS GABAergic neurons that synapse onto glutamatergic neurons of the posterior hypothalamus which project directly to the PVN and by interneurons of the LS that inhibit

LS GABAergic neurons which in turn project to PVN-projecting regions containing GABAergic neurons, such as the peri-PVN, the mPOA and the BNST (Singewald et al., 2011; Myers et al., 2014). However, Anthony and colleagues have shown that a subpopulation of neurons in the LS that express the type 2 CRH receptor and send GABAergic projections to the anterior hypothalamus enhance stress-induced neuroendocrine and behavioural changes. These last data agree with the positive correlation frequently observed between LS activation and the HPA axis response (Úbeda-Contreras et al., 2018).

Taken together, the data aforementioned indicate that the amygdala, the HF, the mPFC and the LS are likely to be involved in the regulation of the HPA response to stressors, with a differentiated and specialised role of specific subdivisions of these areas in conjunction with the particular characteristics of the stressors.

3. Prefrontal cortex and the stress response

The PFC is highly activated by stress and it has an important role in modulating the stress response at different levels. Based on the high complexity and large size of the primate frontal lobes it was previously considered that the PFC was unique to the primate species. However, this view has evolved over the years. Although it has been challenging to establish a functional homology between the human and the rodent PFC, and there is still a long-standing debate on this topic, based on common patterns of connectivity, anatomical and functional characteristics, as well as electrophysiological properties, a part of the frontal lobe of the rodent brain is now accepted to be the equivalent to the primate PFC (Uylings et al., 2003; Dalley et al., 2004).

The rat PFC is usually divided into three topologically different regions: the medial PFC (mPFC), the orbital or ventral PFC and the lateral PFC (Heidbreder and Groenewegen, 2003). In the last decades, studies of the effects of stress on the PFC in rodents have primarily focused on the mPFC, which is the region responsible for most of the executive functions of the PFC. Furthermore, most of the manipulation studies performed in the field of stress have also been conducted in this region, as will be detailed below. Therefore, the present thesis will be focused mainly on the mPFC.

3.1. Medial prefrontal cortex structure

The rat mPFC is usually divided into 4 different areas based on cytoarchitectonic and connectivity criteria, from dorsal to ventral: the medial precentral area (PrCm, also named Fr2), the anterior cingulate cortex (ACC), the PL and the IL (Seamans et al., 2008). It is generally assumed that some regions of the rodent PFC have their equivalents in humans. Focusing on the rodent mPFC, the PrCm and ACC would correspond to the dorsomedial PFC in humans. Although it has been difficult to establish which particular areas in the rat are homologous to the primate dorsolateral PFC (dlPFC), it has been shown that ACC and dorsal PL regions possess dorsolateral-like features. More specifically, the ACC, PL and IL are considered to be homologous in function and connectivity patterns to human Brodmann areas 24b, 32 and 25, respectively. Finally, the ventral PL, IL and medial orbital area, would correspond to the ventromedial PFC (Uylings et al., 2003; Gabbott et al., 2005; Seamans et al., 2008). In this thesis, we will mainly focus on the rat PL and IL subdivisions.

Regarding its cytoarchitectonic characteristics, the most prominent feature of the rat mPFC is that it consists exclusively of agranular cortex lacking layer IV, similar to the primate ACC, but different to the primate granular dlPFC (Fuster, 2008; Seamans et al., 2008). In the rodent mPFC, layer I contains mostly dendritic fibres and axons and some sparse inhibitory neurons, whereas superficial layers II/III and deep layers V and VI contain pyramidal neurons and different populations of interneurons (**Figure 3**; Anastasiades and Carter, 2021). Both superficial and deep layers receive afferent connections from cortical and subcortical regions and send efferent projections to other limbic structures. Furthermore, there are numerous interconnections between the different layers. Layer V receives strong input from layer VI cells and relatively weak input from layer III. In the human PFC, layer IV is the main target for integration of afferent projections (e.g. thalamic input with sensory information) with information from other cortical layers and forwards this information to output layer V. However, as rodents do not possess layer IV, the rodent mPFC lacks a clear information processing structure (Gabbott et al., 2005; Van Aerde and Feldmeyer, 2015).

The mPFC is comprised of glutamatergic pyramidal neurons, which represent approximately 80-85% of the neurons, and a local network of GABAergic interneurons that tightly regulate glutamatergic output and thus maintain an excitation/inhibition balance to ensure adequate mPFC functioning. There are different populations of GABAergic interneurons characterised by the expression of particular proteins, including

parvalbumin (the most abundant subtype), somatostatin (SST) and 5-HT3a receptor, which further includes the subtype expressing vasoactive intestinal polypeptide (VIP), among others (Somogyi et al., 1998; McKlveen et al., 2015).

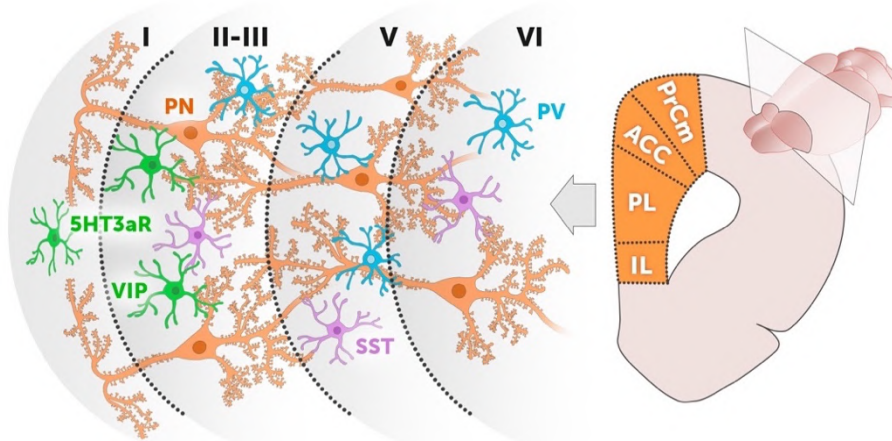


Figure 3. General organisation of the rat medial prefrontal cortex.

Left, schematic diagram of a coronal hemisection of the rat medial prefrontal cortex (mPFC) with the distribution of the subdivisions along the dorsoventral axis. Right, illustrative diagram of the different layers of the rodent mPFC with the main neuronal types located in each layer. Abbreviations: ACC, anterior cingulate cortex; IL, infralimbic; PL, prelimbic; PrCm, medial precentral area.

3.2. Medial prefrontal cortex functions

The PFC is one of the brain regions with the latest development both from a phylogenetic and an ontogenic point of view. Therefore, it has reached its maximum relative growth in humans and it is also the most evolved brain region in our species (Fuster, 2008). A large body of studies in rats, monkeys and humans have concluded that the PFC is highly involved in executive functioning, which comprises all the cognitive processes dedicated to the representation and execution of complex sequences of behaviour. These executive functions include attentional control, planning, attentional set-shifting, behavioural inhibition, behavioural flexibility and decision-making, among others (Heidbreder and Groenewegen, 2003; Dalley et al., 2004; Fuster, 2008). The organisation of these actions requires the representation of information not currently present in the environment, and this ability involves working memory (Goldman-Rakic, 1995). The PFC prevents representations from being affected by the interference of distractions, it inhibits inappropriate actions and promotes task-relevant actions and goal-directed behaviours (“top-down” regulation). Moreover, the PFC is also involved in the regulation of emotions, motivation and

autonomic control, and the behavioural and physiological stress responses (Heidbreder and Groenewegen, 2003; Uylings et al., 2003; Dalley et al., 2004; Fuster, 2008). Studies in primates and rodents have shown functional heterogeneity within the different subdivisions of the PFC regarding its role in different processes, such as addiction, fear memory and behavioural regulation (Heidbreder and Groenewegen, 2003). This functional specialisation will be further discussed in Section 3.5 in the context of stress.

The wide variety of functions carried out by the PFC relies closely on its wide connectivity with many different brain structures, namely the brainstem, the thalamus, the basal ganglia and the limbic system. Afferent connections from these brain regions convey information about the internal milieu of the animal, its drives and motives, and also transmit signals from the external environment, which is highly relevant for the integrative functions of the PFC (Fuster, 2008). In addition, its extensive efferent connections with many different brain structures position it well to coordinate and orchestrate behavioural and physiological responses.

3.3. Medial prefrontal cortex connectivity

The different mPFC subregions can also be differentiated, at least in part, based on distinct afferent and efferent projection patterns with cortical and subcortical structures. Moreover, there are relatively strong reciprocal interconnections between the different mPFC subdivisions (Heidbreder and Groenewegen, 2003; Vertes, 2004).

Efferent projections

Tracing studies in rats have shown that PL and IL regions project both to the orbitofrontal PFC (OFC), the ACC, the anterior piriform cortex, the perirhinal and entorhinal regions, the midline nuclei of the thalamus and the PAG. In general, however, they have largely separated patterns of projections. The PL projects to the agranular insular cortex, the claustrum, the piriform cortex, the core and shell of NAc, the paraventricular, mediodorsal and reuniens nuclei of the thalamus, the BLA, the ventral tegmental area (VTA), and the DRN and MRN of the brainstem (**Figure 4, top**). In contrast, the IL projects to the LS, the lateral BNST, the medial and lateral preoptic nucleus, the shell of the NAc, the medial, basomedial and central nuclei of the amygdala, the dorsomedial, lateral, perifornical, posterior and supramammillary nuclei of the hypothalamus and the parabrachial and NTS of the brainstem (**Figure 4, bottom**; Vertes, 2004). In summary, PL and IL regions have considerably differential brain projections, which could partially explain their distinct functions. Whereas PL predominantly projects to limbic regions associated with cognition, IL primarily targets autonomic and visceral-related sites.

Afferent projections

PL and IL regions receive inputs from other structures, and they are also strongly interconnected. The IL (and ventral PL) receive dense projections from the piriform cortex and the perirhinal and ventral agranular insular regions whereas the dorsal PL is innervated by the posterior agranular insular and retrosplenial cortex, as well as the secondary visual cortex. The HF (mainly the subiculum/CA1) densely projects to IL and PL, whereas there are no direct projections from the mPFC to the hippocampus. The amygdala also sends projections to the mPFC, predominantly from the basal amygdaloid complex and to a lesser extent from the lateral amygdala. Furthermore, the midline thalamus also sends dense projections to both PL and IL and it is believed to be a very important source of limbic information to the mPFC. Finally, while the IL is the target of some subcortical limbic structures that do not project heavily to other mPFC subdivisions (e.g. the LS, PAG and LH), the PL receives projections from other regions of the cortex, including the medial orbital and lateral cortex (for a review see Heidbreder and Groenewegen, 2003; Hoover and Vertes, 2007).

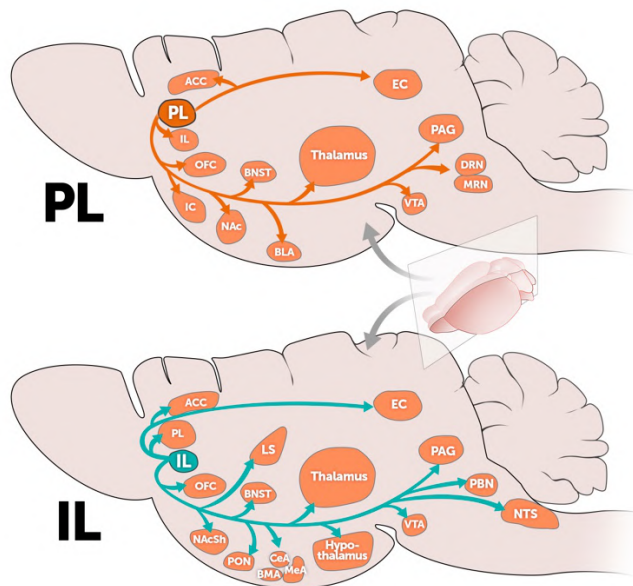


Figure 4. Schematic sagittal section summarising the main projections of the prelimbic (PL) and infralimbic (IL) cortices.

Sections have been adapted from the rat brain atlas of Paxinos and Watson (2014). For illustrative purposes, various planes have been collapsed into a single section. *Abbreviations:* ACC, anterior cingulate cortex; BLA, basolateral amygdala; BMA, basomedial amygdala; BNST, bed nucleus of the stria terminalis; CeA, central amygdala; DRN, dorsal raphe nucleus; EC, entorhinal cortex; IC, insular cortex; IL, infralimbic; LS, lateral septum; MeA, medial amygdala; MRN, medial raphe nucleus; NAc, nucleus accumbens; NAcSh, shell of the nucleus accumbens; NTS, nucleus of the solitary tract; OFC, orbitofrontal cortex; PAG, periaqueductal grey matter; PBN, parabrachial nucleus; PL, prelimbic; PON, preoptic nucleus; VTA, ventral tegmental area.

3.4. Effects of stress in the medial prefrontal cortex

In the last decades, a great deal of effort has been devoted to understanding the effects of acute and chronic stress on mPFC structure and function. There is now compelling evidence from human, monkey and rodent studies that exposure to uncontrollable acute and chronic stress impairs higher-order cognitive PFC functions (for a detailed review see Arnsten, 2015).

Acute restraint in rats impairs spatial delayed alternation task, a test that evaluates spatial working memory, which is dependent on mPFC (Shansky et al., 2006). Similar results have been observed in monkeys exposed to loud white noise (Arnsten and Goldman-Rakic, 1998) and in human subjects exposed to acute psychosocial stress, who show impairments in spatial working memory and attention (Olver et al., 2015). However, Yuen et al. (2011) showed that acute stress (20 min forced swim) enhanced working memory in the T-maze measured at 4h and 1 day after stress in prepubertal rats (3-4 weeks old). The apparent inconsistency with the results reported by others (e.g. Murphy et al., 1996) may be partly explained by two reasons. Firstly, the experimental subjects were prepubertal rats and the effects might be different from those observed in adults. Secondly, they used a milder stressor compared to previous reports using more severe acute stressors or pharmacological treatments. It might be that the effects of stress follow an inverted U-shaped curve, in which too little or too much GC activity or noradrenaline or dopamine levels can have negative effects on cognitive processes. Furthermore, the time between stress and testing usually differs between studies, and this could also affect the behavioural consequences of stress exposure. Finally, the vast majority of this research has been conducted exclusively on male animals. In this respect, Shansky et al. (2006) showed that proestrus females (high levels of estrogens) are more sensitive to the effects of acute restraint stress in a working memory test than males and estrus females (bearing low levels of estrogens).

At the neurochemical level, most studies indicate that acute stress increases the glutamatergic output of the mPFC (Moghaddam, 1993; see revision by (Sanacora et al., 2022)). Acute footshock stress in rats up-regulates glutamate release via a GR-dependent mechanism in the PFC, thereby increasing extracellular glutamate levels (Musazzi et al., 2010). Moreover, the number of docked vesicles in the synapse is up-regulated immediately after footshock exposure (Nava et al., 2015), consistent with a stress-mediated presynaptic structural plasticity. Moreover, Yuen and colleagues (2011) demonstrated in prepubertal rats that acute forced swim increased surface levels of AMPA and NMDA receptors in mPFC neurons. Overall, these results provide evidence for enhanced glutamatergic neurotransmission through pre- and postsynaptic mechanisms in the mPFC after acute stress.

Furthermore, exposure to acute uncontrollable stress also increases the release of the catecholamines NA and dopamine (DA) in the PFC, and high levels of catecholamine release induced by stress seem to be one of the underlying mechanisms of PFC functional impairment (revised by Moghaddam and Jackson, 2004; Arnsten, 2009). Both DA and NA have an inverted U-shaped influence on PFC functioning. Thus, NA levels released during alert enhance working memory by binding the high-affinity adrenergic α_2 receptors, whereas high levels released during a stressful situation impair PFC function by binding the low-affinity adrenergic receptors (α_1 and β_1). In parallel, high levels of DA cause high D1 receptor stimulation, which impairs working memory processes (see revision by Arnsten, 2009). Similarly, some studies have reported increased serotonin (5-hydroxytryptamine, 5-HT) efflux in the mPFC after exposure to inescapable shock (Bland et al., 2003), whereas others have shown decreased 5-HT outflow after other stressors, such as forced swim or saline injection (Adell et al., 1997), suggesting that the release of 5-HT in the mPFC seems to be dependent on the type of stress.

Although the consequences of acute stress on PFC functions are important to consider, exposure to chronic stress seems to have more negative effects on PFC functioning. Remarkably, these deficits in PFC functions driven by chronic stress usually correlate with structural changes in the PFC. Liston et al. (2006) showed that 3 weeks of chronic restraint stress (CRS) induced a selective impairment in an attentional set-shifting, a mPFC-mediated process. The same authors studied the effects of chronic stress in humans and reported that adults exposed to 1 month of psychosocial stress had impaired attentional control in an attention-shifting paradigm and altered functional magnetic resonance (fMRI) measures of PFC function (Liston et al., 2009). Regarding data in rodents, Cerqueira and colleagues (2007) have shown that rats exposed to 4 weeks of chronic unpredictable stress (CUS) had impaired working memory and behavioural flexibility, and these alterations were accompanied by a reduced thickness of layers I/II of the mPFC. Furthermore, Yuen and collaborators (2012) showed in rats that 1 week of repeated restraint stress impaired temporal order recognition memory, a PFC-dependent process, with a concomitant reduction of AMPAR- and NMDAR-dependent synaptic transmission and expression levels of these receptors in the PFC. Interestingly, they showed that these effects were dependent on the activation of GR.

Converging lines of evidence from rodent studies demonstrate that chronic stressors (e.g. 3 weeks of CRS) markedly reduce the apical dendritic length and branching in pyramidal neurons of layers II-III of the ACC and PL regions (Cook and Wellman, 2004; Radley et al., 2005; Liston et al., 2006).

These changes, as previously discussed, are associated with impaired attentional set-shifting performance (Liston et al., 2006). However, this altered dendritic remodelling has been shown to be reversible if animals are allowed to recover for another 3 weeks after CRS (Radley et al., 2005). Later studies in the same neuronal type and brain region have further demonstrated that CRS decrease average dendritic spine volume and surface, most markedly in the distal portion of apical dendrites (Radley et al., 2008; Goldwater et al., 2009). Apical dendritic retraction and dendritic spine loss have also been reported in pyramidal neurons of layer V of the IL after CRS (Goldwater et al., 2009). Finally, alteration of inhibitory networks in the mPFC has also been described after chronic stress in rats. Gilbert-Juan and colleagues (2013) found that 3 weeks of CRS induces dendritic hypertrophy in a subtype of interneurons, Martinotti cells, and reduces the number of glutamate decarboxylase enzyme, 67 kDa isoform (GAD67)-expressing neurons.

Together, these findings indicate that the morphology of mPFC neurons is exquisitely sensitive to stress and that these stress-induced architectural changes may underlie the cognitive deficits observed after stress exposure and may impair the ability of the PFC to properly regulate the behavioural and neuroendocrine response to stress. Therefore, stress-induced PFC morphological and functional changes may partially contribute to many stress-related mental illnesses, such as post-traumatic stress disorder or depression.

3.5. Role of the medial prefrontal cortex in the stress response

Apart from being greatly affected by stress, the mPFC is perfectly positioned to orchestrate the stress response, since it receives sensorial, subcortical and neuroendocrine inputs and sends projections to several limbic diencephalic and brainstem centres (Vertes, 2004). Therefore, it can modulate behavioural, autonomic and neuroendocrine functions in response to challenges. However, studies examining the effects of mPFC manipulation in stress (e.g. lesioning and pharmacological studies) have yielded inconsistent and even contradictory findings. Before delving into this topic, a summary of the methodologies most commonly used for mPFC manipulation will be briefly discussed.

Manipulation techniques used to study mPFC function

Earliest studies mainly used lesioning (e.g. thermal lesion, ibotenic acid injections) and electrical stimulation methodologies for manipulating brain regions. Although they have provided useful insights, these methodologies can only either inactivate or activate, respectively, brain areas of interest,

lacking cell-type specificity and in the case of lesioning, being irreversible. In contrast, pharmacological approaches based on the local infusion of drugs in target brain regions allow good spatial resolution, and relative cellular specificity (e.g. agonists/antagonists of specific neurotransmitter receptors) and they can reversibly activate or inhibit neuronal activity (Russell and Shipston, 2015). However, novel technologies developed in recent years such as optogenetics and chemogenetics provide more precise control of activity in genetically-defined neuronal populations of target brain regions, allowing researchers to elucidate the causal role of specific neural circuits in different behaviours, such as aggression (Lin et al., 2011a) or drug addiction processes (Bossert et al., 2011) (for a review see Cassataro and Sjulson, 2015). Both technologies are based on the use of viral vector expression systems to deliver transgenes into specific brain regions: light-sensitive ion channels (opsins) in the case of optogenetics, and designer receptors exclusively activated by designer drugs (DREADDs) in the case of chemogenetics.

With optogenetics, neurons can be either activated (with channelrhodopsin) or silenced (with halorhodopsin) by using light pulses of specific wavelengths for each opsin in a millisecond time scale (Deisseroth, 2011). In the case of chemogenetics, DREADDs are modified muscarinic G-protein coupled receptors that have a low affinity for their native ligand acetylcholine, but a very high affinity for the synthetic ligand clozapine-N-oxide (CNO), which can be administered systemically (e.g. by intraperitoneal injection, i.p.), via drinking water or food, or locally within the brain. Depending on the type of G protein to which they are coupled, (Gq for hM3Dq and Gi for hM4Di), CNO can either depolarize neurons and induce neuronal activation (hM3Dq) or hyperpolarize and transiently silence neurons (hM4Di) (Rogan and Roth, 2011; Urban and Roth, 2015). Remarkably, these technologies provide high cell-type specificity thanks to the use of cell-type-specific promoters or Cre-inducible viral vectors injected into transgenic Cre animals. Furthermore, they have a high temporal precision, particularly optogenetics.

All the experimental manipulations abovementioned have been fundamental for increasing our understanding of the function of mPFC neurons in the stress response. Nevertheless, the recent major methodological advances have allowed researchers to selectively manipulate specific cell types in defined brain regions and elucidate more precisely their role in different brain processes. In the following section we will summarise the major findings regarding the effects of mPFC manipulation on the stress response, and for the sake of clarity, we will divide them into 1) neuroendocrine, 2) autonomic and 3) behavioural. We will attempt to refer

to specific mPFC subdivisions in studies where they were specifically manipulated. Nevertheless, many studies, especially in the older literature, used generic terms such as “mPFC”, and in this case, we will describe it faithfully to the original source.

mPFC role in the neuroendocrine stress response

Regarding the role of the mPFC in the neuroendocrine response to stress, early studies focused on mPFC lesioning and pointed towards an inhibitory influence of the mPFC in the HPA response to psychological stressors. Thus, mPFC lesions in rats (involving ACC, PL and in some cases also IL) resulted in greater plasma ACTH and corticosterone responses to psychological stressors (e.g. acute restraint), with no changes in basal ACTH and corticosterone levels (Diorio et al., 1993; Figueiredo et al., 2003). Interestingly, these changes were not observed after exposure to a systemic stressor such as ether. Increased c-fos expression in the PVN of restrained, but not in ether-exposed rats, was also observed (Figueiredo et al., 2003), suggesting that the mPFC may differentially modulate the stress response depending on the type of stressor. Other authors, however, found that right or bilateral lesions of the mPFC with ibotenic acid suppressed HPA activity in basal conditions and tended to attenuate HPA response to acute restraint, whereas in repeatedly restrained rats there was a marked reduction in the peak corticosterone response to stress (Sullivan and Gratton, 1999).

In contrast to the previous studies, other experiments have reported non or subtle effects of mPFC neurotoxic or electrolytic lesions on the HPA hormonal response to psychological stressors. Crane and colleagues (2003) found that electrolytic lesions of the mPFC did not affect ACTH response to white noise while increased ACTH response to systemic interleukin-1 , which is opposite to the findings described above. The authors postulated that instead of depending on the stressor category (physical vs psychological), stressor intensity might be the critical factor. In Diorio et al. (1993), response to restraint was milder than to ether, while Crane et al. (2003) obtained a milder response with the injection of interleukin-1 than with noise. Crane and colleagues argued that the mPFC could be considered to have a high-pass filter function, decreasing responses to mild stressors but permitting severe stressors to evoke an adequate response. Similarly, Spencer et al. (2005) also found that mPFC lesion did not change ACTH response to air puff, although it increased the number of activated CRH cells in the mpPVN in response to this emotional stressor.

Radley and colleagues (2006) extended the previous findings in a pivotal study in which they compared the effects of lesioning dorsal versus ventral subdivisions of the mPFC in adult male rats. The dmPFC mainly comprised ACC and dorsal PL, while the vmPFC encompassed the ventral PL and the

whole IL. They showed that dmPFC lesions markedly enhanced ACTH response to acute restraint and also Fos and CRH expression in the PVN, whereas vmPFC lesions attenuated ACTH response and mildly reduced CRH expression in the PVN. This provided evidence for a differential role of dmPFC and vmPFC in the neuroendocrine response to emotional stressors. They further complemented these findings by showing that the inhibitory influence of the PFC in the HPA response to acute restraint could be mediated, at least in part, by a GABAergic relay station in the anterior BNST (Radley et al., 2009). Nevertheless, later studies have shown that silencing glutamatergic neurons (knockdown of the vesicular glutamatergic transporter 1, vGluT1) in the IL of male rats enhanced ACTH and corticosterone secretion after restraint and increased Crh mRNA levels in the PVN, indicating that IL glutamate output may also inhibit the HPA response to acute emotional stress (Myers et al., 2017b).

Complementarily, stimulation experiments by Jones and colleagues (2011) have shown that activation of the PL by the GABA receptor antagonist bicuculline greatly reduced ACTH and corticosterone responses to restraint as well as Fos activation in PVN neurons. Bicuculline administration in the PL did not change ACTH response to hypoxia but significantly enhanced corticosterone response, and the authors claim that it could be due to an increase of ACTH sensitivity of the adrenal gland mediated by an enhancement of sympathetic nervous system activation. Importantly, previous studies had shown that PL lesions do not affect responses to physical stressors such as ether inhalation (Diorio et al., 1993; Figueiredo et al., 2003). This would indicate that PL activation might be sufficient to drive neuroendocrine responses to hypoxia, but may not be necessary for these responses to occur. Therefore, these data suggest that PL stimulation may inhibit the HPA axis response to psychogenic stress but it could enhance the response to systemic stressors (Jones et al., 2011).

Recent studies have used more sophisticated methodologies for manipulating restricted mPFC subdivisions and specific projections to other brain regions. For instance, Johnson et al. (2019) used an optogenetic approach to specifically manipulate projections from the rostral PL to the anteroventral BNST (avBNST). They showed that optogenetic inhibition of PL – avBNST projections in adult male rats increases ACTH and corticosterone response to the tail suspension test (TST), whereas activation of these projections does not change the stress-induced hormonal response, pointing towards a tonic inhibitory role for PL in restraining HPA response to an inescapable stressor. A detailed summary of the effects of mPFC manipulations on the neuroendocrine stress response is shown in **Table 1**.

Table 1. Summary of studies of mPFC manipulation and effects in the neuroendocrine response to stress.

Region	Manipulation method	Model/ strain	Stressor	Type of measurement	Effects	Reference
mPFC	Thermal lesion	LE rats	Acute restraint and ether	Plasma ACTH and CORT	= ACTH and CORT basal = peak levels ACTH and CORT, ↑ ACTH and CORT in the post-stress period after restraint = ACTH and CORT after ether	<i>Diorio et al., 1993</i>
mPFC	Excitotoxic lesion (ibotenic acid)	SD rats	Acute and repeated restraint	Plasma ACTH and CORT	↓ CORT basal levels after bilateral/right lesions Trend to ↓ CORT after restraint ↓ CORT after repeated restraint with bilateral/right lesions	<i>Sullivan and Gratton, 1999</i>
PL + IL	Electrolytic lesion	Wistar rats	Acute white noise and systemic delivery of IL-1β	Plasma ACTH Retrograde tracing and Fos immunostaining	= ACTH basal levels = ACTH after white noise ↑ ACTH and ↓ Fos+ cells in ventral BNST after IL-1β	<i>Crane et al., 2003</i>
PL mainly (some IL and ACC)	Excitotoxic lesion (ibotenic acid)	SD rats	Acute restraint and ether	Plasma ACTH and CORT	= ACTH and CORT basal levels ↑ ACTH and CORT after restraint = ACTH and CORT after ether	<i>Figueiredo et al., 2003</i>
PL + IL	Excitotoxic lesion (ibotenic acid)	Wistar rats	Acute air puff	Plasma ACTH Fos immunostaining	= ACTH basal levels Trend to ↑ ACTH and ↑ Fos+ cells in mpdPVN after air puff	<i>Spencer et al., 2005</i>
PL vs IL	Excitotoxic lesion (ibotenic acid)	SD rats	Acute restraint	Plasma ACTH and CORT ISH <i>Crh</i> Fos IF	PL: ↑ ACTH and CORT, ↑ Fos and CRH mRNA in mpdPVN IL: = ACTH and CORT (but trend to ↓ CORT), ↑ Fos in preautonomic PVN	<i>Radley et al., 2006</i>
ACC + PL	Excitotoxic lesion (ibotenic acid)	SD rats	Acute restraint	Fos IF + fluorogold retrograde labelling	↑ Fos+ cells in the PVN and ↓ Fos+/fluorogold+ cells in the anterior BNST	<i>Radley et al., 2009</i>
PL	Pharmacological stimulation (GABA antagonist bicuculline)	SD rats	Acute restraint and hypoxia	Plasma ACTH and CORT Fos immunostaining	= ACTH and CORT basal levels ↓ ACTH and CORT, ↓ Fos+ cells in the dpPVN after restraint = ACTH and ↑ CORT, ↑ Fos in mpPVN after hypoxia	<i>Jones et al., 2011</i>
PL vs IL	shRNA GR knockdown	SD rats	CUS and acute open field test	Plasma CORT	↑ CORT at 60 min for PL GR knockdown in naïve rats, but ↓ CORT at 60 min in rats previously exposed to CUS ↑ CORT at 30 min for IL GR knockdown in naïve and CUS rats	<i>McKlveen et al., 2013</i>
IL	siRNA vGluT1 knockdown	SD rats	CUS and acute restraint	Plasma ACTH and CORT ISH <i>Crh</i>	↑ ACTH at 15 and 30 min and ↑ CORT at 60 min after initiation of restraint ↑ <i>Crh</i> mRNA in PVN after acute restraint	<i>Myers et al., 2017b</i>
PL	Optogenetic stimulation and inhibition of PL CaMKII neurons projecting to avBNST	SD rats	TST	Plasma ACTH and CORT	PL → avBNST stimulation: = ACTH and CORT levels PL → avBNST inhibition: ↑ ACTH at 10 min and ↑ CORT at 30 min after initiation of TST	<i>Johnson et al., 2019</i>

References are ordered in chronological order. *Abbreviations:* ACC, anterior cingulate cortex; ACTH, adrenocorticotrophic hormone; BNST, bed nucleus of the stria terminalis; CaMKII, Calcium/calmodulin-dependent protein kinase II; CORT, corticosterone; CUS, chronic unpredictable stress; GR, glucocorticoid receptor; IF, immunofluorescence; IL, infralimbic cortex; IL-1β, interleukin 1β; ISH, in situ hybridisation; LE, Long Evans; mpdPVN, medial parvocellular dorsal paraventricular nucleus of the hypothalamus; mPFC, medial prefrontal cortex; PL, prelimbic cortex; PVN, paraventricular nucleus of the hypothalamus; SD, Sprague Dawley; siRNA, small interference RNA; TST, tail suspension test; vGluT1, vesicular glutamatergic transporter 1.

mPFC role in the autonomic stress response

In contrast to the large number of studies evaluating the consequences of mPFC manipulation in the neuroendocrine stress response, only a few have investigated its impact on the autonomic response. Initial studies showed that lesions of the vmPFC with the neurotoxin NMDA reduced the sympathetic tachycardia induced by fear conditioning (FC) in male rats (Frysztak and Neafsey, 1994). Later studies investigated whether mPFC subdivisions could play a differential role in regulating the cardiovascular response to acute restraint stress in rats. Tavares et al. (2009) showed that pharmacological inhibition of the PL increased heart rate during restraint whereas inactivation of IL decreased heart rate. Hence, PL and IL may have different influences on the cardiovascular response to emotional stress. Accordingly, Fassini et al. (2016) demonstrated that rat PL stimulation with bicuculline reduced mean arterial pressure and heart rate in response to restraint, without having any effect on these parameters in basal conditions. Regarding respiratory response, Bondarenko and colleagues (2014) showed PL inhibition with muscimol markedly reduced the respiratory rate in response to various stressors (novel environment, 30 s of intense light and restraint) in male rats.

Recent works using more refined tools have evaluated in more detail different parameters of the stress-induced cardiovascular response. Schaeuble and colleagues (2019) knocked down vGluT1 in the IL cortex with a small interference RNA (siRNA) and studied cardiovascular response to acute restraint in rats previously unstressed (controls) or exposed to chronic variable or unpredictable stress (CUS) for 14 days. Both IL vGluT1 inactivation and previous CUS exposure increased heart rate in response to acute restraint, but the combination of both factors had a more marked increase. This would be at odds with the results of Tavares and colleagues (2009), but the discrepancies could be due to the different manipulation methods (e.g. pharmacological non-specific inhibition vs specifically down-regulating vGluT1). Furthermore, vGluT1 siRNA rose mean arterial pressure in response to restraint in control and previously stressed rats. In a second cohort of rats, which were exposed to CUS or remained unstressed, CUS and vGluT1 knockdown interacted to induce vascular endothelial dysfunction (e.g. impaired vasoconstriction and altered vascular histology). Hence, IL glutamatergic neurons seem to be mainly involved in preventing some cardiovascular consequences to acute and chronic stress.

mPFC role in the behavioural stress response

Numerous studies have been conducted in rodents to evaluate the consequences of activating or inhibiting the mPFC in the behavioural

response to different unconditioned and conditioned stress-related paradigms. There are discordant findings between the different studies, which will be discussed in detail below (**Tables 2 and 3**).

Early work such as the lesioning studies of Jinks and McGregor (1997) showed that electrolytic lesions restricted to the PL or the IL reduced time spent in the open field (OF) centre and in the open arms of the elevated plus maze (EPM), suggesting that both subdivisions play a similar role in reducing anxiety-like behaviour. However, Lacroix et al. (2000) reported that excitotoxic lesions comprising the whole mPFC increased the number of entries and time spent in the centre of the OF and the time in the open arms of the EPM, suggesting an anxiogenic role for the mPFC. Apart from having effects in unconditioned anxiety-related paradigms, mPFC lesions increased freezing in response to contextual cues in a fear conditioning task. Therefore, their results pointed towards decreased anxiety but increased fear conditioning after mPFC lesions. This anxiogenic role of the mPFC is supported by Shah and colleagues (2003; 2004), who showed that pharmacological inactivation of the mPFC induces anxiolytic effects in both the EPM and in the shock probe burying (SPB) test, in which the time burying the probe reflects anxiety-like behaviour. The authors further complemented these findings by separately inhibiting the dmPFC and the vmPFC (Shah and Treit, 2004). They found that inactivating both mPFC subdivisions had the same anxiety-reducing effects, further supporting their previous results. In line with this, Bi and colleagues (2013) reported that pharmacological activation of the IL decreased time spent in the centre of the OF and in the open arms of the EPM, and increased latency to eat in the novelty-suppressed feeding (NSF) test, whereas IL inactivation had the opposite effects. These findings also pointed towards an anxiogenic role for the IL region, but the authors found no differences in any of the parameters abovementioned after PL manipulation, suggesting a differential role for both mPFC subdivisions. Furthermore, Hamani et al. (2010) reported that deep brain stimulation (DBS) of the rat vmPFC resulted in reduced immobility and increased swimming during forced swim, as well as decreased latency to eat in the NSF test, suggesting increased active coping and reduced anxiety-like behaviour, respectively. There were no changes in the OF. Accordingly, Jiménez-Sánchez and colleagues (2016) showed decreased immobility in the forced swim test (FST) and latency to feed in the NSF, accompanied by increased glutamate, serotonin, DA and NA release in the IL after DBS of this subdivision. No effects were observed in the FST after DBS of the PL, although glutamate, DA and NA release was reduced.

Later studies with more sophisticated techniques have also shed light on the role of different neuronal populations of the mPFC. Optogenetic stimulation of PL layer V pyramidal neurons in male mice reduced anxiety-like behaviour in the OF and decreased immobility in the FST (Kumar et al., 2013). Furthermore, in chronically stressed mice it also decreased anxiety-like behaviour in the EPM. Similarly, Son and his colleagues (2018) also reported reduced immobility in the TST after mPFC glutamatergic stimulation in rats. Fuchikami and colleagues (2015) complemented these previous findings by optogenetically stimulating glutamatergic neurons specifically in the PL and the IL. While they did not observe any effects in the FST, NSF test and sucrose preference after PL activation, following IL stimulation they found a significant reduction in immobility in the FST, decreased latency to eat in the NSF test and increased sucrose preference, suggesting an anxiolytic-like and anti-depressant like effect of IL activation.

In parallel, chemogenetic manipulations have contributed to a better understanding of the role of mPFC in the behavioural stress response. Perova and collaborators (2015) evaluated the consequences of inhibiting parvalbumin (PV) interneurons in the PL of mice using DREADDs after exposing them to inescapable and uncontrollable footshocks (learned helplessness paradigm, LHp). PV chemogenetic inhibition during the LHp increased escape latency and number of failures in a shuttle-box testing 24h after, suggesting enhanced susceptibility to LHp. This phenotype was not caused by nonspecific locomotor effects, as PV inhibition did not affect the distance travelled in the OF. Furthermore, Page et al. (2019) analysed the effects of acute and chronic chemogenetic activation of PV neurons in the whole mPFC of male and female mice. They observed that acute PV activation did not have any effect in the OF, but chronic PV activation during 21 days reduced the distance travelled in the OF centre and increased the latency to eat in the NSF test, only in females. Therefore, these findings indicate that chronic activation of PV mPFC neurons elicits anxiogenic-like effects specifically in females. Interestingly, Soumier and Sibille (2014) studied the effects of inhibiting another GABAergic interneuron population, SST-expressing neurons, in the mouse ventral ACC and PL. Acute chemogenetic inhibition of SST neurons in stress-naïve animals reduced time spent in the OF centre and open arms of the EPM and increased latency to eat in the NSF test. Conversely, chronic inhibition or chemical ablation of these neurons both in stress-naïve and CUMS-exposed animals increased time and entries in the open arms of the EPM, pointing towards opposite effects of acute versus chronic blockade of dmPFC SST neurons.

The discrepancies between the studies previously mentioned (i.e. similar vs differential role of PL and IL subdivisions, anxiogenic vs anxiolytic role) could be explained by the existence of distinct neuronal populations in the mPFC differentially regulating the stress response which are not segregated anatomically in mPFC subdivisions but form functionally differentiated circuits that are spatially intermingled. This hypothesis is supported by a pioneering study by the Tye lab reporting that optogenetic stimulation of glutamatergic neurons from the whole mPFC did not induce any changes either in the OF or the FST, whereas the specific activation of those mPFC neurons projecting to the DRN robustly increased active coping in the FST (Warden et al., 2012). Conversely, optogenetic stimulation of mPFC neurons projecting to the lateral habenula (LHb) reduced mobility during the FST. Similarly, Chen et al. (2021) have recently shown that optogenetic stimulation of CaMKII (Calcium/calmodulin-dependent protein kinase II) neurons from the IL that project to the LS induces opposite effects in the OF and EPM (anxiogenic-like effect) to the activation of IL neurons projecting to the CeA (anxiolytic-like behaviour). Notably, they found the same pattern with optogenetic and chemogenetic manipulations. Hence, these key studies have provided solid evidence that different and even opposite behaviours can be mediated by subpopulations of mPFC neurons defined by their specific projection targets.

The work from Steven Maier's lab has focused on the role of the mPFC in the consequences of exposure to controllable vs uncontrollable stress (learned helplessness paradigm). Briefly, the classical design (Weiss, 1972) involves three groups: the MASTER, exposed to controllable stress (CTS), in which animals can escape or avoid the shock performing a particular behaviour; YOKED, exposed to uncontrollable stress (UTS), in which animals receive shocks depending on the behaviour of MASTER animals and independently of their own behaviour and CONTROL, exposed to the same context without receiving shocks. Amat and colleagues (2005) provided clear evidence that vmPFC functioning is fundamental for the positive effects of behavioural control over the consequences of stress. They temporarily inactivated the vmPFC and observed that, in contrast to rats with normal vmPFC activity, vmPFC-inactivated rats previously exposed to CTS had exaggerated fear conditioning and impaired escape learning accompanied by a robust DRN activation, similar to rats exposed to UTS. In later studies, they used the opposite strategy, activating the vmPFC during UTS (Amat et al., 2008). This manipulation abolished escape learning deficits and reduced fear responses, suggesting that vmPFC activation during UTS prevented its negative behavioural consequences, mimicking the effects of CTS. Altogether, these pivotal studies indicate a critical role of vmPFC in modulating the impact of behavioural control over stress.

Finally, several studies in rodents have also shown that mPFC has an important role in the regulation of fear conditioning. Stimulation and inhibition/lesion studies in rodents have shown that the PL cortex is involved in promoting the expression of conditioned fear responses, while the IL cortex plays a role in fear extinction (Sierra-Mercado et al., 2006; Vidal-Gonzalez et al., 2006, and for a detailed review Giustino and Maren, 2015). Therefore, it is generally considered that the two mPFC subdivisions have a functional dichotomy in fear modulation, which could be explained in part by their different connections with other brain regions involved in fear (e.g. the amygdala). PL would be more biased towards fear expression and IL towards fear suppression. However, there are still some discrepancies and the precise contribution of each subdivision is not yet fully understood (Giustino and Maren, 2015).

All these studies clearly indicate that the mPFC is involved in the modulation of the behavioural response to stress. However, there are considerable discrepancies in the results obtained, as some studies report opposite functions of PL and IL, while others find increased anxiety-like behaviours whereas others report decreased anxiety or no effects after mPFC manipulation. Similarly, studies of the role of mPFC in the regulation of the neuroendocrine and autonomic stress response have also yielded inconsistent findings.

Several explanations could account for these divergences. First and foremost, the broad nature of mPFC lesions and the large differences in lesioning methods, lesion size and placement, and the type of manipulation protocols. Furthermore, many of the studies involve physically lesioning or injecting neurotoxins that can affect non-specifically all cell types in the mPFC regardless of their phenotype (e.g. excitatory or inhibitory neurons, glial networks) and in the case of lesioning techniques (e.g. electrolytic lesion), they can destroy fibres of passage and connections. Additionally, techniques such as ibotenic acid injections commonly result in significant gliosis and imply a considerable loss of tissue, which can greatly affect the consequences observed in behaviour (Shah and Treit, 2003; Hamani et al., 2010). Moreover, chronic implantation of foreign objects in the brain (e.g. microelectrode or cannulas) can induce inflammatory responses, mediated primarily by astrocytes and microglia activation (e.g. Szarowski et al., 2003). Furthermore, neuronal phenotype and specific projection patterns to other brain regions may be a clear determinant of behavioural function and therefore, non-specific manipulation of a brain area could drastically hamper an adequate interpretation of the results. Finally, the inconsistent pattern of results on stress-related behavioural paradigms is further complicated by a possible role of mPFC in behaviours such as general

activity, motivation and mnemonic processes, factors which might greatly contribute to the behaviour observed in stress-related tests not related to stress itself.

Nevertheless, despite the inconsistencies in these studies, they have been fundamental to improving our understanding and set the basis for further and more sophisticated studies examining the role of mPFC in stress responses. Further investigation is required to ascertain the contribution of different mPFC neuronal populations to the regulation of the physiological and behavioural response to stress.

Table 2. Summary of studies investigating the effects of mPFC manipulation in the behavioural response to stress.

Lesion and pharmacological manipulation studies

Region	Manipulation method	Strain	Stressor	Tests	Effects	Reference
PL	Electrolytic lesion	Wistar rats	Naïve	OF, EPM, SPB	= distance and time in the centre of the OF, ↑ time and entries in the OA of the EPM, = time burying the shock probe	<i>Maaswinkel et al., 1996</i>
PL vs IL	Electrolytic lesion	Wistar rats	Naïve	OF, EPM	PL: = distance but ↓ time in OF centre and ↓ time in the OA of EPM IL: ↓ distance and time in OF centre and ↓ time in the OA of EPM	<i>Jinks and McGregor, 1997</i>
mPFC	Excitotoxic lesion (NMDA)	Wistar rats	Naïve	OF, EPM, food hoarding	↑ total distance and ↑ entries and time in the centre of the OF, = EPM, ↓ food eaten in food hoarding test.	<i>Lacroix et al., 1998</i>
mPFC vs IPFC	Excitotoxic lesion (ibotenic acid)	Wistar rats	Naïve	OF, EPM, CFC and re-expo to fear context	mPFC: ↑ entries and time in OF centre, ↑ time in the OA of EPM and ↑ freezing to contextual cues IPFC: = OF and EPM but ↑ freezing to contextual cues	<i>Lacroix et al., 2000</i>
mPFC	Excitotoxic lesion (ibotenic acid)	SD rats	Naïve	EPM, SI, SPB	↑ time and entries in the OA of EPM, ↑ time in 1st session of social interaction and ↓ time burying the shock probe	<i>Shah and Treit, 2003</i>
mPFC	Pharmacological inactivation (GABA agonist muscimol)	SD rats	Naïve	EPM, SPB	↑ time and entries in the OA of EPM, ↓ time burying the shock probe	<i>Shah et al., 2004</i>
dmPFC vs vmPFC	Pharmacological inactivation (benzodiazepine midazolam)	SD rats	Naïve	EPM, SPB	dmPFC and vmPFC: ↑ time and entries in the OA of EPM and ↓ time burying shock probe but a trend to ↑ immobility in SBP test	<i>Shah and Treit, 2004</i>
vmPFC	Pharmacological inactivation (muscimol)	SD rats	CS and US	CFC, escape learning	↑ CFC in CS rats and impaired escape learning in CS rats ↑ 5-HT efflux and Fos levels in DRN of CS rats comparable to US rats	<i>Amat et al., 2005</i>
vmPFC	Pharmacological activation (GABA antagonist picrotoxin)	SD rats	CS and US	CFC, escape learning	↓ CFC and reduced escape latency in US rats, mimicking CS effects ↓ 5-HT efflux in DRN of US rats	<i>Amat et al., 2008</i>
vmPFC	Deep brain stimulation	SD rats	Naïve	OF, FST, NSF, LHp	= distance OF, ↓ immobility and ↑ swimming in the FST, ↓ latency to eat in NSF, = latency in LHp	<i>Hamani et al., 2010</i>
PL	Pharmacological inactivation (cobalt)	Wistar rats	Naïve	EPM	↑ time and entries in the OA of EPM	<i>Stern et al., 2010</i>
vmPFC	Deep brain stimulation	Wistar rats	CUS	SPT	↑ sucrose preference after CUS, reversing anhedonic-like behaviour	<i>Hamani et al., 2012</i>
PL vs IL	Pharmacological activation (bicuculline) Pharmacological inactivation (AMPA antagonist CNQX, NMDAR antagonist AP5)	C57BL/6J mice	Naïve	OF, EPM, NSF	IL activation: ↓ time in OF centre, ↓ time in the OA of the EPM and ↑ time in CA, ↑ latency to eat in the NSF IL inactivation (CNQX): ↑ time in OF centre, ↑ time in the OA and ↓ time in the CA of the EPM, ↓ latency to eat in the NSF IL inactivation (AP5): no differences in any test PL activation and inactivation: no differences in any test	<i>Bi et al., 2013</i>
PL vs IL	Deep brain stimulation	Wistar rats	Naïve	OF, FST, NSF	PL: no changes in the FST. IL: no changes in the OF, ↓ immobility and ↑ climbing in the FST, ↓ latency to eat in the NSF.	<i>Jiménez-Sánchez et al., 2016</i>

Optogenetic and chemogenetic studies

Region	Manipulation method	Promoter/Cell type	Model/strain	Stressor or phenotype	Behavioural tests	Effects	Reference
mPFC	Optogenetic stimulation	IE4-5/ not specific cell type	C57BL/6J mice	Chronic social defeat	OF, EPM, SPT, SI	= distance in the OF and = EPM, in susceptible mice fully restored SI and prevention of the reduced sucrose preference in susceptible mice	<i>Covington et al., 2010</i>
mPFC mPFC → DRN mPFC → LHb	Optogenetic stimulation	CaMKII / Glutamatergic	LE rats	Naïve	OF, FST	mPFC: = distance in the OF and = immobility in FST mPFC - DRN: ↑ mobility in FST and = distance in the OF mPFC - LHb: ↓ mobility during FST	<i>Warden et al., 2012</i>
PL	Optogenetic stimulation	Thy1 / Layer V pyramidal neurons	Thy1-ChR2-EYFP mice	Naïve and chronic subordination stress	OF, FST, EPM, SI	Acute: ↑ distance travelled in OF and ↓ immobility in FST Chronic: ↑ time in OA of EPM and = SI	<i>Kumar et al., 2013</i>
PL and ventral ACC	Chemogenetic inhibition (acute and chronic) Ablation of SST neurons with diphtheria toxin	SST / subpopulation of GABAergic neurons	SST-IRES-Cre mice	CUS	OF, EPM, NSF, SPT	Acute inhibition: ↓ time in the centre of the OF, ↓ time in the OA of EPM and ↑ latency to eat Chronic inhibition: = distance OF, ↑ time and entries in the OA of EPM, = latency to feed in NSF and = SPT Ablation of SST neurons: = distance OF, ↑ time and entries in the OA of EPM and ↓ latency to eat in NSF	<i>Soumier and Sibille, 2014</i>
PL → NAc PL → BLA	Optogenetic stimulation and infusion of CCK	CaMKII / Glutamatergic	C57BL/6J mice	Chronic social defeat	EPM, SPT, SI	PL - NAc: = EPM, ↑ sucrose preference and fully reversed social avoidance PL - BLA: ↑ time in OA of EPM, no effects on SPT and on SI	<i>Vialou et al., 2014</i>
PL vs IL	Optogenetic stimulation	CaMKII / Glutamatergic	SD rats	Naïve	FST, NSF, SPT	PL: did not alter behaviour in any of the tests IL: ↓ immobility in FST, ↓ latency to eat in the NSF and ↑ sucrose preference in SPT	<i>Fuchikami et al., 2015</i>
PL	Chemogenetic inhibition	PV / subpopulation of GABAergic interneurons	PV-Cre mice	Footshock	OF, LHp	= distance in the centre of the OF ↑ escape latency and number of failures in LHp	<i>Perova et al., 2015</i>
PL	Chemogenetic activation	CaMKII / Glutamatergic	SD rats	Naïve	OF, EPM	= distance in OF, ↑ time and distance in OA in the EPM ↑ Fos expression in LS, BNST and amygdala	<i>Pati et al., 2018</i>
mPFC	Optogenetic stimulation	CaMKII / Glutamatergic	VGluT2-IRES-Cre:Chr2 mice	Naïve	OF, TST	= distance in the OF ↓ immobility in TST	<i>Son et al., 2018</i>
mPFC	Optogenetic stimulation	Drd1 and Drd2 / Dopaminergic	Drd1-Cre and Drd2-Cre mice	Naïve	FST, EPM, NSF, SPT	Drd1: ↓ immobility in FST, ↑ time in OA in the EPM, ↓ latency in NSF and = SPT Drd2: = immobility in FST, ↓ OA entries in the EPM, = latency in NSF	<i>Hare et al., 2019</i>

PL	Optogenetic stimulation and inhibition	CaMKII neurons (glutamatergic) projecting to avBNST	SD rats	Naïve	TST, SPT	Stimulation: ↓ immobility in TST, ↓ immobility and ↑ time burying the probe in SPT. Inhibition: : ↑ immobility in TST and ↑ immobility and ↓ time burying the probe in SPT.	Johnson et al., 2019
mPFC	Chemogenetic activation (acute and chronic)	PV / subpopulation of GABAergic interneurons	C57BL/6J mice	Naïve	OF, NSF	Acute activation: = distance in centre and total distance in the OF Chronic activation: ↓ distance in the centre of the OF and ↑ latency to eat in NSF	Page et al., 2019
IL	Chemogenetic inhibition (acute and chronic)	PV / subpopulation of GABAergic interneurons	PV-Cre mice	Naïve and CUS	TST, FST, Y-maze	TST ↓ struggling and ↑ immobility, FST (chronic inhibition during CUS) ↑ struggling and ↓ immobility, = locomotor activity in Y-maze	Nawreen et al., 2020
IL	Optogenetic stimulation	Arc / activated cells by social interaction	Arc-Cre-ERT2 mice	IS	OF, Reexpo to IS context	Stimulation of IL social ensembles ↓ freezing in OF and in re-exposure to the footshock context, similar to social buffering effects	Gutzeit et al., 2020
IL IL → LS IL → CeA	Optogenetic stimulation and inhibition Chemogenetic inhibition	CaMKII / Glutamatergic	C57BL/6J mice	Naïve	OF, EPM	IL activation: ↓ time in the centre of the OF, ↓ time and entries in the OA of EPM IL inhibition: ↑ time in the centre of the OF, ↑ time and entries in the OA of EPM IL-LS activation: ↓ time in the centre of the OF, ↓ time and entries in the OA of EPM IL-LS inhibition: ↑ time in the centre of the OF, ↑ time and entries in the OA of EPM IL-CeA activation: ↑ time in the centre of the OF, ↑ time and entries in the OA of EPM IL-CeA inhibition: ↓ time in the centre of the OF, ↓ time and entries in the OA of EPM	Chen et al., 2021

References are ordered in chronological order. Abbreviations: ACC, anterior cingulate cortex; Arc, activity-regulated cytoskeleton-associated; BLA, basolateral amygdala; BNST, bed nucleus of the stria terminalis; CaMKII, Calcium/calmodulin-dependent protein kinase II; CeA, central nucleus of the amygdala; CFC, contextual fear conditioning; ChR2, channelrhodopsin-2; CUS, chronic unpredictable stress; DRN, dorsal raphe nucleus; EPM, elevated plus maze; EYFP, enhanced yellow fluorescent protein; FST, forced swim test; IL, infralimbic cortex; IRES, internal ribosome entry site; IS, inescapable footshock; LE, Long Evans; LHb, lateral habenula; LHp, learned helplessness paradigm; lmpPFC, lateral medial prefrontal cortex; LS, lateral septum; mpdPVN, medial parvocellular dorsal paraventricular nucleus of the hypothalamus; mPFC, medial prefrontal cortex; NAc, nucleus accumbens; NSF, novelty-suppressed feeding; OA, open arms; OF, open field; PL, prelimbic cortex; PV, parvalbumin; PVN, paraventricular nucleus of the hypothalamus; SD, Sprague Dawley; siRNA, small interference RNA; SPT, shock probe burying test; SI, social interaction; TST, tail suspension test; vGluT1, vesicular glutamatergic transporter 1.

4. Immediate early genes and neuronal activation

Much of what we have learned about the brain areas involved in the processing of stressors has been based on the detection of immediate-early genes (IEG), which are genes that are rapidly and transiently induced in response to different stimuli and without requiring de novo protein synthesis. IEGs encode many functionally different products, including effector proteins, such as activity-regulated cytoskeleton-associated (Arc), and transcription factors, including c-Jun, c-Fos and zif268 or NGFI-A (for a review see Herdegen and Leah, 1998). There are various IEGs with distinct time courses of induction, different half-lives as well as distinct subcellular localization, which provide a variety of choices for use depending on the experimental conditions and objectives.

4.1. *c-fos* as a marker of neuronal activation

The IEG *c-fos* is the most widely used marker for neuronal activation. The viral gene “fos” was isolated in 1982 as the oncogene of the Finkel-Biskis-Jenkins murine osteogenic sarcoma virus (FBJ-MSV) and a year later its cellular counterpart *c-fos* was described (see revision by Herdegen and Leah, 1998). The mechanisms underlying the activation of IEG promoters in different cell types have been a subject of study for decades. In neurons, *c-fos* promoter activation is regulated by complex molecular mechanisms, and the most important regulatory elements are the serum response element (SRE) and the calcium and cAMP-responsive element (Ca/CRE). *c-fos* transcription is activated by numerous factors, such as neurotransmitters, growth factors and depolarisation, which cause an influx of extracellular calcium into the cell that, in turn, activates different signalling transduction pathways, including the mitogen-activated protein kinase (MAPK) and calmodulin kinases (CAMKs) (**Figure 5**). Once in the nucleus, the Fos protein dimerises with members of the Jun protein family to form the complex activating-protein 1 (AP-1), which can induce the expression of different genes containing an AP-1 binding site in their promoter (Sheng and Greenberg, 1990; Herdegen and Leah, 1998; Kovács, 1998).

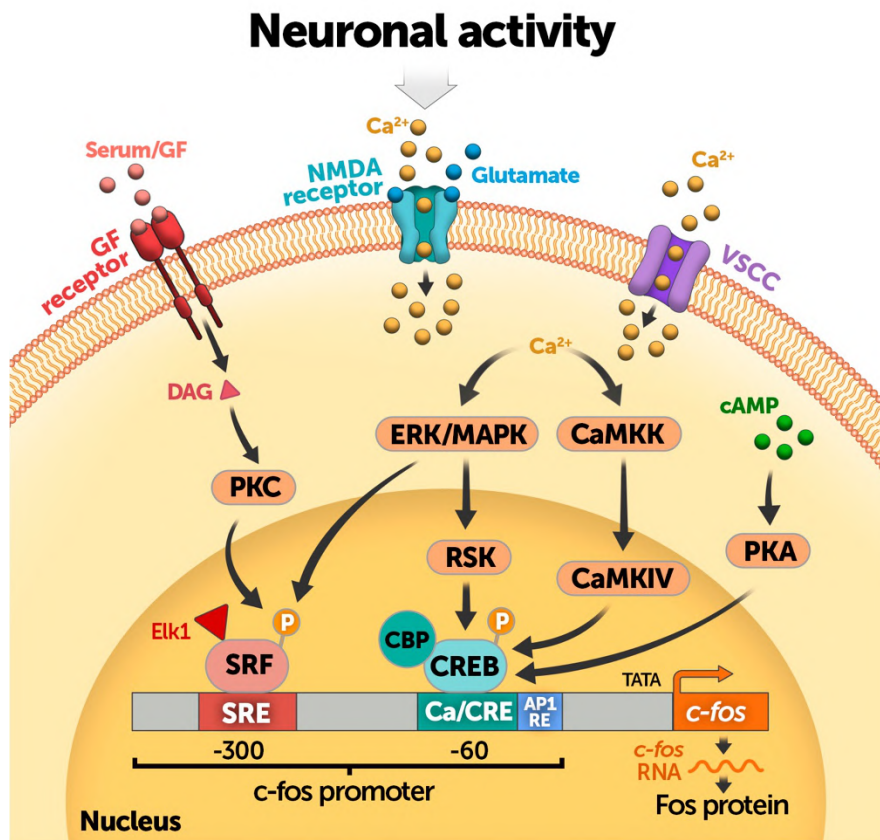


Figure 5. Principal transduction pathways regulating *c-fos* expression.

Calcium influx through N-methyl-D-aspartate receptors (NMDAR) and voltage-gated calcium channels (VSCC) leads to the activation of many calcium-regulated signalling proteins, including extracellular signal-regulated kinase (ERK)/mitogen-activated protein kinase (MAPK) and calcium-calmodulin dependent kinases (CAMK). Furthermore, increases in cyclic adenosine monophosphate (cAMP) activate protein kinase A (PKA). ERK/MAPK activate the ribosomal S6 kinase (RSK), which phosphorylates the cAMP-response element-binding protein (CREB), which is also the target of CAMKIV and PKA. CREB, together with CREB binding protein (CBP) binds to the calcium/cAMP response element (Ca/CRE) in the *c-fos* promoter, a regulatory element critical for activity-dependent *c-fos* transcription. Moreover, serum and growth factors (GF) increase diacylglycerol (DAG) levels, which in turn activates protein kinase C (PKC). PKC and ERK/MAPK activation phosphorylates Elk-1, which binds to the serum response factor (SRF) that, in turn, binds to the serum response element (SRE), a critical regulatory element in the *c-fos* promoter region. This induces the transcription of *c-fos* mRNA, which is then translated into c-Fos protein. Furthermore, there is an AP-1 regulatory (AP-1re) site adjacent to the SRE that binds Fos/Jun heterodimers and other transcription factors and might mediate negative autoregulation for *c-fos* transcription. Adapted from Kovács, 1998 and Cruz et al., 2015.

c-fos induction is transient because diverse repression mechanisms act at different levels. At the transcriptional level, AP-1 can repress *c-fos* transcription via an auto-inhibitory mechanism by binding to an AP1 region in the regulatory regions of the *c-fos* gene (Sassone-Corsi et al., 1988). Furthermore, GR can also suppress *c-fos* promoter activity by binding to SRE and preventing the binding and activation by the serum response factor (SRF). At the mRNA level, the arrest of elongation of nascent transcripts of *c-fos* is signalled by a “premature termination” segment in the first intron, which causes the termination of transcription (Mechti et al., 1991). Moreover, *c-fos* expression is tightly regulated as well by rapid mRNA degradation, which is governed by two elements: an AU-rich element (ARE) in the 3'-untranslated region and a sequence in the protein-coding segment of *c-fos* mRNA. These two distinct pathways confer *c-fos* mRNA a half-life of around 15 min, although if the machinery of degradation is saturated due to high levels of *c-fos*, this might be extended up to 90-100 min (Shyu et al., 1989; Herdegen and Leah, 1998).

At the protein level, there are also different mechanisms of degradation. The c-Fos protein decays in two phases, the first has a half-life of 45 min and the second a half-life of 90-120 min, the latter occurring when most c-Fos molecules (90%) are associated with Jun proteins. Thus, the formation of c-Jun:c-Fos dimers promotes c-Fos degradation. During this window, c-Fos can form dimers with other proteins such as GR, which could influence gene expression in the immediate period after cell activation. The most important c-Fos protein degradation pathway is mediated via the proteasome after polyubiquitination, although mechanisms independent of ubiquitination have also been described. Interestingly, given the rapid synthesis of c-Fos and the more delayed increase in c-Jun, there is a time window when c-Fos is not associated with Jun proteins (Herdegen and Leah, 1998).

Among all the IEGs described throughout decades of research, *c-fos* is the best-characterized and the most commonly used marker for neuronal activity mapping due to its particular characteristics. First and foremost, under basal conditions, *c-fos* mRNA is expressed at very low levels in most brain areas, but it is rapidly induced in response to many different stimuli, including growth factors, neurotransmitters, neuronal depolarization, and exposure to different stressors (Sheng and Greenberg, 1990; Hughes et al., 1992; Armario, 2006b). Moreover, its transcriptional induction is transient, in contrast with other IEGs, such as *zif268*, which have higher basal levels and longer expression patterns (Cullinan et al., 1995). From a technical point of view, *c-fos* mRNA and protein are relatively easy to study by employing in situ hybridization and immunochemistry, respectively, and their detection can be combined with other markers, including cell-type

specific markers or other IEGs (McReynolds et al., 2018). Furthermore, unlike in vivo imaging or electrophysiology approaches, the evaluation of *c-Fos* labelling is not limited to only one brain region but enables the examination of the whole brain. Finally, the methods used to visualize *c-fos* mRNA and protein give superb spatial resolution, not only at the regional level but also at the cellular and even subcellular level.

Although *c-Fos* mapping has been undoubtedly a fundamental tool for studying neuronal activation in response to different stimuli, some caveats need to be considered. Firstly, the absence of *c-Fos* expression does not necessarily mean a lack of neuronal activity. Neuronal depolarisation per se not always results in *c-fos* transcription, but rather a joint action of neuronal depolarization and synaptic inputs, and hence intracellular signalling cascades, are needed (Luckman et al., 1994). Accordingly, Cullinan et al. (1995) showed that after stress exposure, *zif268* expression can be detected in some areas where *c-fos* induction is not found (e.g. the dentate gyrus, medial habenula or the peripeduncular nucleus). Moreover, if *c-fos* activation only happens after robust cellular stimulation, this would mean that *c-Fos* labelling probably does not capture subtle changes in neuronal activation in response to subthreshold stimuli. Secondly, *c-fos* labelling does not allow identifying neurons that are inhibited rather than activated in response to a stimulus. Thirdly, *c-Fos* mapping does not provide information about changes in firing patterns (e.g. tonic to phasic) and it is not a good marker for tonically active neurons. For instance, Hoffman et al. (1994) showed that dopaminergic neurons of the medial basal hypothalamus projecting to the median eminence, which are tonically activated, were devoid of Fos immunoreactivity. Hence, caution should be applied especially when interpreting null findings regarding *c-fos* induction. Fourthly, *c-fos* labelling has the limitation that each measurement in one animal can only represent a single time-point following behaviour. In this line, unlike in vivo electrophysiology or other in vivo imaging approaches, *c-fos* cannot inform about real-time changes in neuronal activity, although it has the important advantage that can provide information about cell-type-specific activation when combined with other markers, in contrast with conventional in vivo electrophysiology.

Finally, although *c-fos* is mainly expressed in neurons within the CNS, its expression is also possible in glial cells, although its regulation and function in astrocytes is thought to differ from that in neurons. For instance, depolarisation stimuli (e.g. increasing calcium uptake, administration of nerve growth factor) that typically induce Fos activation in neurons do not induce it in astrocytes (Hisanaga et al., 1990). Instead, it appears that Fos expression in astrocytes is rather associated with differentiation or

proliferation events, especially after brain injury, but not with depolarisation or activation in response to emotional stressors (Dragunow et al., 1990; Hisanaga et al., 1990; Armario, 2006b). Importantly, although it is assumed that *c-fos* expression in the CNS is restricted to neurons after common stressors, astrocytic expression should not be directly discarded after exposure to some systemic stressors. For instance, Ludwig and colleagues (1997) that administration of hypertonic saline into the supraoptic nucleus (SON) of the hypothalamus induced *c-fos* in astrocytes but not in magnocellular neurons.

4.2. *c-fos* contribution to the field of stress

Despite having some limitations, the *c-fos* mapping strategy has provided invaluable information about the brain processing of stressors. Indeed, is this information what have provided means for a classification of stressors into two broad categories: systemic and emotional, although as previously mentioned, a third category between these two needs to be also considered: mixed stressors (Herman and Cullinan, 1997; Sawchenko et al., 2000; Herman et al., 2003). Systemic stressors activate different brain areas which are specific to each stimulus and indeed, Pacák and Palkovits (2001) termed these specific patterns as “neurochemical signatures” of each systemic stressor. These stressor-specific neuronal populations are important for regulating specific physiological responses to distinct systemic stressors. In contrast, exposure to different types of pure or predominantly emotional stressors, such as immobilisation, forced swim, exposure to novel environments or predator odour, seem to evoke a considerably similar pattern of widespread *c-fos* expression in the brain. The brain regions activated in response to many different stressors have been extensively characterized (for a revision see Kovács, 1998) and include cortical and subcortical areas, such as the mPFC, the LS, the amygdala and the BNST, and brainstem nuclei, such as the PAG, the locus coeruleus (LC), the NTS and the VLM (Cullinan et al., 1995; Campeau et al., 1997; Li and Sawchenko, 1998; Ons et al., 2004; Armario, 2006b).

Reports of stress-induced activation in the BNST and the amygdala have been slightly inconsistent. In the case of the BNST, there is controversy regarding the subdivisions activated in response to stress (Cullinan et al., 1995; Li and Sawchenko, 1998), which can be likely attributed to the anatomical complexity of the nucleus that complicates the analysis of specific subdivisions. Moreover, originally there was also controversy regarding the activation of different subdivisions of the amygdala, although currently it is considered that the CeA may be an important player in controlling the response to systemic stressors while the MeA would be more

involved in the response to emotional stressors (Cullinan et al., 1995; Dayas et al., 2001; Xu et al., 1999). Hence, it appears that different emotional stressors activate a considerable number of common brain areas, even when they markedly differ both in terms of quality and intensity (Cullinan et al., 1995; Ons et al., 2004; Armario, 2006b; Úbeda-Contreras et al., 2018).

Some studies in this field have tried to elucidate specifically the relationship between the intensity of emotional stressors and the degree of neuronal activation in different brain areas. In this line, Campeau and Watson (1997) studied the brain pattern of *c-fos* mRNA induction in response to white noise of different intensities in rats, assessing in parallel the plasma corticosterone response. Interestingly, they found three different patterns of *c-fos* expression. Firstly, exposure to the experimental cages, independently of the noise intensity, elicited a wide *c-fos* induction in cortical areas, thalamic nuclei and the BLA. Secondly, they observed an intensity-dependent pattern in brain areas related to audition (e.g. inferior colliculus, cochlear nuclei). Finally, some areas showed a significantly higher *c-fos* induction only with the highest noise intensities (90 and 105 dB), including some BNST subdivisions, the NAc, the PVN, the LSv, the dentate gyrus, the MRN and the pedunculopontine tegmental nucleus.

Our group and others have also compared the *c-fos* induction pattern in response to emotional stressors of different intensity (Ons et al., 2004; Pace et al., 2005; Rotllant et al., 2013; Úbeda-Contreras et al., 2018), revealing that *c-fos* expression in different brain areas can show three different patterns: (i) marked activation, independently of stressor intensity; (ii) activation proportional to stressor intensity; (iii) activation inversely proportional to stressor intensity. Accordingly, *c-fos* induction in response to a mild stressor (OF) was similar to that of a severe stressor (IMO) in different brain areas such as the PrL, the shell subdivision of the NAC (NACsh) and the MeA, while the LSv, the mpdPVN and the LC show a significantly greater induction by IMO (Ons et al., 2004; Rotllant et al., 2013). Furthermore, Pace and colleagues (2005) evaluated the *c-fos* induction pattern in response to three novel environments (a clean housing tub, a circular arena and a pedestal raised 60 cm off the ground) and to acute restraint, which differed in intensity as indicated by the plasma levels of ACTH and corticosterone. They found a positive correlation between the number of *c-fos*+ cells in the PVN and ACTH and corticosterone levels, whereas the number of *c-fos*+ cells was inversely related to stressor intensity in the HF and the somatosensory, piriform and motor cortices. These results strongly agree with data from our group (Úbeda-Contreras et al., 2018), which also compared *c-fos* induction in response to emotional stressors differing in intensity (OF, cat odour and IMO), as indicated again by ACTH plasma

levels. They showed the three different patterns abovementioned, with some areas showing a positive relationship between neuronal activation and stressor intensity (e.g. DMH, LSv, PVN), others showing a negative relationship (e.g. ACC, NAc, HF) and others whose degree of activation was independent of stressor intensity (e.g. PL, IL and BLA). Notably, these patterns were further corroborated with a different neuronal activation marker, phosphorylation of histone H3 in Serine 10 (Rotllant et al., 2013).

Taking into account these findings, a critical question arises: how is it possible that stressors markedly differing in intensity and nature activate the same number of neurons in the same brain areas, despite having remarkably different physiological and behavioural consequences? It is plausible that this similar activation pattern is reflecting a general activation state or arousal, a common factor among the different stressors. Thus, some brain areas would reflect a general state of stress rather than qualitative aspects of each stressor (Armario, 2006b). However, despite the existence of this predominant neuronal population, there could well be another small population of neurons that respond specifically to each stressor. Should this specific population exist, we hypothesize that it would be present in high hierarchy brain areas, such as the mPFC and other subcortical limbic areas involved in more complex cognitive functions, rather than in areas related to low hierarchy control of the responses, such as the PVN. It could be that this putative specific population has not been described yet because it may be difficult to detect it by conventional histology approaches. Concerning this, novel techniques such as viral labelling and transgenic mice have allowed the characterisation of neuronal ensembles that respond specifically to stimuli with negative valence and others to positive valence (Gore, Schwartz, Brangers, et al., 2015), showing the presence of functionally different neurons which can be anatomically intermingled in a particular brain area. In the case of emotional stressors, this could explain why different stressors can induce *c-fos* in a similar number of neurons and at the same time, have markedly different behavioural and physiological consequences. In the last years, strategies based on the use of IEGs have been designed to address this fundamental question.

4.3. Temporal dynamics of *c-fos* expression

The time-course of expression of *c-fos* RNA isoforms and protein in response to acute stimuli has been well established (Cullinan et al., 1995; Kovács, 1998; Marín-Blasco et al., 2018). The peak expression of unspliced or immature *c-fos* RNA (also called heteronuclear RNA, or hnRNA) transcript occurs as early as 5 min after neuronal activation and it is rapidly degraded due to its very short half-life (Lin et al., 2011a). The mature RNA

(mRNA) also appears rapidly after neuronal activation but tends to reach its peak levels 30 min after stimulus onset and generally return to baseline within 90 to 120 min. *c-Fos* protein peaks between 90-120 min after initial exposure to the stimulus, progressively returning to low or barely detectable levels within 4 - 6 h. Given their transient nature, both *c-fos* mRNA and protein in general return to basal levels after a limited period of time, despite the persistence of the stimulus (e.g. prolonged stressor). This is observed even with emotional stressors of elevated intensity, such as IMO (Imaki et al., 1992; Trnečková et al., 2007a), although it does not occur with some systemic stressors such as endotoxin injection or hypovolemia induced by colloids, in which high *c-fos* mRNA levels have been reported at 3 - 6 h after the stressor (Rivest and Laflamme, 1995; Tanimura et al., 1998). This implies that *c-fos* is appropriate for studying neuronal activation caused by acute stressors of short duration (from minutes to a few hours) and hence, in case one needs to assess the neuronal response to a prolonged or chronic stressor, neuronal activation markers with longer half-lives should be used. The protein FosB and its truncated variant Δ FosB belong to the family of fos-related antigens and possess longer half-lives than *c-Fos*. In particular, the Δ FosB variant has an unusual stability (i.e. it can persist for days), thereby accumulating upon repeated stimulation. This characteristic makes it a useful indicator of repeated neuronal activation, such as the activation induced by chronic exposure to stress (Nestler, 2015).

4.4. Use of *c-fos* for the study of activated neuronal ensembles

Taking advantage of the well-established time course of expression of *c-fos* and the differential time course and subcellular location of *c-fos* intronic and mature transcripts and protein expression, we can examine differential neuronal activation in response to two different experimental manipulations within the same subject. Different experimental strategies have been developed based on this fact.

A pioneering and instrumental method for the study of specific neuronal ensembles was developed by Guzowski and colleagues (1999) and it was called cellular compartment analysis of temporal activity by fluorescence in situ hybridization (catFISH). The original method was based on the temporal characteristics of the IEG Arc. Following a temporally discrete behavioural stimulus, the intronic or nuclear Arc RNA appears within 2 min, peaks at 5 min and returns to baseline levels 16 min after, whereas the mature or cytoplasmic RNA signal appears around 20-45 min after neuronal activation. By exploiting the unique transport kinetics of Arc RNA from nucleus to cytoplasm, Guzowski and collaborators could identify neurons

specifically activated by exposure to two different stimuli separated by a 20 min interval (for a revision see Guzowski et al., 2005). This excellent imaging technique has been key for the examination of neuronal ensembles. Since then, several studies have employed this method with intronic and mature *c-fos* transcripts for describing different neuronal ensembles activated by mating and fighting in the ventromedial hypothalamus (Lin et al., 2011a) as well as by an appetitive (nicotine) and an aversive (footshock) unconditioned stimulus in the BLA (Gore, Schwartz, Brangers, et al., 2015), among others. However, in general, these studies have exclusively focused on studying specific neuronal populations for appetitive vs aversive stimuli, and to our knowledge, catFISH has never been used to study exposure to two stressors (i.e. two aversive stimuli). Furthermore, other labs have used catFISH to study neuronal activation at different time points using a combination of two different IEGs, such as Arc and Homer1a, based on the fact that the timing of induction of the intronic transcript of Homer1a is approximately 25 min, a time point at which Arc intronic RNA has already declined and been processed into mature RNA (Vazdarjanova et al., 2002).

Another useful method to study stimulus-specific neuronal activation, also based on IEG labelling, is the combination of immunofluorescence (IF) to detect Fos protein and FISH to detect *c-fos* RNA (IF-FISH). In this case, however, stimuli have to be separated by 90-120 min, so that at the moment of perfusion the first stimulus results in maximal IEG protein induction and the second stimulus reaches maximal IEG mRNA expression (for a revision see Kovács, 2008). Newer and optimized methods have been developed to concurrently label *c-fos* mRNA and Fos protein, such as tyramide-amplified immunohistochemistry-fluorescence in situ hybridization, which has been used to identify differential neuronal activation in response to appetitive and aversive stimuli in the same animal (Xiu et al., 2014). To the best of our knowledge, only one study has been published using this method to evaluate specific neuronal activation in response to different stressors (immobilisation on board or IMO and forced swim). Marín-Blasco and colleagues (2018) used IF-FISH to show that in some hierarchically superior brain areas such as the mPFC, the LSv and the MeA there is a small proportion of neurons that are specifically activated by forced swim exposure after prolonged exposure to IMO (4h), the majority of neurons being non-specifically activated by the two stressors. Interestingly, in low-hierarchy areas such as the mpdPVN, most neurons respond similarly to the two stressors.

The techniques mentioned above using either *c-fos* RNA isoforms or c-Fos protein have the key advantage of allowing the detection of cells activated specifically by different experiences in the same animal, which is not

possible with conventional IEG labelling methods. Moreover, not only do they allow observing net changes in total neuronal activation with two different experiences, but also determining whether there are neuronal populations activated specifically by each stimulus. Furthermore, the advantage of detecting two Fos products is that both RNA species are subject to the same underlying induction kinetics, which does not occur when two IEGs are used for neuronal ensemble identification (e.g. catFISH with Arc and Homer1a; Vazdarjanova et al., 2002). Moreover, since the techniques are based on the natural dynamics of *c-fos* expression, they do not require the use of transgenic animals and, as long as specific probes and antibodies are available, they are easy to perform and widely applicable in many different species.

Nevertheless, detecting IEG RNA and protein in neurons suffers from three potential limitations compared to catFISH. Firstly, due to tissue processing requirements, combining ISH and immunohistochemistry procedures is much more technically demanding than double FISH (dFISH). The identification of positive neurons using IF or FISH can be strongly dependent on the sensitivity of each technique, which could affect the interpretation of the results. In this sense, by using the same technique for each isoform (e.g. RNA probes, detection with an antibody, same amplification system) the results are likely to be more comparable than using two completely different protocols (IF and FISH). Secondly, the time interval (even of 3 hours) between the two different experiences allows for the expression of proteins that can modify the genomic response to the second stimulus. With catFISH, all behavioural manipulations happen within a time window of approximately 30 min, and therefore there is very little time and hence fewer chances for *de novo* protein synthesis and intranuclear accumulation of proteins that can, in turn, modify the transcriptional response to neuronal activity for the second stimulus.

Moreover, with catFISH, the duration of both stressors is usually the same, while in other approaches such as IF-FISH, the duration of both stimuli sometimes is different, which can also confound the results of double mapping due to different neuronal activation not attributable to specific characteristics of the stressors but to their different duration or intensity (Guzowski et al., 1999, 2005; Marín-Blasco et al., 2018). The combination of different emotional stressors using short exposures with short resting periods (such as catFISH) in between might contribute to more precisely defining stressor-specific neuronal populations. However, this short duration of stimulus exposure also entails a disadvantage, as there is little time to process the stimuli and to differentiate the characteristics of each

stressor, thereby translating into the identification of a bigger proportion of overlapping populations.

In conclusion, IEG labelling methods have been instrumental for identifying groups of neurons selectively activated by different stimuli, although the potential existence of stressor-specific neurons remains poorly investigated. Further exploration of this topic is critical for understanding how different stressors are processed in the brain and what explains the markedly different consequences of stress exposure. Finally, although IEGs have been fundamental for describing the neural circuits engaged in stress, they offer no clue as to the causal role of activated neurons in the stress response. Therefore, manipulation of these stress-activated neurons is undoubtedly needed to establish causality.

5. Technologies for the study of stress-activated neuronal ensembles

For a long time, researchers have been able to identify and characterise sparsely distributed neurons activated by different stimuli by using IEG labelling studies, electrophysiological approaches and, more recently, calcium imaging techniques. Nevertheless, elucidating the causal role of activated neuronal ensembles in different behaviours as well as their molecular profiles has posed a great challenge for neuroscientists (Cruz et al., 2013; Kawashima et al., 2014). In the last years, efforts have focused on solving this challenge, and various technological advances have been made that rely on IEG promoters to drive the expression of reporters and effector proteins, by such means enabling the labelling, molecular profiling and manipulation of neurons activated in response to specific stimuli.

5.1. Neuronal manipulation based on activity-dependent promoters

Existing manipulation methods such as lesions, pharmacology, optogenetics and DREADDs generally alter the activity of either most neurons independently of their phenotype or selected neurons based on their cell type but independently of their actual activation during the exposure to a stimulus, thereby not reflecting the situation in normal conditions. Nevertheless, novel activity-dependent genetic methods enable manipulating neuronal ensembles specifically activated by one stimulus without affecting the activity of surrounding neurons that do not respond to this particular event (Cruz et al., 2013; Kawashima et al., 2014; DeNardo and Luo, 2017). There have been different approaches based mainly on c-fos or Arc promoters-induced expression either in transgenic mice and rats

and/or employing viral vectors. The most relevant strategies will be discussed below.

Transgenic rodents using IEG promoters to drive fluorescent reporters, such as Fos-GFP transgenic mice or rats have enabled researchers to characterize the electrophysiological properties and synaptic characteristics of neurons activated by different stimuli (Barth et al., 2004; Cifani et al., 2012). However, Daun02 inactivation was one of the first approaches that showed a causal role for activated neuronal ensembles in eliciting different behaviours. This method is based on the use of c-fos-lacZ transgenic rats or mice in which the c-fos promoter drives the transcription of lacZ, which translates into β -galactosidase. After the injection of the inactive prodrug Daun02, β -galactosidase converts it into daunorubicin, which inactivates those neurons which were previously activated (Koya et al., 2009; Bossert et al., 2011; Cruz et al., 2013). For instance, with this methodology Bossert and colleagues (2011) showed that a small neuronal ensemble of the vmPFC plays a role in context-induced relapse to heroin.

Later, the c-fos promoter has also been used to directly drive the expression of optogenetic receptors to manipulate recently activated neurons. For instance, by using a lentiviral vector (LV) encoding the light-gated cation channel channelrhodopsin-2 (ChR2) coupled to a fluorescent reporter under the control of the c-fos promoter, Gore and colleagues (2015) described distinct neuronal ensembles that responded differentially to appetitive (nicotine) and aversive (footshock) unconditioned stimuli in the BLA. Moreover, by specifically manipulating these neurons they showed innate valence-specific physiological and behavioural responses. This strategy, however, posed the drawback that the expression of effector proteins is limited to a few hours after stimulus exposure and hence, the manipulation time window is very limited. In this regard, other alternative IEG-based tools have been designed to drive longer-term expression of effector proteins or even permanent expression (DeNardo and Luo, 2017).

The “TetTag method”, initially developed by Reijmers and colleagues (2007), is based on a Fos-tTA transgenic mouse in which the c-fos promoter drives the expression of the protein tTA (Doxycycline-repressible tetracycline transactivator) in activated neurons. Hence, doxycycline (dox) provided to the mice or rats, normally through the diet, inactivates tTA transcriptional activity. However, when dox is removed, tTA can bind to a tet operator in the promoter of a second transgene. This promoter, in turn, controls the expression of a selected gene, which can be either some reporter (Reijmers et al., 2007), or receptors such as opsin for optogenetics (Liu et al., 2012) or DREADDs for chemogenetics (Garner et al., 2012). The pioneering study by Liu and colleagues (2012) exploited this TetTag technology in

combination with an adeno-associated viral vector (AAV) expressing ChR2 to label hippocampal neuronal ensembles activated during the acquisition of contextual fear memory. They showed how light-induced reactivation of these labelled neurons evoked artificial fear responses, consequently demonstrating the role of these hippocampal neurons in fear memory. Furthermore, at the same time, another lab used this same method but combined it with the DREADD technology. They generated a transgenic mouse in which expression of the hM3Dq receptor was induced by the c-fos promoter-driven tTA transgene. They showed that when neurons activated in one context were artificially reactivated during fear conditioning a different context, a “synthetic fear memory trace” was formed in association with the first context (Garner et al., 2012). A large number of subsequent studies have adopted this technology to study the causal role of specific neurons in many processes such as drug addiction and fear (for a review see DeNardo and Luo, 2017). Nevertheless, the slow metabolism of Dox results in a long-time window for labelling or expression (on the order of days), and as a consequence, background expression is probably high. Thus, it must be considered that Fos-tTA could only achieve appropriate signal-to-noise ratios in brain areas with a very low basal expression of Fos. Furthermore, manipulations depend on the half-life of effector proteins and hence they are limited to several days after stimulus exposure (Reijmers et al., 2007; DeNardo and Luo, 2017).

Further strategies aimed at permanent labelling of activated neurons have been designed based on the expression of tamoxifen-dependent Cre recombinase such as CreERT2 under the control of activity-dependent promoters such as c-fos or Arc (Guenthner et al., 2013). With this method, coined by the authors as “ArcTRAP” and “FosTRAP”, from targeted recombination in active populations, Arc:CreERT2 or Fos:CreERT2 transgenic mice (named ArcTRAP and FosTRAP, respectively) are injected with a viral vector encoding a Cre-dependent protein (e.g. ChR2 fused to the reporter mCherry). Hence, in response to neuronal activity, the promoter induces the expression of CreERT2. Then, after tamoxifen injection, Cre recombines the receptor-reporter construct, thereby allowing its persistent expression in those cells which were activated. The labelling window for this approach is much shorter (<12 hours after 4-hydroxytamoxifen injection) than with other methods such as Fos TetTag. Nevertheless, this method greatly depends on the recombination efficiency of CreERT2 in the presence and absence of tamoxifen (Guenthner et al., 2013; DeNardo and Luo, 2017).

More recently, novel viral strategies based on synthetic activity-dependent promoters have been developed to try to solve the limitations of the

abovementioned strategies. Kawashima et al. (2013) firstly developed a combined AAV-based system that expresses CreERT2 under the control of the synthetic promoter E-SARE (enhanced synaptic activity-responsive element). The authors found that different transcription factors such as CREB and SRF bind to this activity-responsive element (SARE) to regulate the induction of Arc. They then fused five repeats of SARE with an Arc minimal promoter to control the expression of CreERT2, thus providing a temporally-controlled system to permanently label activated neurons. Furthermore, another viral-vector based synthetic promoter named RAM (robust activity marking) has also been recently developed (Sørensen et al., 2016) which it is based on 4 synthetic enhancer modules that contain the AP-1 binding site and the binding motif of the neuronal activity-dependent gene Npas4 upstream of the minimal c-fos promoter. This method is also Dox-dependent as it contains tTA and a TRE element, and the tTA protein has been modified to have a lower half-life, which means a significantly lower basal expression and tighter Dox regulation. Notably, these viral strategies with synthetic promoters bypass the need for transgenic mice and are also temporally controlled. However, a caveat of E-SARE is that it requires co-infection with two viral vectors. Moreover, RAM is Dox-dependent and, although improved, the time window for labelling is still relatively longer than with other approaches (DeNardo and Luo, 2017).

Apart from the methods discussed above, there are other approaches that also provide genetic access to activated neurons, such as calcium-based methods or whole-brain visualization of activated neurons by CLARITY combined with Fos-CreERT2 strategies (Ye et al., 2016).

All these methodologies (**Figure 6**) have undeniably shed new light on behaviours driven by active neurons in heterogeneous neural circuits in many different brain regions. Nevertheless, they have mainly focused on addiction research and learning and memory, especially fear memory (Cruz et al., 2015; DeNardo and Luo, 2017). Thus, although the advent of new technologies has allowed greater manipulation of functional ensembles, research focused on the description and functional characterization of neurons activated specifically in response to emotional stressors is still in its infancy and greater attention must turn toward this topic. Furthermore, a relatively unexplored field that is also relevant in stress research is the combination of activity-based genetic strategies with gene sequencing methods for unbiased mapping and profiling of activated neurons.

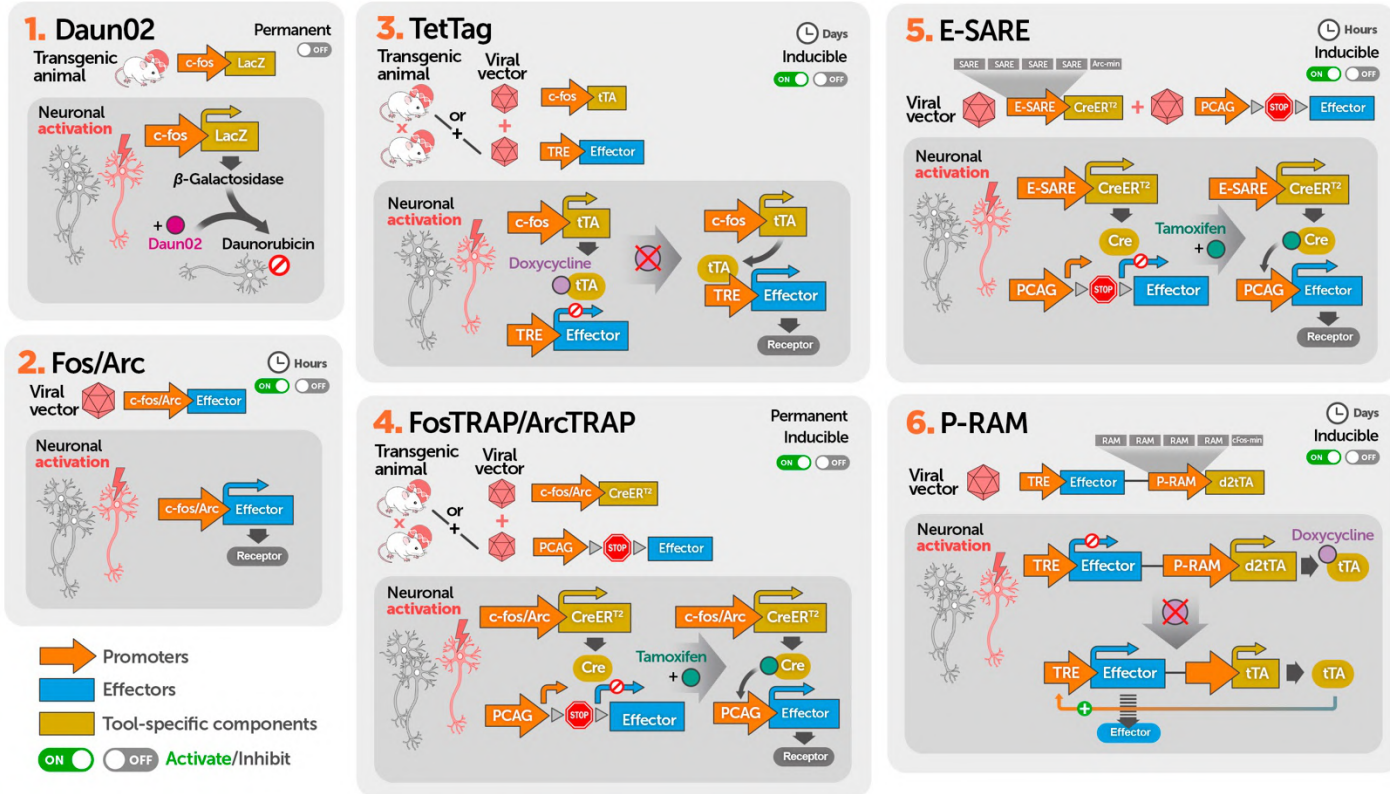


Figure 6. Experimental strategies to manipulate previously activated neurons based on immediate-early gene promoters.

1. In *c-fos*-lacZ transgenic rats the *c-fos* promoter drives the expression of *LacZ* gene that encodes for β -galactosidase, which converts the prodrug Daun02 into daunorubicin, inactivating previously activated cells. 2. Direct strategies involve *c-fos* and *Arc* promoters that drive effector proteins, with peak expression usually a few hours after the experience, lasting no more than a day. 3. The TetTag system involves two transgenes. In the first transgene the *c-fos* promoter drives expression of the doxycycline (Dox)-repressible tetracycline transactivator (tTA). tTA activates the TRE (Tetracycline response element) promoter in the absence of Dox. The second transgene uses TRE to drive expression of an effector gene which lasts for days. 4. In the TRAP method, *c-fos* or *Arc* promoters drive CreERT2 to drive permanent expression of Cre-dependent effector proteins in activated neurons when tamoxifen (TAM) is administered. 5. E-SARE is based on a viral vector carrying a synthetic promoter that drives CreERT2 expression. Hence, translation of effector proteins occurs only when TAM is present. 6. RAM is based on a synthetic enhancer promoter that drives destabilised tTA (d2tTA), which induces the expression of TRE-dependent effectors when neuronal activity occurs in absence of Dox.

5.2. Transcriptomic / Translatomic profiling of activated neurons

As previously described, one of the biggest challenges in neuroscience is to link the activity of specific neuronal types to the different functions of the brain. This is a challenging endeavour because of the huge cellular diversity of the CNS and the high heterogeneity in gene expression across different brain regions (Lichtman and Denk, 2011), as well as the fact that most neurons cannot be identified based only on their morphology or location within the brain. For this reason, the molecular expression pattern of stress-responsive neurons is hardly understood. Unravelling the genetic profile of neurons activated by different stimuli would enable us to define at the molecular level the neuronal populations that control particular behaviours and selectively manipulate them.

Despite the great utility of IEGs such as *c-fos* to identify neurons that respond to stressors in different brain areas (Herman and Cullinan, 1997), IEG labelling does not provide any information about the molecular identity of activated cells. To do so, double or triple-labelling techniques (e.g. double FISH) are required to detect other candidate genes, but there is a limitation on the set of genes that can be studied and it requires a substantial amount of time, money and effort to process such a large number of histological sections. Therefore, genome-wide systematic methods for the molecular identification of specific neuronal ensembles are required.

Studies employing microarrays and RNA-sequencing (RNA-seq) analyses have allowed researchers to assess the genome-wide changes induced by different stimuli. Although numerous studies have exhaustively analysed gene expression changes triggered by chronic stress exposure, very little is known about the molecular changes induced by acute stressors (reviewed by Floriou-Servou et al., 2021). The characterisation of the molecular changes induced by acute stress could provide molecular markers that help to predict adaptive vs maladaptive stress responses. Until now, transcriptomic analyses of the response to acute stress (e.g. FST) have exclusively focused on the HF (Tsolakidou et al., 2008; Roszkowski et al., 2016; Floriou-Servou et al., 2018) and the amygdala (Hohoff et al., 2013) and most of them have been based on microarray analysis. Furthermore, to our knowledge, the study by Floriou-Servou and colleagues (2018) is the only one in which a direct comparison of the transcriptomic changes induced by different acute stressors *in vivo* has been conducted. The authors evaluated gene expression changes in response to 6 min of novelty stress, 6 min of swim stress or 30 min of restraint in the dorsal and ventral hippocampus, assessed 45 min after the initiation of stress. They initially observed considerable differences

in the gene expression changes induced by the different stressors, especially in the ventral hippocampus, with only a minority of the gene changes being shared among the three stressors. However, further re-analyses of the published data with novel and re-evaluated bioinformatic tools revealed that in the original paper they overestimated the differences in stress-induced transcriptomic changes between stressors and that there was a significantly greater overlapping between stressors. The analysis of the variance in the expression of each differentially expressed gene shows that $\approx 74\%$ of the variance attributable to the different experimental groups was well explained by two groups (stress vs control animals), indicating highly similar transcriptional changes induced by different psychological stressors in the HF (Floriou-Servou et al., 2021). Furthermore, an important consideration is that the duration of the stressors in the study was different. The duration and the intensity of stressors are crucial factors for determining the stress response (Armario et al., 2012) and hence, this fact could have greatly contributed to the differences observed.

Notably, it must also be considered that not all transcriptional changes directly correlate with the expression levels of corresponding proteins, with some abundant transcripts being poorly translated, and vice versa (Zhang et al., 2020). A direct approach to evaluate changes in protein levels is to perform proteomic analyses, but some studies have detected very few changes 24h after stress, and current proteomic strategies have lower sensitivity than transcriptomic analyses due to limitations in the range of proteins detected (Floriou-Servou et al., 2018; Zhang et al., 2020). Altogether, this emphasizes the need for RNA analysis after stress exposure at a step closest to the protein. An approach that has proven very useful in this regard is the analysis of the mRNAs that are associated with ribosomes, namely the translome. Although an mRNA bound to a ribosome does not necessarily imply that it is being actively translated, protein levels correlate much better with mRNAs bound to ribosomes than with total mRNA levels (Zhang et al., 2020). Several strategies have been recently developed to study the translome in vivo, including the translating ribosome affinity purification (TRAP) method (Heiman et al., 2014) or the Ribotag approach (Sanz et al., 2009). These techniques are based on the cell-type-specific expression of tagged ribosomal proteins, which then allow the capture and isolation of the ribosome-bound mRNAs in the cell types of interest for further gene expression analyses. These methodologies provide a more refined characterization of the changes triggered by stimulus exposure than previous microarrays and bulk RNA sequencing so far as they are specifically selecting mRNAs bound to ribosomes and hence, those that are expected to be actively translated into proteins, in a cell-type-specific manner. Nonetheless, the selectivity of these systematic approaches is based

on cell-type-specific promoters or marker genes, and the genes that define functional neuronal ensembles are currently poorly understood.

In this regard, novel technological advances have been developed to specifically gain genetic access to neurons activated in response to a stimulus. Knight and colleagues (2012) developed a pioneering method called PhosphoRiboTRAP, which is based on the fact that the ribosomal protein S6, a structural component of the ribosome, becomes phosphorylated after neuronal activation. Hence, this phosphorylated S6 protein (pS6) can be used as a molecular tag to selectively capture those RNAs expressed in neurons activated by a particular stimulus and isolate and analyse these ribosome-bound RNAs through quantitative reverse-transcription PCR (RT-PCR) or RNA-seq without the need for transgenic animals or viral vector strategies. Several studies have since then successfully used this approach to identify and molecularly define activated neuronal populations, such as warm-sensitive neurons within the hypothalamus (Tan et al., 2016) and a subpopulation of neurons activated by food in the HF (Azevedo et al., 2019).

Phosphorylation of S6

S6 protein can be phosphorylated at five evolutionarily conserved C-terminal sites, which undergo phosphorylation in an ordered manner, beginning with Ser236 as the primary phosphorylation site and followed sequentially by Ser235, Ser240, Ser244 and Ser 247. Hence, the most C-terminal sites (244 and 247) are phosphorylated at a lower stoichiometry than N-terminal residues in basal conditions (Meyuhas, 2008). S6 is phosphorylated by different kinases at the different phosphorylation sites. The p70/p85 S6 Kinase 1 (S6K1) can phosphorylate pS6 at all sites, whereas the p90 Ribosomal S6 Kinases (RSK1-4), Protein Kinase C (PKC), Protein Kinase A (PKA), Protein Kinase G (PKG) and Death-Associated Protein Kinase (DAPK) phosphorylate selectively the Ser235 and Ser236 residues. Conversely, the dephosphorylation of the five residues is carried out by only one phosphatase, Protein Phosphatase-1 (**Figure 7**; for a review see Biever et al., 2015; Meyuhas, 2015). Remarkably, several biochemical pathways that have been described to regulate the phosphorylation of S6 such as cAMP/PKA signalling and MAPK (Meyuhas, 2008; Biever et al., 2015), are also known to modulate the transcription of activity-regulated genes such as c-fos (Sheng and Greenberg, 1990).

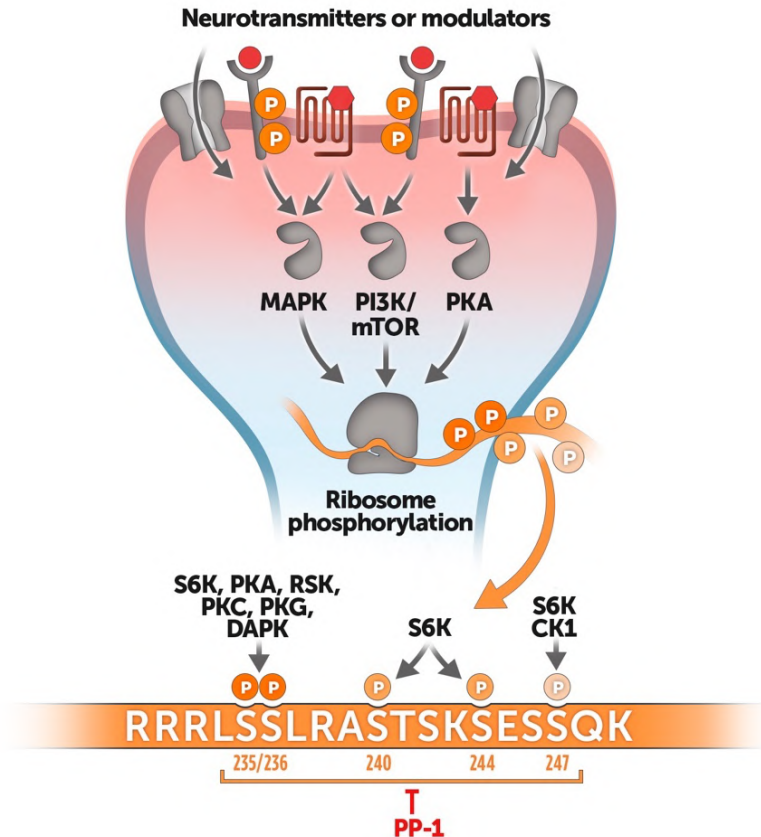


Figure 7. Regulation of S6 phosphorylation.

Activation of signalling pathways that trigger the phosphorylation of S6. Phosphorylation of S6 residues is carried out by different kinases at different serine residues and dephosphorylation by PP-1. Abbreviations: CK1, casein kinase 1; DAPK, death-associated protein kinase; MAPK, mitogen-activated protein kinase; PI3K/mTOR, phosphatidylinositol-3-kinase/mammalian target of rapamycin; PKA, protein kinase A; PKC, protein kinase C; PKG, protein kinase G; PP-1, protein phosphatase-1; RSK, p90 ribosomal S6 kinase; S6K, ribosomal S6 kinase.

Although the exact physiological role of S6 phosphorylation remains currently unsolved, in the last years a growing number of studies have used pS6 as a marker of neuronal activity in response to a wide variety of stimuli both in vitro and in vivo. Many different pharmacological agents (e.g. kainate, haloperidol and cocaine) have been reported to induce in mice and rats S6 phosphorylation in various brain areas such as the hypothalamus, the striatum or the cortex (for a detailed review see Biever et al., 2015). Other authors have reported increased S6 phosphorylation associated with synaptic plasticity. For instance, Salgado-Pirbhot and colleagues (2016) have reported that high-frequency stimulation rapidly increases phosphorylation of S235/236 of pS6 in the HF, and exposure to a novel environment induces S6 phosphorylation throughout the forebrain.

Furthermore, Bertran-Gonzalez et al. (2012) have shown that the state of phosphorylation of S6 at more C-terminal sites (S240/244) can be used to estimate the activation state of cholinergic interneurons in the striatum. Nevertheless, there has been very little research on S6 phosphorylation after exposure to emotional stressors.

Phosphorylation of S6 and stress exposure

Most of the research regarding S6 phosphorylation and stress has mainly focused on physical stressors and different regions of the hypothalamus. For instance, Knight et al. (2012) conducted a thorough immunofluorescence analysis of pS6 in mice after exposure to systemic stressors such as salt challenge, dehydration and fasting in various areas of the hypothalamus (e.g. PVN, ARC and SON, among others) and showed increased pS6 compared to control animals. Remarkably, the authors observed that all these stimuli also induced Fos expression in neural populations largely overlapping with pS6 signal. However, they only evaluated S6 phosphorylation after two emotional stressors, the resident-intruder test and exposure to cat odour, in the PAG and the premammillary nucleus of the hypothalamus, respectively. They concluded that both stressors increase S6 phosphorylation at S235/236. Unfortunately, no other areas involved in stress processing (e.g. mPFC, amygdala, LS) were assessed.

Notably, given that all neurons have a certain basal level of ribosome phosphorylation, if a stimulus induces inhibition in particular neuronal populations, it would result in decreased pS6 levels and hence, a depletion of transcripts from pS6 immunoprecipitates (Knight et al., 2012; Azevedo et al., 2019). This is a crucial aspect of this approach that contrasts with traditional IEGs approaches that do not label cells that are inhibited or insufficiently activated by a stimulus.

In summary, there is a lack of information regarding S6 phosphorylation after exposure to emotional stressors, particularly in areas of the limbic system and the mPFC. Furthermore, the kinetics of S6 phosphorylation after exposure to different stimuli have not been fully characterized. The characterization of S6 phosphorylation after emotional stressors in the mPFC as well as the immunoprecipitation of ribosome-RNA complexes with pS6 antibodies and subsequent RNA-seq analysis will help us to gain an understanding of the genetic identity of neurons specifically-activated in response to different stressors.

Materials and methods

1. Animals

2-months-old male Sprague-Dawley rats obtained from Janvier Labs (France) were used in our experiments. After arrival, they were housed in pairs in standard conditions of temperature (21 ± 1 °C) on a 12h light/12h dark cycle (lights on at 8.00 am) with food and water available ad libitum. The experimental protocol was approved by the Ethics Committee on Animal Experiments of the Universitat Autònoma de Barcelona and the Generalitat de Catalunya and it was carried out in accordance with the European Communities Council Directive (2010/63/EU) and Spanish legislation (RD53/2013).

2. General procedures

2.1. Animal housing and handling

The animals were allowed at least 1 week to acclimate themselves to the housing conditions before the experiment. During the second week after their arrival, all animals were handled 3-4 times for approximately 2 minutes (min) on different days before the start of the experiments to habituate them to manipulation and transport. Animals were randomly assigned to the different experimental groups taking into account their weight. Animals were always tested in a room different from the housing and blood sampling rooms to avoid interferences. The two cage-mates were always simultaneously exposed to stressors. All behavioural testing was conducted during the animals' light cycle from 8:30 a.m. to 2:30 p.m.

2.2. Blood samples collection

Blood samples were taken by tail-nick immediately after the behavioural tests (OF and FST) to evaluate the HPA response to stressors. In brief, the procedure consisted of gently wrapping the animal with a piece of cloth, making a 2 mm incision at the end of one of the tail veins and then performing tail massage until collecting 300 µL of blood into ice-cold EDTA capillary tubes (Sarsted, Granollers, Spain). The procedure was performed within 2 min and the two cage-mates were sampled simultaneously, two researchers obtained blood at the same time while a third one was gently holding the two rats. Afterwards, blood was centrifugated at 4 °C to obtain plasma, which was stored at -30 °C until radioimmunoassay (RIA) procedures.

2.3. Recording and analyses of behavioural tests

Behavioural tests were recorded with a video camera either in frontal or in zenithal position, connected to a TV monitor and a digital video recorder for later observation. For analyses of behaviour, two software were used. The SMART program (version 2.5.19-21, Panlab-Harvard) allowed us to analyse the track of the subjects during the tests (v.g. distance travelled), and The Observer XT 11 (Noldus Information Technology) was used to analyse several behaviours (v.g. rearings, grooming episodes) simultaneously and obtain not only their frequency of appearance but also their duration. In all experiments, the analyses were performed at blind.

3. Stress paradigms and behavioural tests

3.1. Immobilisation (IMO)

Rats were immobilised in a prone position by taping their four limbs to metal mounts attached to a board (e.g. Gagliano et al., 2008). Head movements were restricted with two plastic pieces (7 × 6 cm) placed at each side of the head and the body was additionally subjected to the board by a piece of plastic cloth (10 cm wide) attached with Velcro® surrounding the trunk of the animal.

3.2. Inescapable footshock (IS)

Footshock exposure was conducted in standard Skinner boxes (Ref. LE1005, Panlab-Harvard, Barcelona, Spain). Each chamber (25 x 25 x 25 cm) had a clear Plexiglas door, a black stainless-steel back wall and two aluminium sidewalls. The floor was composed of 19 stainless-steel rods (3 mm in diameter), spaced 1 cm centre to centre, and it was wired to a shock generator and scrambler. A house light (4 cm diameter 2.4-W, 24-V) was placed on the wall at 22 cm to the floor. The software (Packwin 2.00.2, Panlab-Harvard, Barcelona, Spain) controlled the delivery of shocks. The chambers were placed inside a sound-attenuating box (67 × 53 × 55 cm) provided with a fan that helped to mitigate environmental sound. The boxes were carefully cleaned between animals with a solution with ethanol in tap water (70% v/v). The IS protocol was the following for each chapter of the present thesis:

- Chapter 1: 1.5 mA shocks of 3 seconds duration with an inter-trial interval (ITI) of 30 seconds for a total time of 5 min.

- Chapter 2: 1.5 mA shocks of 3 seconds duration with an ITI of 1 min for 60 min.
- Chapter 3: 1 mA shocks of 3 seconds duration with a 2 min ITI for 20 min.

Given that one of the main aims of the thesis was to compare neuronal activation in response to different emotional stressors, for the experiments performed in chapters 1 and 2 a high shock intensity (1.5 mA) was selected based on previous experiments in our group showing that this shock intensity elicits a similar peak HPA axis response to IMO exposure (Márquez et al., 2002).

In chapter 3 of the thesis, we evaluated contextual fear memory in the second session of IS by measuring the time spent freezing during the first 2 min before the delivery of the first shock. Freezing was defined as the cessation of all movement except for respiration-related movement and non-awaken or resting body posture (Fendt and Fanselow, 1999).

3.3. Restraint (RES)

Rats were introduced for 60 min in open-ended Plexiglas cylindrical restrainers (WPI, UK, STR554) measuring 21.5 cm in length and 6 cm in diameter. The rear top of the cylinder was adapted to the weight of each animal to maintain a constant level of restraint regardless of the animal size. Several holes in the walls (1 cm in diameter) of the cylinder provided air to the animal (Rabasa et al., 2015).

3.4. Open field (OF)

The open field (OF) test is a widely used paradigm designed by Hall and Ballachey (1932) for analysing general activity and exploratory behaviour in a new environment in rodents. In this thesis, two different OFs were used.

For the behavioural experiments with viral vectors, the OF arena consisted of a square grey plastic cage (56 x 36.5 x 31 cm) which included an object in the centre of the arena (measuring 7 x 6 x 6 cm) to further study the exploratory behaviour of the animals. Animals were initially placed facing one of the corners of the arena, and their behaviour was videotaped for 15 min from the top. Testing was performed in dimly light conditions and without the presence of the investigator. The cages were cleaned between trials with a solution of soap water and dried with paper.

The variables measured in this test were the distance travelled by the animals, the number of rearings, the number and time of interaction with the object, the number of grooming episodes and the total duration of

grooming. The distance travelled was analysed with the SMART software whereas the other variables were measured by The Observer XT 11 program. The criteria for behavioural evaluation were the following:

- Rearings were considered when the animals' posture consisted on standing on both hind paws in a vertical upright posture.
- Interaction with the object was defined as making direct contact with the object, including sniffing, smelling or touching it with the front paws or nose. Non-directed contacts, such as touching it with the tail, were not included.
- Grooming was defined as a rapid wiping of the head usually with both forepaws. Grooming episodes are highly stereotyped and include different behaviours: licking the fur, washing the face, and scratching with a hind leg. Both the number of grooming episodes and the duration of these episodes were counted.

For the experiment of characterisation of the short-term behavioural effects of inescapable footshock exposure, a circular OF was used. The circular OF (80 cm diameter x 34 cm height) had white wooden walls and was placed over a black base. Testing was performed in dimly light conditions and without the presence of the investigator. Animals were initially placed facing the walls and their behaviour was videotaped for 5 min. The OF was carefully cleaned between animals with soap and water. For the behavioural analysis, the OF was divided into two concentric circles to separate the centre and periphery, and the inner circle had a 30 cm diameter. The variables measured in this test were the distance travelled by the animals in the centre and the periphery, as well as the total distance travelled.

3.5. Hole Board (HB)

The hole board (HB) test (see File and Wardill, 1975) is used to evaluate the activity and exploratory behaviour of rodents confronted with a new environment by measuring the distance travelled by the animal and the number head-dips and head-dipping time in the holes of the apparatus.

The apparatus consisted of a white wood box (62 x 53 x 28 cm) with four 4,5-cm diameter equidistant holes on the floor. Rats were placed in a corner of the box facing the wall and tested for 5 min. After each session, the apparatus was cleaned with soap water. Behaviour was videotaped from the top. The distance travelled in the periphery and the centre, as well as the total distance were measured in the SMART software, while the number of rearing episodes and the number and time of head-dipping behaviour (introducing the head in the holes at least until the level of the eyes) were measured by The Observer XT 11 program.

3.6. Forced Swim Test (FST)

The FST was developed by Porsolt and collaborators (1977) to evaluate the efficacy of antidepressant treatments and depression-like states in rodents. However, currently, its use is mainly directed at evaluating coping strategies in an inescapable situation. Furthermore, FST can be also considered as a predominantly emotional stressor per se (for a review see Armario, 2021). In this thesis, the FST was employed to study active (struggling) vs passive (immobility) coping strategies in a stressful situation.

The test was performed in plastic Plexiglas transparent cylinders of 40 cm height and 19 cm inner diameter mounted on a base of 25 x 25 cm containing water at 36-37 °C to a level of 25 cm. Water was always changed for each rat, and the temperature of the water was monitored before exposure of each animal. Classical FST is performed in water at around 20 °C, but this results in hypothermia (Dal-Zotto et al., 2000), so we exposed animals to water at 36-37 °C to avoid the physical component of swimming at a low temperature (Armario, 2021). Two animals from the same home cage were exposed simultaneously in 2 cylinders, separated by opaque screens to prevent visual contact with each other. The duration of the test was 15 min, and immediately after the subjects were removed from the water and dried with a towel. Since it has been previously described that rats show very low levels of activity after the first 5-min period of the FST (Martí and Armario, 1993), we focused on this time block for analysis of the behaviour.

Behaviour was videotaped from the front and all behavioural scoring was performed by an experimenter blind to the treatment in the Observer XT 11. The parameters measured were:

- Struggling, making active movements, including strongly moving the four limbs, breaking the surface of the water with the forelimbs, scratching the walls, or diving or jumping.
- Mild swim, swimming around the tank, moving all four limbs but with less intensity than struggling. Mild swim was calculated by subtracting from the total test time the animal spent immobile and struggling.
- Immobility, floating in the water and making only those movements necessary to keep the head above water.

4. Biochemical analysis

Corticosterone levels in plasma were determined by a double-antibody radioimmunoassay (RIA). The procedure followed was based on the RIA protocol recommended by Dr G. Makara (Institute of Experimental Medicine, Budapest, Hungary). A sodium phosphate buffer 0.2M, pH 7.4 with Milli-Q water was used. Samples were incubated with citric acid 0.1M for 2 h at room temperature (RT) to inactivate plasma corticosteroid-binding globulin (CBG). Corticosterone RIA used ¹²⁵I-corticosterone-carboxymethyl oxime-tyrosine-methyl ester (MP Biomedicals, Germany, Ref. 07-120128 Tracer 50 µCi, specific activity 1500-2000 µCi/µg, working solution 5000-5500 CPM/200 µL), synthetic corticosterone (Sigma, Barcelona, Spain) as the standard and an antibody against corticosterone (kindly provided by Dr G. Makara) diluted 1:60 in assay buffer with 0.15% normal rabbit serum (NRS). The free fraction was separated using a second antibody (donkey anti-rabbit IgG, Ref. R2004, Sigma) diluted 1:50 in assay buffer, polyethyleneglycol 7.5% (in Milli-Q water) containing 10 µL/tube of cow serum. After incubation, samples were centrifuged for 30 min at 4700 rpm at 4 °C (SIGMA-Laboratory Centrifuges 6K15). Samples were run in duplicate, and all samples to be statistically compared were run in the same assay to avoid inter-assay variability. The intra-assay coefficient of variation was 7 % for corticosterone and the sensitivity was 2 ng/mL for 1 µL of sample. Radioactivity of the precipitates was measured with a gamma counter (Wallac 1272, Clinigamma) and calculations to determine corticosterone concentration were obtained by using a log-B/B0 transformation.

5. Perfusion and histological processing

5.1. Perfusion

The two animals in the same home cage were always euthanized simultaneously in order to minimise distress and alteration of basal levels of RNA expression in the brain samples. Animals were anaesthetised by inhalation in a chamber saturated with isoflurane (Laboratorios Esteve) and with an oxygen flow of 1-2L/min within 30 seconds after they were removed from the animal room or from the room in which they were exposed to stress. The deeply anaesthetised state was maintained during the beginning of the perfusion by introducing the rat head in a container with a cotton piece soaked in isoflurane. They were perfused transcardially via the

ascending aorta, firstly with sterile saline solution (0.9% NaCl) for 1-2 min (depending on the experiment), and then with 3,7 - 4% paraformaldehyde (PFA, Casa Álvarez Material Científico S.A., Spain) for 10 min. Perfusion solutions were kept at 4 °C during the procedure. After perfusion, their brains were extracted, post-fixed in PFA and stored at 4 °C overnight (O/N). Then, they were embedded in a cryoprotectant solution containing 30% sucrose (in potassium phosphate-buffered saline (KPBS; 0.2 M NaCl, 43 mM potassium phosphate) until they were totally submerged (3 - 4 days at 4 °C). The brains were then frozen in dry ice-cooled isopentane (at approximately - 40 °C) for 2 min and stored at - 80 °C until sectioning.

5.2. Brain sectioning

Sections were obtained serially with a cryostat (Ref. CM3050-S, Leica Microsystems). In the cryostat, the brains were warmed to -21 °C and then fixed to a platform with Tissue-Tek (O.C.T.[™], LabTech). For all the experiments of the thesis, coronal sections of 20 µm thickness were taken from all the brain (for other experimental purposes), except for the PVN that was sectioned at 14 µm due to the high density of c-fos+ cells after stress exposure, which would complicate the quantification of individual cells. Sections were collected in anti-freeze solution (0.05 M sodium phosphate buffer, pH 7.3, 30% ethylene glycol, 20% glycerol) and stored at -20 °C until further processing.

6. Fluorescent in situ hybridisation (FISH)

6.1. Probes generation

The c-fos mRNA antisense probe was generated from the EcoRI fragment of rat c-fos DNA (Dr I. Verma, The Salk Institute, La Jolla, CA), subcloned into a pBluescript SK-1 (Stratagene, La Jolla, CA) and linearised with SmaI (Ref. R0141S, New England BioLabs) The intronic c-fos probe was a kind gift from Dr Lin (California Institute of Technology, Caltech, CA) and it was linearised with Sall (Ref. R0138S, New England BioLabs). The c-fos intronic probe targets specifically the first intron of the c-fos gene and hence, only detects immature or nuclear intronic c-fos RNA. In contrast, the c-fos mature RNA (mRNA) antisense probe was directed against the first three exons of the c-fos gene and half of the four exon (**Fig. 8**). We and others noticed that due to the length of the mRNA probe and the nature of the

hybridisation process, the probe can also bind to the intronic transcript, which also contains the exonic sequences (Lin et al., 2011b).

In each transcription to produce the probes, 1 µg of digested plasmid was used as DNA template and UTP labelled with Digoxigenin or Fluorescein (DIG/Fluorescein RNA Labelling Mix 10X conc, Roche) was used as labelled ribonucleotide for *c-fos* intronic RNA and *c-fos* mRNA antisense probes, respectively. After transcription, the cDNA template was digested with RNase-free DNase I (T7 transcription Kit, Roche). Then 45 µL of a sodium chloride-Tris-EDTA buffer solution (STE, 0.1 NaCl, 10 mM Tris-HCl, 1 mM EDTA pH 8.0) were added and the mixture was incubated at 65 °C for 5 min to inactivate enzymes. The probes were isolated through gel filtration columns (mini Quick Spin RNA Columns, Ref. 11814427001, Roche) and stored at -20 °C until use.

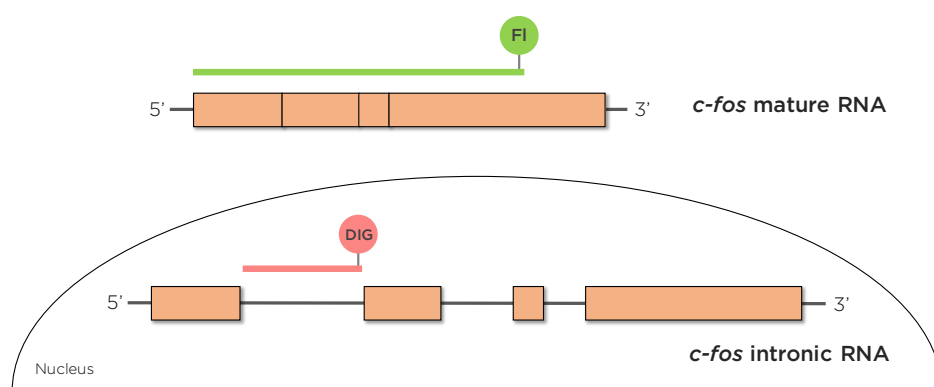


Figure 8. Schematic representation of the two probes used to detect both *c-fos* transcripts and their location.

The probe directed against the *c-fos* mature RNA, mainly located in the cytoplasm, targets the first three and half of the fourth exon of the *c-fos* gene and it is labelled with fluorescein (FI). The probe specific for the *c-fos* intronic RNA, located in the nuclear compartment, is directed against the first intron, only present in the immature or intronic transcript and it is labelled with digoxigenin (DIG). The colours used for representing the probes and labels have been used to aid visualisation and understanding of the scheme, but the fluorescence at these particular wavelengths is provided by the tyramide signal amplification process (detailed below).

6.2. In situ hybridisation assay (ISH)

Sections used for the In situ hybridisation assay (ISH) were rinsed three times with KBPS to remove the anti-freeze solution and they were mounted on slides (Superfrost Plus, Thermo Scientific). Sections were left overnight (O/N) drying and then they were stored at -20 °C in sealed boxes containing a drying agent (Silica Gel PS, Fluka) until the FISH procedure was performed.

The FISH protocol used was adapted from Simmons et al. (1989). All the solutions used in the pre-hybridisation and hybridisation steps were pre-treated with diethylpyrocarbonate (DEPC; Ref. D5758, Sigma-Aldrich) and sterilised in the autoclave prior to use to ensure they were RNase-free. Sections were first post-fixed in 3.7 - 4% PFA (Casa Álvarez) for 20 min and then they were washed in KPBS 4 times to remove the remaining fixation solution. Afterwards, sections were digested with proteinase K (Ref. 3115879001, Roche) at a concentration of 0.01 mg/mL in 100 mM Tris-HCl pH 8.0, and 50 mM EDTA, pH 8.0, for 15 min at 37 °C. After digestion, sections were washed with DEPC-treated water and then in 0.1 M triethanolamine pH 8.0 (TEA; Ref. T58300, Sigma) and acetylated with 0.25% acetic anhydride (Ref. 320102, Sigma) in 0.1 M TEA pH 8.0. Then sections were washed in 2x saline-sodium citrate solution (SSC; Ref. S4641, Sigma) which contained 0.3 M NaCl, 0.03 M sodium citrate tribasic, and dehydrated through graded increasing concentrations of ethanol (50%, 70%, 95% and 2x 100%) and finally air-dried for at least 1h.

Once the sections were dried, 150 µL of hybridisation buffer (50% formamide, 0.3 M NaCl, 10 mM Tris-Cl pH 8.0, 1 mM EDTA pH 8.0, 1x Denhardt's solution, 10% dextran sulphate, yeast tRNA 500 µg/mL, and 10 mM dithiothreitol [DTT]), containing the DIG-labelled c-fos intronic RNA probe (1:2000) and the Fluorescein-labelled c-fos mRNA probe (1:2000) were added onto each slide. Then slides were covered with a coverslip and incubated in a humid chamber for 18h at 60 °C. After hybridisation, sections were washed 4 times in 4x SSC at 37 °C and were digested with RNase A (Ref. 10109169001, Roche) at 200 µg/mL in an appropriate buffer (0.5 M NaCl, 10 mM Tris-HCl pH 8.0, 1 mM EDTA pH 8.0) at 37 °C for 30 min. Then sections were washed at RT in descending concentrations of SSC (from 2x to 0.5x), then heated at 60 °C in 0.1x SSC for 30 min and rinsed in 0.1x SSC at RT. Then sections were stored in a Tris-buffered saline with Tween 20 [T-TBS; 0.1 M Tris-HCl pH 7.5, 0.15 M NaCl, 0.05% Tween 20 (Ref. P7949, Sigma)].

Sections were incubated with H₂O₂ (Ref. 216763, Sigma) at 3% in a Tris-buffered saline (TBS: 0.1 M Tris-HCl, pH 7.5, 0.15 M NaCl) for 30 min at RT. After peroxidase (POD) blocking, non-specific binding was blocked during 1h at RT with blocking buffer [2% bovine serum albumin (BSA; Ref. A7906, Sigma) and 3% fetal calf serum (FCS) in T-TBS]. Slides were then incubated with an anti-Digoxigenin antibody (Anti-DIG-POD, Ref. 11093274910, Roche) at a concentration of 1:2000 in antibody blocking solution (1% BSA in T-TBS) using incubation chambers (CoverWell, Ref. C18151, Grace Bio-Labs), O/N at 4 °C. After incubation, sections were washed 4 times with T-TBS to remove the excess antibody solution and the

signal was amplified using the tyramide signal amplification kit (TSA-Plus Cyanine 5, Ref. NEL745001KT, Akoya Biosciences) which generates a precipitate with an emission peak at 667 nm. 80 μ L of TSA-Cyanine 5 were added to each slide at a concentration of 1:50 in amplification solution, slides were covered with a coverslip and the amplification reaction was left for 10 min. Then sections were washed twice in T-TBS and POD was blocked as described before to prevent the crossing of the signal from the first amplification to the second amplification, given the fact that both antibodies used are conjugated to POD. After this, non-specific signal was blocked with a blocking solution for 1h at RT. Then, excess blocking solution was removed and an anti-Fluorescein antibody (Anti-Fl-POD, Ref. NEF710007EA, PerkinElmer) was added at 1:500 in antibody blocking solution using incubation chambers. After incubation O/N at 4 °C, sections were washed 4 times with T-TBS and the signal was amplified using the tyramide signal amplification kit (TSA-Plus Fluorescein, Ref. NEL741001KT, Akoya Biosciences) which generates a green precipitate with an emission peak at 517 nm. Again, 80 μ L of TSA-Fluorescein were added to each slide at a concentration of 1:50 in amplification solution, slides were cover-slipped and incubated for 10 min.

After the amplification reaction, slides were rinsed in T-TBS and nuclei were counterstained with Hoechst 33258 pentahydrate (Ref. H3569, Invitrogen) at 1:10000 in TBS for 5 min. Finally, slides were washed with TBS and rinsed with deionized H₂O to remove the excess of salts. Slides were air-dried and cover-slipped (Menzel™, Ref. 101BB024060, Sudelab) with an aqueous mounting medium (Fluoromount™, Ref. F4680, Sigma) and their edges sealed with rapid mounting medium (Entellan, Ref. 1079600500, Merck). Slides were stored at 4 °C in an opaque box to avoid exposure to light and were used for confocal microscopy within 1-2 months after performing the FISH for optimal image quality.

6.3. Image acquisition and quantification

The brain areas analysed were the PL and IL subdivisions of the mPFC and the coordinates used for histological analysis were between Bregma 3.20 mm and 2.70 mm, based on the stereotaxic atlas by Paxinos and Watson (2014). A stack of 12 sections with a thickness of 0.7 μ m per step was taken for each stained mPFC section in the Leica TCS SP5 confocal microscope (Servei de Microscòpia, UAB). Each channel was acquired in “Sequential Mode, Frame” to excite only that particular fluorophore and therefore avoid bleed-through and emission spectral overlap. A total of 4-6 images for mPFC superficial layers and 4-6 images for mPFC deep layers of the PL and IL of each animal were taken at 40X magnification to ensure proper visualisation

of the intronic RNA staining. Hoechst was visualized at 405 nm, c-fos mRNA at 488 nm (FITC channel) and c-fos intronic RNA at 633 nm (Rho/TRed channel).

For image analysis, the free software ImageJ (FIJI, version 1.51) was used. Original images were never modified for their subsequent analysis and both throughout image acquisition and quantification the researcher was blind to the treatment. A total of 4 images per animal were analysed for each region and averaged to produce a mean cell count per region. The quantification was based on manually determined regions of interest (ROI) using ImageJ since the scattered signal pattern of c-fos mRNA prevented automated analysis. The specificity of the FISH signal was verified by colocalization of the labelled probes with DAPI. The three channels of the image were separated into nuclear staining, c-fos mRNA and c-fos intronic RNA, and data were analysed as follows:

- 1) The threshold for c-fos mRNA quantification was determined by calculating the background signal for c-fos mRNA+ cells counting the mean integrated density (IntDen) value of 30 ROIs per image. The positivity threshold for c-fos mRNA was considered when the IntDen value of a selected cell exceeded 3 standard deviations (STD) above the average background.
- 2) Those cells presenting cytoplasmic labelling were selected and were considered c-fos mRNA+ cells if their IntDen was above the background + 3STD.
- 3) Those cells that presented mRNA labelling in both the cytoplasm and the nucleus (it must be considered that the c-fos mRNA probe can also bind to the nuclear transcript, see Lin et al., 2011 for an example) were also selected. For these cells, an extra criterion was applied to the background + 3STD, which considered the fluorescence corresponding to the nuclear labelling for each image.
- 4) c-fos intronic RNA+ cells were identified by the presence of one or two intense intranuclear fluorescent foci. Cells that contained low-intensity diffused intranuclear RNA signal were not considered intronic RNA+ cells.
- 5) Then the colocalization between c-fos mRNA and intronic RNA was calculated by counting the number of cells which were double-positive for c-fos mRNA and intronic RNA.

The number of positive cells per group was calculated as the average obtained of all analysed images per animal and then averaged per group. This number was then converted to cells per mm². For cell counts, N refers to the number of animals.

7. Immunofluorescence

The primary and secondary antibodies used for immunofluorescence procedures in this thesis are shown in the following table (**Table 4**).

Table 4. Primary and secondary antibodies used for immunofluorescence.

	Target antigen	Host	Dilution	Reference	Company
<i>Primary antibodies</i>	c-fos	Goat	1:500	sc-52-G	Santa Cruz Biotechnology
	GFAP	Rabbit	1:1000	Z0332	Dako
	mCherry	Rabbit	1:500	Ab167453	Abcam
	NeuN	Chicken	1:500	ABN91	Millipore
	pS6 (S244/247)	Rabbit	1:1000	44-923G	ThermoFisher Scientific
<i>Secondary antibodies</i>	Anti-chicken A488	Goat	1:500	A11039	Life Technologies
	Anti-goat A488	Donkey	1:500	A11055	Life Technologies
	Anti-rabbit A488	Goat	1:500	A11008	Life Technologies
	Anti-rabbit A647	Donkey	1:500	A31573	Life Technologies

7.1. Immunostaining protocols

All the procedures of immunohistochemistry used in this thesis were performed on free-floating sections. For NeuN/mCherry and GFAP/mCherry colocalization experiments, sections were washed three times in Phosphate Buffer Saline (1x PBS) and then incubated in blocking solution (1% BSA in 1x PBS with 0.2% Triton X-100) for 1h at RT. Then sections were incubated either with the NeuN antibody (for neuronal staining) or with the GFAP antibody (for astrocyte labelling) in blocking solution O/N at 4 °C. The next day, sections were left for 1h at RT and then washed in 1x PBS three times and incubated with the secondary antibodies (Alexa Fluor 488-conjugated anti-chicken for NeuN and anti-rabbit for GFAP) in a blocking solution for 1h at RT. The slices were then washed in 1x PBS and stained with Hoechst 33258 (1:10000 in 1x PBS) for 3 min at RT, washed again with PBS 1x and mounted on slides as previously described in the FISH protocol.

For double-labelling of pS6 (S244/247) and c-Fos, sections were washed three times in 1x TBS and then incubated in blocking solution (5% Normal Donkey Serum, NDS in 1x TBS with 0.4% Triton X-100) for 1.5h at RT. Then sections were incubated with both c-Fos and pS6 antibodies in blocking solution O/N at 4 °C (note that a prior titration of the primary antibody for pS6 was conducted to determine the optimal conditions for this antibody). After three washes in 1x TBS, sections were incubated with the secondary antibodies (Alexa Fluor 488-conjugated anti-goat for c-Fos and Alexa Fluor 647-conjugated anti-rabbit for pS6) in a blocking solution for

2h at RT. The slices were then washed in 1x TBS and counterstained with Hoechst 33258 (1:10000 in 1x TBS), washed twice in 1x TBS and mounted onto slides. All dry-mounted sections were stored at 4°C in an opaque box until image acquisition.

mCherry immunostaining was performed to amplify endogenous mCherry fluorescence. To do so, mPFC sections were washed three times in 1x KPBS and then incubated in blocking solution (5% NDS in 1x KPBS with 0.4% Triton X-100) for 1.5h at RT. Sections were then incubated with anti-mCherry antibody in blocking solution O/N at 4 °C. After three washes in 1x KPBS, sections were incubated with the secondary antibodies (Alexa Fluor 647-conjugated anti-rabbit) in a blocking solution for 2h at RT. The slices were then washed in 1x KPBS and counterstained with Hoechst 33258 (1:10000 in 1x Milli-Q H₂O), washed twice in 1x KPBS and mounted onto slides. All dry-mounted sections were stored at 4 °C in an opaque box until image acquisition. It must be noted that mCherry immunofluorescence was only performed in the experiments shown in Section 3.1. of the results. In the experiments that followed, mCherry signal was visualised without antibody amplification given that a prior quantification pilot showed that there was a very high correlation between the number of mCherry cells counted with mCherry antibody and without antibody.

7.2. Image acquisition and quantification

The brain area used for image capture was the PL subdivision of the mPFC and the coordinates used for histological analysis were between Bregma 3.20 mm and 2.70 mm, based on the stereotaxic atlas by Paxinos and Watson (2014). Stained mPFC sections were examined either by epifluorescence microscopy in the case of NeuN and GFAP staining or by confocal microscopy in the case of pS6 and c-Fos double immunofluorescence and mCherry immunofluorescence (detailed below). All the image quantification analyses of this thesis were performed using the program ImageJ (FIJI, version 1.51). Moreover, all image captures and quantification analyses were performed blind to the experimental conditions. Throughout the thesis, the terms “Intensity” of signal or “fluorescence intensity” described in the results correspond to the measurement of the “Integrated Density or IntDen”.

For NeuN and GFAP immunofluorescence, the epifluorescence microscope EVOS™ M5000 Imaging system (Invitrogen) kindly provided by the Quintana lab was used. Three filters were used for image capture, DAPI for nuclear staining, GFP for either NeuN or GFAP staining, and Texas Red for mCherry labelling. Light, exposure and gain settings were optimised for each staining and maintained constant throughout the entire acquisition

process. 4-6 images from 4-6 sections were taken per animal and from all the images, the two showing the highest mCherry signal from each animal were further selected to perform the quantification analysis. The colocalization analysis for GFAP and mCherry was manually performed by selecting the cells expressing both GFAP and mCherry with the ROI tool. The quantification of the NeuN and mCherry was also performed manually by selecting with the ROI tool all the cells with cytoplasmic red labelling (mCherry+ cells) and with green labelling (NeuN+ cells) and then calculating the percentage of colocalization by dividing the number of mCherry+ cells + NeuN+ cells / mCherry+ cells to determine the percentage of cells transduced by the viral vector that are neurons.

For pS6 and Fos immunofluorescence, stained PL sections were analysed using the Olympus Fluoview 1000 confocal microscope (Servei de Microscòpia, UAB). A stack of 4 sections (2 µm/step) was taken at 20X magnification and 6 images were acquired from 6 sections of each animal. Three lasers were used: 1) 405 nm laser for Hoechst staining, 2) 488 nm laser for Fos staining and 3) 633 nm laser for pS6 labelling. The number of pS6 positive cells was counted using a semi-automated analysis macro generated using the “Analyze Particle” tool from the program ImageJ (FIJI, version 1.51), with a defined level of background intensity and cell size (previously validated manually). Cells that passed this threshold were selected using the ROI tool and then the IntDen of each cell in the original image was also measured. The number of Fos positive nuclei was counted by selecting with the ROI tool those cells whose IntDen was above the background intensity of the image (determined with the average IntDen of 20 ROIs randomly distributed in regions without specific signal) + 3STD. Both the number of positive cells and the IntDen of each cell were quantified. Both channels were merged with the Hoechst nuclear staining to confirm that the selected ROIs corresponded to a cell and discard non-specific labelling. Then the number of cells positive for both pS6 and Fos was also quantified to calculate the percentage of colocalization.

For mCherry immunofluorescence, stained PL sections were analysed using the Olympus Fluoview 1000 confocal microscope (Servei de Microscòpia, UAB). For the experiment in section 3.1, three lasers were used: 1) 405 nm laser for Hoechst staining, 2) 559 nm laser for mCherry endogenous fluorescence and 3) 633 nm laser for mCherry amplified signal. For experiments in the rest of chapter 3 of the results, only two lasers were used: 1) 405 nm laser for Hoechst staining, and 2) 559 nm laser for mCherry endogenous fluorescence. Serial stack images (8 planes, 2 µm each) were acquired at 20x magnification. For each subject, 2 images per section covering the full extent of viral expression were captured from the 6 sections

with the highest mCherry signal (a total of 12 images per animal). mCherry-positive cells were counted manually by setting an intensity threshold (the same for all the subjects) to filter out background levels of fluorescence. Total fluorescence intensity signal per image and averaged per cell were also measured.

In all cases, the number of cells and IntDen shown for each experimental group was calculated as the average obtained from all the analysed images for each animal and then averaged for all the animals of the experimental group. The number of positive cells was converted to cells per mm² and N refers to the number of animals.

8. Viral vector generation and delivery

8.1. Viral vectors design

All the viral vectors used in this thesis were designed in the free design VectorBuilder platform and the plasmid constructs were also generated by the company VectorBuilder, Inc (Chicago, IL, USA).

The expression construct AAV-fos:hM3Dq:mCherry was designed by introducing the c-fos minimal promoter sequence (720 bp, based on Gore et al., 2015) driving the expression of the excitatory DREADD (hM3Dq) fused to the fluorescent reporter mCherry (2502 bp, based on the plasmid pAAV-hSyn-hM3D(Gq)-mCherry from the Roth lab, Ref. 50474, Addgene). Then the woodchuck hepatitis virus posttranscriptional regulatory element (WPRE) and the polyadenylation signal from the bovine growth hormone (BGH pA) were also introduced, all flanked by the 5' and 3' inverted terminal repeats (ITRs).

The expression constructs AAV-fos(Int+Ex):hM3Dq:mCherry:PEST and AAV-fos(Int+Ex):hM4Di:mCherry:PEST were designed by introducing the c-fos promoter followed by the sequence of the first exon and intron of the c-fos gene (1659 bp, based on the construct pFos-ChR2:EYFP:PEST from the Deisseroth lab; Ye et al., 2016) driving the expression of either the excitatory DREADD (hM3Dq) or the inhibitory DREADD (hM4Di) fused to mCherry (Ref. 50474 and Ref. 50475 plasmids from the Roth lab, Addgene, respectively). The stop codon TAA from the mCherry sequence was removed and the rest of the sequence was fused to the PEST sequence, a 120 bp fragment from the ornithine decarboxylase gene from the rat. Finally, the BGH pA was also added to the plasmid sequence. All the sequence was flanked by the 5' and 3' ITRs. To overcome transgene size

limitations inherent to the use of AAVs we had to remove the WPRE sequence.

8.2. Viral vector production

The plasmid AAV-fos:hM3Dq:mCherry was amplified from a glycerol stock using the ZymoPURE II Plasmid Maxiprep Kit (Ref. D4202, Zymo Research) following the manufacturer's instructions. The expression construct AAV-fos:hM3Dq:mCherry was produced by the co-transfection method with Human Embryonic Kidney (HEK) 293T cells with a helper plasmid as described by Quintana et al. (2012). Specifically, HEK293T cells kindly provided by the Quintana lab were grown in complete Dulbecco's Modified Eagle Medium without pyruvate (DMEM, Ref. 41965039, Gibco) supplemented with 10% heat-inactivated fetal bovine serum (HIFBS, Ref. 10270106, Gibco) and 2% penicillin/streptomycin (Ref. 15140122, Gibco). HEK293T cells were seeded at a density of 3.7×10^6 cells/100 mm plate in 110 plates and maintained at 37 °C and 5% CO₂ for 24 h. The day after, HEK293T cells were transfected with the pAAV-fos:hM3Dq:mCherry plasmid and the helper plasmid pDP1 (Ref. PF431, Plasmid Factory, Germany), which encodes the genes needed for the replicative cycle and the capsid (rep and cap genes) and the adenoviral helper genes needed for AAV replication (E4, E2a and VA) (see **Table 5**). This helper encodes for the serotype AAV1. The transfection protocol was based on the calcium phosphate transfection method. Briefly, the DNA solution was added dropwise to the HEPES solution while constant vortexing and then incubated at RT for 10 min. 800 µL of transfection solution were added dropwise to each cell plate, and 14-16h post-transfection the culture medium was exchanged for serum-free DMEM. 72h post-transfection cells were harvested and subjected to 4 freeze-thaw cycles followed by vortexing after each thaw to lyse the cells and release the viral vector particles.

Table 5. Components of the transfection solution.

DNA solution	Volume/amount per plate
2 M CaCl ₂	50 µL
Plasmid of interest	10 µg
Helper plasmid (pDP1)	20 µg
H ₂ O (Cell culture grade water)	Up to 400 µL
HEPES solution	Volume per plate
2x HBS (280 mM NaCl + 50 mM HEPES, pH = 7.05)	394 µL
Phosphate solution (49.5 mM NaH ₂ PO ₄ + 100.5 mM Na ₂ HPO ₄)	6 µL

Cells were centrifuged at 2000 rpm for 30 min at 4 °C and the vector-containing supernatant was transferred to sterile ultracentrifuge tubes (Ref. 344058, Beckman Coulter, Life Sciences) containing 13 mL of a 40% sucrose solution in 1x PBS. Tubes were centrifuged at 25000 rpm O/N at 4 °C. Then the pellet was resuspended with 5 mL of a CsCl solution at a density of 1.37 g/mL in an ultracentrifuge tube (Ref. 355537, Beckman Coulter, Life Sciences) and centrifuged at 41000 rpm O/N at 4 °C. After centrifugation, the solution was dialyzed using a dialysis cassette (Ref. 66810, Fisher Scientific) against 1.5 L of HBSS 1x (Ref. 14175095, Gibco) for 3 h at 4 °C. Then HBSS solution was replaced by fresh HBSS and the dialysis process was left O/N at 4 °C. The equilibrated solution was centrifuged at 4000 rpm for 5 min and the supernatant was transferred to a Beckman tube with 15 mL of a 40% sucrose solution and centrifuged at 25000 rpm O/N at 4 °C. The pellet was resuspended in HBSS 1x, aliquoted and frozen at -80 °C.

The viral titre was determined using real-time quantitative PCR (qRT-PCR) using primers for mCherry (Forward: 5' GAACGGCCACGAGTTCGAGA and Reverse: 5'-CTTGGAGCCGTACATGAACTGAGG). Titres were calculated as viral genome copies based on a standard curve of the plasmid AAV-fos:hM3Dq:mCherry diluted in nuclease-free H₂O to obtain concentrations ranging from 10⁰ to 10⁹ molecules/μL. A viral aliquot was diluted at different concentrations (1/40, 1/400 and 1/1000 in nuclease-free H₂O). All samples were run in triplicate using the PowerUp™ SYBR™ Green Master Mix (Ref. A25741, Applied Biosystems, ThermoFisher Scientific) as detailed in Table 6 following the manufacturer's instructions in the Applied Biosystems 7500 Real-Time PCR System. The viral titre obtained for the viral vector AAV1-fos:hM3Dq:mCherry was 5x10¹² genome copies (gc)/mL.

Table 6. Reagents and volumes used for SYBR Green RT-PCR reaction.

Reagent	Volume (10 μL/well)
SYBR Green Master Mix (2x)	5 μL
Forward primer (10 μM)	0.5 μL
Reverse primer (10 μM)	0.5 μL
DNA template	Variable
Nuclease-free water	Up to 10 μL

The plasmids of the expression constructs AAV-fos(Int+Ex):hM3Dq:mCherry:PEST and AAV-fos(Int+Ex):hM4Di:mCherry:PEST were amplified and encapsulated in serotype 9 (AAV9) by the Viral Vector Production Unit (UPV) from Universitat Autònoma de Barcelona (UAB). The viral titres obtained were 1x10¹³ gc/mL for both viral vectors.

8.3. Viral vector delivery: stereotaxic surgery

For brain region-specific viral vector delivery, rats were deeply anaesthetised with isoflurane (4-5%, v/v) firstly in an induction chamber, and then placed in the stereotaxic frame (Kopf Instruments, Tujunga, CA). Isoflurane at 2-2,5% (v/v) in oxygen, at a rate of 1-1.5 L/min was delivered through a facemask for maintaining anaesthesia. Body temperature was maintained at 37 °C using a heating pad. Ophthalmic ointment (Viscotears® 2mg/g) was applied to both eyes to prevent drying. Three rounds of iodine povidone 10% (v/v, Betadine®) and ethanol 70% (v/v) wipes were applied to the previously shaved scalp for disinfection and a midline incision was made. The head position was adjusted in order to place Bregma and lambda in the same horizontal plane and a drill (Ref. 67-1204, Ideal Micro-Drill™, CellPoint Scientific) was used to gain access to the injection site. Injections of the viral vector were performed bilaterally in the following coordinates (PL; +3.0 mm anteroposterior; \pm 0.6 mm mediolateral; -4.0 mm dorsoventral from Bregma, 0° angle). 0.5 μ L of viral vector was bilaterally infused at a rate of 0.1 μ L/min using a 5 μ L Hamilton syringe attached to a 32-gauge needle (Ref. HV721822, Panlab, Harvard Apparatus). The needle remained in place for an additional 7.5 min to allow viral vector diffusion into the tissue and prevent its back-flow through the injection tract and then it was slowly withdrawn during 2.5 min. At the end of the surgery, rats were administered one subcutaneous injection of the analgesic buprenorphine (0.05 mg/Kg; Buprex®) and the incision was sewed using a sterile silk suture (Laboratorio Aragón, S.L, Spain). Rats were monitored daily for several days after the surgery and behavioural tests started 3 weeks after surgery to allow enough time for the animals to recover and for the viral vector to be adequately expressed. Animals with spatially inaccurate viral injections were excluded from analyses.

8.4. Histological verification of viral vector injections

To determine the injection placement and the viral vector spread, sections from Bregma 4.7 mm to 2.5 mm comprising the whole mPFC were washed three times in KPBS 1x and then incubated with Hoechst 33258 (1:10000 in KPBS) for 3 min at RT. Then they were washed twice in KPBS 1x and mounted onto slides. Slides were allowed to dry for a minimum of 4-6h and then rinsed in Milli-Q water to remove the excess of salts. They were then allowed to dry for at least 1h and covered using mounting medium. Serial images of the viral vector injection were acquired using the EVOS™ M5000 Imaging system (Invitrogen) at a 10x magnification and then viral

expression was mapped onto different Bregma coordinates by outlining the spread of mCherry expression onto corresponding brain atlas illustrations Paxinos and Watson (2014). Occasional rats not showing bilateral AAV expression in the PL or that showed important targeting of neighbouring areas were excluded from the analysis.

9. Drugs

Clozapine-N-Oxide (CNO, Cat. No. 4936, Tocris, UK) dissolved in 1% DMSO in saline (0.9% NaCl) at a dose of 1 mg/kg was intraperitoneally injected into the rats 30 min prior to behavioural testing. For control rats, the same volume of vehicle (1% DMSO in saline) was injected.

10. PhosphoRiboTRAP and RNA-sequencing

10.1. Stimuli and brain dissection

The procedure of ribosome immunoprecipitation using an anti-pS6 antibody was based on Knight et al. (2012) with some modifications. Control and stress animals (1h restraint, 1h IMO, 1h IS) were sacrificed by decapitation and the PL cortex between Bregma 4.20 and 2.76 mm was rapidly dissected using an ice-cold stainless brain matrix (World Precision Instruments) as shown in **Fig. 9**. The region of interest was collected into nuclease-free Eppendorf tubes and immediately frozen in liquid nitrogen, and then stored at -80 °C.

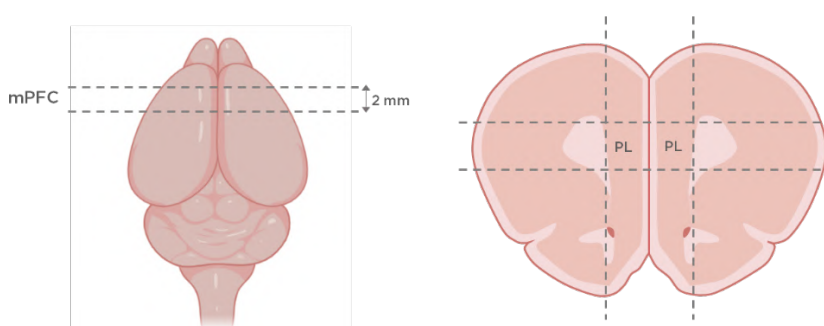


Figure 9. Graphical representation of the cuts performed in the rat brain (discontinued lines) to dissect the prelimbic cortex.

First, the brain was cut in dorsal position in the brain matrix with an interval of 2 mm (left) to dissect the medial prefrontal cortex (mPFC) and then the dissected section was cut in a coronal position to isolate the prelimbic (PL) cortex (right).

10.2. Coupling beads with pS6 antibody

The day before immunoprecipitation, protein A dynabeads (Ref. 10002D, ThermoFisher Scientific) were loaded with the anti-pS6 antibody previously described. We added the necessary amount of protein A dynabeads for the total number of IPs to be performed (100 μ L/IP). Beads were washed twice with 0.15M KCl wash buffer using the microtube rotator (Thermo Fisher Scientific, Ref. 88881002) in the cold room (4 °C) at a speed 20 for 5 min using the magnet (Ref. 1232D, Invitrogen™). Beads were then resuspended in 0.15M KCl wash buffer (300 μ L/IP, **Table 7**), loaded with 4 μ g/IP of anti-phosphoS6 244/247 antibody (anti-pS6 from now on) and incubated O/N at 4 °C in the microtube rotator with gentle end-over-end mixing. The antibody used was different from the originally used by Knight and colleagues and we did not use any blocking peptides during immunoprecipitation as done by them, since this anti-pS6 antibody is specifically directed at the last two phosphorylation sites at the C-terminal domain (S244 and S247) and it has been described that phosphorylation at these two serines exhibits greater enrichment of cell-type-specific transcripts and lower background than other antibodies recognising more proximal sites (Knight et al., 2012).

Table 7. Composition of the 0.15M KCl wash buffer for the PhosphoRiboTRAP procedure.

Reagent	Reference	Company	Final concentration	Volume per sample
HEPES pH 7.4	H3784	Sigma	100 mM	20 μ L
KCl	P-3911	Sigma	150 mM	150 μ L
MgCl ₂	M2670	Sigma	5 mM	10 μ L
IGEPAL® CA-630	18896	Sigma	1 % (v/v)	200 μ L
BSA IgG-free	001-000-161	Jackson Immunoresearch	0.05 % (w/v)	1 mg
Nuclease-free H ₂ O	46-000-CM	Corning	-	1620 μ L

Note: the concentration and volume of all the reagents used for a total volume of 2 mL of 0.15M KCl wash buffer are shown. The reference and source of each reagent are also shown.

10.3. Homogenisation

Frozen PL were transferred to an ice-cold glass homogenizer (2 mL, Ref. 8938, Sigma) previously cleaned with RNaseZAP™ (Ref. 2020, Sigma) and rinsed thoroughly with RNase-free water and containing 1 mL of chilled homogenisation buffer (see **Table 8** for further details). Tissue was homogenized using 40 strokes of the loose-fitting pestle (type A) and 40 more strokes with the tight-fitting pestle (type B). Homogenates were transferred to a nuclease-free Eppendorf tube and clarified at 2.000xg for 10

min at 4 °C. The supernatant was transferred to a new tube and the pellet was discarded. Then 70 µL of 10% IGEPAL and 70 µL of 1,2-diheptanoyl-sn-glycero-3-phosphocholine (DHPC, Ref. 850306P, Avanti Polar Lipids, Sigma-Merck) were added to the supernatant and tubes were mixed by inversion and incubated on ice for 2 min. The clarified supernatant was centrifuged at 17.000xg for 10 min at 4 °C. The supernatant was transferred to a new nuclease-free Eppendorf and a 25 µL aliquot was removed and added to a new tube containing 325µL of buffer RLT (Ref. 74004, Qiagen) supplemented with DTT (20 µL per 1 mL buffer) and stored at -80 °C for future purification as input RNA. The remaining supernatant was used for immunoprecipitation.

Table 8. Composition of the homogenisation buffer for the PhosphoRiboTRAP procedure.

Reagent	Reference	Company	Final concentration	Volume per sample
HEPES pH 7.4	H3784	Sigma	10 mM	20 µL
KCl	P-3911	Sigma	150 mM	150 µL
MgCl ₂	M2670	Sigma	5 mM	10 µL
Nuclease-free H ₂ O	46-000-CM	Corning	-	1820 µL
Supplements				
DTT (1,4-Dithiothreitol)	D0632	Roche	2 mM	2 µL
Protease inhibitor EDTA-free	539134	Calbiochem (Millipore)	1:200	10 µL
RNasin® Ribonuclease Inhibitor	2511	Promega	100 units/mL	5 µL
Cycloheximide	C-7688	Sigma	100 ug/mL	2 µL
Phosphatase inhibitors (PhosSTOP)	4906845001	Merck	1 tablet/10 mL	1/5 tablet
Calyculin A	HY-18983	Eurodiagnostico	100 nM	2 µL

Note: the source and final concentrations of reagents used for a total volume of 2 mL of homogenisation buffer are shown. The reference and source of each reagent are also shown. The supplements (below) were added within 1h before starting the IP protocol because they are highly sensitive to temperature.

10.4. Immunoprecipitation

The pS6 antibody-loaded beads were washed twice with 0.15M KCl wash buffer as previously explained. Then beads were resuspended in 0.2 mL of homogenisation buffer supplemented with IGEPAL and DHPC (so that the buffer had an identical composition to the clarified homogenate) and kept in ice. The remaining supernatant was added to the antibody-loaded beads and placed on the microtube rotator to mix end-over-end for 10 min at 4 °C at a speed of 12. After incubation, beads were washed four times with 0.35M

KCl wash buffer (Table 9). During the third wash, beads were transferred to a new tube and incubated at RT for 5 min to remove any RNA that might have non-specifically stuck to the original tube. After the final wash, the RNA was eluted by adding 350 μ L buffer RLT supplemented with DTT, and incubated at RT for 4 min. Then tubes were vortex thoroughly, placed on the magnet and supernatant was transferred to a new nuclease-free Eppendorf and stored at -80 °C for further purification as IP RNA.

Table 9. Composition of the 0.35M KCl wash buffer for the PhosphoRiboTRAP procedure.

Reagent	Reference	Company	Final concentration	Volume per sample
HEPES pH 7.4	H3784	Sigma	10 mM	40 μ L
KCl	P-3911	Sigma	350 mM	700 μ L
MgCl ₂	M2670	Sigma	5 mM	20 μ L
IGEPAL® CA-630	18896	Sigma	1 % (v/v)	400 μ L
Nuclease-free H ₂ O	46-000-CM	Corning	-	2840 μ L
Supplements				
DTT	D0632	Roche	2 mM	4 μ L
RNasin® Ribonuclease Inhibitor	2511	Promega	100 units/mL	10 μ L
Cycloheximide	C-7688	Sigma	100 μ g/mL	4 μ L
Calyculin A	HY-18983	Eurodiagnostico	100 nM	4 μ L

Note: the source and final concentrations of reagents used for a total volume of 4 mL of 0.35M KCl wash buffer are shown. The reference and source of each reagent are also shown. The supplements (below) were added within 1h before starting the IP protocol because they are highly sensitive to temperature.

10.5. RNA purification and sequencing

RNA was extracted using the RNeasy Micro kit (Ref. 74004, Qiagen) following the manufacturer's instructions and including the in-column DNase treatment to eliminate genomic DNA contamination. RNA concentration was quantified using the Quant-iT RiboGreen RNA Reagent kit (Ref. R11490, Invitrogen™) according to the manufacturer's protocol. Before cDNA library generation, sample RNA integrity (RIN) was assessed using a RNA Picochip on an Agilent 2100 Bioanalyzer (Agilent Technologies, USA). Four biological replicates, each one including the PL of 1 rat, were used for RNA-seq analysis. RNA-seq analysis was performed in the Sequencing Unit of the CNAG-CRG (Barcelona, Spain). cDNA was amplified following the protocol described by Picelli and colleagues (2014) and sequenced in an Illumina NovaSeq6000 platform with an average coverage of 30x106 reads per sample. Each fragment was bidirectionally

sequenced (pair-end) in 2 x 50 bp and the sequencing facility provided the “.fastq” files individually for each sample.

10.6. qRT-PCR analyses

The analysis and validation of the expression of the different transcripts was performed by one-step qRT-PCR using the TaqMan® RNA-to-Ct™ 1-Step Kit (Ref. 4392938, ThermoFisher Scientific) with specific TaqMan probes. Relative expression values were determined by using the method of standard curve (Sanz et al., 2015) and then they were normalised to the levels of the housekeeping gene Actb. For each reaction, the amplification efficiency was calculated using the software AriaMx Real-Time PCR System (Agilent Technologies) and efficiencies between 80-120% were considered acceptable. The genes of interest were determined using specific Taqman gene expression assays (Rn02396759_m1 for c-fos and Rn4453320_m1 for Actb; ThermoFisher Scientific). All samples were run by duplicate, including the standard samples for the curve and the experimental samples, and in all reactions a negative control (non-template control) was included. For qRT-PCR, RNA was diluted to a final concentration of 0.5 ng/L in H2O with yeast tRNA (10 µg/mL, Ref. AM7119, Invitrogen). The reference and amount used of each component is detailed in **Table 10, left** and the amplification cycles, time and temperature are specified in **Table 10, right**.

Table 10. Components and reaction conditions of the TaqMan qRT-PCR reaction.

Reagent	Volume (20 µL/well)	Step	Temp.	Time	Cycles
TaqMan RT-PCR Mix (2x)	10 µL	Reverse transcription	48 °C	15 min	1x
TaqMan RT enzyme (40x)	0.5 µL	Enzyme activation	95 °C	15 min	1x
TaqMan GE assay (20x)	1 µL	Denaturation	95 °C	15 sec	40x
RNA template	1 µL (0.5 ng)	Annealing/ extension	60 °C	1 min	
Nuclease-free water	Up to 20 µL				

A) Details of the reagents used for the qRT-PCR protocol and their corresponding volumes. B) Information about the parameters used in the qRT-PCR protocol. Temp: temperature.

10.7. Bioinformatic analysis of RNA-seq data

Sequencing quality control of the “.fastq” files was assessed using the software FastQC (Andrews et al., 2012). Files were aligned using STAR (version 2.7.10a; Dobin et al., 2013) to mRatBN7.2 reference rat genome and gene counts were obtained using mRatBN7.2.105 genome annotation from Ensembl using the default parameters. The read counts per gene were obtained using “GeneCounts” function from STAR software. Gene counts

were imported to Rstudio (version 4.1.0, R Core Team, 2020) and analysed downstream using R package DESeq2 (version 1.32.0; Love et al., 2014) for normalisation, scaling and negative binomial distribution differential analysis, including batch effect modelling. We used a prefiltering on genes with overall low alignment rate (less than 10 reads among all the samples). The thresholds used for differentially enriched genes between input and IP samples for each condition or between the inputs and/or the IPs of different conditions were an absolute fold change (FC) above 1.5 and an adjusted p-value below 0.05. P-value adjustment was performed with the false discovery rate (FDR) from Benjamini-Hochberg's method (Benjamini and Hochberg, 1995), referred in the results as adjusted p-values (padj). For graphical representation of the data, we used mainly ggplot2 package (version 1.3.1; Wickham et al., 2019) to represent Volcano plots, with the padj values in -log₁₀ scale and the FC in log₂ scale (Log₂FC), and FC plots, which represented Log₂FC values filtering for genes with padj < 0.05. For principal component analysis (PCA), the most variable 500 genes were used and we applied batch correction using the limma package (Ritchie et al., 2015). Heatmaps were created using the pheatmap package for R (Kolde, 2019) with the scaled rlog counts and hierarchically clustering computed by Euclidean distance.

10.8. Statistical analysis

The statistical package for social science' (SPSS) program was used for statistical analysis (version 23 for Windows). Homogeneity of variances was always checked and if needed, variables were log-transformed to improve the homogeneity of variances. When only two independent groups were compared, normality was checked and the unpaired Student's t-test was performed. In the case there were more than two variables to compare, statistical analysis was performed using the generalized linear model (GzLM; McCulloch and Searle, 2001). The GzLM is a more flexible statistical method than the standard general model because several types of data distribution can be selected, it does not require homogeneity of variances and importantly, it admits missing values without removing all data subject. The significance of the effects was determined by the Wald chi-square statistic (X^2) and appropriate post hoc pairwise comparisons followed when needed (sequential Bonferroni's correction or Fisher's least significant difference). Pearson correlation test (two-tailed) was also used to measure the correlation between two variables. In all cases, the criterion for statistical significance was set at $p < 0.05$. All the data, except for the bioinformatic analysis of RNA-seq, are represented as mean and standard error of the mean (SEM) and graphically represented using GraphPad Prism 9.0 (La Jolla, California, USA).

Results

Chapter 1: Identification of neuronal ensembles activated specifically by different emotional stressors in the mPFC

1. Introduction

Numerous studies have characterised the neuronal response to physical and emotional stressors in a wide range of brain areas, including the mPFC, by employing classical IEG labelling techniques (reviewed by Herman and Cullinan, 1997; Pacák and Palkovits, 2001). However, the neuronal activation pattern in response to stress has been mainly studied with relatively prolonged exposure to stressors (e.g. 30 min). Therefore, there is limited knowledge on activation induced by stressors of short duration and the neuronal response after punctual exposure to stress followed by a recovery time, which is the design required for catFISH experiments. Moreover, classical IEG labelling does not allow the characterisation of neurons activated in response to different stimuli within the same animal.

In this thesis, we aim to identify potential stressor-specific neuronal populations in the mPFC, an issue that has been addressed in very limited studies. Previous work from our lab using IF-FISH has suggested that there seem to be some neuronal populations in hierarchically higher areas, such as the mPFC and LSv, that respond specifically to forced swim after prolonged exposure to IMO (Marín-Blasco et al., 2018). These potentially swim-specific neurons are not present in hierarchically lower areas, such as the PVN. Based on this, we proposed to identify whether there are neurons in the mPFC that respond specifically to two different, predominantly emotional, stressors: IMO and IS. We selected IMO and IS because they are considered severe stressors and elicit a similar HPA response immediately after stress (e.g. peak ACTH and corticosterone levels). However, the post-stress recovery of ACTH and corticosterone is delayed in immobilised versus IS-exposed animals (Márquez et al., 2002). Therefore, by selecting two stressors that induce a similar peak HPA response, we could ensure that they mainly differ qualitatively (stressor nature); hence, the potential specificity of response that we observe could be attributed to a different quality of the stressors rather than to a different intensity. In order to assess the potential of each stressor to activate specific neuronal populations, we have quantified the overlap between neurons activated by IMO and IS using a double *c-fos* FISH (also termed catFISH) with one probe directed against the spliced or mature *c-fos* RNA and the other probe against the first intron of *c-fos*, which is present exclusively in the intronic transcript.

Based on the above, our **hypotheses** are:

- 1) After brief exposure to stressors (e.g. 5 min), the dynamics of induction of intronic *c-fos* RNA will be extremely fast, with peak levels shortly after stress and decline levels thereafter, whereas the expression of *c-fos* mature RNA will require a period of 15-30 min to reach the peak.
- 2) Since *c-fos* activation in the mPFC has been found to be similar after exposure to different types of emotional stressors, we did not expect major differences in the number of activated neurons between IMO and IS.
- 3) The catFISH technique will allow us to detect neurons activated specifically by the first stressor (only expressing the mature *c-fos* transcript), neurons activated specifically by the second stressor (only expressing the intronic transcript) and neurons activated non-specifically, which will express both transcripts. We expect in the mPFC a large overlapping neuronal population that responds to IMO and IS, and a small population specific for each stressor.

The specific **objectives** of the present chapter are:

- 1) To characterise the dynamics of expression of mature and intronic *c-fos* RNA in the mPFC after a short exposure to an emotional stressor and determine the optimal duration of stressor exposure that ensures, first, that the second stressor mainly induces *c-fos* intronic RNA and not *c-fos* mature RNA and second, that the intronic transcript corresponding to the first stressor has declined.
- 2) To compare neuronal activation in response to IMO and IS and to analyse whether neuronal activation in response to the second stressor is affected by exposure to a first stressor (either sensitisation or desensitisation of the response).
- 3) To identify whether there are stressor-specific neuronal populations in the mPFC using sequential exposure to two different emotional stressors (IS and IMO).

2. Temporal dynamics of *c-fos* RNA expression after IMO exposure

2.1. Experimental design

To study the temporal dynamics of *c-fos* RNA expression in response to a predominantly emotional stressor (IMO), 22 adult male SD rats were randomly assigned to 6 different groups (**Fig. 10**). Three groups consisted of exposing animals to 5, 8 or 15 min of IMO and immediately perfusing them: IMO5 (n=3), IMO8 (n=4) and IMO15 (n=3), respectively. Two additional groups were exposed to IMO and perfused after a recovery period (n=4/group): the IMO8 + R group was exposed to 8min IMO and perfused 46 min after the initiation of stress, whereas the IMO15 + R was exposed to 15 min IMO and perfused 2 h after the initiation of stress. Furthermore, a basal group not exposed to any stimulus was used as a control (n=4). We evaluated by dFISH the number of cells expressing *c-fos* intronic RNA, the number of cells expressing *c-fos* mRNA as well as the total intensity of fluorescence signal globally and averaged intensity per cell in the PL cortex.

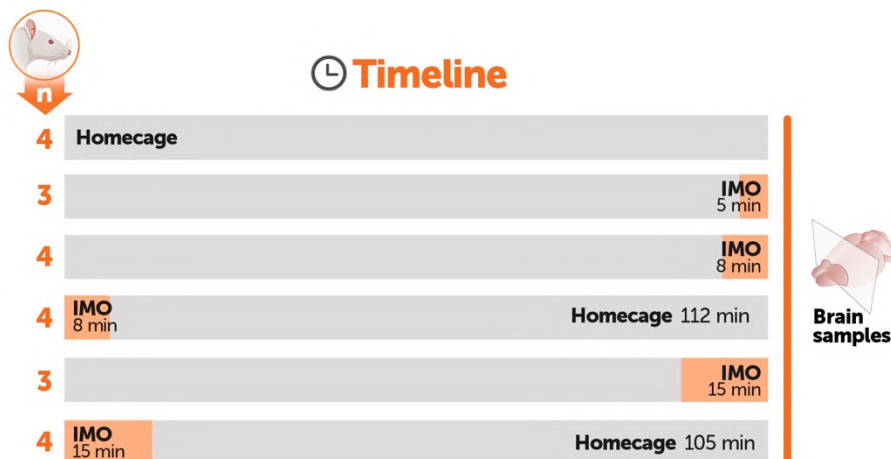


Figure 10. Experimental groups and design for the study of *c-fos* RNA expression after different times of IMO.

Orange colour represents the duration of exposure to IMO and grey represents no stress exposure (home cage conditions). Animals were euthanised by intracardiac perfusion and their brains were obtained for histological analyses.

2.2. Results

Representative images of the dFISH in the PL are shown in **Fig. 11**.

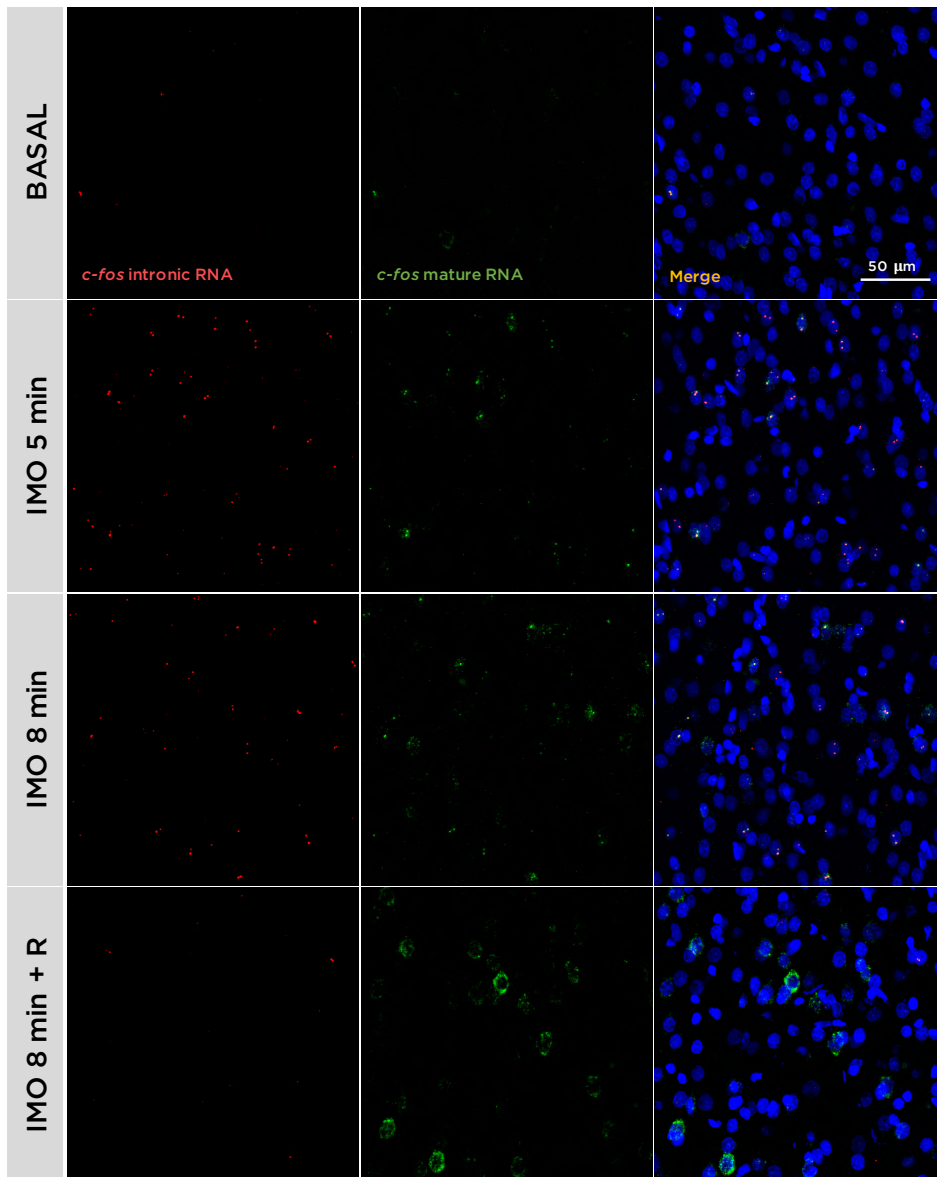


Figure 11. Representative images for expression of *c-fos* intronic and mature RNA in the PL cortex of animals of the experimental groups basal, IMO5, IMO8 and IMO8+R. Left column, labelling of *c-fos* intronic RNA (red); middle column, labelling of *c-fos* mature RNA (green); right column, a composite image showing the merge of the labelling of *c-fos* intronic RNA (red), *c-fos* mature RNA (green) and nuclear staining Hoechst (blue). All images are represented with the same scale.

The expression of both *c-fos* transcripts was quantified in the PL cortex of all the experimental groups (**Fig. 12**). The analysis of the number of cells expressing *c-fos* intronic RNA at different times after exposure to the emotional stressor IMO (**Fig. 12A**) showed a significant effect of the factor group ($X^2(3) = 370.6$, $p < 0.001$). Post-hoc comparisons revealed an increase in the number of *c-fos* intronic RNA+ cells already after 5 min of IMO ($p < 0.001$) and a peak of expression at 8 min of IMO ($p < 0.001$), slightly above values observed in IMO5 ($p = 0.033$). The levels of *c-fos* intronic RNA+ cells markedly declined in the 8 min IMO group after the recovery period ($p < 0.001$ vs IMO8 group), although they remained above basal levels ($p < 0.001$). A GzLM analysis of the number of cells expressing *c-fos* mature RNA (**Fig. 12D**) also showed a group effect ($X^2(3) = 361.3$, $p < 0.001$). In contrast to the intronic RNA, it increased progressively after IMO exposure, reaching its maximum levels at 46 min after the initiation of stress ($p < 0.001$). After 5 min of IMO, the number of *c-fos* mature RNA positive cells was already significantly elevated compared to basal conditions ($p < 0.01$), although still considerably lower than at 8 min of IMO ($p < 0.01$).

To better characterise the expression of *c-fos* RNA in response to IMO, we also determined neuronal activation by measuring the total intensity of fluorescence of the intronic and mature *c-fos* transcripts in all positive cells as well as the fluorescence signal per cell. Exposure to IMO increased the total intensity of fluorescence of *c-fos* intronic RNA ($X^2(3) = 68.3$, $p < 0.001$; **Fig. 12B**), which already increased after 5 min of IMO compared to basal levels ($p < 0.001$) and remained elevated after 8 min of IMO ($p < 0.001$), without significant differences between IMO5 and IMO8 groups. Similar to the number of intronic RNA+ cells, the levels of total fluorescence intensity for *c-fos* intronic RNA were drastically reduced in the IMO8+Rec group compared to IMO8 ($p < 0.001$), but they remained significantly increased compared to the basal group ($p < 0.001$). This increase was similar in proportion to the observed for the count of *c-fos* intronic RNA+ cells. Analysis of the *c-fos* intronic RNA fluorescence per cell revealed no significant group effect (**Fig. 12C**).

Regarding the total fluorescence signal of *c-fos* mature RNA (**Fig. 12E**), the GzLM analysis revealed an effect of group ($X^2(3) = 333.2$, $p < 0.001$). In parallel with the increase in the number of mature RNA+ cells, the intensity of the signal also increased after 5 min IMO ($p < 0.001$) until reaching its peak levels in the IMO8+R group ($p < 0.001$). In this case, fluorescence intensity was significantly elevated in the IMO8 group compared to the IMO5 group ($p = 0.001$). Analysis of *c-fos* mature RNA signal per cell indicated a significant effect group effect ($X^2(3) = 32.1$, $p < 0.001$). Pairwise comparisons showed that already after 5 min IMO, fluorescence

levels per cell were significantly increased compared to the basal group ($p < 0.015$), and they remained increased after 8 min IMO ($p < 0.000$) until reaching peak levels in the IMO8+R group ($p < 0.000$). Moreover, fluorescence intensity per cell was significantly higher in the IMO8 group compared to the IMO5 group ($p = 0.017$; **Fig. 12F**).

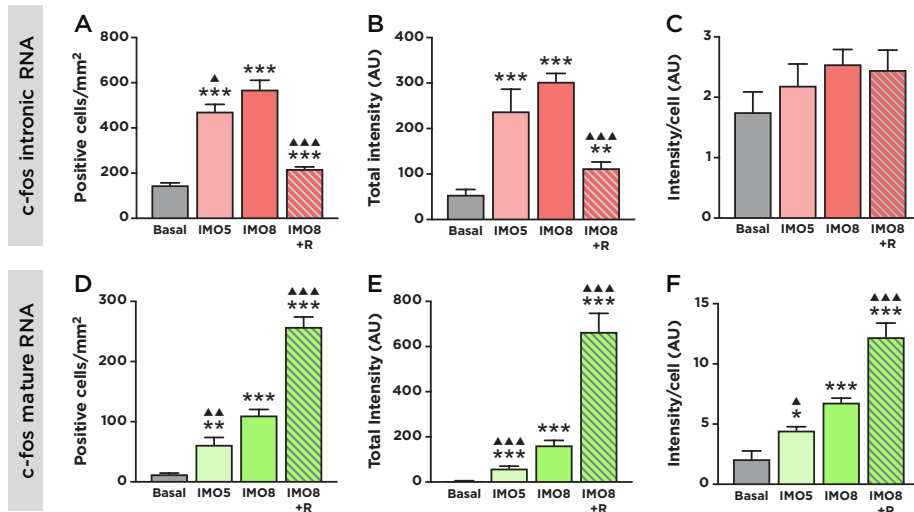


Figure 12. Quantification of *c-fos* intronic and mature RNA levels in the experimental groups basal, IMO5, IMO8 and IMO8+Rec.

The upper panel shows quantification of the *c-fos* intronic RNA, A) the number of positive cells per mm², B) total intensity of fluorescence and C) intensity of fluorescence per cell. The lower panel shows quantification for the *c-fos* mature RNA, D) the number of positive cells per mm², E) total intensity of fluorescence and F) intensity of fluorescence per cell. Data represented as mean + SEM (n = 3-4/group, * $p < 0.05$, ** $p < 0.01$, *** $p < 0.001$ vs basal; ▲ $p < 0.05$, ▲▲ $p < 0.01$, ▲▲▲ $p < 0.001$ vs IMO8 group). Part of the data of this experiment was analysed by the MSc student Sandra Beriain and was presented in her Master's thesis.

We further studied the correlation between the different parameters used to assess neuronal activation after stress. There was a highly significant correlation between the number of *c-fos* intronic RNA+ cells and the total intensity of fluorescence ($r = 0.931$, $p < 0.001$; **Fig. 13A**), but we did not find a significant correlation between the number of positive cells and the fluorescence intensity of *c-fos* intronic RNA per cell (**Fig. 13B**). There was a strong correlation between the number of positive *c-fos* mature RNA cells and the total fluorescence intensity ($r = 0.964$, $p < 0.001$; **Fig. 13C**) and the intensity of fluorescence per cell ($r = 0.939$, $p < 0.001$; **Fig. 13D**).

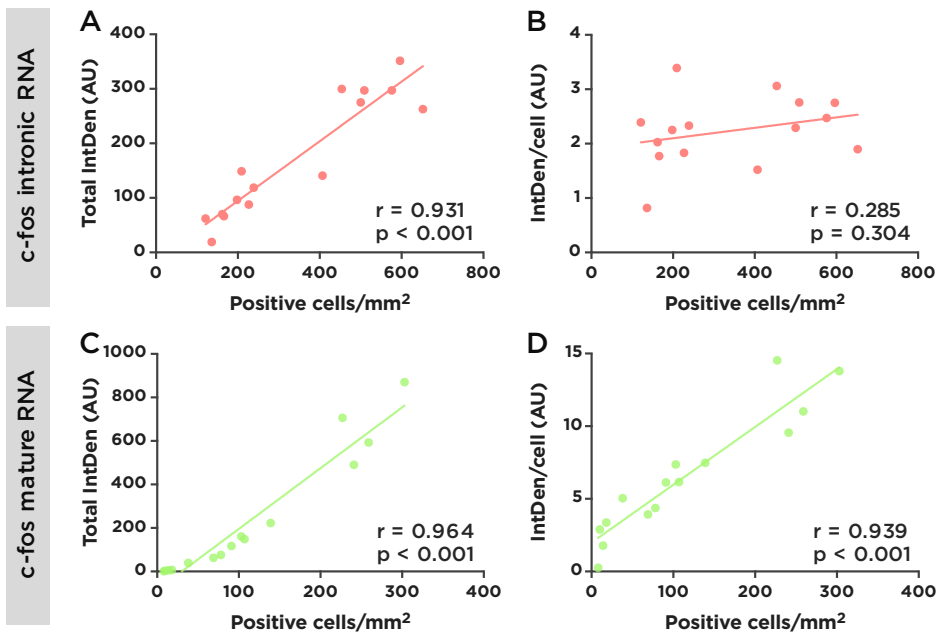


Figure 13. Correlation between the distinct parameters used to measure neuronal activation in all experimental groups.

Correlation coefficients (r) between A) the number of positive cells for *c-fos* intronic RNA and the total intensity of signal; B) the number of positive cells for *c-fos* intronic RNA and the intensity of signal per cell; C) the number of positive cells for *c-fos* mature RNA and the total intensity of signal and D) the number of positive cells for *c-fos* mature RNA and the intensity of signal per cell.

To further explore the dynamics of expression of the intronic and mature *c-fos* transcripts with longer times of stress exposure (IMO 15 min) and recovery (1h 45 min after exposure to 15 min of IMO), we performed a FISH using both *c-fos* RNA probes and quantified the number of cells expressing *c-fos* intronic RNA and cells expressing *c-fos* mRNA as well as the intensity of both signals in the PL cortex (**Fig. 14**). We also included again the IMO8 group as a reference to compare with the previous experiment.

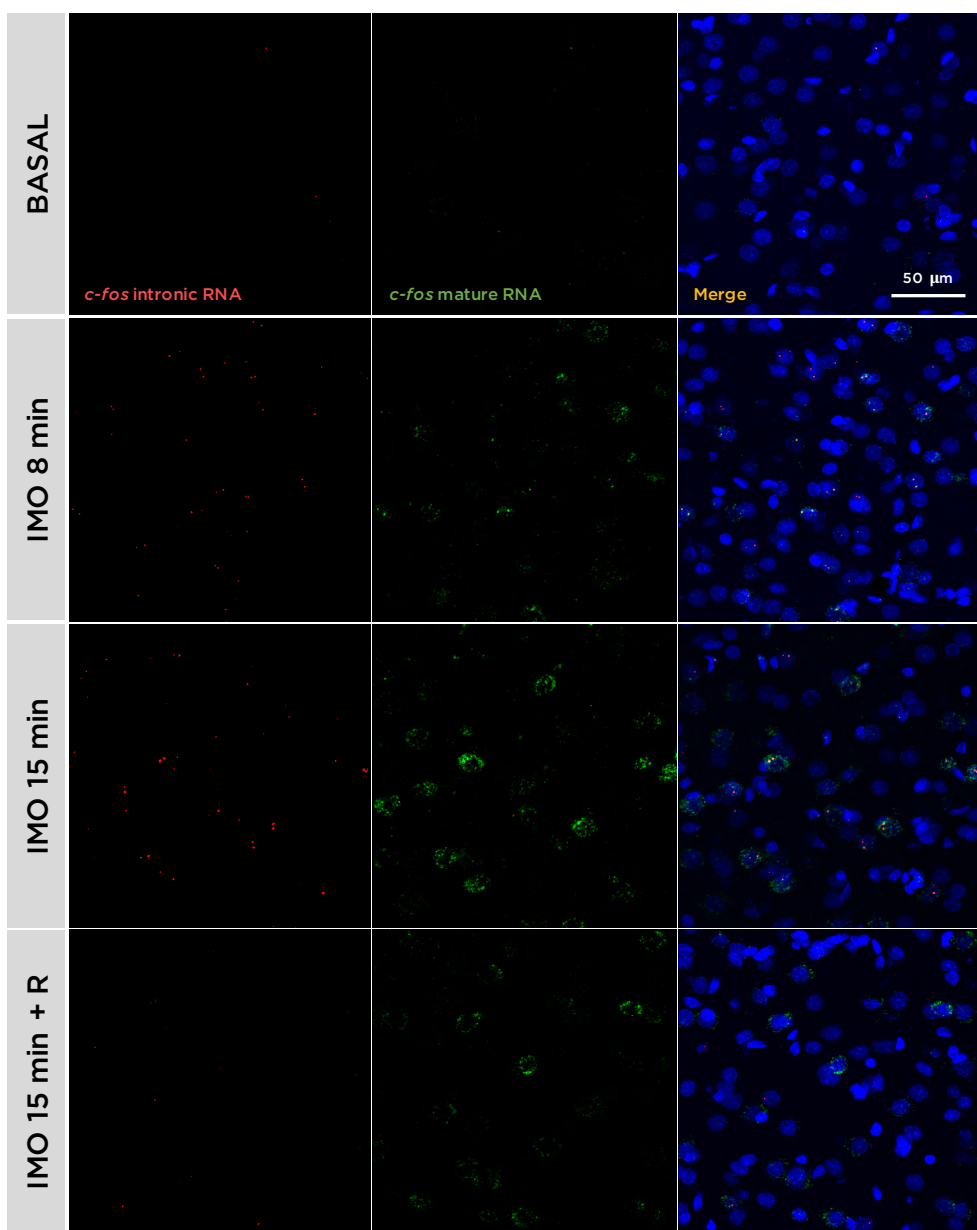


Figure 14. Representative images for expression of *c-fos* intronic and mature RNA in the PL cortex of animals of the experimental groups basal, IMO8, IMO15 and IMO15+R.

Left column, labelling of *c-fos* intronic RNA (*red*); middle column, labelling of *c-fos* mature RNA (*green*); right column, composite image showing the merge of the labelling of *c-fos* intronic RNA (*red*), *c-fos* mature RNA (*green*) and nuclear staining Hoechst (*blue*). All images are represented with the same scale.

The study of the number of positive cells for *c-fos* intronic RNA at different times after IMO exposure (**Fig. 15A**) indicated an effect of the factor group ($X^2(3) = 154.1$, $p < 0.001$). As expected, the number of *c-fos* intronic RNA+ cells was elevated after 8 min of IMO relative to controls ($p < 0.001$) and this increase was similar after 15 min of IMO ($p < 0.001$). The count of *c-fos* intronic RNA+ cells in the IMO15+R group drastically declined compared to IMO15 ($p < 0.001$), with no differences versus controls. Concerning the cells expressing *c-fos* mature RNA, the GzLM analysis also revealed a group effect ($X^2(3) = 99.7$, $p < 0.001$). The number of cells expressing *c-fos* mature RNA (**Fig. 15D**) was elevated at 8 min of IMO compared to basal conditions ($p < 0.001$), with a further increase after 15 min of IMO ($p < 0.001$ vs basal group and $p = 0.049$ vs IMO8). Notably, in this case, the number of cells expressing the mature transcript remained significantly higher in the IMO15+R group ($p < 0.001$), without significant differences between animals exposed to 15 min of IMO and immediately perfused and animals that were left to recover after the 15 min of IMO. We then analysed the total intensity of fluorescence of the intronic and mature RNA of *c-fos* as well as the average fluorescence intensity per cell.

Exposure to IMO increased the total intensity of fluorescence of the intronic *c-fos* transcript ($X^2(3) = 109.9$, $p < 0.001$; **Fig. 15B**). Post-hoc analysis indicated increased intensity of intronic RNA signal after 8 min ($p < 0.001$) and 15 min of IMO ($p < 0.001$), with IMO15 having a small trend to higher levels than the IMO8 group ($p = 0.085$). There was a marked drop in fluorescence intensity in the IMO15+R group compared to the IMO15 group ($p < 0.001$), although it remained above resting levels ($p < 0.001$). The magnitude of increase of the total intensity of the *c-fos* intronic RNA signal was proportional to the rise observed in the number of positive cells.

Moreover, analysis of the *c-fos* intronic RNA fluorescence intensity per cell showed a significant group effect ($X^2(3) = 24.6$, $p < 0.001$; **Fig. 15C**). Pairwise comparisons indicated that the IMO8 group had a trend to increased fluorescence intensity per cell compared to the basal group ($p = 0.06$), whereas the IMO15 and IMO15+R groups had significantly increased intensity of signal per cell compared to the basal group ($p < 0.001$). No differences were observed either between 8 and 15 min of IMO or between animals immediately perfused and those perfused 1h 45 min later after 15 min IMO.

Analysis of the total intensity of fluorescence of the mature transcript of *c-fos* revealed a significant group effect ($X^2(3) = 126.1$, $p < 0.001$; **Fig. 15E**). Post-hoc analysis showed increased levels in the IMO8 group ($p < 0.001$), which reached a peak at IMO15 ($p < 0.001$). Furthermore, similarly to the pattern of the number of activated cells, the total fluorescence intensity of

the mature transcript remained significantly higher in the IMO15+R group ($p < 0.001$), without significant differences with the IMO15 group. The magnitude of increase in the total fluorescence intensity of *c-fos* mature RNA was much greater than the increment in the count of positive cells in all the groups exposed to IMO. In the maximum peak of expression of the mature transcript (IMO15) the number of cells increased 22-fold compared to the basal group, whereas the total fluorescence intensity increased by more than 200-fold compared to basal conditions.

Finally, analysis of the intensity of fluorescence of *c-fos* mature RNA per cell (Fig. 15F) also showed an effect of group ($X^2(3) = 115.8$, $p < 0.001$). Post-hoc analysis indicated an increased intensity of fluorescence of *c-fos* mature RNA per cell after 8 min of IMO compared to basal conditions ($p < 0.001$) and a further increase after 15 min of IMO ($p < 0.001$ vs basal group and $p < 0.002$ vs IMO8 group). Remarkably, fluorescence intensity levels per cell were significantly reduced when animals were left to recover after IMO ($p < 0.001$ vs IMO15 group), although levels were still above basal conditions ($p < 0.001$). Together, this shows that although the number of *c-fos* mRNA+ cells after a recuperation time is similar to the number of recruited cells with sustained stress, the intensity of signal globally and per cell are considerably reduced if the stressor is not maintained.

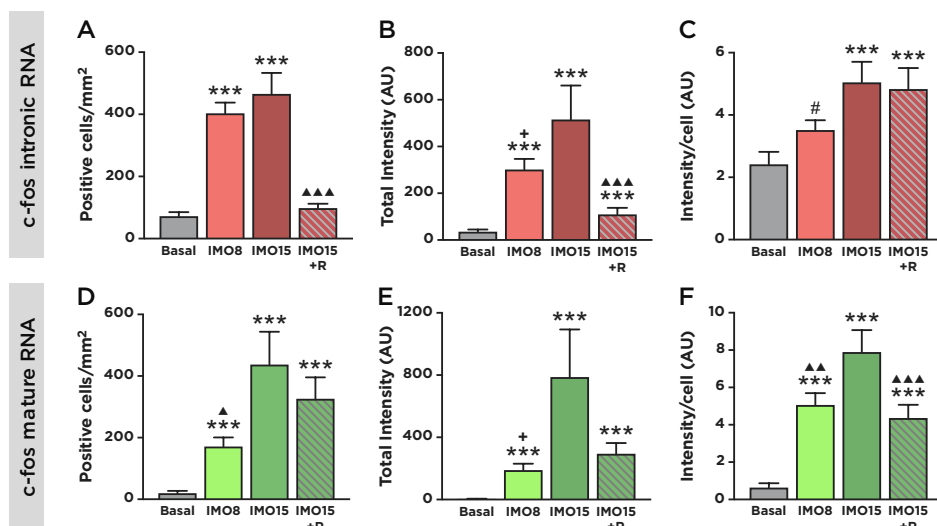


Figure 15. Quantification of *c-fos* intronic and mature RNA levels in the experimental groups basal, IMO8, IMO15 and IMO15+R.

Top panel shows quantification of A) number of *c-fos* intronic RNA positive cells per mm², B) total intensity of fluorescence of *c-fos* intronic RNA and C) intensity of fluorescence per cell of *c-fos* intronic RNA. Bottom panel shows quantification of D) number of *c-fos* mature RNA positive cells per mm², E) total intensity of fluorescence of *c-fos* mature RNA and F) intensity of fluorescence per cell of *c-fos* mature RNA. Data represented as mean + SEM (n = 3-4/group, *** $p < 0.001$, # $p < 0.1$ vs basal; ▲ $p < 0.05$, ▲▲ $p < 0.01$, ▲▲▲ $p < 0.001$, + $p < 0.1$ vs IMO15 group).

We also analysed the correlation between the different measurements employed to study neuronal activation after IMO, and found a very similar pattern to the previous experiment. The number of *c-fos* intronic RNA+ cells strongly correlated with the total fluorescence intensity ($r = 0.923$, $p < 0.001$), but not with fluorescence intensity per cell. Furthermore, the number of *c-fos* mature RNA+ cells showed a highly significant correlation with the total intensity of fluorescence ($r = 0.879$, $p < 0.001$) and fluorescence intensity per cell ($r = 0.755$, $p = 0.001$).

Hence, the study of the dynamics of expression of *c-fos* RNA showed a very fast induction for the intronic transcript, with a very high number of cells expressing the transcript already after 5 min IMO and a pronounced decay over time. In contrast, although at 5 min of IMO the levels of mature *c-fos* RNA are slightly above basal levels, the transcript shows a marked increase with longer stress times. The present findings have provided relevant insights about optimal duration of stress exposure and the interval between stressors in which base our following experiment aimed at determining the potential existence of specific neuronal ensembles for different emotional stressors.

3. Specificity of neuronal activation in response to IMO and IS in the mPFC

3.1. Experimental design

To study whether there are neurons that respond specifically to different emotional stressors 62 adult male SD rats were randomly distributed into nine groups. Four groups were exposed twice to one of the two stressors (IMO or IS) for 5 min, separated by an interval of 25 min ($n=8/\text{group}$). The stressors were either the same (IMO-IMO and IS-IS) or different (IMO-IS and IS-IMO). Five groups were used as controls (Ctrl, $n=6/\text{group}$): Ctrl-IMO and Ctrl-IS, only exposed to 5 min of stress and immediately perfused; IMO-Ctrl and IS-Ctrl, exposed to 5 min of stress and perfused 30 min after, and the basal group, not exposed to any stressor and perfused in basal conditions. A summary of the experimental groups and procedure is shown in **Fig. 16**. We evaluated by dFISH the number of cells positive for *c-fos* mRNA, for *c-fos* intronic RNA and also the number of cells expressing both markers in two mPFC subdivisions: the PL and the IL, differentiating between the superficial (external) layers and the deep (internal) layers.

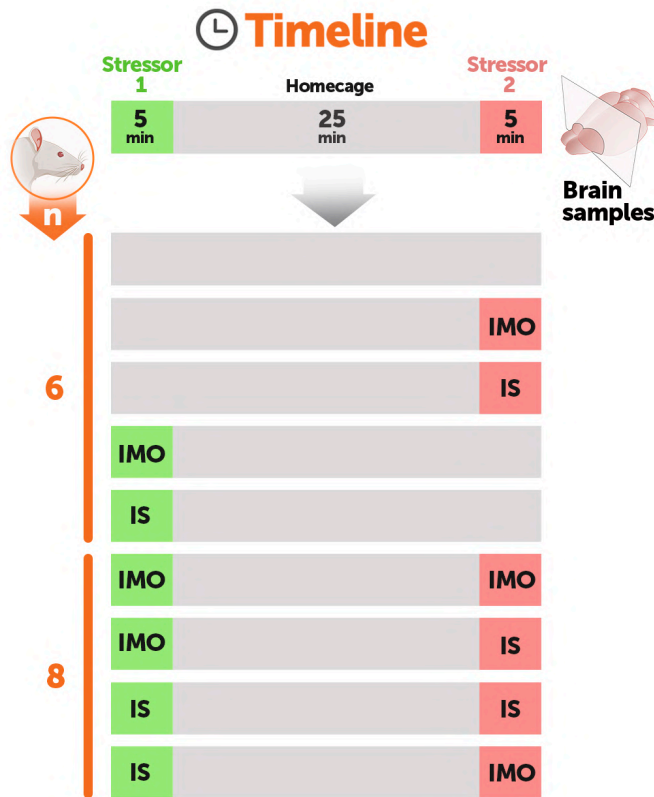


Figure 16. Experimental groups and design for identification of potential stressor-specific activated neurons.

5 experimental groups were used as controls (n=8/group). The basal group (Ctrl-Ctrl) was not exposed to any stressor and remained undisturbed in their home cage until perfusion. Four groups were exposed to a single IMO or IS, and two groups were perfused immediately after (Ctrl-IMO and Ctrl-IS, respectively) and two groups 30 min after (IMO-Ctrl and IS-Ctrl, respectively). Finally, 4 groups were sequentially exposed to two stressors (n=6/group), either the same or different (IMO-IMO, IMO-IS, IS-IS and IS-IMO). In all cases, stress exposure lasted for 5 min and the interval between stressors was 25 min.

3.2. Results

Validation of the time course of expression of c-fos intronic and mature RNA after exposure to different emotional stressors in the PL cortex

Based on the data above mentioned and adapting the timings employed in published papers using the catFISH technique (Lin et al., 2011; Gore et al., 2015), we defined the time course for this experiment, which consisted of exposing animals to two consecutive stressors of 5 min duration separated by an interval of 25 min. Given our observations of increased *c-fos* mRNA

expression in the IMO5 group, we decided to reduce the time of isoflurane exposure before perfusion as well as the time of cleaning with saline in order to reduce the time since the beginning of exposure to IMO until the fixation of the brain. We then performed dFISH using the probes against the *c-fos* intronic and mature RNA and quantified the expression of both RNA species in the PL and IL regions of the mPFC. To validate the selected time course for our experiments, we quantified the number of *c-fos* intronic and mature RNA in animals exposed either to IMO or IS for 5 min and immediately perfused, which should mainly express intronic *c-fos* RNA, and in animals exposed either to IMO or IS for 5 min and perfused 30 min later, which should mainly express *c-fos* mature RNA. We compared all these groups with the basal group (not exposed to any stimulus). A GzLM analysis was performed to analyse the differences between these 5 experimental groups.

The images and quantification of the dFISH performed in the superficial layers of the PL cortex to study neuronal activation in response to IMO and IS is represented in **Fig. 17**. Analysis of the number of cells expressing *c-fos* intronic RNA in response to IMO (**Fig. 17D**) showed a significant group effect ($X^2(2) = 180.9$, $p < 0.001$) and pairwise comparisons revealed that the number of *c-fos* intronic RNA+ cells was significantly increased in animals exposed to 5 min IMO and perfused immediately compared to basal conditions ($p < 0.001$). However, the number of cells expressing *c-fos* intronic RNA returned to baseline levels in animals exposed to 5 min IMO and perfused 30 min later. On the other hand, the analysis of the number of *c-fos* mRNA+ cells showed an effect of group ($X^2(2) = 271.6$, $p < 0.001$), but the expression pattern of the mature transcript was opposite to the observed with the *c-fos* intronic transcript. The number of cells expressing *c-fos* mRNA in animals exposed to 5 min of IMO and immediately perfused was comparable to basal conditions, whereas it significantly increased when animals were perfused 30 min after IMO ($p < 0.001$).

The quantification of both *c-fos* RNA species after IS showed the same pattern as exposure to IMO (**Fig. 17E**), with a significant effect of group for the intronic transcript ($X^2(2) = 132.5$, $p < 0.001$) and the mature transcript ($X^2(2) = 105.2$, $p < 0.001$). Post-hoc analysis revealed that immediately after 5 min IS, animals exhibited increased *c-fos* intronic RNA positive cells compared to the basal group ($p < 0.001$), whereas the number of *c-fos* mRNA positive cells remained comparable to basal conditions. In contrast, 30 min after IS, the number of *c-fos* mRNA positive cells was significantly elevated compared to basal levels ($p < 0.001$) while the number of *c-fos* intronic RNA positive cells returned to resting levels.

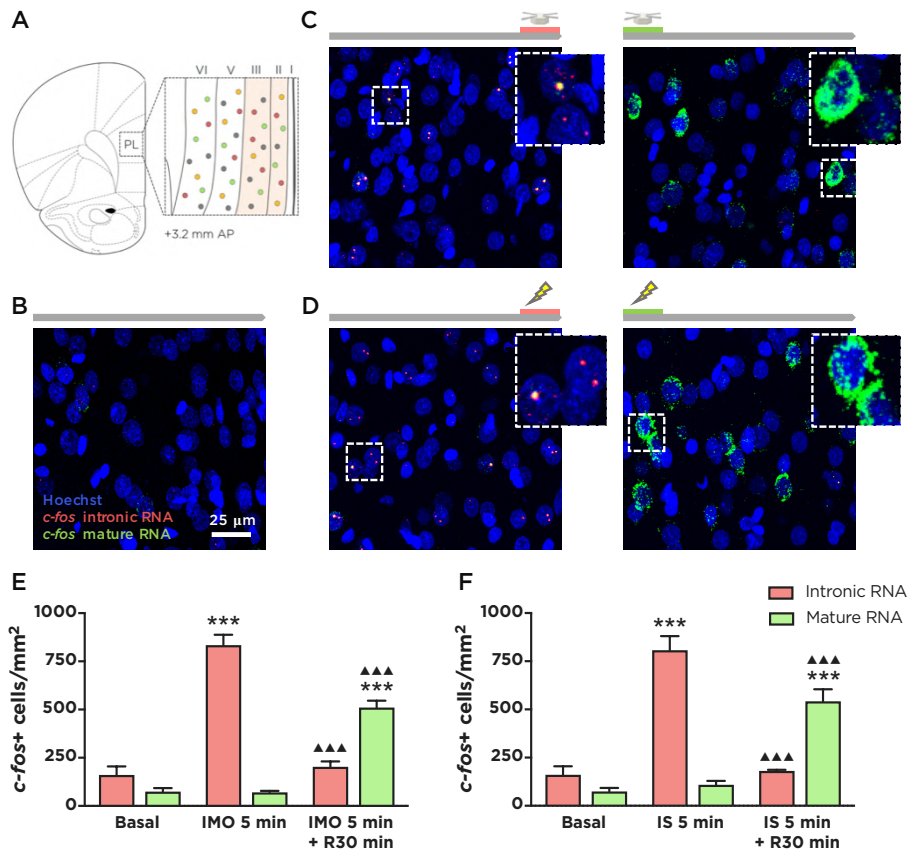


Figure 17. Representative images from the superficial layers of the PL cortex of the control groups and quantification of the number of activated cells.

A) Schematic of the brain region and layers analysed for quantification. B) Representative image of the superficial layers of the PL of rats in basal conditions. Representative images of the superficial layers of PL cortex of rats exposed C) to 5 min of IMO and perfused immediately after (left) and 30 min later (right) and D) to 5 min of IS and perfused immediately after (left) and 30 min later (right). Blue, Hoechst nuclear staining; Red, *c-fos* nuclear transcript or intronic RNA; Green, *c-fos* mature transcript or mRNA. E) Quantification of *c-fos* positive cells per mm² for intronic and mature RNA immediately after 5 min IMO or 30 min after and F) immediately after 5 min IS or 30 min after. All images are represented with the same scale. Data shown as mean + SEM (n=6 animals/group; ***p < 0.001 vs basal group; ▲▲▲ p < 0.001 vs 5 min stress).

We also quantified neuronal activation in response to IMO and IS in the deep layers of the PL cortex (**Fig. 18**). The statistical analysis of the number of positive cells for intronic *c-fos* RNA in response to IMO (**Fig. 18A**) showed a group effect ($X^2(2) = 81.5$, $p < 0.001$) and post-hoc comparisons indicated that the number of *c-fos* intronic RNA+ cells was significantly increased in animals exposed to 5 min IMO and perfused immediately

compared to basal animals ($p < 0.001$). The number of *c-fos* intronic RNA+ cells returned to basal levels in animals exposed to 5 min IMO and perfused after 30 min. The analysis of the number of *c-fos* mRNA+ cells also showed a significant group effect ($X^2(2) = 56.3$, $p < 0.001$), but the expression pattern of the mature RNA was completely opposite to the observed with the intronic RNA. The number of *c-fos* mRNA+ cells in animals exposed to IMO for 5 min and immediately perfused was comparable to basal conditions, whereas it significantly increased when animals were perfused 30 min after IMO ($p < 0.001$).

The quantification of both *c-fos* RNA species after IS exposure showed a similar pattern to IMO (**Fig. 18B**), with a significant group effect for the intronic ($X^2(2) = 51.8$, $p < 0.001$) and the mature transcripts ($X^2(2) = 37.8$, $p < 0.001$). Post-hoc analysis revealed that immediately after 5 min IS, animals had significantly more *c-fos* intronic RNA+ cells than the basal group ($p < 0.001$), whereas the number of *c-fos* mRNA+ cells remained comparable to baseline levels. Remarkably, 30 min after IS, the number of cells expressing *c-fos* mRNA was significantly higher than in the basal group ($p < 0.001$) whereas the number of cells expressing *c-fos* intronic RNA returned to resting levels.

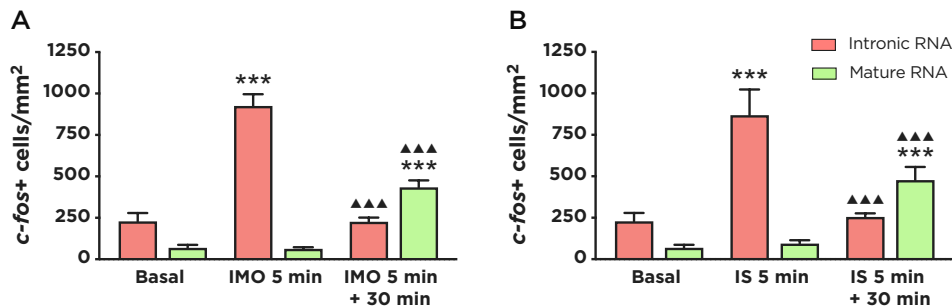


Figure 18. Quantification of the number of activated cells in the deep layers of the PL in basal conditions and after exposure to a single IMO and IS.

A) Quantification of *c-fos* positive cells per mm² for intronic and mature RNA immediately after 5 min IMO or 30 min after and B) immediately after 5 min IS or 30 min after. Data shown as mean + SEM (n=6 animals/group; *** $p < 0.001$ vs basal group; ▲▲▲ $p < 0.001$ vs 5 min stress).

As a complementary quantification, we further assessed the percentage of cells expressing exclusively intronic, mature or both intronic and mature *c-fos* transcripts in each control group (Fig. 19). We found that animals perfused immediately after 5 min stress exhibited almost exclusively intronic *c-fos* transcripts in both superficial and deep PL layers. In contrast, most of the activated cells in animals perfused 30 min after stress expressed only mature transcripts. In basal conditions, the most abundant type of activated cells were those expressing exclusively intronic RNA.

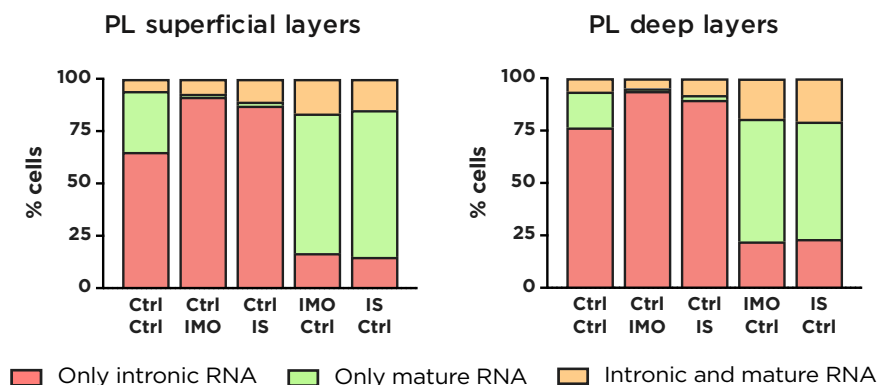


Figure 19. Percentage of total c-fos+ cells exhibiting exclusively intronic, mature or intronic and mature c-fos transcripts in basal conditions, immediately after 5 min stress or 30 min later in the PL cortex.

Left, superficial layers of the PL; right, deep layers of the PL.

Overall, these findings suggest that with this methodological approach and experimental design we can determine the neuronal activity at two different time points within the same animal, and hence, potentially identify neurons specifically activated in response to two different emotional stressors in the PL cortex.

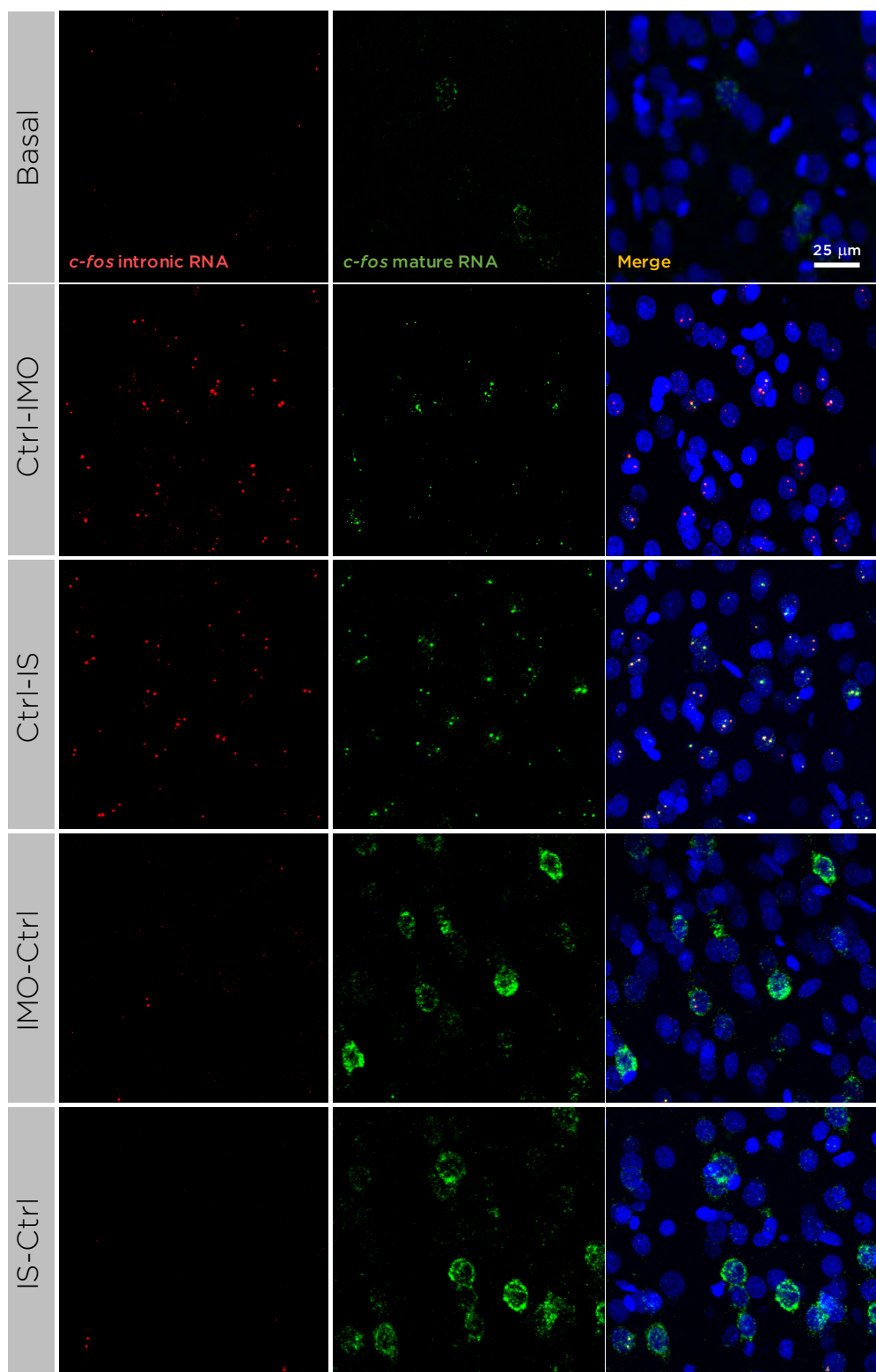
Expression of c-fos intronic and mature RNA in the PL cortex after exposure to different emotional stressors

To evaluate neuronal activation in response to each emotional stressor and assess whether the neuronal response to the second stressor could be influenced by previous exposure to another stressor, we quantified in the PL cortex the total number of cells expressing the intronic and mature transcripts of *c-fos* in all the experimental groups (**Fig. 21**). We performed a GzLM analysis with 2 factors (first and second stimulus) and 3 levels (Ctrl, IMO and IS).

The analysis of the number of cells expressing ***c-fos* intronic RNA** in the superficial layers of the PL cortex (**Fig. 22A**) showed a significant effect of the first stimulus ($X^2(2) = 28.8$, $p < 0.001$), the second stimulus ($X^2(2) = 240.9$, $p < 0.001$) and a significant interaction between the first and the second stimulus ($X^2(4) = 20.1$, $p < 0.001$). Planned comparisons revealed differences between both Ctrl-IMO and Ctrl- IS and the basal group ($p < 0.001$ in both cases) and no differences between basal animals and animals exposed to 5 min IS or IMO and perfused 30 min later. Remarkably, no significant differences in the number of *c-fos* intronic RNA+ cells were

found between the two stressors, IMO and IS (Ctrl-IMO vs Ctrl- IS). Furthermore, animals exposed to IMO and immediately perfused had a higher number of *c-fos* intronic RNA+ cells than animals previously exposed to either IMO or IS (IMO-IMO and IS-IMO, $p < 0.001$ in both cases). Similarly, animals from the Ctrl-IS group had increased *c-fos* intronic RNA+ cells than the double stressor groups IMO-IS and IS-IS ($p < 0.001$ in both cases). In addition, the number of cells in the IMO-IS and IMO-IMO groups was higher than in the IMO-Ctrl group ($p < 0.001$ in both cases) and in the IS-IMO and IS-IS groups compared to the IS-Ctrl group ($p < 0.001$ for both comparisons). Finally, all the groups exposed to two stressors exhibited a similar number of *c-fos* intronic RNA+ cells (IMO-IMO vs IS-IMO and IMO-IS vs IS-IS), independently of whether the stressor used was the same or different and regardless of the order of exposure.

In contrast to the intronic *c-fos* RNA, the analysis of the number of *c-fos* mature RNA positive cells in the superficial layers of the PL cortex (**Fig. 22B**) revealed a main effect of the first stimulus ($X^2(2) = 369.2$, $p < 0.001$), but no effect of the second stimulus or the interaction between both stimuli. Further comparisons indicated significant differences between groups exposed to IMO and IS as the first stressor compared to those groups that remained in basal conditions in the first time-block ($p < 0.001$ for both IMO and IS vs Ctrl). Finally, no differences in the number of *c-fos* mRNA+ cells were found after IMO versus IS.



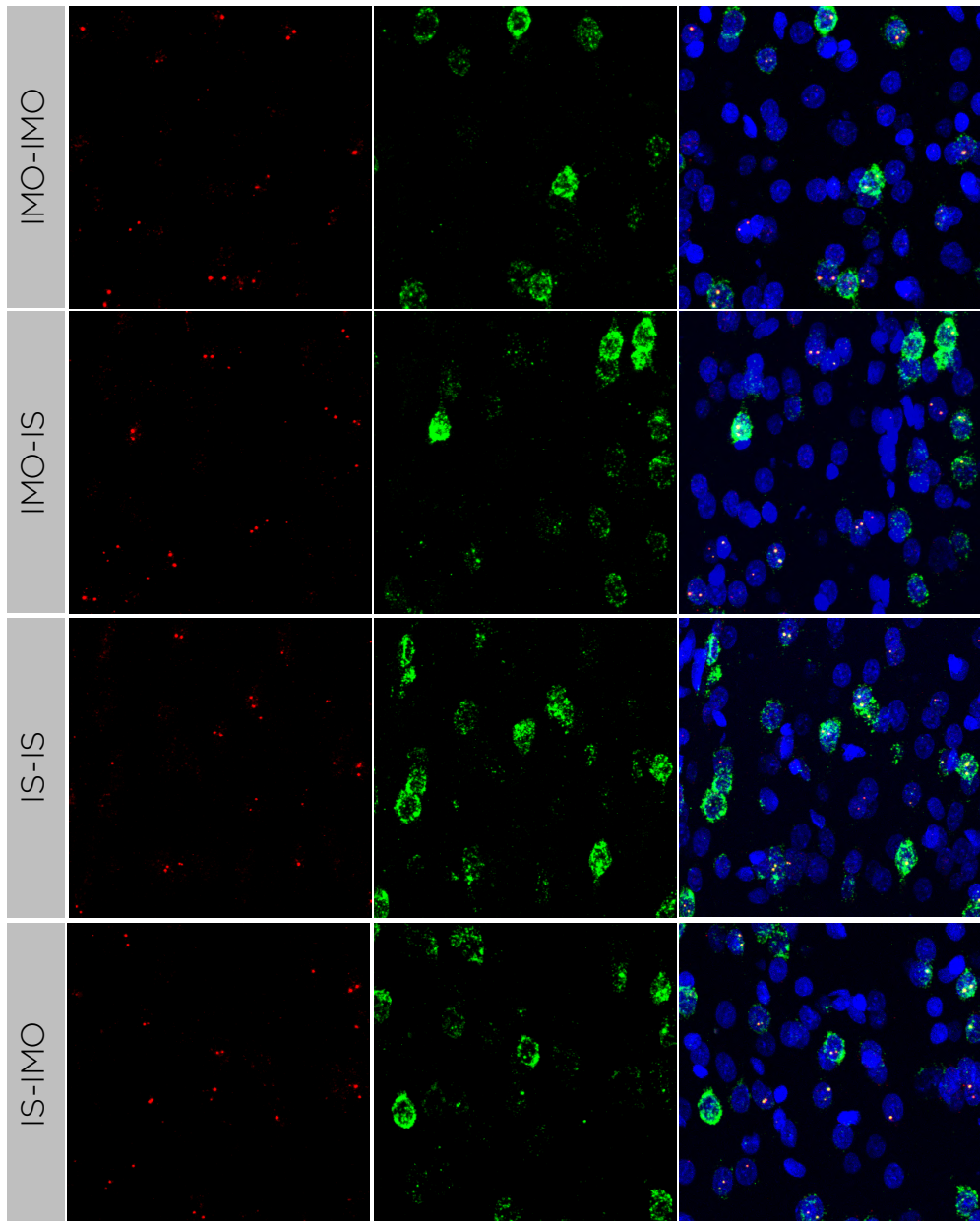


Figure 21. Representative images for expression of *c-fos* intronic and mature RNA in the superficial layers of the PL cortex of all the experimental groups.

Left column, labelling of *c-fos* intronic RNA (red); middle column, labelling of *c-fos* mature RNA (green); right column, composite image showing the merge of the labelling of *c-fos* intronic RNA (red), *c-fos* mature RNA (green) and nuclear staining Hoechst (blue). All images from the panel are represented with the same scale.

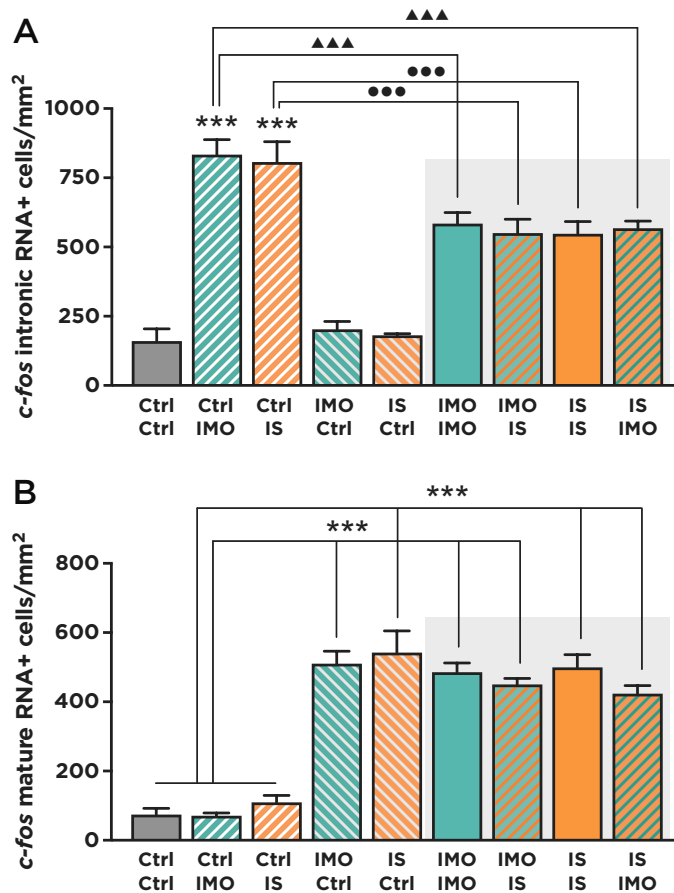


Figure 22. Expression of *c-fos* RNA in the superficial layers of the PL cortex of animals exposed to different emotional stressors.

Quantification of the number of A) *c-fos* intronic RNA and B) *c-fos* mature RNA positive cells in basal conditions and after either one exposure to IMO or IS, or to two exposures of the same stressor twice or a combination of the two stressors. The grey square highlights the groups sequentially exposed to two stressors. Data represented as mean + SEM (n=6-8 animals/group; ***p < 0.001 vs Ctrl; ▲▲▲ p < 0.001 vs Ctrl-IMO group; ●●● p < 0.001 vs Ctrl-IS group).

The expression pattern of both probes in the deep layers of the PL cortex in all the experimental groups was highly similar to the superficial layers. The analysis of the number of positive cells for *c-fos* intronic RNA (**Fig. 23A**) showed a main effect of the first stimulus ($X^2(2) = 14.5$, $p = 0.001$), the second stimulus ($X^2(2) = 116.1$, $p < 0.001$) and a significant interaction between the first and the second stimulus ($X^2(4) = 15.4$, $p = 0.004$). Planned comparisons indicated significant differences between both Ctrl-IMO and Ctrl-IS and the group not exposed to any stressor ($p < 0.001$ in both cases).

No differences were observed between basal animals and the IMO-Ctrl and IS-Ctrl groups, as previously described. Furthermore, Ctrl-IMO and Ctrl-IS groups had a similar number of *c-fos* intronic RNA+ cells.

Moreover, animals perfused immediately after 5 min of IMO had significantly more cells expressing *c-fos* intronic RNA than animals previously exposed to either IMO (Ctrl-IMO vs IMO-IMO, $p = 0.003$) or IS (Ctrl-IMO vs IS-IMO, $p = 0.001$). Similarly, the Ctrl-IS group was also significantly different from the double stressor group IMO-IS (0.034). In addition, significant differences were observed between the groups exposed to one stressor and perfused 30 min after, and their corresponding double stressor groups. In this regard, the IMO-Ctrl group had significantly fewer *c-fos* intronic RNA positive cells than IMO-IMO and IMO-IS groups ($p < 0.001$ in both cases), and the same for the IS-Ctrl group compared to the IS-IMO ($p = 0.015$) and IS-IS ($p < 0.001$) groups. Finally, all the groups exposed to two successive stressors exhibited a similar number of *c-fos* intronic RNA positive cells, independently of whether the stressor was the same or different and regardless of the order of exposure.

The analysis of the number of cells expressing *c-fos* mature RNA in the deep layers of the PL cortex (**Fig. 23B**) showed a main effect of the first stimulus ($X^2(2) = 299.3$, $p < 0.001$), but no effect of the second stimulus or the interaction between both stimuli. Pairwise comparisons indicated that groups exposed to IMO and IS as the first stressor had a higher number of *c-fos* mature RNA+ cells than those groups not exposed to any stressor 30 min before perfusion ($p < 0.001$ for both comparisons). Remarkably, quantification of activated cells revealed no differences in the number of *c-fos* mRNA+ cells after IMO or IS, as observed for the PL superficial layers.

Taken together, the results obtained with both *c-fos* RNA probes in the superficial and deep layers of the PL cortex suggest that the neuronal ensembles activated by IS and IMO are of similar size. Furthermore, our findings indicate that previous exposure to another stressor reduces the number of cells expressing *c-fos* intronic RNA in response to the second stressor compared to animals not exposed to any stressor before, suggesting a desensitisation mechanism. Remarkably, this phenomenon occurs regardless of whether the first stressor is the same or not as the second one.

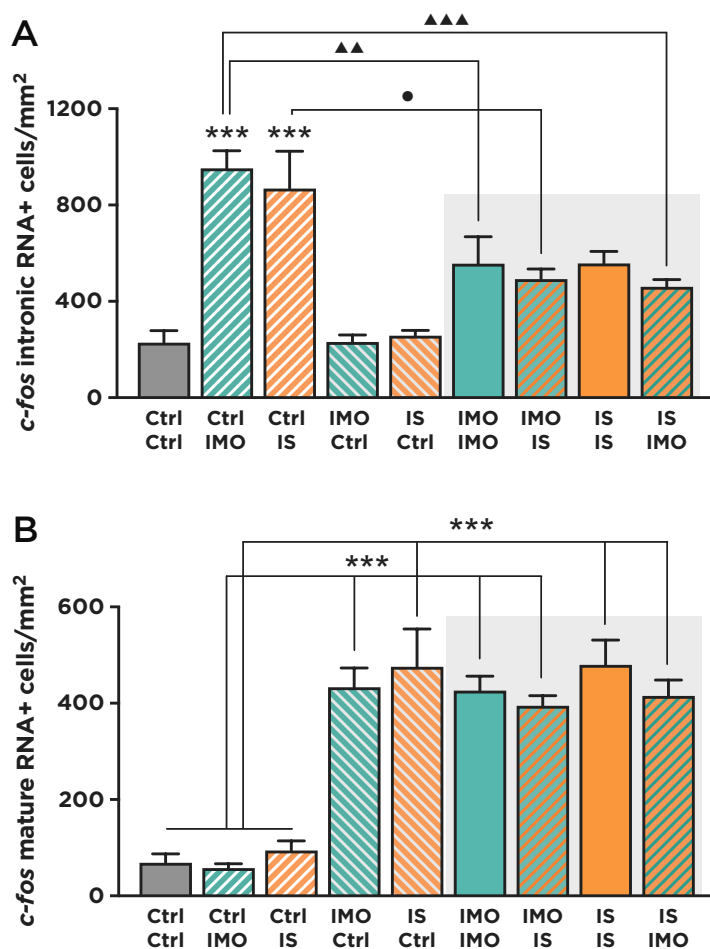


Figure 23. Expression of c-fos RNA in the deep layers of the PL cortex of animals exposed to different emotional stressors.

Quantification of the number of A) *c-fos* intronic RNA positive cells and B) *c-fos* mature RNA positive cells in basal conditions and after either one exposure to IMO or IS, or to two exposures of the same stressor twice or a combination of the two stressors. The grey square highlights the groups sequentially exposed to two stressors. Data represented as mean + SEM (n=6-8 animals/group; ***p < 0.001 vs Ctrl; ▲▲ p < 0.01, ▲▲▲ p < 0.001 vs Ctrl-IMO group; ● p < 0.05 vs Ctrl- IS group).

Identification of stressor-specific neuronal populations in the PL cortex

The quantification analysis performed with all the experimental groups indicated an analogous pattern of activation after exposure to IMO or IS in the PL cortex, with a similar number of cells activated by both stressors. A possible explanation for these results would be that both stressors recruit the

same neuronal population. However, another plausible hypothesis would be that each stressor activates specific neuronal populations and different but similar size ensembles. To test this hypothesis, a colocalization analysis was performed in animals exposed to the same stressor twice and to two different stressors, allowing us to assess the overlap between the two labelled populations within each animal.

A GzLM analysis for the number of double labelled cells (*c-fos* mRNA+ and intronic RNA+ cells) in the superficial layers of the PL cortex (**Fig. 24A**) indicated no main effects of the first or the second stimulus but a significant interaction between stimuli ($X^2(1) = 23.9$, $p < 0.001$). Post-hoc comparisons revealed that there were significant differences in the number of double-labelled cells between IMO-IMO and IMO-IS groups ($p < 0.001$) and IMO-IMO and IS-IMO groups ($p = 0.001$). Similarly, the number of double-labelled cells was significantly higher in animals exposed to IS twice compared with the animals exposed to different stressors, IS-IMO ($p = 0.02$) and IMO-IS ($p = 0.005$). We further complemented these results by calculating the percentage of overlap (**Fig. 24B**), which consisted of dividing the number of double labelled cells between the total number of intronic RNA+ cells ($c-fos$ mRNA+ intronic RNA+ / *c-fos* intronic RNA+) in order to normalise the results to the response to the second stressor. A GzLM analysis indicated no main effects of either of the stimuli separately but a significant interaction between stimuli ($X^2(1) = 20.2$, $p < 0.001$). Decomposition of the interaction indicated significant differences between IMO-IS and IMO-IMO group ($p = 0.002$) and the IS-IMO with the IMO-IMO group ($p = 0.002$). Furthermore, there were also significant differences between the IS-IMO and IS-IS groups ($p = 0.001$) and the IMO-IS and IS-IS groups ($p = 0.001$).

In the deep layers of the PL cortex, analysis of the number of double labelled cells (**Fig. 24C**), revealed no significant effect of either the first stimulus or second stimulus, but a significant interaction of the first and second stimulus ($X^2(1) = 8.4$, $p = 0.004$). Planned comparisons indicated a small trend to a reduced number of double-labelled cells in the IMO-IS group compared to IMO-IMO ($p = 0.09$) and a significantly reduced number in IMO-IS and IS-IMO compared to the group exposed to IS twice ($p = 0.011$ and $p = 0.016$, respectively). Similarly, analysis of the percentage of overlap in the four groups (**Fig. 24D**) revealed no main effects of the first or the second stimulus but a significant interaction between both ($X^2(1) = 4.252$, $p = 0.039$). Decomposition of the interaction indicated nearly significant differences between the IMO-IS and IMO-IMO groups ($p = 0.055$) and a small trend between the IMO-IS and IS-IS groups ($p = 0.096$).

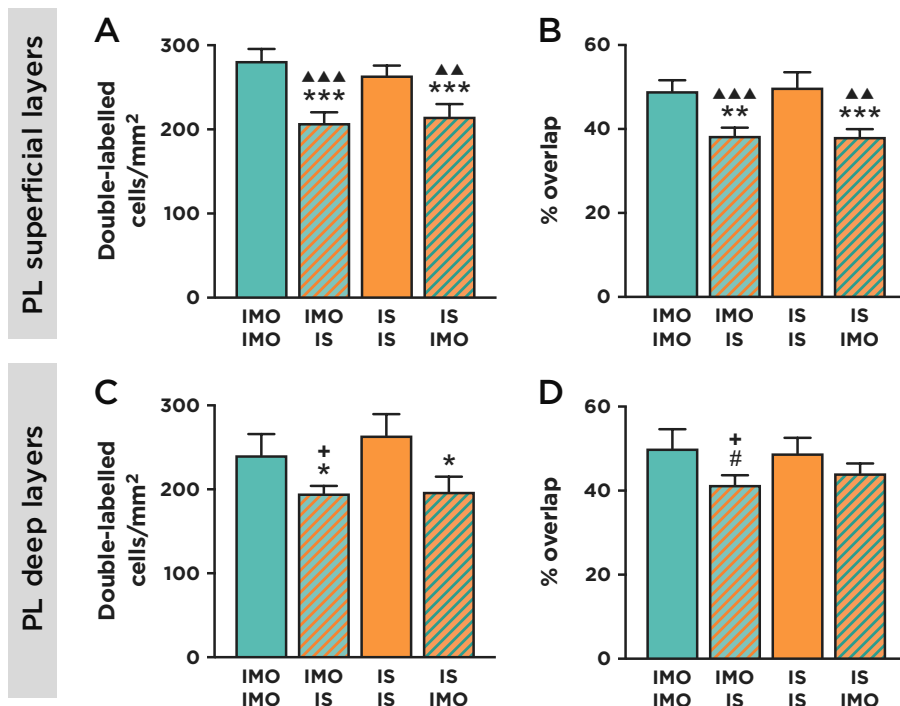


Figure 24. Overlap of *c-fos* intronic and mature RNA positive PL neurons in the experimental groups exposed to two stressors.

Top panel, PL superficial layers. A) Total number of double labelled cells and B) number of double labelled cells normalised to the number of *c-fos* intronic RNA+ cells. Bottom panel, PL deep layers. C) Total number of double labelled cells and D) number of double labelled cells normalised to the total number of *c-fos* intronic RNA+ cells. Data represented as mean + SEM (n = 7-8 animals/group; * p < 0.05, ** p < 0.01, *** p < 0.001, # p < 0.1 vs IMO-IMO group; ▲▲ p < 0.01, ▲▲▲ p < 0.001, + p < 0.1 vs IS-IS group).

Taken together, these results suggest that distinct emotional stressors might recruit partially distinct neuronal ensembles in the PL cortex, especially in the superficial layers. Furthermore, we found a very strong correlation between the number of activated cells (expressing intronic RNA+, mature RNA+ or both RNA isoforms) in the superficial and deep layers in all the experimental groups (Fig. 25).

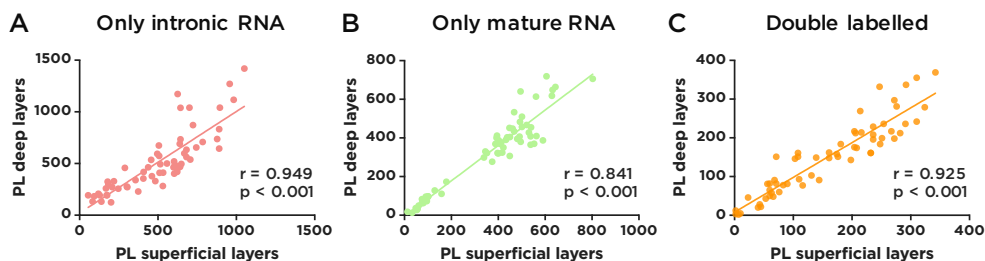


Figure 25. Correlation between the number of activated cells in the superficial and deep layers of the PL cortex in all the experimental groups.

Pearson correlation between the number of A) *c-fos* intronic RNA positive cells, B) *c-fos* mature RNA positive cells and C) double-positive cells (expressing both *c-fos* intronic and mature transcripts) between the superficial and deep layers of the PL cortex. Pearson correlation coefficient (r) and statistical significance are shown for each graph.

Validation of the time course of expression of *c-fos* mRNA and intronic RNA after exposure to different emotional stressors in the IL cortex

After studying the temporal dynamics of expression of the *c-fos* RNA in the PL cortex, we further analysed the time course of expression of this IEG in another mPFC subdivision, the IL cortex. Given the strong correlation found between the superficial and deep layers of the PL cortex and due to time constraints, we only performed the quantification of FISH images in the superficial layers of the IL cortex (**Fig. 26**).

Analysis of the number of cells expressing intronic *c-fos* RNA (**Fig. 26A**) after exposure to IMO showed a significant effect of group ($X^2(2) = 19.2$, $p < 0.001$), and pairwise comparisons indicated that animals exposed to 5 min IMO and immediately perfused had an increased number of *c-fos* intronic RNA positive cells compared to basal animals ($p < 0.001$), returning to baseline levels after 30 min. The analysis of the number of *c-fos* mature RNA positive cells also showed a significant effect of group ($X^2(2) = 371.8$, $p < 0.001$). The number of cells expressing *c-fos* mRNA in animals exposed to IMO for 5 min and immediately perfused was similar to basal animals, while it significantly increased in animals perfused 30 min after IMO ($p < 0.001$).

The quantification of *c-fos* intronic and mature RNA after IS showed the same pattern as IMO (**Fig. 26B**), with a significant effect of group for both the intronic ($X^2(2) = 24.8$, $p < 0.001$) and mature transcripts ($X^2(2) = 213.2$, $p < 0.001$). Paired comparisons revealed that immediately after 5 min of IS, animals exhibited an increased number of *c-fos* intronic RNA positive cells compared to the basal group ($p < 0.001$), with no changes in the number of *c-fos* mRNA positive cells. In contrast, 30 min after IS, the number of *c-fos*

mRNA positive cells was significantly increased ($p < 0.001$) while the number of *c-fos* intronic RNA positive cells dropped sharply to baseline levels.

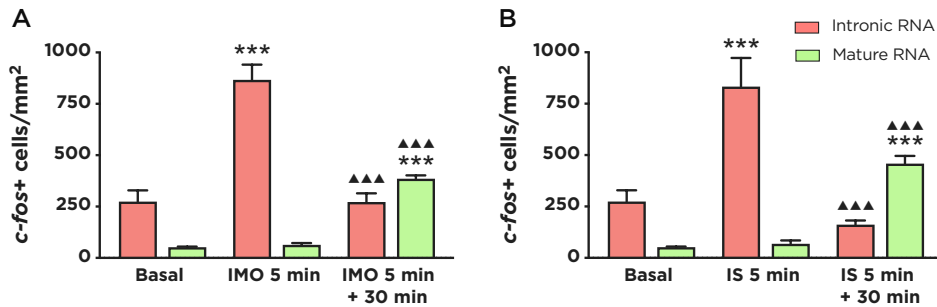


Figure 26. Quantification of the number of activated cells in the superficial layers of the IL in basal conditions and after exposure to IMO and IS.

A) Quantification of *c-fos* positive cells per mm² for intronic and mature RNA immediately after 5 min IMO or 30 min after and B) immediately after 5 min IS or 30 min after. Data shown as mean + SEM (n=6 animals/group; *** $p < 0.001$ vs basal group; ▲▲▲ $p < 0.001$ vs 5 min stress).

Expression of c-fos intronic and mature RNA in the IL cortex after exposure to different emotional stressors

We aimed to further evaluate in the IL subdivision of the mPFC cortex neuronal activation induced by IMO and IS and investigate whether the response triggered by exposure to the second stressor could be affected by previous exposure to another stressor. For this, we quantified the number of cells expressing *c-fos* intronic RNA and the number of cells expressing *c-fos* mature RNA in the IL cortex of the animals from all the experimental groups.

The analysis of the number of *c-fos* intronic RNA positive cells in the superficial layers of the IL cortex (**Fig. 27A**) indicated a main effect of the first stimulus ($X^2(2) = 16.1$, $p < 0.001$), the second stimulus ($X^2(2) = 71.9$, $p < 0.001$) and no interaction between both stimuli. Further comparisons of the first stimulus revealed significant differences between control and IS ($p < 0.001$) and control and IMO ($p = 0.027$). Moreover, comparisons of the second stimulus indicated significant differences also between control and IS and control and IMO ($p < 0.001$ in both cases).

The analysis of the number of *c-fos* mature RNA positive cells in the superficial layers of the IL cortex (**Fig. 27B**) indicated a significant effect of the first stimulus ($X^2(2) = 390.2$, $p < 0.001$), no significant effect of the second stimulus or interaction between both stimuli. Further comparisons

indicated significant differences between groups exposed to IMO and IS as the first stressor compared to those groups not exposed to any stressor in the first time-block ($p < 0.001$ for both IMO and IS vs Ctrl). Remarkably, there were no differences between the number of *c-fos* mRNA+ cells after IMO or IS.

Together, the data obtained with both *c-fos* RNA probes in the superficial layers of the IL cortex also suggest that IS and IMO activate a similar number of neurons in our experimental conditions and that previous stress exposure partially reduces the response to a second stressor, regardless of whether it is the same or different.

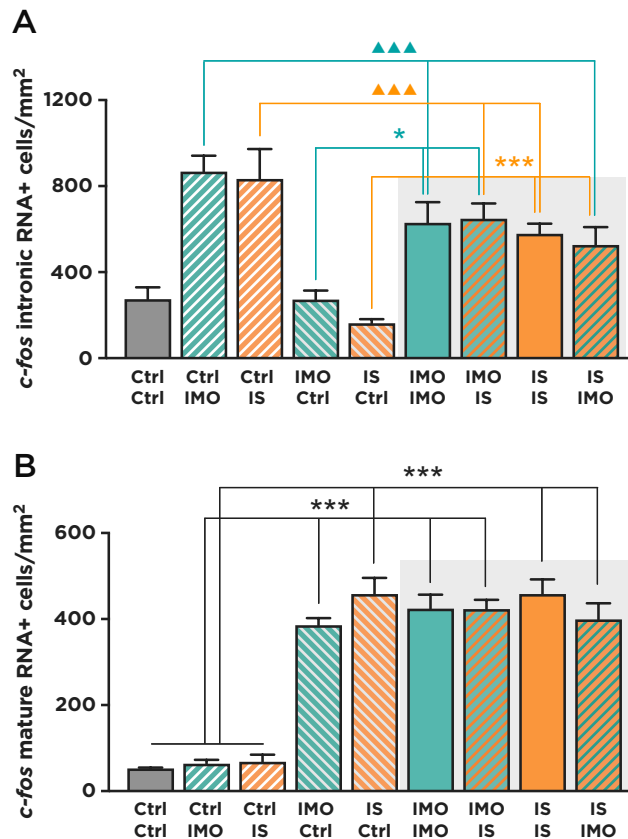


Figure 27. Expression of *c-fos* RNA in the deep layers of the IL cortex of animals exposed to different emotional stressors.

Quantification of the number of A) *c-fos* intronic RNA positive cells and B) *c-fos* mature RNA positive cells in basal conditions and after either one exposure to IMO or IS, or to two exposures of the same stressor twice or a combination of the two stressors. The grey square highlights the groups sequentially exposed to two stressors. Data represented as mean + SEM ($n=6-8$ animals/group; * $p < 0.05$, *** $p < 0.001$ vs Ctrl first stimulus, ▲▲▲ $p < 0.001$ vs Ctrl second stimulus. Only in this panel, in graph A lines of statistical significance were colour-coded with the corresponding colour of each stimulus because of the complexity of the statistical representation).

Identification of stressor-specific neuronal populations in the IL cortex

To identify potential stressor-specific neurons in the superficial layers of the IL cortex, we analysed the overlap between intronic RNA and mRNA labelling in those groups exposed to two stressors. GzLM analysis of the number of double labelled cells (**Fig. 28A**) indicated no main effects of the first or the second stimulus but a significant interaction between stimuli ($X^2(1) = 4.991$, $p = 0.025$). Pairwise comparisons revealed significant differences between the IS-IMO group and the IMO-IMO ($p = 0.046$) and the IS-IS groups ($p = 0.028$). Furthermore, analysis of the percentage of overlap in the four groups (**Fig. 28B**) showed again no effects of the first or the second stimulus separately but a significant interaction between stimuli ($X^2(1) = 7.008$, $p = 0.008$). Planned comparisons indicated that the IMO-IS group had a lower percentage of overlap than the IMO-IMO group ($p = 0.027$) and the IS-IS group ($p = 0.008$).

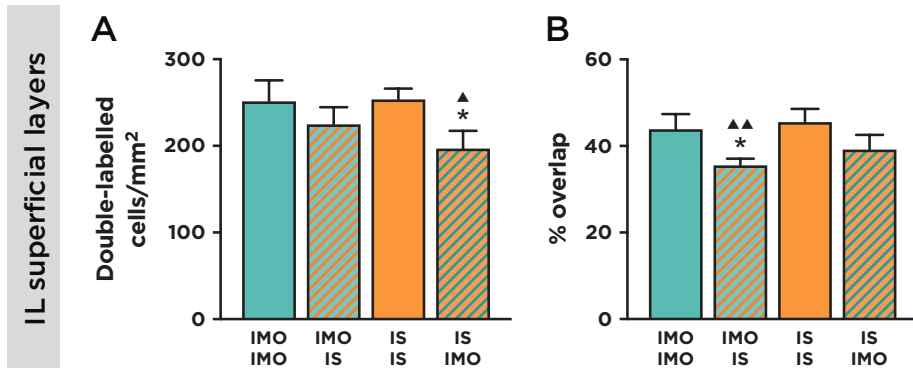


Figure 28. Overlap of *c-fos* intronic and mature RNA positive IL neurons in the experimental groups exposed to two stressors.

A) Total number of double labelled cells (intronic RNA+ mRNA+) and B) number of double labelled cells normalised to the number of *c-fos* intronic RNA+ cells. Data represented as mean + SEM ($n = 7-8$ animals/group; * $p < 0.05$ vs IMO-IMO group; ▲ $p < 0.05$, ▲▲ $p < 0.01$ vs IS-IS group).

Collectively, these results indicate that the catFISH technique allows us to distinguish between neurons activated by sequential exposure to two emotional stressors in the mPFC. Our data suggest that IMO and IS activate a large population of overlapping neurons, but a small population of neurons would be specifically recruited by each stressor. Furthermore, we observed a very high correlation between the number of activated cells in the superficial and deep layers of the PL cortex, and the results in the IL cortex also followed the same pattern.

Chapter 2: Molecular profiling of neurons activated in response to emotional stressors differing in intensity and nature in the PL

1. Introduction

There is currently little knowledge on the transcriptomic changes induced by exposure to acute stressors since most studies have focused on the consequences of chronic stress exposure. Furthermore, to our knowledge, only one study has directly compared the transcriptomic changes induced by different acute emotional stressors (Floriou-Servou et al., 2018). However, the exposure time was different for the three stressors (e.g. 6 min FST vs 30 min restraint, RES) and the analysis was performed only in the HF. Furthermore, it is known that not all changes at the transcriptomic level directly correlate with changes in the expression levels of the corresponding proteins (Zhang et al., 2020).

Novel approaches have been developed directed specifically at analysing RNAs bound to ribosomes (i.e. the translato~~m~~ome), and further sophistications have allowed selectively targeting the ribosomes of particular cell types or depending on the activation state of the cells. In this regard, the PhosphoRiboTRAP approach developed by Knight and colleagues (2012), takes advantage of the fact that phosphorylation of the ribosomal protein S6 correlates with the state of activation of specific neuronal populations. Hence, after exposure to a stimulus, immunoprecipitation with a pS6 antibody allows enrichment for the mRNAs selectively expressed in the neuronal populations that respond to this stimulus. In the present thesis, we have employed this methodology to analyse the molecular profiling of activated cells in response to emotional stressors differing in nature and intensity.

Based on the above, our **hypotheses** are:

- 1) Exposure to emotional stress will increase pS6 levels in the PL cortex as a result of neuronal activation. We hypothesise that this increase will be independent of the intensity of the stressors. Moreover, considering that c-fos and S6 phosphorylation share many signalling mechanisms of activation, we expect a high colocalization between both markers after exposure to stress.
- 2) We expect that the PhosphoRiboTRAP approach allows us to highly enrich samples for mRNAs associated with ribosomes of activated neurons.
- 3) We hypothesise that the PhosphoRiboTRAP approach will increase the sensitivity to observe differential gene expression changes after exposure to different stressors. This, in turn, will enable a better characterisation of the translato~~m~~ic signature linked to the intensity or the nature of emotional stressors.

To validate these hypotheses, the **objectives** of this chapter are:

- 1) To characterise the expression of pS6
 - a. In basal conditions, in response to different times of IMO and after exposure to two emotional stressors greatly differing in intensity (IMO vs NE).
 - b. To assess the colocalization between pS6 and c-Fos markers in animals exposed to IMO.
- 2) To validate the PhosphoRiboTRAP methodology for capturing RNA from activated neurons after emotional stressors in the PL cortex.
- 3) To perform molecular profiling of the gene expression changes in neurons activated by distinct emotional stressors differing in nature and intensity (RES, IMO and IS).

2. S6 phosphorylation after different times of IMO and different emotional stressors

2.1. Experimental design

The experimental design for the characterisation of pS6 expression after exposure to emotional stress is shown in **Fig. 29**. Adult SD male rats exposed to 30 min IMO (IMO30, n=3) or 90 min IMO (IMO90, n=5) and immediately perfused were used. A group of animals not exposed to any stressor and perfused in basal conditions was included as control (BASAL, n=5). We also compared pS6 levels in the PL of rats exposed to 90 min of IMO with rats exposed to 30 min of IMO followed by a recuperation period of 60 min before perfusion (IMO30 + 60, n=5), as well as between animals of the IMO30 group with another group of rats exposed to NE for 30 min, a milder stressor than IMO (NE30, n=5). The number of cells in the PL expressing pS6 and the intensity of the signal were quantified by immunofluorescence.

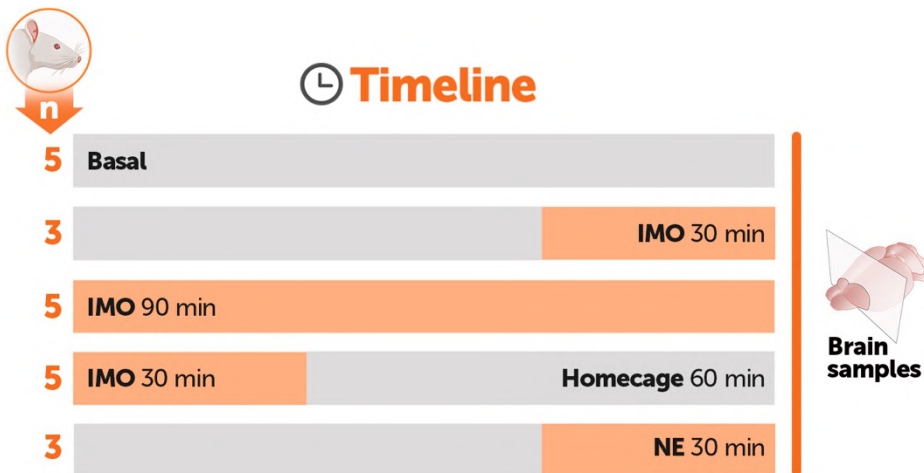


Figure 29. Experimental design for characterising pS6 expression after exposure to different times of IMO and to a novel environment (NE).

In orange is represented the stress exposure period and grey represents no stress exposure (home cage conditions). The sample size used in each group is represented inside the temporal line. Animals were euthanised by intracardiac perfusion and their brains were obtained for histological analyses.

2.2. Results

The quantification of the number of pS6-positive cells in response to different times of IMO in the PL cortex (**Fig. 30A**) revealed a significant effect of time ($X^2(2) = 42.3$, $p < 0.001$; **Fig. 30B**), with an increase in the number of pS6-positive cells already at 30 min ($p = 0.001$), and maximum levels at 90 min of IMO ($p < 0.001$). Furthermore, analysis of the total intensity of pS6 signal revealed a significant group effect ($X^2(2) = 60.8$, $p < 0.001$; **Fig. 30C**), with increased intensity of pS6 signal already at 30 min of IMO ($p = 0.02$) and a peak at 90 min of IMO ($p < 0.001$). Concerning pS6 fluorescence intensity per cell, there was also an effect of time ($X^2(2) = 81.7$, $p < 0.001$; **Fig. 30D**). Moreover, when pS6 levels of rats exposed to 90 min of IMO were compared with those exposed to 30 min of IMO and left undisturbed in their home cages for 60 min (**Fig. 30E**), no differences were observed in the number of pS6-positive cells (**Fig. 30F**), but the total intensity of pS6 signal tended to be reduced (**Fig. 30G**) and the intensity of pS6 fluorescence per cell was significantly reduced ($t_{(5,522)} = 3.7$, $p = 0.012$; **Fig. 30H**).

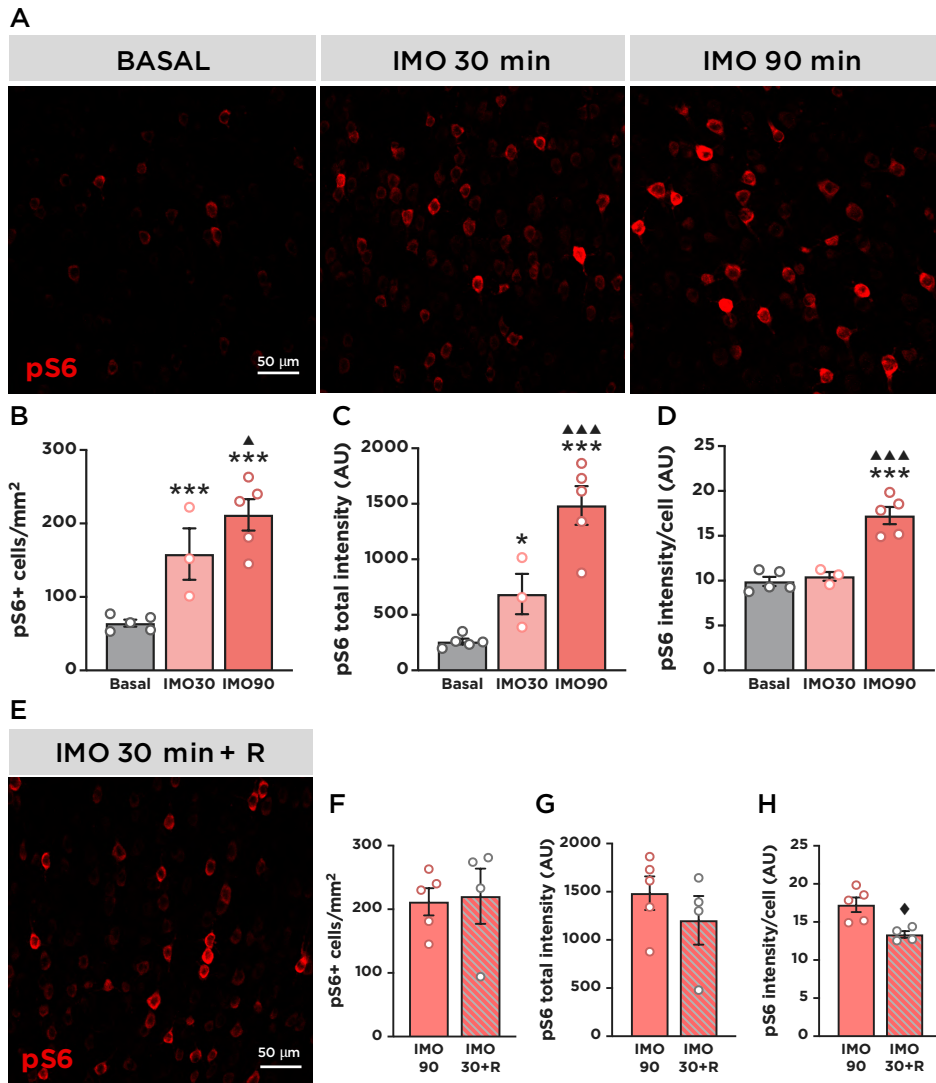


Figure 30. Quantification of pS6 expression in the PL cortex in basal conditions and after different times of IMO.

A) Representative images of pS6 expression (red) the experimental groups basal (left), IMO30 (middle) and IMO90 (right). All images are represented with the same scale. B) Quantification of the number of pS6 positive cells per mm², C) total intensity of fluorescence of pS6 and D) intensity of fluorescence per cell of pS6. E) Representative image of pS6 expression (pS6) in the experimental group IMO30 + R. F) The number of pS6 positive cells per mm², C) total intensity of fluorescence of pS6 and D) intensity of fluorescence per cell of pS6. Data represented as mean + SEM (n = 3-4/group, * p < 0.05, *** p < 0.001 vs basal; ▲ p < 0.05, ▲▲▲ p < 0.001 vs IMO30 group; ♦ p < 0.05 vs IMO90 group).

Furthermore, the comparison of the phosphorylation levels of S6 after two distinct emotional stressors differing in intensity (IMO vs NE; **Fig. 31A**) revealed no significant differences either in the number of pS6-positive cells (**Fig. 31B**) or the total intensity of pS6 signal (**Fig. 31C**), whereas the intensity of signal per cell had a marginal increase in the NE group ($t_{(6)} = -2.374$, $p = 0,055$; **Fig. 31D**).

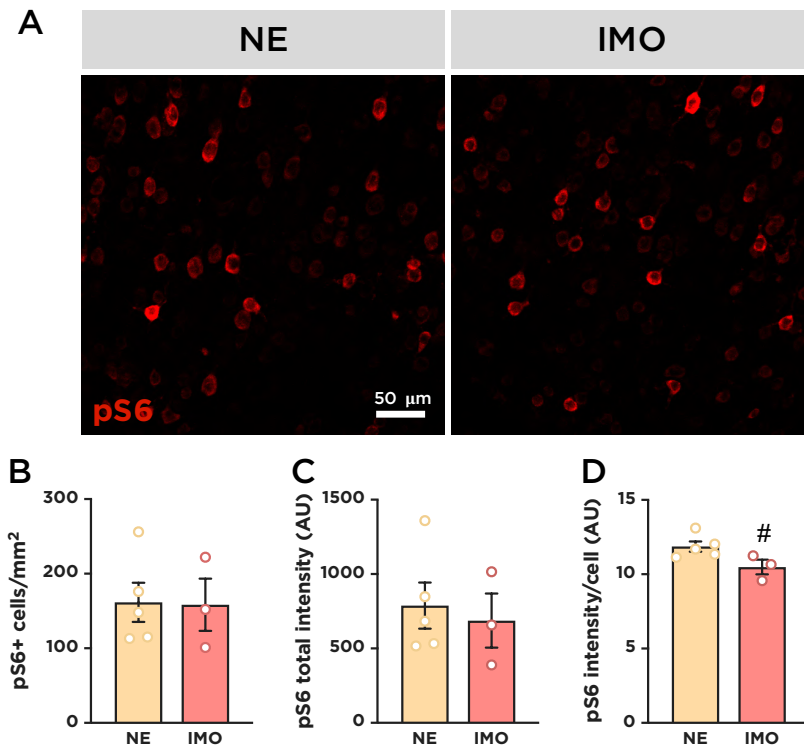


Figure 31. Quantification of pS6 expression in the PL cortex after exposure to a novel environment (NE) and exposure to IMO.

A) Representative images of pS6 expression (red) in animals exposed to NE (left) and IMO (right). All images are represented with the same scale. B) Quantification of the number of pS6 positive cells per mm², C) total intensity of fluorescence of pS6 and D) intensity of fluorescence per cell of pS6. Data are represented with mean \pm SEM; # $p < 0.1$ vs NE group).

3. Colocalization between pS6 and c-Fos after IMO exposure

3.1. Experimental design

After assessing the temporal dynamics of S6 phosphorylation after exposure to 30 and 90 min of IMO, we performed a pilot experiment with animals exposed to 60 min of IMO (IMO60, $n = 2$) to confirm whether S6 phosphorylation increases compared to animals not exposed to any stimulus (BASAL, $n = 2$) and to assess the colocalization between pS6 and the widely used activation marker c-Fos. 60 min of stimulus exposure is a time widely applied in studies that use the phosphoRiboTRAP technique and is a period very well-characterised in terms of the hormonal response. pS6 and c-Fos positive cells as well as the intensity of signal, and the colocalization between both markers were quantified by double immunofluorescence.

3.2. Results

To minimise the number of animals used, we utilised brain samples from other experiments performed in our group. Hence, we had a small sample size and for this reason no formal statistical analysis is shown for this data (**Fig. 32**). Our results clearly pointed towards increased number of pS6+ cells (**Fig. 32B**) and pS6 signal intensity: total (**Fig. 32C**) and per cell (**Fig. 32D**) after 60 min IMO compared to basal conditions. We also aimed to compare pS6 expression pattern in response to stress with the well-characterised c-Fos marker. The number of c-Fos+ cells (**Fig. 32E**), the total c-Fos fluorescence intensity (**Fig. 32F**) and the c-Fos fluorescence intensity per cell (**Fig. 32G**) were also increased in stressed animals compared to the basal group. Then to determine whether pS6 labels the same neuronal populations as c-Fos, we quantified the colocalization between both markers in the stressed animals (**Fig. 32H**). The colocalization analysis revealed that around 70% of pS6+ cells also expressed c-Fos and around 75% of c-Fos+ cells expressed pS6 (**Fig. 32I**).

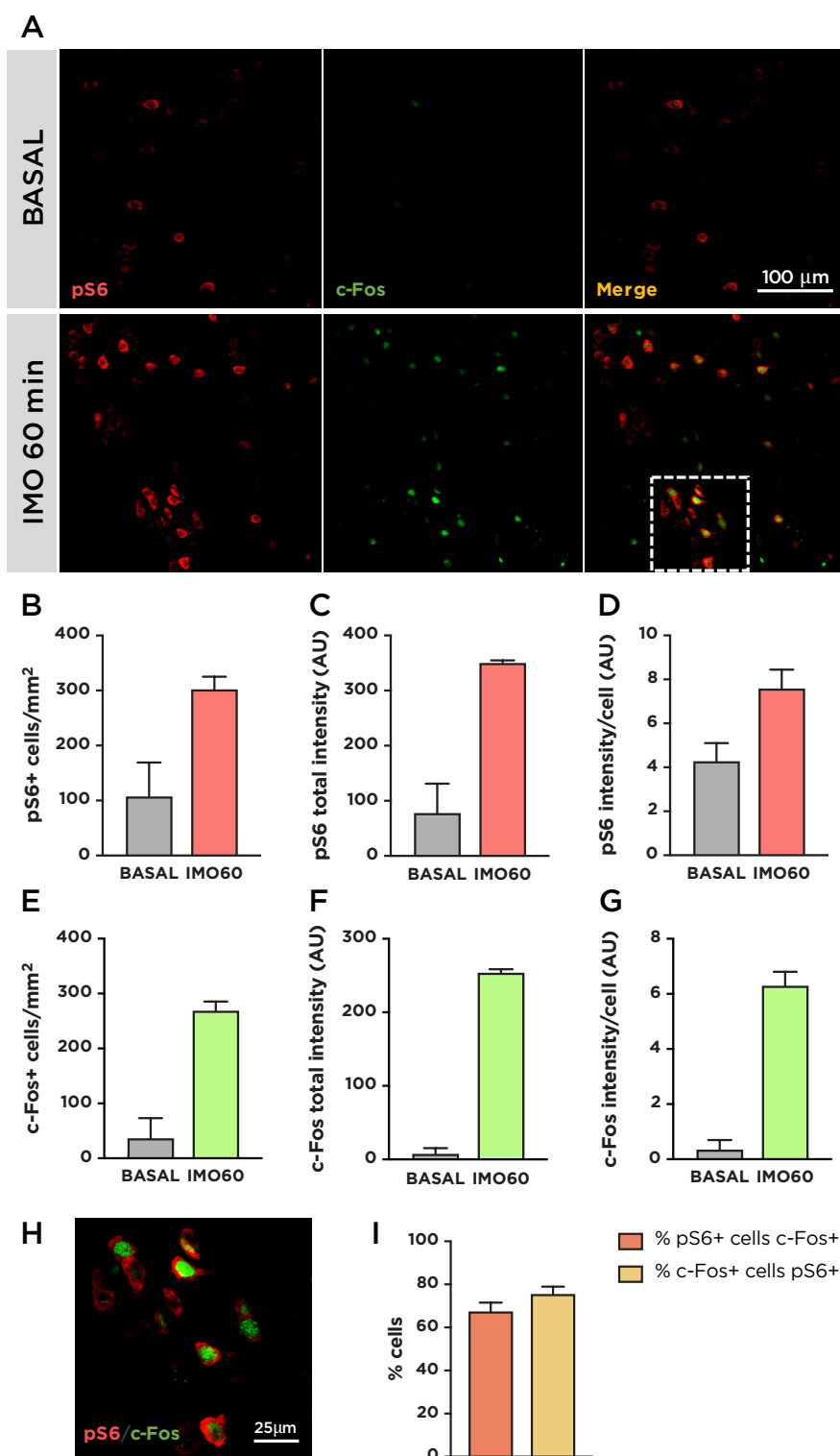


(Figure legend on next page)

Figure 32. pS6 and c-Fos expression in basal conditions and after exposure to 60 min IMO in the PL cortex.

A) Representative images of animals in basal conditions (*upper panel*) and exposed to 60 min IMO (*lower panel*). Left, pS6 labelling (*red*); middle, c-Fos labelling (*green*) and right, merge between pS6 and c-Fos labelling. The white dashed square represents the area selected for showing a higher magnification image in H. All images are represented with the same scale. B) Quantification of the number of pS6 positive cells per mm², C) total intensity of fluorescence of pS6 and D) intensity of fluorescence per cell of pS6. E) Quantification of the number of c-Fos positive cells per mm², F) total intensity of fluorescence of c-Fos and G) intensity of fluorescence per cell of c-Fos. H) Magnification of the white square shown in the condition 60 min IMO (A). Red, pS6 labelling and green, c-Fos labelling. I) Quantification of the colocalization between pS6 and c-Fos positive cells.

In summary, our results indicate that pS6 expression is increased after exposure to IMO in the PL cortex and colocalizes with the neuronal activation marker c-Fos, suggesting that S6 phosphorylation is a reasonably good correlate of neuronal activation.

4. PhosphoRiboTRAP: translatic profiling of PL neurons activated after acute exposure to different emotional stressors

4.1. Experimental design

We aimed to identify molecular markers of stress-responsive populations in the PL cortex after restraint (RES), immobilisation (IMO) and inescapable footshock (IS) exposure. 40 rats were randomly and equally distributed into 4 experimental groups. A group of rats was exposed to 60 min restraint (RES, n=10), another group to 60 min IMO (IMO, n=10) and another group to 60 min IS (IS, n=10). Finally, a group of rats remained in their home cages in basal conditions until euthanasia (BAS, n=10) (**Fig. 33, top**). Gene expression changes in the different conditions were evaluated by RNA-seq of ribosome-bound RNAs obtained by immunoprecipitation of pS6 (**Fig. 33, bottom**).

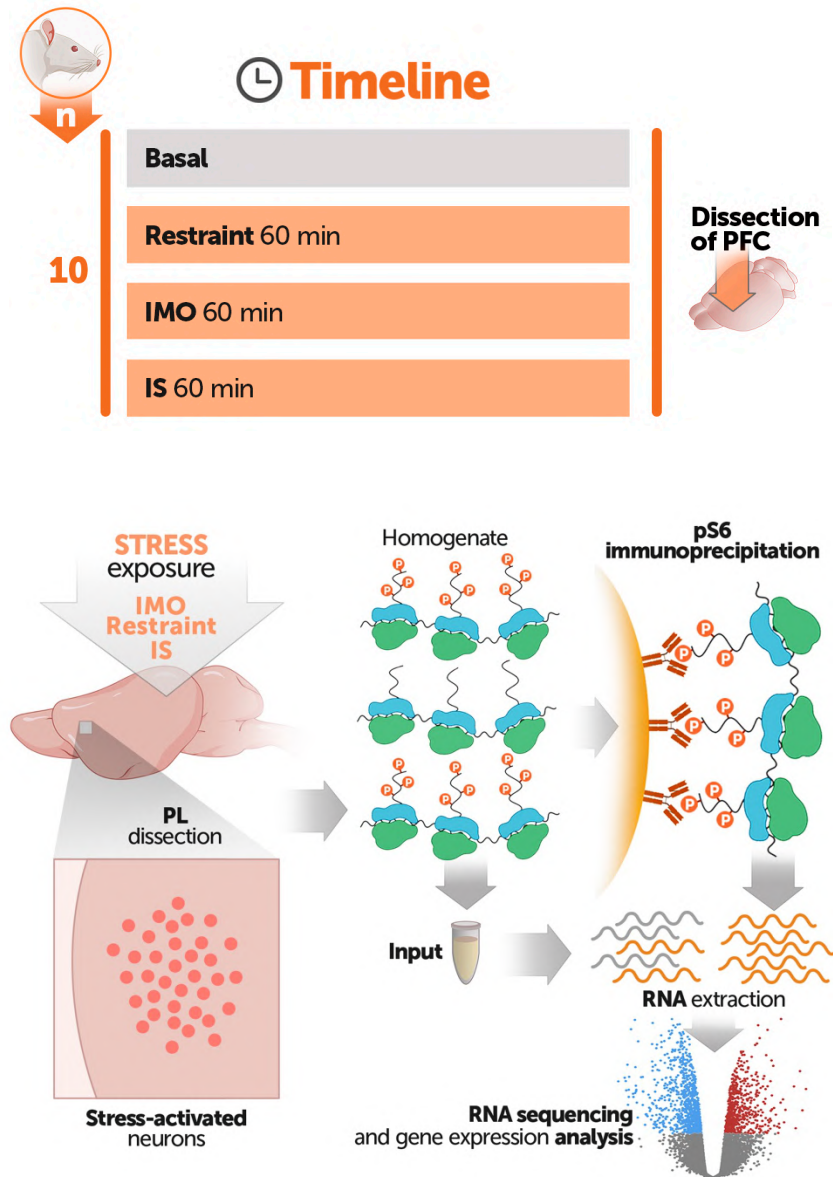


Figure 33. Experimental design and methodology for the study of gene changes after exposure to different stressors and in basal conditions.

Top, The stressors used were restraint (RES), immobilisation (IMO) and inescapable footshock (IS) for 60 min. Another group of animals remained undisturbed in their home cages (BAS).

The experiment was performed with 10 animals per group. Animals were euthanised by decapitation and the PL cortex was rapidly dissected in fresh and frozen. Bottom, schematic diagram of the PhosphoRiboTRAP procedure.

The election of the three stressors is based on two important aspects: 1) their intensity and 2) their nature or quality. First, IMO and restraint are of a very similar nature, as they imply a restriction of the free movement of the animal. Nevertheless, IMO represents a more severe type of movement restriction, as it involves taping the limbs and body of the animal to a wooden table, and it also restricts head movement. In fact, we have experimental evidence that IMO elicits a much higher ACTH and corticosterone response than restraint (García et al., 2000; Belda and Armario, unpublished data). Therefore, despite being comparable in terms of quality, IMO is of higher intensity than restraint. In contrast, IMO and IS elicit a similar peak HPA response (Márquez et al., 2002) but they mainly differ qualitatively in terms of movement possibilities and nociceptive signals, among others. Thus, analysing gene expression changes triggered by different emotional stressors in the immunoprecipitated samples will enable us to decipher genes activated in response to stress as well as different gene expression changes depending on the intensity and the nature of stressors.

4.2. Results

We immunoprecipitated the ribosomes with the phosphorylated S6 fraction from homogenates of dissected PL region from animals in basal conditions or exposed to the different emotional stressors. We then isolated and analysed the RNA to compare the gene expression patterns. qRT-PCR and RNA-seq analyses were performed with 4 animals per group.

qRT-PCR validation of pS6 immunoprecipitation

Before performing RNA-seq with all the samples, we first validated that the technique worked properly. To do so, we conducted a qRT-PCR analysis of the IEG *c-fos* in the input fraction (non-immunoprecipitated supernatant containing RNA from all cell types of the PL cortex) and the immunoprecipitated fraction (containing phosphorylated ribosomes-bound RNAs) in all the experimental groups (**Fig. 34**). GzLM statistical analysis of the levels of *c-fos* RNA in the input fraction revealed a significant GROUP effect ($X^2(3) = 120,2$, $p < 0.001$; **Fig. 34A**). Pairwise comparisons indicated that *c-fos* RNA levels were increased in the input fraction of all groups exposed to stress compared to the basal group ($p < 0.001$ for all stressors). Furthermore, *c-fos* RNA was higher in the IS group compared to the RES ($p < 0.001$) and IMO groups ($p < 0.001$). Remarkably, there were no differences between restraint and IMO animals.

Analysis of *c-fos* RNA levels in the IP fraction indicated a GROUP effect ($X^2(3) = 104,7$, $p < 0.001$; **Fig. 34B**). Further comparisons revealed that *c-*

fos RNA was increased in all stress groups compared to the basal condition ($p < 0.001$ for all stressors), with the highest levels in IS animals as compared to RES ($p < 0.001$) and IMO ($p < 0.001$). No differences were found between restraint and IMO animals. Importantly, comparison of the relative abundance of *c-fos* after pS6 immunoprecipitation and the input fraction that contains transcripts from all cell types revealed a significant enrichment of this gene. There was GROUP effect ($X^2(3) = 19.1$, $p < 0.001$; **Fig. 34C**) and pairwise comparisons revealed a significant enrichment in the IP fraction of restraint animals compared to basal ($p = 0.01$), IMO animals compared to basal ($p = 0.001$) and IS compared to basal ($p = 0.001$). A similar enrichment was found with all stressors.

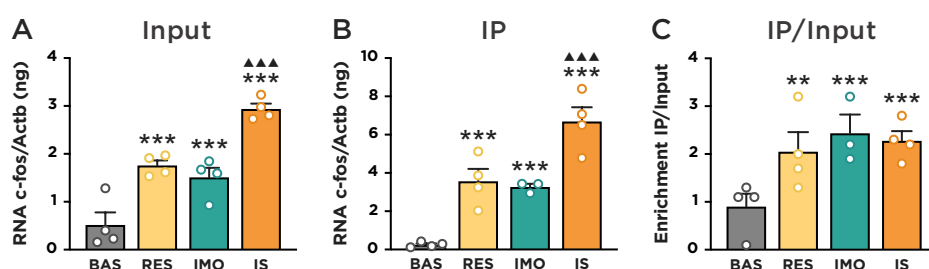


Figure 34. Validation of the PhosphoRiboTRAP approach by qRT-PCR.

qRT-PCR analyses of *c-fos* RNA levels A) in the input fraction and B) in the pS6 immunoprecipitated of all groups normalised to the housekeeping Actb. C) Validation of the enrichment of *c-fos* after pS6 immunoprecipitation compared to the input fraction. Data represented as mean \pm SEM ($n=3-4$ /group; ** $p < 0.01$, *** $p < 0.001$ vs basal; ▲▲▲ $p < 0.001$ vs IS).

RNA-seq analysis of input and pS6 immunoprecipitated samples

We then performed RNA-seq of all the experimental groups in both input and IP samples. Firstly, we aimed to assess overall differences and similarities between all the groups and conditions. To do so, we used principal component analysis (PCA) of all the samples (both inputs and immunoprecipitated) (**Fig. 35**). This indicated that the origin of the RNA (whole tissue input vs phosphorylated ribosome-bound RNA) explained most of the variance between samples (PC1: 82.6%). The second source of variance (PC2: 7.3%) was associated with exposure to a stressor (basal conditions vs exposure to either RES, IMO or IS). These differences between the basal and stress groups dramatically intensified in the case of IP samples. Moreover, the IP samples from RES and IMO conditions showed more overall similarities between them than with the IS group, which clustered separately. This differential clustering between stressors became more evident in the IP samples.

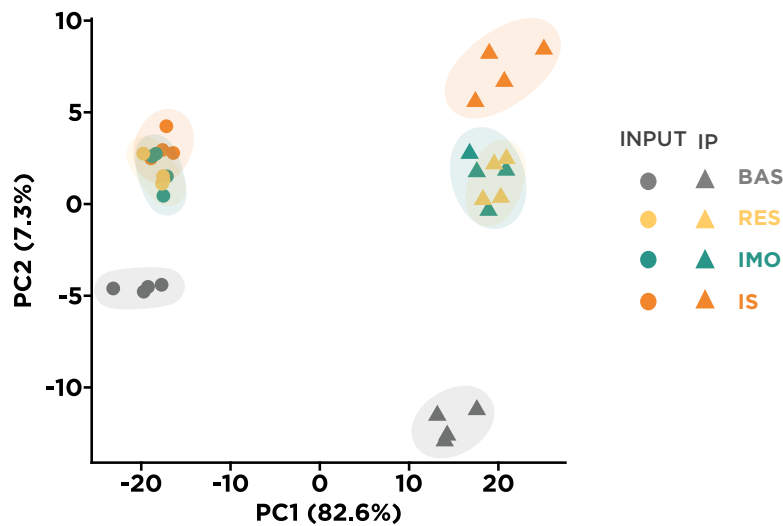


Figure 35. Principal component analysis (PCA) of RNA-seq gene expression of inputs and ribosome-bound RNAs from all the experimental groups.

Each symbol correspond to a sample of tissue from 1 rat (n=4/group). Circles represent input samples and triangles represent IP samples.

After an exhaustive bibliographic search we selected a list of IEGs used in studies of neuronal activation (e.g. Herdegen and Leah, 1998; Guzowski et al., 2001; Tyssowski et al., 2018; Yap and Greenberg, 2018) and we compared their relative expression levels in the input and IP samples from all groups, as shown in the heatmap (**Fig. 36A**). Hierarchical clustering showed a clear separation between the IP samples of the three stressors and the rest of the conditions (Basal IP and input samples, and stress input samples), revealing a clear impact of pS6 immunoprecipitation on the RNA content. Further clustering separated samples from basal animals from the inputs of all the stressors. Furthermore, in the cluster of IP stress samples, samples from the IS group in general tended to cluster separately from the rest, as already observed in the PCA analysis.

The overall pattern of the different IEGs showed higher expression levels in the input samples from stress groups vs input samples of basal animals and higher expression levels in the IP samples than in the inputs of each condition, further illustrating the aforementioned enrichment after pS6 immunoprecipitation. However, the heatmap also displayed some remarkable differences between the expression pattern of IEGs in the different conditions, as some IEGs were depleted after immunoprecipitation (e.g. *Atf1*, *Atf2* and *Creb1*), while others were higher in IP samples in basal conditions in comparison to stress conditions (e.g. *Homer1*).

The relative expression changes and statistical analysis of the IEGs most used in the field of stress (*Fos*, *Fosb*, *Arc*, *Egr1*, *Egr2*, *Npas4* and *Jun*; for examples see Cullinan et al., 1995; Ons et al., 2004) in IP samples from the stress groups compared to IP samples from basal animals are represented in **Fig. 36B**. All IEGs were significantly upregulated in the three stress conditions compared to the basal group ($p < 0.001$) except for *Jun*, which was only significantly upregulated in the IS group compared to the basal ($p = 0.008$). In fact, some IEGs like *Fos* and *Egr2* (also named *Krox-20*) showed a fold-change (FC) from 8 to 15 after stress exposure compared to basal conditions.

We further studied the number of significantly upregulated and downregulated genes ($|1.5| > \log_2 \text{FC}$) in the different stress conditions compared to the basal group in both input and pS6 immunoprecipitated samples. As shown in **Fig. 37**, pS6 immunoprecipitation significantly increased the number of differentially expressed genes detected in all stress conditions compared to the input fraction (Pearson's Chi-square test; $X^2(5) = 70.3$, $p = 8.8\text{e-}14$). Furthermore, the stressor with the highest number of differentially expressed genes relative to the basal group was IS.

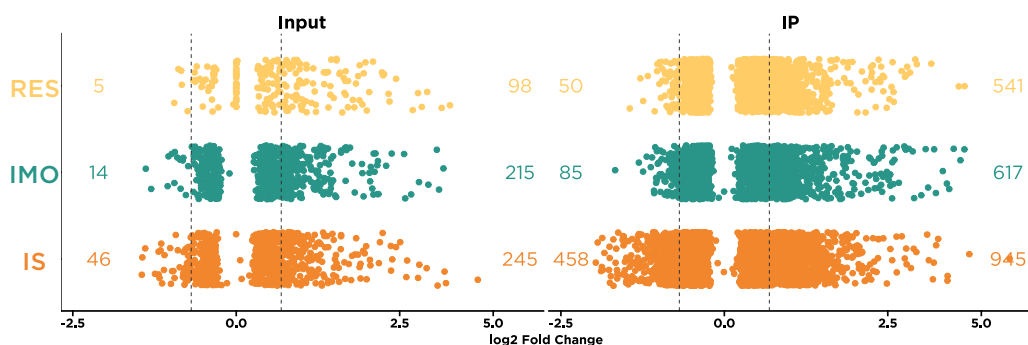


Figure 37. Fold-change plots of the significantly upregulated and downregulated genes in the input and IP samples of the three stressors compared to basal conditions.

Top, RES condition; middle, IMO condition and bottom, IS condition. Dots represent individual genes and numbers represent the total number of significantly downregulated (left) and upregulated (right) genes compared to the basal group for each stressor ($\text{padj} < 0.05$).

Dashed lines represent a FC threshold of ± 1.5 .

Given the apparent higher sensitivity provided by the pS6 IP procedure to find differentially expressed genes, we then focused the subsequent analysis of the RNA-seq data only in the IP samples to capture all the genes with differential expression in activated in cells in response to the distinct stressors, regardless of their general expression profiles outside of activated

cells. Firstly, we compared each stressor to basal conditions. This differential enrichment analysis of each stressor versus the basal group is depicted in the Volcano plots of **Fig. 38**. With the three stressors, the number of upregulated genes vs basal conditions was much higher than the number of downregulated genes. As expected, we found many IEGs among the genes with the highest FC and statistical significance in the three stressors compared to the basal (e.g. *Fosb*, *fos*, *Nr4a2*, *Arc*, *Npas4*, *Crem*) as previously described. Interestingly, other genes such as *Klf4* (encoding for the transcription factor Krueppel-like factor 4), *Gem* (encoding for the GTP binding protein overexpressed in skeletal Muscle), *Ccn1* (encoding for the secreted protein Cellular communication network factor 1) and *Coq10b* (encoding for the Coenzyme Q10B) were consistently highly upregulated with all stressors. To our knowledge, this list of genes has not been studied in the context of neuronal activation and emotional stress so far.

Furthermore, apart from the well-known IEGs we found that other genes were consistently upregulated in all the stressors compared to basal conditions. Among the most upregulated genes in the three stressors there were *Dio2* (encoding for iodothyronine deiodinase 2) related to thyroid hormone metabolism and *Ntsr2* (encoding for Neurotensin receptor 2), related to GPCR downstream signalling processes. Furthermore, genes related to extracellular matrix organisation such as *Lama5* and *Lamb2* were also significantly upregulated. Other genes such as *Mt1*, *Mt2a*, which belong to the Metallothionein family, were also highly upregulated in the three stressors. On the other hand, other genes were downregulated in all groups compared to basal conditions, such as *Nefh*, which encodes for a neurofilament protein involved in intracellular transport to axons and dendrites or *Satb1*, which is involved in transcription regulation and chromatin remodelling and has been related to apoptotic processes. The information for the described function of these genes was obtained from the Reactome database (Gillespie et al., 2022) and the Gene database from the National Center for Biotechnology Information (NCBI; Sayers et al., 2022).

Next, we aimed to investigate more in detail the proportion of genes shared and those stressor-specific that were induced or downregulated genes in response to the stressors. To do so, we overlapped the respective differentially expressed genes for each stressor compared to basal conditions. As seen in **Fig. 39**, using a $FC > \pm 1.5$, we found a total of 385 differentially upregulated genes shared by all the stressors in comparison to the basal group, including the genes above mentioned. This accounted for the 40% of all the genes upregulated in IS vs basal, 60% of all the genes upregulated in IMO vs basal and 70% of all the genes upregulated in RES vs basal.

IS and IMO shared specifically 86 differentially upregulated genes, accounting for 8% and 13% of their total of differentially expressed genes vs basal, respectively. Meanwhile, IS and restraint shared between them, but not with IMO, 94 genes, which accounted for the 9% and 17% of their total of differentially expressed genes vs basal, respectively. On the other hand, RES and IMO shared an 7% and 8%, respectively, of their total of differentially upregulated genes compared to basal conditions (48 genes). Finally, a 43% of the total upregulated genes in the IS group compared to the basal were specific for IS. In contrast, a 19% and a 5% of the total upregulated genes for IMO and RES groups were specific for each respective stressor.

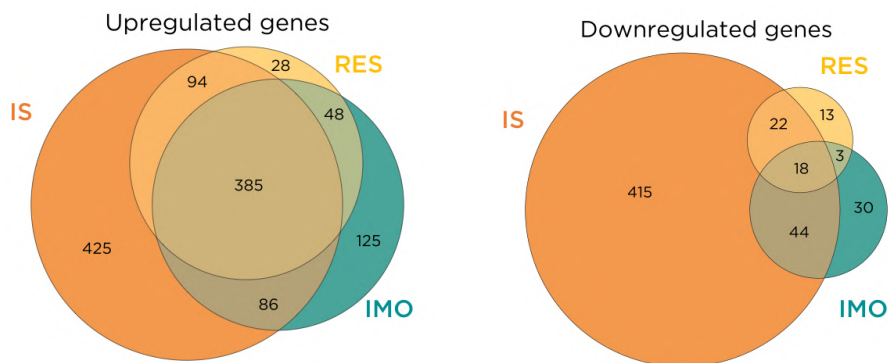


Figure 39. Gene expression changes in response to different stressors compared to basal conditions.

Euler diagrams showing the overlap of RNAs significantly upregulated (*left*) and downregulated (*right*) by RES, IMO and IS compared to basal conditions. The threshold for gene selection was $FC \pm 1.5$ and $padj < 0.05$.

Together, these results show that whereas IMO and RES highly overlap with each other, they only share a portion of the total genes upregulated by IS, thereby indicating a partially common translome profile between the

different stressors but also stressor-specific transcriptional signatures, especially notable with IS.

Regarding the pattern of stress-downregulated genes, we found only 18 shared by all the stressors relative to the basal group. This represented 4% of the genes downregulated in IS vs basal conditions, but a 19% and a 32% of the total of genes downregulated in IMO and restraint compared to basal conditions, respectively. Conversely, 415 genes were specifically downregulated in IS vs basal conditions, which accounted for a 83% of its total downregulated genes. In contrast, a 31% and a 23% of the total downregulated genes for IMO and RES groups were specific for each stressor, respectively. Hence, this suggest that IS has a much greater proportion of downregulated genes specific as compared with IMO and RES.

Since one of the main objectives of the thesis was to compare the gene changes in neurons activated by exposure to different emotional stressor, we also performed a differential gene analysis comparing IMO vs IS, RES vs IS and RES vs IMO (**Fig. 40**; $FC > \pm 1.5$, $p_{adj} < 0.05$). Strikingly, whereas IMO vs IS and RES vs IS showed some differences in the upregulated and downregulated genes, there were almost no significant changes between RES and IMO. We found only three genes that were significantly upregulated in RES compared to IMO (*C5*, *Rsrp1* and *Siah2*), whereas only 7 genes had higher relative expression in the IMO group compared to the RES group (*Apold1*, *Tmem252*, *Fundc2*, *Cpxm1*, *Ifit3*, *Paqr5* and *Adamts1*). These genes might be candidates to detect intensity of qualitatively similar stressors. In contrast, IMO vs IS comparison displayed 60 differentially upregulated genes and 33 differentially downregulated, whereas RES vs IS showed 67 upregulated and 32 downregulated. Collectively, these data indicates a more similar translome profile between RES and IMO than with IS, albeit all stressors share a great portion of their molecular profile.

Taken together, these data indicate that the PhosphoRiboTRAP approach selectively captures mRNAs from activated neurons, as there is a clear enrichment of IEGs in the IP samples compared to the input fractions. Furthermore, this methodology increases the sensitivity of the differential molecular signature analysis in PL activated neurons in response to distinct emotional stressors. Overall, we have observed that IMO and RES share a great portion of their total upregulated genes. Conversely, while IS also shares a great number of its differentially expressed genes with the other stressors, it also presents a considerable number of specifically differentially expressed genes. This would point to shared gene expression pattern between the distinct stressors, but also to specific molecular signatures of each stressor, particularly in the case of IS.

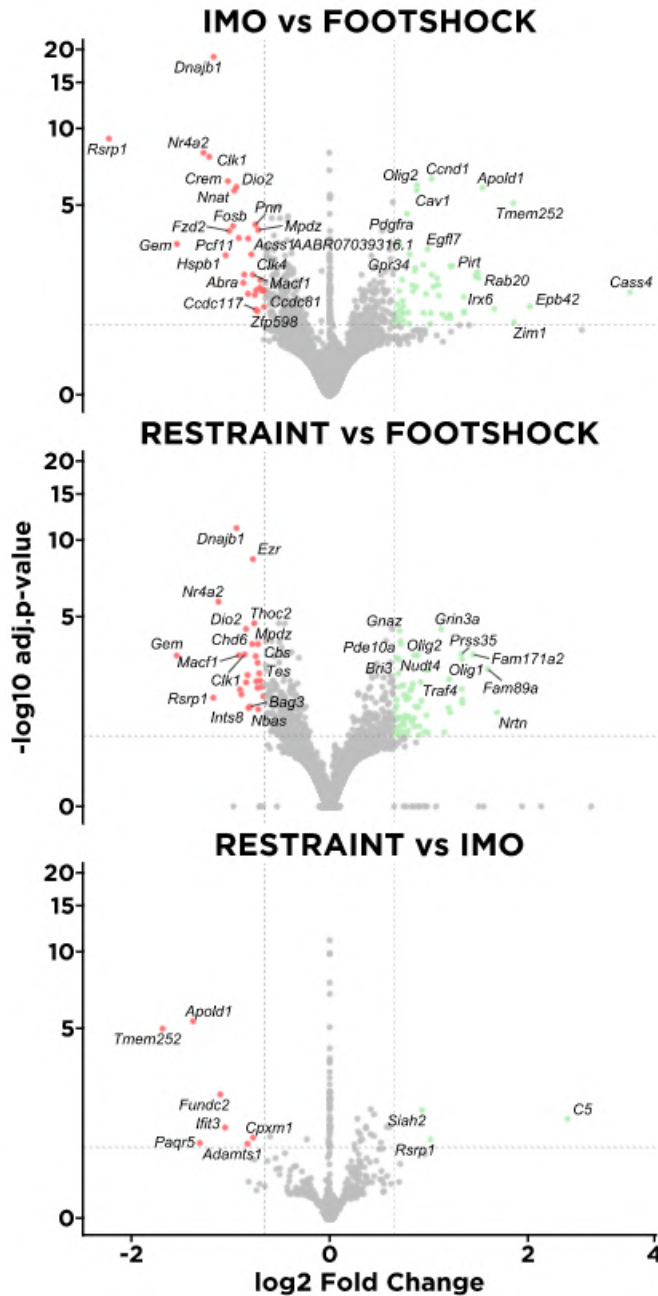


Figure 40. Comparison of the transcriptome profile of activated neurons between different emotional stressors.

Volcano plots depicting genes enriched and depleted in the IMO vs the IS group (top panel), the RES vs the IS groups (middle panel) and the RES vs the IMO groups (bottom panel) groups compared to basal conditions. Each dot represents a gene, significantly upregulated genes are labelled in green whereas significantly downregulated genes are labelled in red (threshold FC > ± 1.5 and padj < 0.05)

Chapter 3: Chemogenetic manipulation of stress-activated neurons in the PL

1. Introduction

Activation of mPFC neurons after exposure to emotional stressors has been reported in many studies (e.g. Cullinan et al., 1995; Ons et al., 2004) and the profound effects of stress exposure on mPFC structure and function have also been elegantly demonstrated (revised in Arnsten, 2015). In fact, in the previous chapters of this thesis, we have shown that *c-fos* levels in the mPFC rapidly increase in response to IMO and IS and that marked genetic changes occur in the PL region after exposure to different emotional stressors. In particular, the expression of many IEGs, such as *c-fos* and *Egr1*, is robustly up-regulated after exposure to RES, IMO and IS. However, the role of this brain region in the regulation of the neuroendocrine and behavioural stress response remains poorly understood, and studies have yielded inconsistent findings (see Section 3.5 of the Introduction).

A great challenge in neuroscience has been to elucidate the causal role of neuronal ensembles in particular behaviours. Technological advancements have been developed based on the use of IEG promoters, which allow the modulation of the activity of neuronal populations previously activated in response to a stimulus (revised in DeNardo & Luo, 2017). Based on our previous findings, in the present chapter, we aim to employ a manipulation strategy based on the use of the *c-fos* promoter and artificial chemogenetic receptors (DREADDs) to manipulate neurons in the PL previously activated by a stressor. We have selected IS as the stressor for different reasons: 1) the intensity of stress can be easily modulated by changing shock intensity; 2) the RNA-seq data showed that IS was the stressor which generated the most robust increase in several IEGs, 3) IS exposure results in the development of contextual fear conditioning, which does not occur after exposure to IMO (Daviu et al., 2012) and 4) the paradigm offers additional possibilities for future experiments, allowing to study the role of controllability.

The **hypotheses** on which we have based the present work are the following:

- 1) The use of a viral vector in which the expression of DREADDs is driven by the activity-regulated *c-fos* promoter will allow us to specifically manipulate stress-activated neuronal populations in the mPFC.
- 2) Given the fact that *c-fos* expression after exposure to emotional stressors is induced mainly in neurons and does not seem to be activated in glial cells, we predict that the viral vector will display an exclusively neuronal expression.

- 3) The manipulation of neurons previously activated by IS may result in typical stress-related behavioural changes (e.g. exploratory activity, coping strategies) and may modulate the HPA response to stress.

To validate the above-mentioned hypotheses, the **objectives** of this chapter are to:

- 1) Design a viral vector approach that enables the manipulation of neurons activated by stress exposure (IS) in the mPFC.
- 2) Validate the induction of viral vector expression after stress exposure and analyse its expression in neuronal and glial cells.
- 3) Assess the behavioural and hormonal consequences of activating neurons previously activated by IS with the excitatory DREADD (hM3Dq) construct in stress-sensitive behavioural tests.
- 4) Assess the behavioural and hormonal consequences of inhibiting neurons previously activated by IS with the inhibitory DREADD (hM4Di) construct in stress-sensitive behavioural tests.

The working hypothesis and general experimental design are summarised in **Fig. 41**.

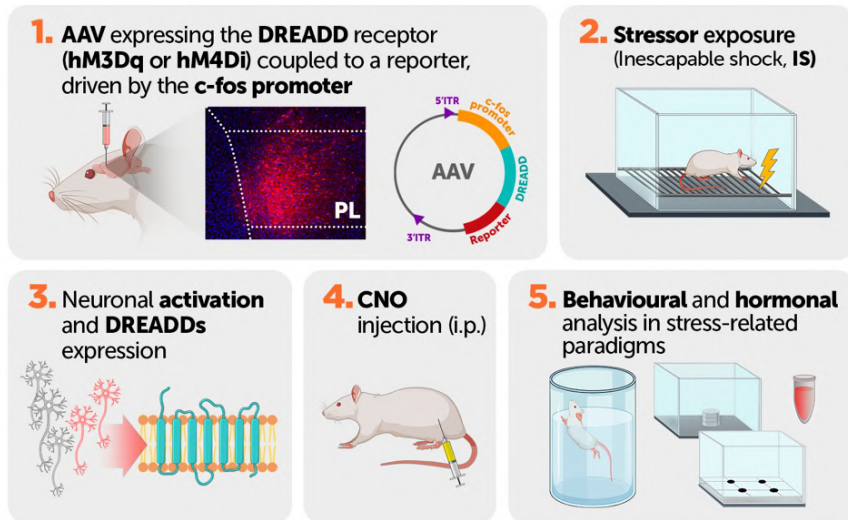


Figure 41. Working hypothesis and experimental design for evaluating the effects of manipulating stress-activated neurons at the behavioural and hormonal level.

Abbreviations: AAV, adenoassociated viral vector; CNO, clozapine-N-oxide; DREADD, Designer Receptors Exclusively Activated by Designer Drugs; i.p., intraperitoneal; IS, inescapable shock.

2. Design and validation of expression of AAV1-pfos:hM3Dq:mCherry

2.1. Experimental design

For the validation of the first viral vector designed in this thesis, two groups of animals were injected with the AAV1-pfos:hM3Dq:mCherry vector bilaterally in the PL cortex. One group was exposed to inescapable footshock and perfused 18h hours later (IS, n=5), a time based on previous studies using *c-fos*-driven viral vectors (Gore, Schwartz, & Salmanz, 2015). The other group remained undisturbed in the home cage and was perfused under basal conditions (Control, n=4).

2.2. Results

We engineered an expression construct in which the excitatory artificial receptor DREADD (hM3Dq) fused to the reporter mCherry was driven by the minimal *c-fos* promoter and packaged into AAV particles (**Fig. 42A**) in order to manipulate stress-activated neurons in the rat mPFC. **Fig. 42B** depicts the injection site and spread of the viral vector transduction, detected by the presence of mCherry fluorescence in the cohort of rats bilaterally injected with the viral vector in the PL cortex. The analysis showed that the viral vector was appropriately expressed in the mPFC, mainly restricted to the PL region, with minor expression in the IL and ACC. Higher magnification to characterise the subcellular localization of the receptor (**Fig. 42C**) revealed a membrane expression pattern for mCherry, typical of the general topography of DREADD expression, both in the soma and in dendrites and axons. Next, to assess whether the viral vector AAV-pfos:hM3Dq:mCherry was appropriately induced by neuronal activity, we compared AAV expression in stressed animals (18h after IS) versus control animals (**Fig. 42D**). We hypothesised that if the viral vector was expressed after neuronal activation under the control of the *c-fos* promoter, the reporter mCherry should be significantly higher in stressed than control animals. However, the histological analysis revealed no significant differences in the number of mCherry+ cells between the control and the stressed groups (**Fig. 42E**) suggesting no significant increase in viral vector expression associated with stress exposure. In this analysis, we also compared the quantification of the viral vector expression detecting mCherry directly or by immunofluorescence amplification. The correlation between both quantifications was very high ($r = 0.835$, $p < 0.001$; not shown). Moreover, given that mCherry signal was easily visualised without

amplification by immunofluorescence, we decided to not use the mCherry antibody for the next experiments of the thesis.

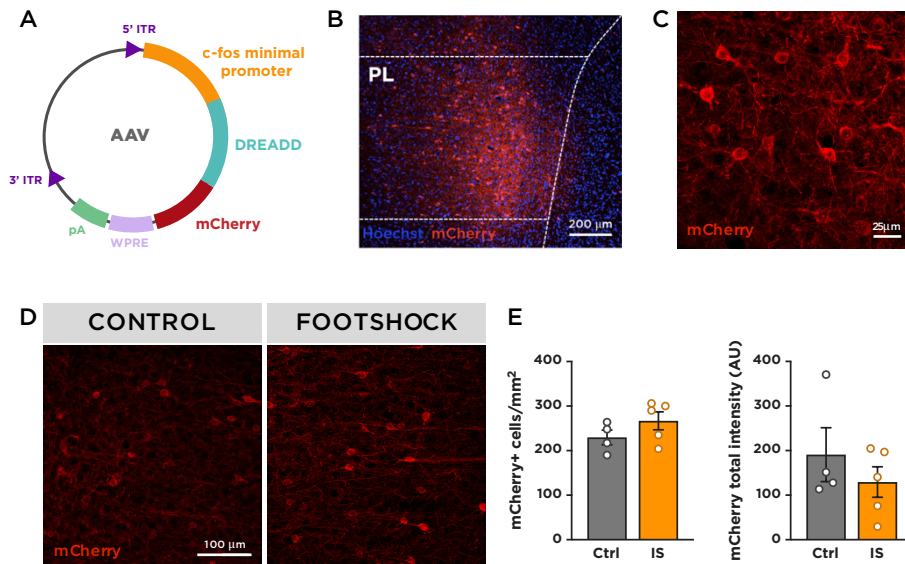


Figure 42. AAV1-pfos:hM3Dq:mcherry sequence design and expression in control animals and animals exposed to inescapable footshock (IS).

A) Schematic representation of the AAV1-pfos:hM3Dq:mCherry vector. The minimal *c-fos* promoter drives the expression of the excitatory artificial receptor DREADD (hM3Dq), which is fused to the reporter protein mCherry. B) Representative image from one animal showing the injection site and viral vector spread based on mCherry fluorescence. White dashed lines delineate the PL cortex. Blue, Hoechst nuclear staining; red, mCherry. C) Higher magnification of viral vector expression showing mCherry staining. D) Representative images of mCherry levels in animals in basal conditions and at 18h after exposure to IS. E) Quantification of the number of cells expressing mCherry and total intensity of mCherry in animals in basal conditions (Ctrl) and 18h after exposure to IS. Values represent mean \pm SEM (n=4-5/group). AAV, adeno-associated viral vector; ITR, inverted terminal repeat; pA, bovine growth hormone polyadenylation signal; PL, prelimbic cortex; WPRE: woodchuck hepatitis virus posttranscriptional regulatory element.

3. Design and validation of AAV9-pfos(Int+Ex):hM3Dq: mCherry:PEST

3.1. Experimental design

Next, we designed a new viral vector implementing some changes that we hypothesised could be important for regulating its activity-dependent expression. Firstly, the *c-fos* first intron and a segment of the first exon were added to the minimal promoter region of *c-fos*, as it has been shown that the

first intron contains key regulatory elements for *c-fos* transcription (Robertson et al., 1995; Coulon et al., 2010). Secondly, the STOP codon from mCherry was removed and a 70 bp PEST sequence was added to the C-terminal end of mCherry (**Fig. 43A**). The PEST sequence is a conserved amino acid sequence enriched in Proline, Glutamic acid, Serine and Threonine, which is present in short half-life proteins that are rapidly degraded (Rogers et al., 1986). For our viral vector, we added a fragment from the C-terminal rat ornithine decarboxylase (OCD), which contains a PEST sequence that, when fused to the C-terminal end of other proteins such as EGFP, drastically reduces their half-life by increasing their degradation (X. Li et al., 1998). Given the results obtained with the previous viral vector, we inserted the degradation domain of rat OCD to promote construct degradation and prevent the fusion protein DREADD:mCherry from accumulating over time, thereby reducing background levels of the viral vector.

For the validation of the second viral vector approach, three groups of animals were injected with the AAV9-pfos(Int+Ex):hM3Dq:mCherry:PEST vector bilaterally in the PL cortex. Two groups were exposed to IS and perfused 4h (IS 4h, n=4) or 18h later (IS 18h, n=4), whereas the other group remained undisturbed in their home cage and was perfused in basal conditions (Control, n=5). In this experiment, we added an additional stress group perfused at an earlier time point (4h after IS) in case the PEST sequence would promote such a fast degradation of the construct that at 18h it would not be possible to detect stress-induced viral vector expression. Brain samples were obtained to assess viral vector expression through the visualisation of mCherry.

We first verified the appropriate expression of the viral vector and analysed the extent of viral spread in animals bilaterally injected in the PL cortex with the AAV-pfos(Int+Ex):hM3Dq:mCherry:PEST viral vector (**Fig. 43B**). Histological analysis revealed that the viral vector was appropriately expressed as shown by mCherry fluorescence and its spread was primarily limited to the PL cortex, with low expression in the ACC and IL. Injection sites and viral vector spread were found from Bregma 4.2 to 2.7 mm (Paxinos and Watson, 2014). Next, to evaluate whether the viral vector was expressed in an activity-dependent manner, we compared mCherry expression in basal versus stress conditions.

The histological analysis (**Fig. 43C**) revealed a significant GROUP effect ($X^2(2) = 17.6$, $p < 0.001$), with animals perfused 4h after IS showing a significantly higher number of mCherry+ cells than the control group ($p < 0.001$), which returned to basal levels at 18h after IS (**Fig. 43D, left**). We further characterised viral vector expression after stress by analysing the

global fluorescence intensity of mCherry (**Fig. 43D, middle**). We observed the same pattern as with the number of cells: a significant GROUP effect ($X^2(2) = 14.3$, $p = 0.001$), with increased mCherry fluorescence intensity levels at 4h after IS ($p = 0.003$) that normalised at 18h after IS. Finally, the analysis of the levels of viral vector levels per cell (**Fig. 43D, right**) also showed a significant GROUP effect ($X^2(2) = 7.8$, $p = 0.020$), with a clear trend to be higher in the group exposed to IS and perfused 4h later than in basal conditions ($p=0.055$), and no differences after 18h.

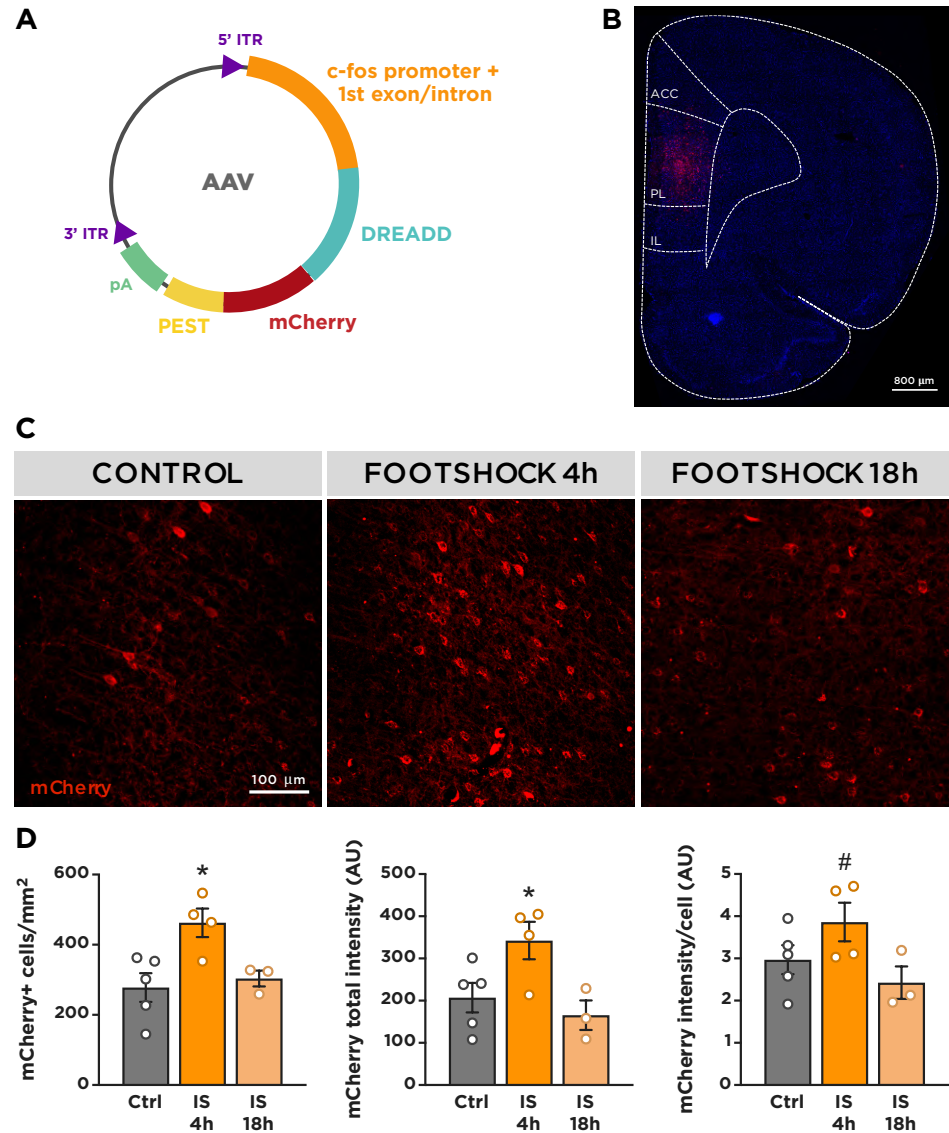


(Figure legend on next page)

Figure 43. AAV9-pfos(Int+Ex):DREADD:mcherry:PEST sequence design and expression levels in control animals and animals exposed to inescapable footshock (IS).

A) Schematic representation of the viral vector AAV9-pfos(Int+Ex):DREADD:mcherry:PEST. The *c-fos* promoter region, the first intron and a segment of the first exon of the *c-fos* gene control the expression of the artificial receptor DREADD, which is fused to the mCherry and the degradation sequence PEST. B) Representative image from one animal showing the injection site and spread of infection based on mCherry fluorescence. Blue, Hoechst nuclear staining; red, mCherry. C) Representative images showing activity-dependent labelling of PL neurons (mCherry+) in basal conditions, 4h and 18h after IS. D) Quantification of the number of mCherry-positive cells (*right*), total mCherry fluorescence intensity (*middle*), and fluorescence intensity per cell (*left*) in control and stressed animals 4h and 18h after IS. Values represent mean \pm SEM (n=3-5/group, *p < 0.05 vs control group, # p < 0.1 vs control group). AAV, adeno-associated viral vector; ITR, inverted terminal repeat; pA, bovine growth hormone polyadenylation signal; PL, prelimbic cortex.

We further studied whether or not the *c-fos* viral vector displayed an exclusively neuronal expression. Immunofluorescent analysis (**Fig. 44**) showed that mCherry protein widely colocalised with NeuN, an extensively used neuronal marker (**Fig. 44C**). In contrast, astrocytes did not seem to express the viral vector, as there was no colocalization between mCherry and the astrocytic marker GFAP (glial fibrillary acidic protein) (**Fig. 44F**).

Importantly, it seems that neuronal viability was maintained after transduction with the viral vector, as mCherry+ neurons show intact NeuN immunolabelling and similar neuronal morphology compared to other non-transduced neighbouring neurons (**Fig. 44C**). Quantification of the number of cells expressing mCherry that corresponded to neurons from both control and IS 4h group (n = 4/group) indicated that a 98.9% of mCherry+ cells were also neurons (mCherry+NeuN+/mCherry+). In the case of GFAP (**Fig. 44D**), the number of mCherry+ cells that colocalised with GFAP+ cells was null (mCherry+GFAP+/mCherry+; **Fig. 44F**).

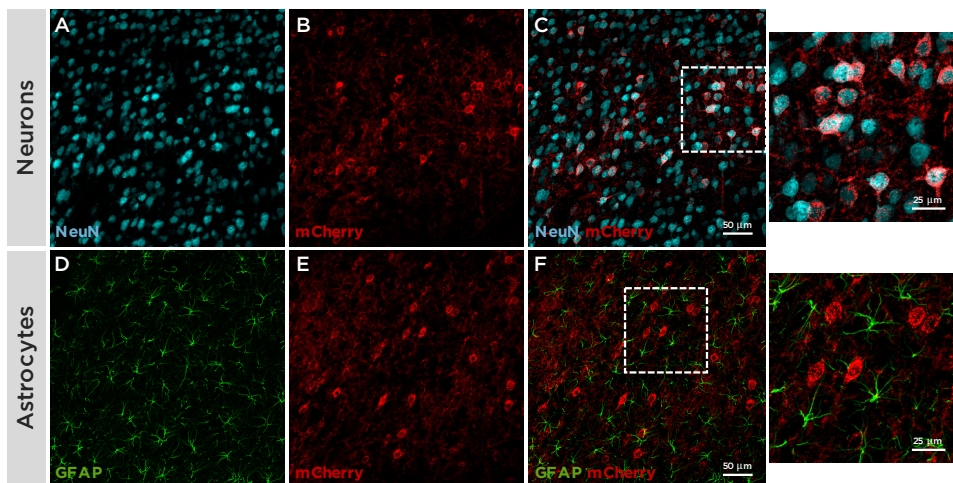


Figure 44. Assessment of AAV-pfos(Int+Ex):hM3Dq:mcherry:PEST expression in neurons and glial cells (astrocytes) in the PL cortex of animals exposed to inescapable footshock.

Top panel, representative images of A) a NeuN immunolabelled section (blue), B) viral vector expression (mCherry, red) and C) composite of NeuN and mCherry labelling showing extensive colocalization between neurons and the viral vector. Bottom panel, representative images of a section showing D) immunolabelling for glial fibrillary acidic protein (GFAP, green), E) viral vector expression (mCherry, red) and F) composite of GFAP and mCherry, indicating no colocalization between astrocytes and the viral vector. White dashed squares represent a higher magnification of the original images.

Together, these results indicate that the viral vector used in this thesis (AAV9-pfos(Int+Ex):hM3Dq:mCherry:PEST) is specifically expressed in neurons (not in astrocytes) of the rat PL cortex and its expression is induced by neuronal activation after IS exposure. Thus, this vector enables activity-dependent labelling and manipulation of neurons after stress.

3.2. Behavioural consequences of inescapable footshock exposure

In the previous experiment, we found significantly increased expression of mCherry 4 hours after IS. However, we have never studied the behavioural consequences of IS exposure in such a time period. Therefore, we decided to do an experiment in rats not subjected to stereotaxic surgery. Non-stressed (Ctrl, $n = 10$) or IS (IS, $n = 9$) rats were tested at various times after IS exposure: immediately after IS to study the activity of animals in the home cage for 5 min; 4 h later to study activity in an OF for 5 min, to evaluate changes in locomotor and exploratory behaviour at the peak of mCherry expression. The rectangular OF contained an object in the centre to assess

motivation to interact with a novel object. Finally, to better characterise the behavioural consequences of IS, we also assessed the activity of rats in a circular open field 48-72h after IS (**Fig. 45**). The procedure allowed us to gain an understanding of the immediate impact of IS on the overall activity as well as the short-term and long-term behavioural effects on activity and exploratory behaviour.

Stressed animals already showed hypoactivity in the home cage immediately after IS exposure, as evidenced by a significantly reduced distance travelled in this group compared to control animals ($t_{(17)} = 5.002$, $p < 0.001$; **Fig. 45A**). Analysis of the behaviour in the rectangular OF (**Fig. 45B**) indicated that previously shocked rats tended to travel less distance ($t_{(17)} = 2.068$, $p = 0.054$). Although no significant differences were found in terms of object interaction episodes, stressed animals spent significantly less time interacting with the object than non-shocked animals ($t_{(17)} = 2.3$, $p = 0.034$). Furthermore, shock-exposed animals tended to perform less rearings ($t_{(12,920)} = 1.975$, $p = 0.070$) and displayed significantly increased grooming episodes ($t_{(17)} = -3.116$, $p = 0.006$) and time ($t_{(17)} = -3.707$, $p = 0.002$). Finally, shock-induced hypoactivity in a circular OF was also observed at 48-72h after IS ($t_{(17)} = 3.061$, $p = 0.007$; **Fig. 45C**), although no differences were found in the distance travelled in the central, more anxiogenic, zone.

Together, these results provide evidence that IS exposure in rats reduces general activity and exploratory behaviour, while increasing grooming behaviour 4h later. Moreover, shock-induced hypoactivity in novel environments is maintained at least 48-72h after IS exposure.

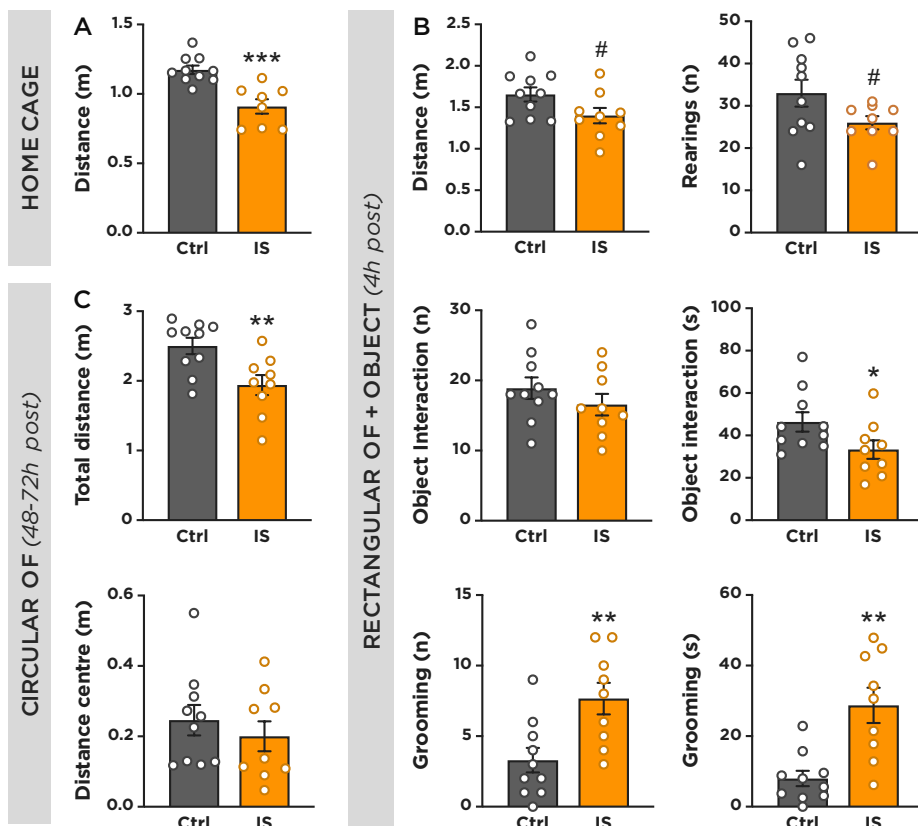


Figure 45. Behavioural effects in novel environments at different time points after inescapable footshock (IS) exposure and in the home cage immediately after.

A) Distance travelled in the home cage immediately after IS exposure. B) Behaviour of rats in the rectangular open field (OF) with an object in the centre 4h after IS exposure, including the distance travelled, number of rearings, object interaction episodes and time, grooming episodes and time of grooming. C) Distance travelled in total and in the central zone of a circular OF 48-72h after IS. Values represent mean \pm SEM ($n=9-10$ /group, * $p < 0.05$; ** $p < 0.01$; *** $p < 0.001$; # $p < 0.1$ compared to control group).

3.3. Re-activation of stress-activated neurons in the PL

The validation experiments previously described demonstrated an effective induction of the expression of the viral vector 4h after IS exposure and also altered behaviour at this time. Next, we aimed to modulate neuronal activation using DREADDs in order to study if stress-activated PL neuronal ensembles play a role in regulating the behavioural and hormonal response to emotional stressors.

The experimental design for the re-activating IS-activated neurons is shown in **Fig. 46**. We bilaterally injected the viral vector AAV9-

pfos(Int+Ex):hM3Dq:mCherry:PEST into the rat PL (n=24, 6 animals/group). Three weeks later, half of the animals were exposed to a 20 min IS session (stress) whereas the other half remained undisturbed in their home cage (control). 3 h and 30 min after initiation of IS exposure, control and stress groups were injected with either vehicle (0.9% saline solution with DMSO) or CNO (1 mg/kg, i.p.) and 30 min later exposed to the OF. This resulted in the following groups: **Control-vehicle**, **Control-CNO**, **Stress-vehicle** and **Stress-CNO**. OF exposure lasted 15 min and immediately after, blood samples were obtained to assess HPA response to the OF. One day later, all animals were exposed to the HB test to evaluate if previous activation or inhibition of IS-responsive neurons had any effects 24h later. One week later, the same animals were exposed again to IS and the same injection protocol previously described, except that they were tested for 15 min in the FST 30 min after appropriate injections. Again, blood samples were obtained immediately after the FST. Finally, 2h later, they were perfused to obtain brain samples for histological analyses.

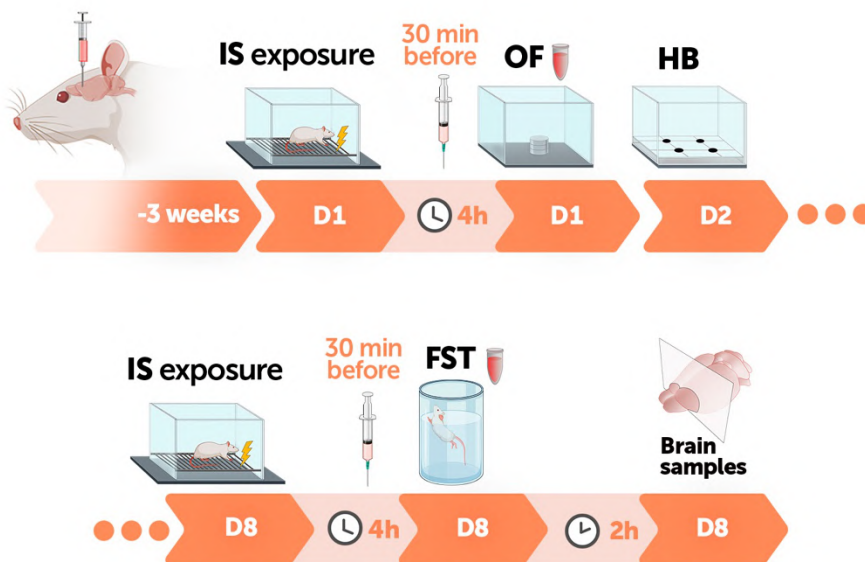


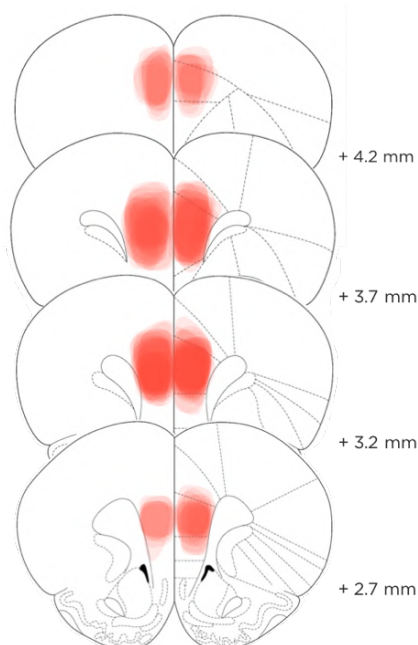
Figure 46. Experimental design for re-activation of IS-activated neurons.

Abbreviations: FST, forced swim test; HB, hole board; OF, open field.

The effects of re-activating neurons previously activated by IS in the activity and exploratory behaviour of the animals were first assessed during a 15-min session in an OF test with an object placed in the centre. A 15-min exposure would allow us to simultaneously study the response of the HPA axis (e.g. plasma corticosterone levels). Nevertheless, in this thesis, we will only represent and discuss the behavioural results of the first 5 min of the

test, since this is the standard procedure for behavioural studies and no additional clear information emerged when we analysed the following 10 min of the test. The coordinates of injection from the animals included in the overall analysis are shown in **Fig. 47**.

Figure 47. Schematic drawing of the injection site and spread of infection of AAV-pfos(Int+Ex)-hM3Dq:mCherry: PEST in all the animals included in the statistical analysis. Note that viral vector spread (determined by mCherry fluorescence) was within the Bregma range 2.7 mm to 4.2 mm (n=22).



The statistical analysis of the behaviour in the OF was performed with a GzLM with 2 factors: **STRESS** (control vs IS) x **DRUG** (vehicle vs CNO). When the interaction between factors was significant, appropriate post-hoc pairwise comparisons (LSD test) were performed. We observed a significant effect of STRESS in reducing the distance travelled in the OF ($X^2(1) = 8.8$, $p = 0.003$; **Fig. 48B**), but no effect of either the DRUG or the interaction STRESS x DRUG. No significant differences were observed in the frequency of rearings performed by the animals (**Fig. 48C**). Analysis of the interaction with the object indicated a significant effect of STRESS for object interaction episodes ($X^2(1) = 9.6$, $p = 0.002$; **Fig. 48D**) and time ($X^2(1) = 25.2$, $p < 0.001$; **Fig. 48E**), but no effect of DRUG and no STRESS x DRUG interaction. Regarding grooming frequency, there was a trend for an effect of STRESS ($X^2(1) = 2.9$, $p = 0.087$), no effect of DRUG and a trend for a significant STRESS x DRUG interaction ($X^2(1) = 2.9$, $p = 0.087$; **Fig. 48F**). Post-hoc comparisons indicated significantly higher grooming frequency in the Stress-CNO group than in the control-CNO group ($p = 0.012$). No differences were observed in grooming time (**Fig. 48G**).

Finally, analysis of the corticosterone response to the OF indicated no effect of STRESS, but a significant main effect of DRUG ($X^2(1) = 4.3$, $p = 0.039$; **Fig. 48H**). The interaction between STRESS x DRUG was not significant. Both control and stressed animals injected with CNO showed a reduced corticosterone response to the OF compared with vehicle-injected animals. We further assessed whether the HPA response to OF correlated with any of the parameters measured. We did not find any significant correlation between corticosterone levels and the behavioural variables analysed, except for a small trend to a negative correlation between object interaction time and corticosterone levels ($r = -0.38$, $p = 0.09$; **Fig. 48I**).

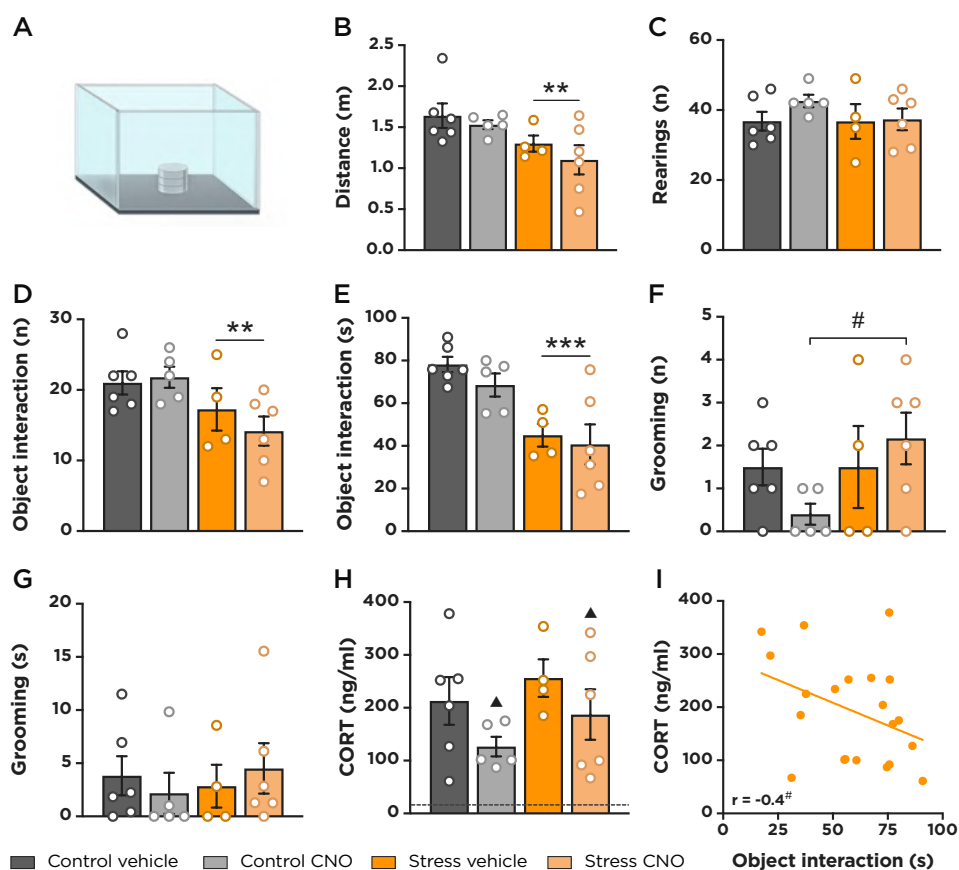


Figure 48. Behavioural and hormonal effects of reactivating stress-induced neurons in a modified OF test.

A) Representation of the OF arena depicting the object placed in the centre. B) Total distance travelled, C) Number of rearings performed. D) Frequency of interaction and E) time spent interacting with the object in the centre. F) Frequency of grooming episodes and G) time of grooming. H) Corticosterone response to the OF. The dashed line represents corticosterone historical basal levels from our lab in this rat strain. I) Correlation between object interaction time and corticosterone response to the OF. Data represented as mean \pm SEM ($n=4-6$ /group; ** $p < 0.01$, *** $p < 0.001$, # $p < 0.1$ vs control; ▲ $p < 0.05$ vs vehicle).

The day after IS and neuronal manipulation with CNO, animals were exposed without prior stress and drug injection to the hole-board (HB) for 5 min to evaluate whether their activity and exploratory behaviour were affected by the reactivation of stress-activated neurons on the day before.

The analysis of the distance travelled in the periphery of the HB revealed an effect of previous STRESS exposure ($X^2(1) = 5.3$, $p = 0.021$; **Fig. 49A**), whereas no effects were found in the central zone (**Fig. 49B**). Furthermore, no effect of DRUG or the interaction STRESS x DRUG were found for any of the two variables. Previous STRESS had a marginally significant effect on the total distance travelled in the HB ($X^2(1) = 3.7$, $p = 0.055$; **Fig. 49C**), without significant effect of previous DRUG treatment or the interaction STRESS x DRUG. Analysis of the number of rearings (**Fig. 49D**) revealed a significant effect of prior STRESS ($X^2(1) = 4.6$, $p = 0.032$), but no effect of DRUG or the interaction between STRESS x DRUG.

Furthermore, analysis of the number of head-dips (**Fig. 49E**), more specifically related to exploratory behaviour, revealed a main effect of STRESS ($X^2(1) = 7.0$, $p = 0.008$), no effect of DRUG and a significant STRESS x DRUG interaction ($X^2(1) = 4.0$, $p = 0.044$). Further pairwise comparisons revealed a significant reduction in the frequency of head-dips in the Stress-CNO compared to the Control-CNO group ($p = 0.001$) and the Stress-vehicle group ($p = 0.045$). Moreover, there was a main effect of STRESS in head-dipping time ($X^2(1) = 10.3$, $p = 0.001$; **Fig. 49F**) and no effect of previous DRUG treatment, but a significant STRESS x DRUG interaction ($X^2(1) = 9.3$, $p = 0.002$). Decomposition of the interaction revealed that head-dipping time was increased in Control-CNO compared to the Control-vehicle group ($p = 0.038$). Moreover, animals from the Control-CNO group spent significantly more time head-dipping than animals from the Stress-CNO group ($p < 0.001$). Finally, Stress-CNO animals spent significantly less time head-dipping than Stress-vehicle animals ($p = 0.026$).

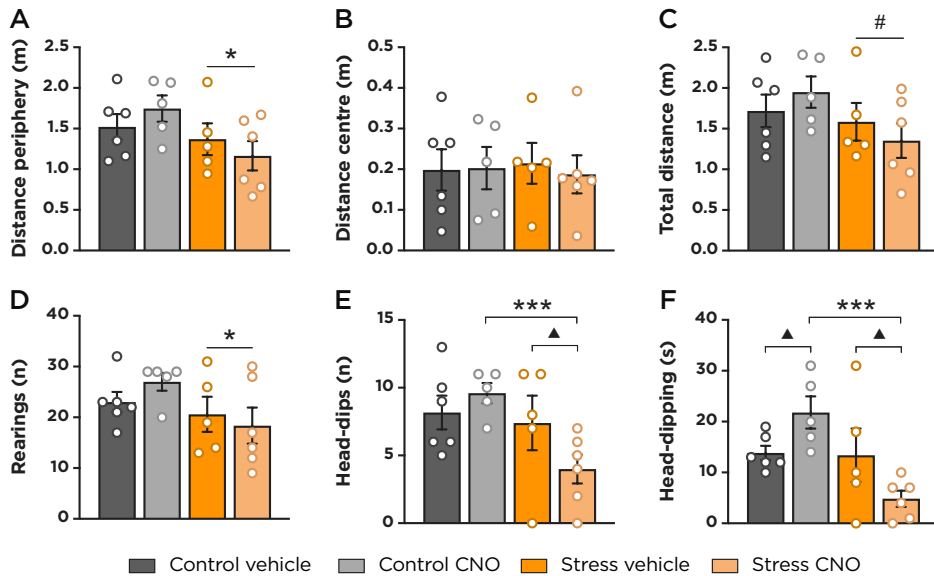


Figure 49. Exploratory behaviour in the HB test one day after inescapable footshock (IS) exposure and PL neuronal re-activation.

A) Distance travelled in the periphery of the HB, B) in the central zone and C) total distance travelled. D) Number of rearings. E) Frequency of head-dips and F) time of head-dipping behaviour. All data are represented as mean values \pm SEM ($n=5-6$ /group; * $p < 0.05$, *** $p < 0.001$, # $p < 0.1$ vs control; \blacktriangle $p < 0.05$ vs vehicle).

One week later, the same group of animals previously exposed to IS were re-exposed to the same IS paradigm to induce the expression of the viral vector in PL neurons activated by stress. 3h and 30 min after the start of the IS session, rats received systemic injections of CNO or vehicle to re-activate the IS-activated neurons. 30 min later they were exposed to FST for 15 min (**Fig. 50**). However, the behaviour analysis focused on the first 5 min of the test, since animals typically show low levels of active behaviour in the second and third 5-min periods (Marti and Armario, 1993).

Analysis of immobility time in the FST revealed no effect of STRESS or DRUG, but a significant STRESS \times DRUG interaction ($X^2(1) = 6.9$, $p = 0.008$; **Fig. 50A**). Subsequent comparisons showed that Stress-vehicle animals tended to spend less time immobile than Control-vehicle animals ($p = 0.096$), whereas the Stress-CNO group displayed more immobility than the Control-CNO group ($p = 0.041$). Remarkably, CNO injection in the stress group significantly increased the time the animals spent immobile compared to the stressed animals injected with vehicle ($p = 0.032$). Regarding mild swim, there were no effects of STRESS or DRUG, but a significant STRESS \times DRUG interaction ($X^2(1) = 3.9$, $p = 0.05$; **Fig. 50B**). Pairwise comparisons revealed significant differences between control animals injected with vehicle and control animals injected with CNO ($p =$

0.048). In terms of active coping, which was reflected by the time that the animals spent struggling (Fig. 50C) there was no significant effect of STRESS but a clear trend to a DRUG effect ($X^2(1) = 3.6$, $p = 0.057$). No STRESS x DRUG interaction was found. Remarkably, CNO reduced struggling time, especially in those animals previously exposed to IS. Finally, the analysis of the corticosterone response to the FST (Fig. 50D) showed no effect of previous STRESS exposure but a significant main effect of DRUG ($X^2(1) = 7.6$, $p = 0.006$) to reduce the corticosterone response, with no STRESS x DRUG interaction. We investigated the relationship between corticosterone levels in the FST and coping behaviour and found no significant correlation.

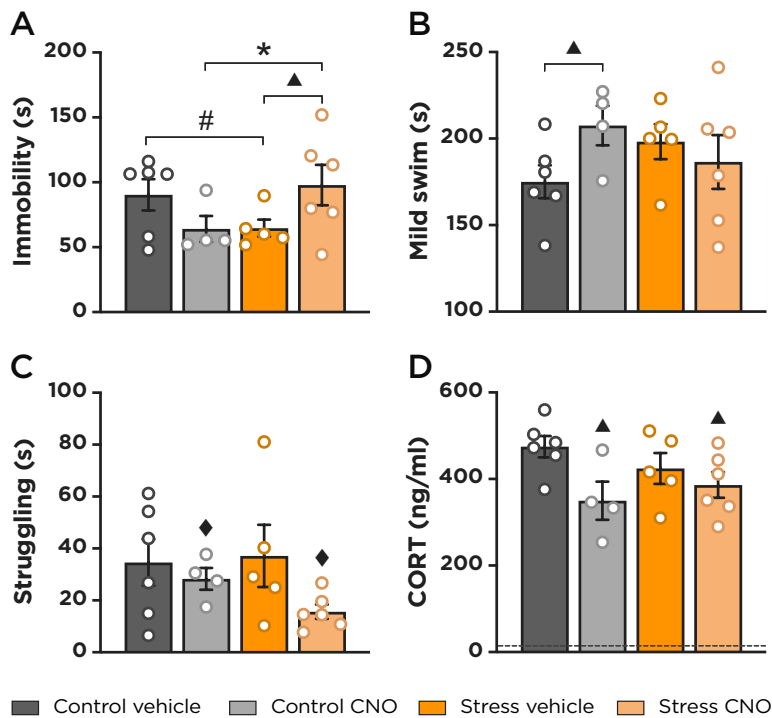


Figure 50. Behavioural and hormonal effects of reactivating stress-induced neurons in the FST.

A) Total time spent immobile. B) Time of mild swim. C) Time of struggling behaviour. D) Corticosterone response to the FST. Dashed lines represent corticosterone historical basal levels from our lab in this rat strain. Values represent mean \pm SEM ($n=4-6$ /group; * $p < 0.05$, # $p < 0.1$ vs control; ▲ $p < 0.05$, ◆ $p < 0.1$ vs vehicle).

We took advantage of the fact that shocked animals had been exposed one week before to the same IS paradigm to measure their contextual fear memory during the first 2 min of re-exposure to the same context (the time before the delivery of the first shock). Previously shocked animals injected

with CNO after the first IS exposure spent less time freezing in the shock context than animals injected with vehicle ($t_{(9)} = 2.345$, $p = 0.044$; **Fig. 51**).

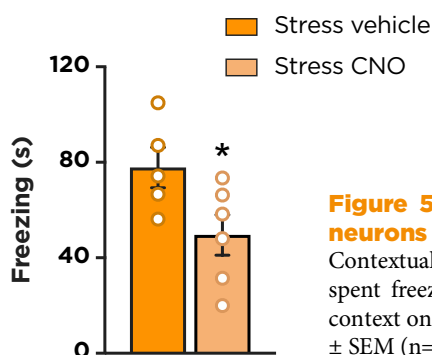


Figure 51. Effects of re-activation of IS-activated neurons in contextual fear memory.

Contextual fear memory was evaluated by measuring the time spent freezing during the first 2 min of re-exposure to the IS context one week after the first exposure. Values represent mean \pm SEM ($n=5-6$ /group; * $p < 0.05$ vs vehicle).

In summary, IS exposure had a negative impact on behaviour in the OF (reduced activity and exploration) and a minor impact on the HB (less peripheral activity) and the FST (less active coping). Re-activation of IS-responsive neurons did not exert a major effect on behaviour, but when observed, the direction of the changes tended to improve behaviour in stress-naïve and accentuated negative consequences of IS. Remarkably, the neuronal activation of PL neurons in control and stressed animals reduced the corticosterone response to the OF and the FST. Finally, re-activation of PL neurons after IS reduced long-term contextual fear memory, probably interfering with consolidation.

3.4. Inhibition of stress-activated neurons in the PL

After describing the behavioural and hormonal consequences of reactivating stress-activated neurons in the PL, we aimed to study the consequences of inhibiting these neurons. To do so, we employed the viral vector **AAV9-pfos(Int+Ex):hM4Di:mCherry:PEST**, which contained the same genetic sequence as the one used above except that the hM3Dq sequence of the excitatory DREADD was substituted by the gene sequence of the inhibitory DREADD (hM4Di). Considering that the promoter region, the reporter protein and the PEST sequence were identical to the previously employed vector (AAV9-pfos(Int+Ex):hM3Dq:mCherry:PEST), which had already been thoroughly validated, we did not repeat the validation process.

Rats ($n = 22$) were bilaterally injected in the PL with the viral vector AAV9-pfos(Int+Ex):hM4Di:mCherry:PEST and behavioural testing began 3 weeks later to allow recovery from the surgery and adequate viral vector expression. The experimental design was exactly the same as the protocol described for the excitatory DREADD (**Fig. 46**).

The viral vector injection site and spread of the subjects included in the statistical analysis are depicted in **Fig. 52**. AAV expression was mainly restricted to the PL, with some minor spread into the surrounding regions. One animal was not included in the statistical analysis because it did not show bilateral PL expression.

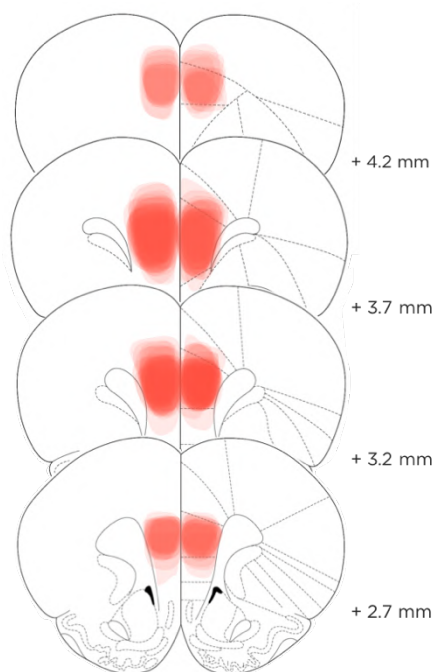
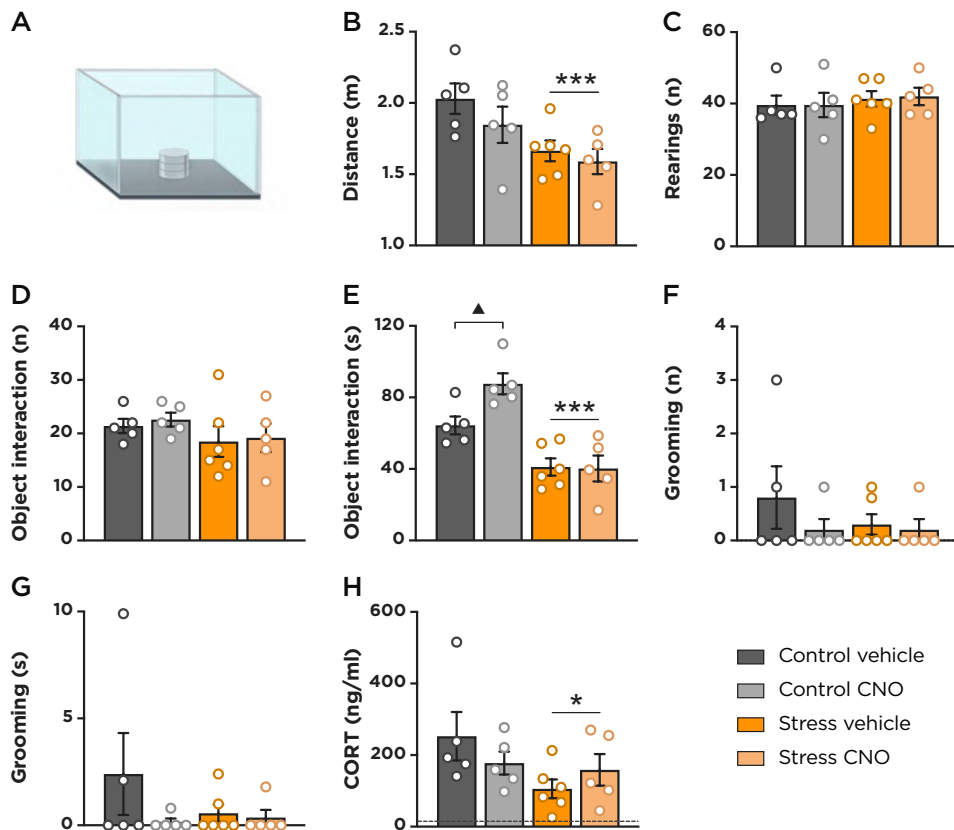


Figure 52. Schematic drawing of the injection site and spread of infection of AAV-pfos(Int+Ex)-hM4Di:mCherry:PEST in all the animals included in the statistical analysis. Note that viral vector spread (determined by mCherry fluorescence) was within the Bregma range 2.7 mm to 4.2 mm (n=22).

Three weeks after surgery, half of the rats were exposed to the same stress paradigm (IS) as in the previous experiment (stress, n = 11) and the other half remained undisturbed (control, n = 10). The behavioural consequences of inhibiting stress-activated neurons were first tested by exposing animals to the OF 4h after IS exposure (**Fig. 53A**). Similar to the previous experiment, 3h and 30 min after IS, rats were systemically injected either with vehicle or CNO and 30 min later exposed to the OF.

The GzLM analysis of the distance travelled (**Fig. 53B**) revealed a significant effect of STRESS ($X^2(1) = 12.2$, $p < 0.001$), but no effect of DRUG or STRESS x DRUG interaction. No significant differences were observed in the number of rearings (**Fig. 53C**) and in the frequency of object interaction (**Fig. 53D**). In contrast, regarding object interaction time (**Fig. 53E**), there was a significant effects of STRESS ($X^2(1) = 46.3$, $p < 0.001$), DRUG ($X^2(1) = 4.7$, $p = 0.031$) and STRESS x DRUG interaction ($X^2(1) = 5.4$, $p = 0.02$). No differences were observed in grooming frequency (**Fig. 53F**) or time (**Fig. 53G**). Pairwise comparisons indicated that control animals injected

with CNO interacted more time with the object than those injected with vehicle ($p = 0.002$). Furthermore, object interaction time was reduced in the Stress-vehicle group compared with the Control-vehicle group ($p = 0.001$) and also in the Stress-CNO group compared with the Control-CNO group ($p < 0.001$). Finally, analysis of the corticosterone response to the OF (**Fig. 53H**) indicated an effect of STRESS ($X^2(1) = 6.0$, $p = 0.014$), but no effect of DRUG or the interaction STRESS x DRUG. We further studied whether corticosterone levels after OF exposure correlated with any of the behavioural data, but no significant correlations were found.



One day after IS and the subsequent inhibition of stress-responsive neurons, animals were exposed with no additional intervention to the HB during 5 min. GzLM analysis of the distance travelled in the periphery of the HB (**Fig. 54A**) showed no main effect of STRESS but a significant effect of DRUG ($X^2(1) = 9.7$, $p = 0.002$), without a significant STRESS x DRUG interaction. Analysis of the distance travelled in the centre (**Fig. 54B**) followed the same pattern, with a significant effect only of DRUG ($X^2(1) = 3.6$, $p = 0.057$). There were no differences in the total distance travelled in the HB (**Fig. 54C**). Analysis of the number of rearing episodes (**Fig. 54D**) revealed no effects of STRESS or DRUG, but a significant STRESS x DRUG interaction ($X^2(1) = 6.3$, $p = 0.012$). Pairwise comparisons indicated that control animals injected with CNO the day before performed significantly fewer rearings than animals injected with vehicle ($p = 0.046$) and stressed animals injected with CNO ($p = 0.039$). Regarding head-dipping behaviour, analysis of the number of head-dips (**Fig. 54E**) indicated only a trend to an effect of STRESS ($X^2(1) = 2.9$, $p = 0.089$). Finally, no effect of previous STRESS exposure was found in head-dipping time, but there was trend to an effect of DRUG treatment ($X^2(1) = 3.1$, $p = 0.077$; **Fig. 54F**), with no significant interaction STRESS x DRUG.

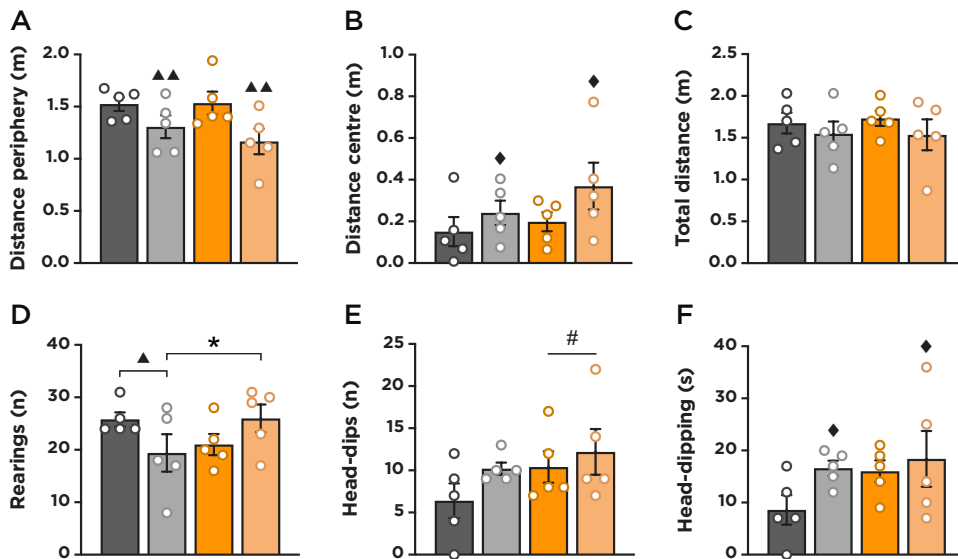


Figure 54. Exploratory behaviour in the HB test one day after inescapable footshock exposure and PL neuronal inhibition.

A) Distance travelled in the periphery of the HB, B) in the central zone and C) total distance travelled. D) Number of rearings. E) Frequency of head-dips and F) time of head-dipping behaviour. All data are represented as mean values \pm SEM ($n=5/\text{group}$ * $p < 0.05$, # $p < 0.1$ vs control; ▲ $p < 0.05$, ▲▲ $p < 0.01$, ◆ $p < 0.1$ vs vehicle).

One week after the first IS exposure, animals were re-exposed to the same IS protocol. 3h and 30 min after the IS session, rats received systemic injections of CNO or vehicle to inhibit IS-responsive neurons. 30 min later they were exposed to FST to evaluate their coping strategies and HPA response (Fig. 55). The duration of the test was 15 min. Analysis of behaviour during the first 5 min of the test revealed no significant effects of STRESS, DRUG or STRESS x DRUG interaction in any of the variables measured (Fig. 55A-C). Finally, regarding the corticosterone response to the FST (Fig. 55D), there was no effect of STRESS, a marginally significant effect of DRUG ($X^2(1) = 3.6, p = 0.094$) and no interaction STRESS x DRUG. CNO tended to increase corticosterone levels in response to the FST, particularly in animals previously exposed to IS.

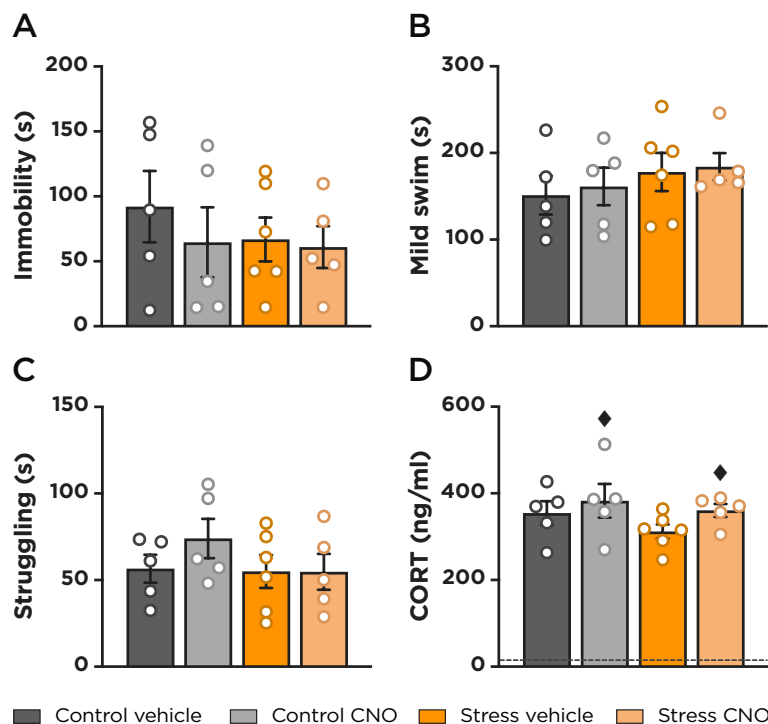
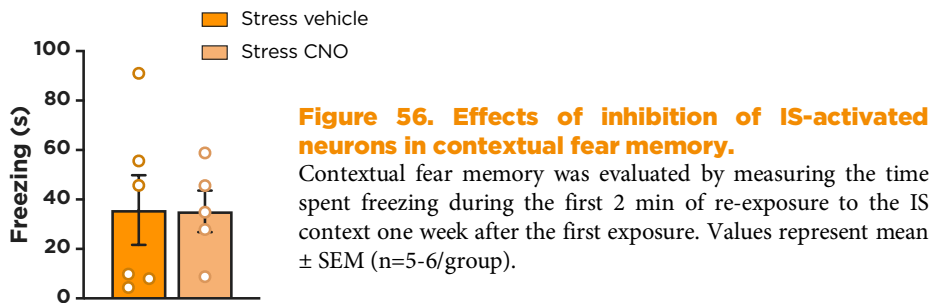


Figure 55. Behavioural and hormonal effects of inhibiting stress-induced neurons in the FST.

A) Total time spent immobile. B) Time of mild swim. C) Time of struggling behaviour. Behaviours were analysed for the first 5 min of the FST. D) Corticosterone response to the FST. The dashed line represents corticosterone historical basal levels from our lab. All data is represented as mean values \pm SEM ($n=5-6$ /group; # $p < 0.1$ vs corresponding vehicle group).

As with the cohort of animals injected with the excitatory DREADD, we measured contextual fear memory during the first 2 min of exposure to the

IS chamber in animals previously exposed to IS one week before. No differences in freezing time were observed between animals injected with vehicle and CNO after the first IS exposure (**Fig. 56**).



Taken together, the results confirmed IS-induced reduction of activity/exploration in the OF, but no effect was basically observed in the HB and FST tests. Inhibition of IS-activated neurons only modestly affected behaviour, changing pattern of activity/exploration in the OF and HB (central versus peripheral HB activity and less rearings but more head-dipping time in the HB). The impact of prior IS or PL neuronal inhibition on corticosterone response was weak and not entirely consistent, but prior IS tended to reduce and PL inhibition to increase corticosterone response, particularly in the stress group. Finally, inhibition of PL neurons after IS did not affect contextual fear memory evaluated 1 week later.

Discussion

The main goal of this thesis has been to characterise the neuronal populations responding to different emotional stressors in the mPFC of the rat at the molecular and functional levels. We have identified mPFC neurons that are activated specifically by different stressors (IMO and IS) and described the molecular expression pattern of neurons responding to emotional stressors differing either in nature or intensity of stress (RES, IMO and IS). Finally, we aimed at manipulating neurons activated by IS in the PL cortex (either activating or inhibiting them) to elucidate their role in the behavioural and endocrine response to stress.

Before delving into the discussion of the results obtained in each chapter, we have to make an important consideration: throughout this thesis, we use “activation” as equivalent to *c-fos* expression, although we are aware that there is no single IEG that is an ideal proxy for cellular or neuronal activation.

1. Identification of neuronal ensembles activated in response to IMO and IS in the mPFC

The expression of *c-fos* RNA has been widely used to study neuronal activation after stress exposure, but its temporal dynamics in response to short stress exposure have not been well characterised, especially *in vivo*. Furthermore, studying the expression of both the intronic and the mature transcripts of *c-fos* provides a unique opportunity to investigate more in-depth different features of the neuronal response to stress. Among them, detecting neurons specifically activated in response to different stressors, an aspect that has been poorly investigated.

1.1. Temporal dynamics of *c-fos* expression after exposure to IMO

Basal levels of *c-fos* mRNA positive cells and intensity (total and per cell) were very low in all the experiments analysed in the present thesis, in accordance with the existing literature and previous data from our group (Cullinan et al., 1995; Úbeda-Contreras et al., 2018). However, we observed a notable intensity of fluorescence and number of intronic RNA positive cells in basal conditions. *c-fos* intronic RNA levels in basal conditions have been not studied in the literature, but it has been reported to increase very rapidly after stress (Lin et al., 2011; Gore et al., 2015). Due to its fast

induction, any environmental alteration in the housing room, the transport of the animals for euthanasia, the manipulation, the anaesthesia or the perfusion process before brain fixation could activate to some degree the transcription of *c-fos* (intronic RNA) in the mPFC. Among these factors, it is important to consider the effect of anaesthetics. It has been reported that many anaesthetics can induce *c-fos* expression in several brain regions. For instance, Yang and colleagues (2020) have shown increased levels of neuronal activation measured by calcium imaging in layer II/III pyramidal neurons of the primary somatosensory cortex of mice exposed to sevoflurane, an inhaled anaesthetic, only for 1 min. To our knowledge, there are no studies assessing the effects of short exposure to isoflurane specifically in the PFC, but some authors have reported in mice increased c-Fos expression in the piriform cortex and LS after exposure to this anaesthetic (Smith et al., 2016). However, in this case, isoflurane exposure was longer than in our experiments (5 min at 4% followed by 120 min at 1%). Considering that induction of *c-fos* intronic RNA is much faster than c-Fos protein, it is plausible to assume that isoflurane in our experiments could also increase to some extent *c-fos* intronic RNA levels. To mitigate this possibility, we reduced isoflurane exposure time in the catFISH experiment of identification of stressor-specific neuronal populations to a minimum (from 1.5 min to 30 s). In any case, the number of cells expressing *c-fos* intronic RNA was much higher after exposure to stress than in basal conditions.

In all the experiments we observed that the dynamic of *c-fos* intronic RNA was very fast, with a marked increase already after 5 min of IMO, as previously reported with other stimuli (Lin et al., 2011; Gore et al., 2015). The number of intronic RNA positive cells showed a further but slight additional increase after 8 min IMO, with no further increase after 15 min IMO. Total intronic RNA signal dramatically increased also after 5 min IMO and remained at peak levels at longer IMO times. This strikingly rapid induction may be in part due to the fact that, even prior to neuronal activation, several transcription factors and the preinitiation form of the RNA polymerase II complex are already bound to the *c-fos* promoter (revised by Lyons and West, 2011), a primed promoter state that enables very rapid activation of transcription after stimulus exposure.

In contrast, *c-fos* mRNA reached its peak later, as expected due to the time required for its maturation process and transport into the cytoplasm (Alpert et al., 2017). In parallel with this RNA maturation process, in the two groups exposed to IMO and let to recover in their home cages, the number of *c-fos* intronic RNA+ cells and the total intensity of the signal was drastically reduced, although still remained slightly above basal levels. Although

reaching peak levels was clearly slower for the mature than for the intronic transcript, it is still an extremely fast process: in the first experiment, there was a significant increase in *c-fos* mRNA in the IMO5 group. To our knowledge, there are no studies convincingly showing increased *c-fos* mRNA levels as early as 5 min after stress exposure in the mPFC. The only study that reports a significant increase already after 5 min of restraint was performed by Imaki and colleagues (1996) in the PVN with a radioactive *c-fos* mRNA probe. Unfortunately, the mRNA probe also binds to the nuclear transcript as shown by us and others (e.g. Lin et al., 2011). Given that radioactive ISH cannot distinguish between nuclear and cytoplasmic signals, it is highly probable that the observed *c-fos* signal corresponds mainly to intronic RNA and not mRNA, as the authors claim. Furthermore, the induction dynamics could depend on the brain region and might be faster in the PVN than in the mPFC.

Our results indicate an extremely fast stimulus-transcription coupling for the *c-fos* gene as compared with other activity-regulated genes, generally showing a delay of approximately 10-20 minutes between the activity of transcription factors in the promoter and enhancers elements of a gene and the appearance of the corresponding mRNA in the cytoplasm (revised by Lee and Fields, 2021). In agreement with this, Listerman et al. (2006) have shown in cell cultures that there is a temporal and probably a mechanistic coupling between transcription and recruitment of splicing factors and RNA splicing in the *c-fos* gene.

1.2. Analysis of the number of activated neurons and intensity of signal

Another crucial aspect that has become apparent from our data is that the different parameters used to assess neuronal activation (i.e. number of positive neurons and intensity of signal) sometimes can provide different information and must be considered as important complementary measurements to get a more accurate picture of the changes and reach more robust conclusions.

For the intronic *c-fos* transcript, the information provided by the number of positive neurons and the total intensity of fluorescence is very similar, as the magnitude of change in both parameters in the different experimental conditions was similar and proportional. However, in the case of the mature transcript, the magnitude of the increase in the total fluorescence intensity was much greater than in the number of positive cells in all groups exposed to IMO (e.g. after 15 min IMO the number of cells increased 22-fold compared to basal conditions, whereas the total fluorescence intensity increased by 200-fold). This means that exposure to IMO not only increases

the number of activated neurons but also the magnitude of *c-fos* expression per neuron, which was corroborated by the gradual increase in *c-fos* mRNA signal per cell after different times of IMO.

If we assume that the level of activation of individual neurons has a functional implication, it is fundamental to quantify the degree of activation and not only the number of recruited neurons. A clear example of this is the study by Gómez-Román and colleagues (2016), who found that exposure to FST in combination with amphetamine activated in the PVN a similar number of neurons than FST alone, which could have led to the erroneous conclusion that amphetamine does not alter PVN activation in response to stress. However, the degree of activation of neurons (total *c-fos* intensity) was significantly reduced in the FST-exposed group given also amphetamine, indicating that this drug actually reduces PVN activation in response to stress. Hence, it might be appropriate in some cases to include measures of the total intensity of signal, which can provide complementary information to the number of positive cells, typically the only measure used in neuronal activation studies.

In the case of the intronic *c-fos* RNA, the number of positive cells showed a strong correlation with total intensity levels, but no significant correlation with the intensity of signal per cell. This could be in part because most cells show two intense intranuclear foci of *c-fos* intronic RNA signal, which are considered to represent the sites of transcription at the genomic alleles for *c-fos* (see Guzowski et al., 2005 for a revision). Nevertheless, in some cells, we only observed one focus. This could be due to biological or technical reasons (e.g. the disposition of the cell in the space causes one focus to be placed above the other when we capture the image in the microscope). Thus, the presence of one or two foci can greatly influence intensity measurement without necessarily having any biological significance. Moreover, with such a limited area of signal compared to the mRNA, quantification of intensity is very difficult, which could mask subtle differences. Data from Guzowski and colleagues (2006) are in accordance with our findings, as *Arc* catFISH in the HF revealed that whereas exposure to different environments caused an increase in the number of *Arc*+ cells compared to control (caged) animals, there were no differences in the fluorescence intensity per cell between groups.

1.3. Validation of the experimental design

To validate the design for the experiment of identification of stressor-specific neuronal populations, we exposed two groups of animals to 5 min stress (IMO or IS) and immediately perfused them, and two groups to 5 min stress and perfused them 30 min after. The quantification of the number of

activated cells after exposure to IMO and IS in the PL and IL regions provided evidence that with the catFISH technique and with this design, we can distinguish between neurons activated by the first stressor, which mainly present *c-fos* mRNA, and neurons activated by the second stressor, which mostly express *c-fos* intronic RNA. The discrepancies between the low mRNA levels after 5 min exposure in this experiment and the significant increase observed in the first catFISH experiment can be due to the fact that we implemented several modifications to the experimental protocol to minimise mRNA expression after 5 min IMO: (1) less isoflurane exposure time, (2) shorter time of perfusion with saline before perfusion with PFA and (3) the process of immobilisation of the animal per se and the release from the IMO table were included in the 5 min of IMO. Therefore, we substantially reduced the time elapsed between starting stress exposure and brain fixation with PFA. These changes were key to improving the experimental design.

A key finding was that both after IMO and after IS the peak number of *c-fos* intronic RNA+ cells was higher than the number of mRNA+ cells 25 min later. There are several possible, not mutually exclusive, explanations for this result. First, it could be that the time used for measuring *c-fos* mRNA is not ideal and that some mRNA has already been degraded 25 min after the termination of the first very brief stress exposure. Several studies have shown peak *c-fos* mRNA levels after 30 min of stress (Cullinan et al., 1995; Imaki et al., 1996), but stress exposure was sustained. In contrast, in our experiment, there was a post-stress period in the home cage, which could imply a faster reduction of the levels of the *c-fos* mature transcript. In this regard, we already reduced the time interval between stressors to 25 min compared to published studies (e.g. 35 min in Gore et al., 2015 and 30 min in Lin et al., 2011 and Pfarr et al., 2018) to prevent potential mRNA degradation. Further reducing the time between stressors could imply that there could still be some intronic RNA present, so we opted for a compromise between both transcripts.

Second, it might be that not all the intronic RNA synthesised after 5 min stress is being processed into mature RNA. In this regard, there is experimental evidence indicating that in some conditions that are stressful to the cell there can be a shutdown of RNA maturation, nuclear export and translation, in order to have enough resources for the urgent production of proteins needed to sustain important cellular processes, such as heat shock proteins (Zander and Krebber, 2017). However, this is most frequently observed with regular or housekeeping genes and it has not specifically been studied with *c-fos*. Third, it might be that some neurons not activated in response to IMO are activated specifically by signals of termination of stress

(i.e. release from the immobilisation process) (Marín-Blasco et al., 2018). Finally, we cannot exclude that the intronic and mRNA probes used in our experiments have different detection sensitivities.

1.4. Study of neuronal ensembles specifically activated by emotional stressors in the mPFC

Before quantifying the overlapping between neuronal populations activated by IMO and IS, we compared the response to each stressor in the PL and IL regions. We found that the number of activated cells after exposure to IMO and IS was similar in the PL and IL regions, both with the *c-fos* intronic and mature RNA probes, which gave consistency to our data. We have evidence that IMO and IS generate a similar ACTH and CORT peak response to stress (Márquez et al., 2002). Moreover, even if they differed in intensity, several studies have reported that mPFC neurons are activated independently of the intensity of stressors (Ons et al., 2004; Úbeda-Contreras et al., 2018). It is important that the size of both IMO and IS ensembles is similar since we expect that the differences observed in the overlapping of neurons when animals are exposed to different stressors are due to specific characteristics of the stressors and not to the magnitude of the response that they elicit.

The use of the catFISH technique also allowed us to examine how earlier exposure to stress influences further transcription of the IEG *c-fos* in response to subsequent episodes of stress. Our results indicated that the number of neurons that responded to either IMO or IS was reduced in those animals that had been exposed to a stressor before, regardless of whether this stressor was the same or different, indicating a **desensitisation** process. To our knowledge, there is no precedent in the literature using such short-term exposures.

It has been previously described in the literature that prolonged exposure to emotional stressors results in a progressive reduction of *c-fos* expression in several brain regions (e.g. 4h of exposure to IMO; Trnečková et al., 2007; Marín-Blasco et al., 2018). There are two main possibilities that explain these reduced *c-fos* levels: intracellular repression mechanisms or changes in the excitatory/inhibitory inputs to activated neurons.

First, a possible cellular mechanism involved in this refractory state of *c-fos* is the recruitment of histone deacetylases (HDAC) to the promoter region of the gene, which forms a transcriptionally inactive chromatin structure in the *c-fos* promoter. Numerous *in vitro* studies have shown that sustained ERK activity and subsequently enhanced Elk-1 phosphorylation induces binding of HDAC activity to the *c-fos* promoter, implying that Elk1 bound

to the SRE can also, to some extent, mediate negative regulation of the *c-fos* gene (Kukushkin et al., 2002; Usenko et al., 2003). Further processes could involve repressor mechanisms, such as enhanced ICER (inducible cAMP early repressor) activity. For instance, Misund et al. (2007) have shown that when HEK273 cells were stimulated and ICER was overexpressed, stimulus-induced *c-fos* gene expression was drastically reduced, suggesting that ICER represses *c-fos* transcription. Moreover, it could be due to an auto-inhibitory mechanism of *c-fos* through the AP-1 complex (Sassone-Corsi et al., 1988). When c-Fos levels increase, the protein, in combination with other factors, forms the nuclear transcription factor AP-1 and downregulates transcription of *c-fos* by binding to the AP-1 site in the promoter region of this gene. Furthermore, it could be that neurons are unable to respond in terms of *c-fos* to another stimulus because their machinery is somehow saturated or cannot be maintained active over time.

However, the existence of cellular repressive processes or incapability to respond would be at odds with studies showing that endotoxin administration or hypovolemic shock can maintain an elevated *c-fos* response for several hours (Rivest and Laflamme, 1995; Tanimura et al., 1998). It is important to note that these are systemic stressors, which could be subjected to different regulatory mechanisms since they can severely alter homeostasis. In accordance with this, previous work from our lab (Marín-Blasco et al., 2018) has shown that re-exposure to either IMO or FST after prolonged exposure to IMO (4h) activates some neurons which were previously activated, suggesting that the decline in *c-fos* expression is not due to transcriptional repression.

Considering all the above studies, we consider that in the case of prolonged stressors the contribution of intracellular repressive mechanisms would be small, and the most important would be increased inhibitory signals or reduced stimulatory signals that neurons receive associated with the evidence that the stressor is not an actual threat to homeostasis (i.e. “safety signals”; see Marín-Blasco et al., 2018). Nevertheless, safety signals are specific for a particular stressor, and thus they should not affect the response to a different stressor.

To our knowledge, there is very little available information with the short exposure times and the short interval elapsed between stressors we used. Based on the information from studies with prolonged stress, we hypothesise that in our case it does not seem evident that the key mechanism is a reduction of excitatory signals or increased inhibitory signals (e.g. safety signals), because we do not only observe desensitisation with the homotypic but also with the heterotypic stressor. Furthermore, 5 min of stress may be a very short time to generate strong safety signals, which might require

longer exposure times. We consider that in our case the most important contributing factor would be intracellular repression mechanisms (e.g. ICER, HDAC), as previously described. Nevertheless, the desensitization observed was not dramatic, as only a 25% reduction was found, perhaps because exposure to the first stressor was only 5 min. It is likely that under more prolonged exposure to acute stressors a combination of repressor mechanisms and safety signals could contribute to reduce *c-fos* expression.

It would be of interest to assess whether this attenuated response after short-term repeated exposure to emotional stressors affects specifically *c-fos*, also to other IEGs or to neuronal processes, including the electrophysiological response of the cells. Although this phenomenon might affect the interpretation of the double-labelling results, our experiment was carefully designed to include all the combinations of stressors, as the influence on the response to the second stressor could have been different depending on whether the first stressor was homotypic or heterotypic.

In order to identify potential stressor-specific neuronal populations, we evaluated the number of double-labelled (*c-fos* mRNA+/intronic RNA+) cells in the groups exposed to two sequential stressors. We hypothesised that if there was some degree of specificity in the neuronal activation response to stress, we should observe a higher number of double-labelled neurons in animals exposed to the same stressor twice than those exposed to two different stressors. We clearly observed this for the PL region. In the IL region, the number of intronic RNA+ cells was more variable within groups, and this variability partly masked the differences between groups in the double-labelled cells. Furthermore, in order to have a measurement comparable to the literature and also to normalise the double-labelled cells to the neuronal response to the second stressor, we also calculated for each animal the percentage of overlap (double-positive/total intronic RNA+). In general, both measurements indicated higher levels of overlapping in the superficial and deep PL layers of those animals exposed to the same stressor twice than in animals exposed to distinct stressors, and again, the effect was similar but more subtle in the IL region.

Previous studies about stimulus-specific neuronal populations have always compared appetitive (e.g. nicotine, mating) versus aversive stimuli (e.g. IS, fighting) (Lin et al., 2011; Gore et al., 2015; Pfarr et al., 2018) and far too little attention has been paid to studying neuronal populations responding to distinct stressors, which obviously have the same valence. These above mentioned studies reported greater overlapping in the neuronal populations responding to similar than to different stimuli using the *c-fos* catFISH technique, with lower levels of overlapping between distinct stimuli. For instance, Gore et al (2015) reported in the BLA only a 10% overlapping

when animals were exposed to nicotine and IS and around 80% when animals were exposed twice to nicotine or IS. Lin and colleagues (2011) studied the neuronal activation response to fighting and mating in the ventrolateral VMH, the premammillary nucleus and the MeA. They observed around a 90% overlapping when animals were exposed to two successive episodes of the same behaviour, whereas there was a 20-30% overlap in animals that sequentially engaged in two different behaviours.

However, it is expected that comparing positive versus negative valence stimuli will result in bigger differences than when the two stimuli are of the same valence, as in our case. IMO and IS are both highly aversive, so it is logical that the percentage of overlap between neurons activated by each stressor is bigger than in the above-mentioned studies, even though they are distinct stimuli. Furthermore, the brain regions they studied were different from the mPFC, which could have greatly impacted the results. In this regard, a vast body of literature points to the amygdala as the critical node of the circuits assigning valence to stimuli, and particularly the BLA has emerged as a key region for valence coding (revised by Pignatelli and Beyeler, 2019). Thus, it is possible that neuronal populations in different brain regions respond differently to different characteristics of stimuli. Concerning this, Cai and colleagues (2016) have reported by calcium imaging that the overlap between the HF ensembles activated by two different contexts was around 40% of activated neurons, which is more in line with our results.

Furthermore, previous work by Marín-Blasco et al (2018) has also reported using IF-FISH, that a relatively modest population of neurons in higher-level processing areas, such as the mPFC and the LSv appear to respond specifically to forced swim after prolonged exposure to IMO, whereas in low-hierarchy areas, such as the PVN, all neuronal populations seem to respond non-specifically. They also found in the PL that some neurons also respond to IMO despite they were exposed to prolonged IMO before, and they hypothesise that this neuronal population could be specifically responding to the release of the animal from IMO, and thus it would be different from the population activated by IMO itself. This is, to our knowledge, the only study comparing neuronal populations activated by two stressors, and although there are some considerable methodological differences, it is in accordance with our findings.

We consider that the relatively high overlapping we observe in cells responding to the two different stressors could be easily explained by arousal processes or generalised activation induced by stress, which might be common to all stressors. It is well described that there are monoaminergic projections from the brainstem to the mPFC that regulate arousal and

indeed, the LC noradrenergic system is a key element in inducing an arousal response in telencephalic regions (Berridge, 2008). In this regard, Spencer and Day (2004) have shown that lesioning mPFC catecholaminergic terminals in the mPFC (both dopaminergic and noradrenergic) drastically reduces the number of Fos+ cells after exposure to air puff, indicating a key role for these projections in the mPFC response to stress. The relatively low overlapping between activated neurons after exposure to the same stressor twice might be partially explained by the desensitisation process that affected a certain number of previously activated neurons, thus reducing the number of neurons apparently activated by two exposures to the same stressor and affecting our conclusions. If they were neurons activated non-specifically or due to arousal processes, which is highly likely, these neurons would be the more particularly affected by desensitisation. This would result in an underestimation of the overlapping after exposure to the same stressor.

Furthermore, technical aspects may be also affecting our results. For instance, we could have overestimated the number of neurons activated specifically by the second stimulus if some mRNA from the first stressor has already been degraded, thereby reducing the neuronal overlapping observed when animals are exposed to the same stressor twice. In contrast, we do not consider that technical aspects have influenced our ability to detect neurons activated specifically by the second stressor. We hypothesised that those neurons responding specifically to the second stimulus (mRNA-/intronic RNA+) should be differentiated from those that were activated by the first stressor (mRNA+/intronic RNA- or mRNA+/intronic RNA+, in case they are re-activated). Our results confirmed this hypothesis, as we did not observe significant differences in the number of mRNA+ cells between groups exposed to 5 min stress and immediately perfused and the basal group, and between those groups exposed to two stressors and their corresponding control groups exposed only to the first stressor (e.g. IMO-IMO or IMO-IS vs IMO-Ctrl), indicating that exposure to the second stressor for 5 min does not increase *c-fos* mRNA levels.

In summary, our results indicate that in the mPFC there is an important population of neurons that respond non-specifically to different emotional stressors, probably due to arousal processes, whereas a small population of neurons seems to be activated specifically by IMO and IS, especially in the PL cortex. This suggests that in the mPFC there is a representation of aspects related to particular characteristics of stressors, such as restriction of free movement or inescapability of the situation (and perhaps in general, applicable to other type of stimuli). Further studies assessing the overlapping between activated neurons in response to different emotional

stressors in other brain regions would shed light on the brain circuitry of stress processing and the neurobiological mechanisms underlying the markedly different behavioural consequences of distinct emotional stressors.

1.5. Important methodological considerations

One possible limitation of our experimental design lies in the fact that animals have very little time to process the stressful situation and hence less chance to distinguish the particularities of each stressor. This could lead to an overestimation of the overlapping of neuronal populations activated by different stressors. Furthermore, the experimental design needs to be validated in each brain region, since the dynamics of induction of the *c-fos* gene could vary depending on the brain region examined. This has been elegantly illustrated by Bonapersona et al. (2022) after IS exposure.

Given the considerable time constraints of catFISH and the limitations of *c-fos* labelling techniques, it would be interesting to replicate our findings with other double-labelling approaches allowing a greater interval time between stressors. For instance, injecting a *c-fos*-dependent viral vector to label activated cells (e.g. mCherry) and combining it with Fos protein or *c-fos* mRNA labelling to detect the response to the second stressor (e.g. Gore et al., 2015), and/or use a combination of other cellular activation markers.

Our data remark the importance of controlling the duration of the procedures, particularly the time elapsed between the start of the second stressor and the fixation of the brain with PFA. When brief exposures are required, such as with catFISH, improperly adjusting can result in elevated mRNA levels as a consequence of the second stressor exposure, leading to inadequate conclusions. For instance, if an animal is exposed to 5 min of stress but it takes some minutes to transport it to the room for euthanasia (i.e. the room is far from the experimental room or it is even in a separate building), to anaesthetize it or to prepare it for PFA perfusion, the time from the start of stimulus exposure until brain fixation can be much longer than 5 min (> 10 min). The importance of these factors is usually underestimated and details are frequently not reported in publications, but attention should be paid to describing experimental protocols in the context of catFISH.

Notwithstanding these limitations, the catFISH technique has shown to be an excellent tool for identifying neurons activated by different stimuli and has contributed to a better understanding of the neuronal populations that respond to distinct emotional stressors in the mPFC. Experiments aimed at manipulating these stressor-specific neuronal populations would help to elucidate the precise role of these neuronal ensembles in the stress response.

2. Molecular profiling of cells activated by different emotional stressors in the PL cortex

One of the main purposes of the present thesis was to unravel the molecular profile of PL neurons activated by emotional stressors differing either in nature or intensity. To do so, we employed the PhosphoRiboTRAP technology, which is based on the fact that ribosomal protein S6 is phosphorylated after neuronal activation, thus enabling the isolation and analysis of RNAs selectively expressed in neurons activated by a particular stimulus (Knight et al., 2012). Prior to this experiment, we investigated the expression of pS6 after different times of IMO, in response to different stress intensities and its colocalization with the well-known activation marker c-Fos, aspects that have been poorly investigated until now.

2.1. Characterisation of pS6 expression after exposure to stress and colocalization with c-Fos

Our results indicated that S6 phosphorylation in PL neurons occurs rapidly after acute stress exposure, as after 30 min of IMO the number of pS6+ cells and the total intensity of signal were significantly increased, with a further increase after 90 min of IMO. Indeed, in another experiment we found an elevated number of pS6+ cells already after 5 min of stress (*data not shown*). In this regard, Pirbhoy et al., 2016 have shown increased intensity of pS6 (at S235/236) already after 5 min of high-frequency stimulation in the HF with peak levels after 30 min. In our experiments pS6 intensity per cell did not show a significant increase until 90 min IMO. These data again reveal a partial dissociation between the different parameters used to assess neuronal activation. Similarly to the observed with *c-fos* RNA, this lack of consistency between total intensity and intensity per cell could suggest that cells do bear pS6 shortly after activation by stress, but it accumulates as the stressor continues.

The comparison between animals exposed to 30 min IMO and left to recover for 60 min and animals maintained immobilised for 90 min revealed that the number of pS6+ cells is maintained despite termination of stress, but the intensity of pS6 signal per cell was significantly reduced during the recovery period. To our knowledge, no previous study has investigated the post-stress dynamics of S6 phosphorylation in pS6+ cell number. Our data indicate that the recovery after stress does not alter the number of neurons recruited, but their degree of activation decreases. This decrease in pS6 intensity per cell was only partial, which could be due to the severity of IMO.

It is then possible that the post-stress decline would be faster with stressors of lower intensities.

We further compared pS6 phosphorylation after exposure to stressors markedly differing in intensity (NE, which consisted of exposing animals to an OF, and IMO), and we observed that both stressors activated a similar number of pS6+ cells with similar intensity. We consider two alternative hypotheses for these results. It could be that pS6 cannot distinguish between different intensities of stressors or that it could detect differences in areas other than the PL, an area where activation in terms of *c-fos* expression is also independent of the intensity of stressors (e.g. Ons et al., 2004; Úbeda-Contreras et al., 2018). In order to contrast these hypotheses, we measured pS6 levels in the LSv, a brain region where *c-fos* activation is positively related to stressor intensity. Interestingly, in this region the number of pS6+ cells was significantly higher in animals exposed to IMO than to NE (157 ± 21 vs 95 ± 12 ; $t_{(6)} = 2.8$, $p = 0.03$). These results indicate that phosphorylation of pS6 could also be able to discriminate between stressors differing in intensity in some brain areas, showing a similar pattern to *c-fos* (Úbeda-Contreras et al., 2018).

We further analysed in the PL cortex pS6 levels after 60 min of IMO, a time widely used in studies that employ the PhosphoRiboTRAP technique (e.g. Knight et al., 2012; Azevedo et al., 2020). To minimise the use of animals, brain samples of the animals used for this validation were reutilised from previous experiments in our lab. Given the small sample size, no formal statistical analysis was performed. However, our data indicated that at 60 min IMO the number of pS6+ cells and total pS6 signal intensity were increased above basal levels, with a trend also for increased pS6 signal per cell. In line with our results, Salgado-Pirbhoy et al. (2016) also showed significantly increased pS6(S240/244) positive cells in the dentate gyrus of the HF after 60 min of exposure to a NE.

We also studied c-Fos expression in the PL cortex after 60 min of IMO with the purpose of comparing the expression of both markers. It is worth mentioning that the fold-change in all the parameters measured (e.g. number of cells and intensity) was higher for c-Fos than for pS6, mainly due to a higher number of pS6+ cells in basal conditions compared to c-Fos. We observed a reasonably high co-localisation between both markers at 60 min IMO: around 65-70% of pS6+ cells also expressed c-Fos and 75-80% of c-Fos+ cells also expressed pS6. We expected a high co-localisation because both markers share common signalling pathways (e.g. MAPK) and Knight and colleagues (2012) already showed an extensive colocalization between pS6 and c-Fos in several hypothalamic regions, the HF and the striatum after exposure to physical stressors (e.g. dehydration or salt challenge) or some

drugs. The finding that some pS6+ cells do not express c-Fos and vice versa could be explained by the differential quantitative contribution of distinct signalling pathways that regulate the expression of each marker. Moreover, at the technical level, we cannot rule out that the sensitivity and specificity of the antibodies used for pS6 and c-Fos are different. In any case, this partial dissociation illustrates the limitations of using a single marker for studying neuronal activation. In this regard, Salgado-Pirbhoy and colleagues (2016) coimmunostained for Arc protein and pS6(235/236) in the dentate gyrus of rats exposed to a NE and found that 73% of pS6+ cells also expressed Arc, providing further evidence that different stimuli activate pS6 in many of the same neurons in which IEG expression is induced.

Based on the above findings and given that most studies employing PhosphoRiboTRAP have used 60 min of stimulus (e.g. Knight et al., 2012; Azevedo et al., 2020) we selected this time-point for our experiments of pS6 immunoprecipitation. However, considering the results of other markers of neuronal activation (e.g. c-fos, Arc), it is likely that the temporal dynamics of pS6 expression would depend on the brain region studied and thus, validation experiments should be performed for each area of interest. Gaining a better understanding of the dynamics and regulation of pS6 expression after stress is fundamental to laying the foundations for describing the transcriptome of activated neurons in response to emotional stress.

2.2. Translatomic profiling of PL activated cells after exposure to different stressors

We performed pS6 immunoprecipitation of the PL region of animals in basal conditions and after exposure to RES, IMO and IS in order to compare the molecular profile of activated cells in each condition. Heatmap and clustering analysis illustrated that most IEGs were highly enriched after pS6 immunoprecipitation in all conditions, in line with previous reports (e.g. Knight et al., 2012; Azevedo et al., 2020). Moreover, IEG relative levels were significantly higher in the IP samples from all stress groups than in basal conditions. Remarkably, the results obtained with RNA-Seq for the *c-fos* gene were highly consistent with the results obtained by qRT-PCR, including the greater FC after IS exposure vs basal conditions than after RES and IMO.

Moreover, we found that pS6 IP strikingly increased the number of differentially expressed genes detected in each of the stress groups versus basal conditions when compared to the expression pattern in input samples, thereby evidencing that the sensitivity and the potential to detect gene expression changes after stress exposure is largely improved with this

approach. The results from the FC plots, together with the clear differences between input and IP samples in the PCA, illustrate the importance of using techniques aimed at studying the population of activated cells in response to stimuli and more specifically the mRNAs bound to ribosomes rather than performing bulk RNA sequencing, which has much background noise.

In addition, the analysis of differential expression changes between different stress and basal conditions revealed a large number of well-known IEGs upregulated with all the stressors compared to basal conditions but also unmasked some between-stressor differences in their expression patterns. For instance, some of them were more enriched in IP from IS than from IMO, such as *Dusp5*. Interestingly, some genes were highly enriched after IP in basal conditions, such as *Homer1* and *Jun*. This could be due to some basal levels of pS6 phosphorylation in resting conditions and greater rate of translation of these genes in activated neurons of basal animals. For instance, *Homer1* gene has a variant mRNA (*Homer1a*) which is highly induced after neuronal activation, but *Homer1b* and *Homer1c* are constitutively expressed (Bottai et al., 2002) and we are not discriminating between these variants with our approach. In any case, our results illustrate some particularities in the expression pattern of each IEG in the different groups (e.g. IP vs input, stressors vs basal), which could be of interest when choosing activation markers for different experimental conditions or objectives.

Concerning the pattern of upregulated and downregulated genes after exposure to the different stressors compared to basal conditions, we found a great proportion of common upregulated genes between RES, IMO and IS. A large portion of this shared genes corresponded to well-known IEGs, which were highly upregulated after all the stressors. Furthermore, other genes such as *Mt1* and *Mt2a* were robustly upregulated in all the three stressors compared to basal conditions, in agreement with reports in the literature. Belloso et al. (1996) found increased mRNA levels of these transcripts in the brain after exposure to IMO, whereas increased levels of the corresponding protein in the frontal cortex of rats exposed to prolonged IMO have also been described (Hidalgo et al., 1991). Our results evidence that apart from IMO, these genes are also upregulated after exposure to other emotional stressors.

However, there were also other genes which were exclusively upregulated in each of the stressors, especially in IS, thereby suggesting a specific molecular signature of each stressor in the PL. To our knowledge, there is only one study that has compared gene expression changes in response to different acute stressors, albeit in mice. Floriou-Servou and colleagues (2018, 2021) compared by bulk RNA-seq the transcriptomic changes in the HF after

exposure to different stressors (e.g. NE, forced swim and RES). They found that most of the stress-induced genes were highly similar between stressors, although there was a small proportion of transcripts specifically upregulated by each stressor. Although the methodology and brain region were different, their results support our findings. At the biological level, it is expected that they share a great proportion of genes, assuming that they would all activate a common set of stress responses, including general arousal, activation of emotionally relevant circuits, increased glutamate levels and enhanced HPA axis response, among others (e.g. see Armario, 2006; Sanacora et al., 2022). Furthermore, the relatively small proportion of stressor-specific induced genes might partially explain the differential behavioural consequences of each stressor. Future research is needed aimed at specifically studying these stressor-specific genes (e.g. silencing or manipulating neurons with viral vectors driven by the specific promoters of these genes).

Regarding the downregulated genes, we found a similar pattern to the upregulated genes, although a lower overlap was observed between the three stressors. In this case, a great proportion of the downregulated genes in IS conditions vs basal were specific exclusively of IS. Given that pS6 decrease is believed to be a marker of cellular inhibition, these results are suggestive of the potential presence of inhibited neuronal populations. Nevertheless, since the upregulation of genes in the IS sample vs basal condition is considerably higher, we cannot rule out an effect of competition for binding of RNAs to ribosomes (Raveh et al., 2016) that may lead to a downregulation of some genes when compared to basal animals.

Specific comparison of the gene expression pattern in the IP samples of the three stressors revealed that IMO and RES were strikingly similar, whereas there were more differences between each of them and IS. IMO and RES greatly differ in intensity in terms of HPA response (García et al., 2000; Belda and Armario, unpublished data), but they are very similar with regard to quality or nature. Hence, our data suggest that, in the PL cortex, the gene expression changes induced by different stressors would be more related to the nature of the stressors rather than to their intensity. This hypothesis would predict relatively minor differences between different shock intensities. Moreover, it would be of great interest to perform this study in other brain regions which could be more sensitive to the intensity of stress rather than their nature, such as the PVN or the LSv, and observe whether this pattern is conserved or not.

Collectively, these data suggest that there is a more similar transcriptome profile between RES and IMO than with IS, although the three stressors share a considerable proportion of the differentially expressed genes. To our

knowledge, this study constitutes the first *in vivo* direct translatomic comparison between different emotional acute stressors in rats.

2.3. Important considerations

The PhosphoRiboTRAP method opens up new avenues for research in the field of stress and neuronal activation and provides the opportunity to profile genes uniquely expressed in neurons that respond to a particular stimulus. Importantly, it has the great advantage that, in contrast to other methods employed to study the translatomic of specific neurons, PhosphoRiboTRAP does not require to work with transgenic animals and there is no need to inject viral vectors, as it only requires commercially available antibodies to immunoprecipitate ribosomes. Furthermore, this approach utilises an endogenous pS6 site to capture ribosomes without requiring the use of ectopic proteins such as EYFP or EGFP, or other tags that could alter the structure and perhaps the normal function of ribosomes.

However, there are some caveats that need to be considered. One of the major challenges is the dynamic nature of transcription and translation. Stress exposure modifies the transcriptome in an interactive and dynamic manner, with some gene changes appearing as early as 10 min after acute fear conditioning (Cho et al., 2015), whereas others can take hours. In this regard, Jackson and Moghaddam (2006) have shown by unit activity recording in the PFC of animals exposed to restraint that there are neurons that encode fast (phasic increase in firing rate during restraint exposure) and slow responses (slow onset increase that is sustained for more than 2h). Transcriptional waves of gene expression were not captured in our experiments as we only analysed changes immediately after 1h of stress. Further experiments at different time points would help to thoroughly characterise the molecular pattern in response to stress.

Furthermore, throughout this thesis, we have used pS6 as a surrogate of neuronal activity induced by stress but caution should be taken when making this assumption. First, it is not completely known whether pS6 marks all activated neurons, and it is not fully understood to what degree S6 phosphorylation correlates with changes in the firing rate of neurons. Moreover, S6 contains different phosphorylation sites, and these sites might be differentially regulated in distinct brain areas or cell types within the same brain area. Nevertheless, our characterisation after different times of IMO and its high colocalization with c-Fos, suggest that pS6 is a very valid marker for stressor-induced neuronal activation.

This is the first study, to our knowledge, specifically aimed at characterising the translatomic changes in neurons activated in the PL cortex after acute

exposure to distinct emotional stressors. Our differential gene expression data, which we plan to make publicly available, will provide a valuable framework for all researchers interested in changes in particular genes or pathways after acute stress exposure, a topic largely unexplored. Moreover, although this was out of the scope of the present thesis, we plan to exhaustively analyse the molecular and cellular pathways affected by exposure to each stressor compared to the basal conditions, and also to compare between stressors.

Future studies with more brain regions and distinct stressors would provide valuable information to better define the molecular characteristics of neuronal circuits involved in the stress response. Unravelling the molecular changes induced by acute exposure to stress can help to understand how it can lead to long-lasting changes in behaviour and it would be a step forward in the study of the pathogenesis of several stress-related disorders and the development of potential and more specific therapeutic strategies. In this regard, a great limitation of these experiments is that they were performed exclusively in males; we plan to perform this experiment also in females in the close future and study whether sex differences exist at the translational level in response to stress.

3. Behavioural and hormonal consequences of manipulating stress-activated neurons in the PL cortex

A major goal and challenge of neuroscience are to elucidate how neuronal ensembles drive particular behaviours. The technological advances in recent years have allowed researchers to study the role of molecularly-defined neuronal phenotypes. Nevertheless, since neurons from the same molecular type could be spatially intermingled but functionally heterogeneous (Pinto and Dan, 2015), it would be critical to manipulate neurons based on their activity in order to better define the neural circuits underlying behaviour. To do so, strategies based on activity-dependent or IEG promoters have been developed (for a review see DeNardo and Luo, 2017).

In this thesis, we have employed a manipulation strategy based on the use of the *c-fos* promoter to drive the expression of either the excitatory or the inhibitory DREADDs with the purpose of activating or inhibiting, respectively, neurons activated by IS in the PL cortex of male rats. This would allow us to assess the behavioural and hormonal consequences of

such manipulation and the putative role of these neurons in stress-related paradigms.

3.1. Design and validation of an IEG-based viral vector for manipulating stress-activated neurons

To gain access to neuronal populations that are activated by stress we developed a strategy which consisted of driving the expression of the excitatory DREADD (hM3Dq) with the *c-fos* minimal promoter. However, contrary to our hypothesis, the levels of the reporter mCherry in PL neurons the day after IS were not significantly different from those of basal animals. This posed a problem since when manipulating neurons with this viral vector, we do not know if the behavioural consequences would be related to the IS neuronal ensemble or other neurons activated in the PL by other habitual stimuli.

Other authors have successfully employed this strategy to label and manipulate BLA neurons activated by particular stimuli in mice 18h after stimulus exposure (Gore et al., 2015). The inconsistency with our results might be due to the fact that they used lentiviral vectors instead of AAV, which integrate into the genome, and this might have bypassed the problems related to the lack of additional regulatory elements in the *c-fos* promoter. Thus, integration in the genome could allow regulatory mechanisms of *c-fos* expression such as RNA polymerase pausing to occur (Fivaz et al., 2000). Importantly, the success of this direct strategy may also depend on the brain area manipulated. The mPFC has higher levels of activity under regular animal living conditions (e.g. circadian rhythm, locomotor activity, response to typical environmental factors in animal facilities) than other brain regions like the BLA, the region targeted by Gore and colleagues. In fact, the mPFC has been postulated as a core region of the brain's default network, a group of areas that show considerable levels of brain activity during resting states or non-task dependent conditions (see revision by Buckner et al., 2008). This would translate into higher levels of non-stress-related viral vector expression in the mPFC than in other brain regions.

We then implemented several modifications in our viral vector system, which consisted of combining the *c-fos* minimal promoter with key regulatory elements in the first exon and intron (Schilling et al., 1991; Smeyne et al., 1992; Coulon et al., 2010) and adding the degradation sequence PEST from the C-terminal rat OCD (X. Li et al., 1998), similar to the strategy used by Ye et al. (2016). Previous studies have shown that incorporating the PEST sequence into a protein dramatically reduces its half-life (Li et al., 1998). More specifically, Ye and colleagues transfected

cultured hippocampal neurons with a *c-fos*-based construct carrying the reporter EYFP fused to the PEST sequence and showed that 4h after neuronal stimulation with KCl, EYFP levels were significantly higher than in basal conditions (neurons electrically silenced with tetrodotoxin), whereas 24h after KCl stimulation EYFP levels normalised again.

Based on these validated temporal dynamics, we also compared levels of our reporter mCherry in animals injected with the viral vector and exposed to IS or left undisturbed in their home cages. As expected for an activity-dependent construct, animals exposed to IS and euthanised 4h later had increased levels of mCherry than basal animals, with a similar fold-change in the number of cells expressing the reporter and signal intensity to that obtained by Ye et al. (2016) after exposure of mice to IS. Similarly to what they had observed in cultured neurons, expression levels of the reporter mCherry were normalised the day after IS in our validation experiment. This indicates that the modifications implemented in the viral vector sequence contributed to the induction of activity-dependent expression in the PL cortex 4h after IS. Another aspect that changed from the first viral vector designed to this second one is the serotype of the AAV (AAV1 vs AAV9, respectively), due to reasons associated with the production procedure. We do not consider that this was the fundamental difference given that both serotypes have been described to primarily infect neurons with similar transduction levels (for a review see Haery et al., 2019). However, we cannot completely rule out that this also influenced our results given that we only tested the new viral vector with the serotype 9.

Given that *c-fos* expression has also been reported in some glial cells under some conditions (e.g. direct injection of a hypertonic saline solution in the supraoptic nucleus; Ludwig et al., 1997) and that the AAV9 serotype can also infect astrocytes (Haery et al., 2019), we assessed whether astrocytes also expressed the viral vector. However, we found virtually no co-localisation between GFAP and the reporter mCherry in animals exposed to IS, and almost 100% of mCherry+ cells co-localised with the neuronal marker NeuN, thereby allowing us to state that the possible behavioural and hormonal changes are due to the manipulation of PL neurons and not astrocytes. We in fact expected that the co-localisation with GFAP was very low as it is generally assumed that regulation of *c-fos* in astrocytes differs from that in neurons, being more associated with proliferation or differentiation events and systemic stressors, rather than with depolarisation and exposure to emotional stressors (Hisanaga et al., 1990; Armario, 2006).

3.2. Short-term behavioural consequences of IS exposure in general activity and exploratory behaviour

To demonstrate a behavioural impact immediately after IS exposure, the activity of rats in their home cages was analysed, and we observed that IS induced marked hypoactivity. Similarly, exposure to 20 min IMO also induced hypoactivity in the home cage (*data not shown*). Lehnert and colleagues (1984) reported that rats tested in a novel environment 15 min after exposure to electric tail-shocks showed reduced locomotion and frequency of rearings and head dips, without differences in grooming behaviour, which would be in line with our results of reduced locomotor activity. Furthermore, rats exposed to a passive avoidance task (1 mA intensity shock) showed reduced activity in the OF 1h after (Heinsbroek et al., 1988). Moreover, Armario and collaborators (1991) measured the exploratory behaviour of adult male rats in the HB immediately after exposure to different stressors for 1 h. Noise, restraint and tail shock did not induce changes in behaviour in the HB, whereas 1h IMO caused a profound inhibition of exploratory activity. Other studies in rodents, however, report that acute stress increases activity immediately after. For instance, Katz and colleagues (1981) reported increased activity in an OF immediately after exposure to noise and light, and Füzezi and colleagues (2016) found that mice exposed to IS travelled more distance in the home cage immediately after than their controls.

The reasons for these apparent discrepancies are most likely related to the intensity of the stressors used (e.g. Katz and colleagues used light and noise and Füzezi and colleagues used a much lower shock intensity than us, 0.5 mA), with less severe stressors having opposite consequences than high-intensity stressors. It seems therefore that exposure to severe stressors causes hypoactivity either in the familiar environment of animals or in novel environments.

Based on the viral vector expression results, we tested animals in a novel environment (OF) 4h after IS to assess the short-term consequences of IS exposure. We observed a clear trend for reduced distance and number of rearings compared to control animals. Furthermore, we introduced an object in the centre of the OF as previously done by others (e.g. Maaswinkel et al., 1996) to assess motivation to explore, and we found that object interaction time was significantly reduced in animals exposed to IS. There are very few studies in the literature evaluating the consequences of stress exposure at this specific time point, as behaviour is usually evaluated 24h after and in some cases immediately after the stressor (e.g. Lehnert et al., 1984; Armario et al., 1991), with many of them evaluating changes some days after. Furthermore, many reports focus on the impact of chronic stress.

To our knowledge, one of the few studies measuring locomotor and exploratory activity in a novel environment 4h after acute IS was performed by Van Dijken and colleagues (1992). They found a trend to reduced locomotion and rearings and significantly less sniffing in IS-exposed rats when compared to controls. This hypoactivity was more robust on the day after IS and it was maintained for several days (up to 14 days after). Other authors have also studied this time but with other stressors. For instance, Yuen et al. (2009) exposed animals to forced swim for 20 min and 4h later evaluated the behavioural consequences in the OF and the TST. Forced swim did not induce changes in the time spent in the centre of the OF, suggesting no effect on anxiety, or coping strategies in the TST. Furthermore, although we are not aware of a study that has performed a detailed comparison of the intensity of HPA response to FST and IS, comparison of different experiments performed in our laboratory shows that forced swim is of lower intensity than IMO or IS in terms of ACTH and CORT response. Hence, FST would be considered an stressor of intermediate intensity compared to IMO and IS, which could explain the lack of differences in the study by Yuen and colleagues.

It could be that the hypoactivity observed in the OF after IS exposure might be an unconditioned debilitating effect of shock exposure, but we believe that it is most likely due to a process termed “cognitive generalisation of conditioned fear”, which has been described by our lab and others after IS exposure. It has been reported that the conditioned fear generated by IS in adult male rats can be generalised to other contexts markedly differing from the IS context, resulting in decreased exploratory activity in the first 5 min of exposure to any novel environment, not only in the short-term (e.g. at 24h after IS; Weyers et al., 1989; Radulovic et al., 1998; Belda et al., 2016) but also in the long-term (e.g. 7-14 days; Daviu et al., 2010, 2014). Remarkably, the total distance travelled in the circular OF at 48-72h after IS was also decreased in the present experiments, concordant with a long-lasting fear generalisation process. We consider that this is not a mere consequence of shock exposure because immediate shock delivery when the rat is placed in the IS chamber, which does not induce contextual fear conditioning (Fanselow, 1986), does not result in hypoactivity and generalisation of fear to novel environments (Daviu et al., 2010). Thus, this indicates that animals need to associate the aversive experience with a distinct unknown environment to develop cognitive generalisation of fear.

3.3. Consequences of IS stress and PL neuronal manipulation in locomotor and exploratory activity

Once we evaluated the immediate and short-term consequences of IS exposure in a novel environment, we studied the consequences of either activating or inhibiting IS-activated PL neurons in the OF test. In this section, the effects of previous stress exposure and the comparison with the pilot experiment will be first discussed, and then the consequences of neuronal re-activation or inhibition will follow.

In both neuronal stimulation and inhibition experiments, the impact of prior IS exposure in the OF was mostly noted in distance travelled and interaction with the object. Firstly, in the neuronal stimulation cohort, IS-exposed animals travelled less distance in the OF and displayed reduced time and frequency of interaction with the object. No differences were observed in the number of rearings. Secondly, in the neuronal inhibition cohort, previous IS exposure significantly reduced distance travelled and time of interaction with the object, without changes in rearing frequency. The null effects of IS in rearing frequency in any of the two cohorts are discordant with the results of the pilot experiment. A possible reason underlying this discrepancy could be that experimental manipulations, including surgical procedures and i.p. injections before behavioural tests, could interfere with the effects of previous stress exposure. However, other authors have also reported no effects of IS in rearing frequency 4h later (Van Dijken et al., 1992), suggesting that perhaps this variable is less sensitive to stress than horizontal activity.

Together, these data in conjunction with the pilot experiment, indicate that time of interaction with the object is the most sensitive parameter to prior stress exposure with a high level of consistency since it was significantly reduced in the three experiments. Second, concerning the effects of neuronal re-activation or inhibition, no changes were found in any of the behaviours measured, except for object interaction time in the inhibitory DREADD cohort. In this case, time interacting with the object was increased in control animals injected with CNO compared with vehicle, suggesting that basal inhibition of the PL cortex could increase the motivation to interact with novel objects.

Regarding the congruity of our findings with the literature, the effects of mPFC manipulation are controversial (*see Section 4 of the Introduction*), and many of the studies manipulate all mPFC or PL neuronal types without distinguishing between previously activated and non-activated neurons. Optogenetic stimulation of PL pyramidal neurons in mice increased the distance travelled in the OF (Kumar et al., 2013), although others reported

no changes after optogenetic stimulation of CaMKII mPFC neurons in mice (Son et al., 2018) or chemogenetic activation of CaMKII PL neurons in rats (Pati et al., 2018). Moreover, chemogenetic studies have reported no impact of inhibiting PL SST (Soumier and Sibille, 2014) or PV neurons (Perova et al., 2015) on the OF.

We also exposed animals to the HB test on the day after stress exposure to study if neuronal manipulation after IS exposure and during the OF test had any delayed effect on exploratory behaviour. Importantly, we wanted to ensure that the behavioural changes observed in the HB were not due to residual CNO effects, given that at the doses typically used (0.1 – 5 mg/kg i.p.) DREADD activation usually lasts about 2-4h (Roth, 2016), although in some cases it has been reported to last longer (9h; Alexander et al., 2009). In the excitatory DREADD cohort, IS exposure 24h before induced hypoactivity, with significantly reduced distance travelled in the periphery of the HB and lower number of rearings, without affecting head-dipping behaviour, a parameter more specifically related to exploration (File and Wardill, 1975). In contrast, in the inhibitory DREADD cohort no significant effects of stress were found. Although there is an apparent discrepancy, in fact, most of the differences between control and stressed groups in the excitatory cohort could be attributed to the stress-CNO group, and the effect of IS per se in the stress-vehicle compared to the control-vehicle group was less evident.

As discussed in the previous section, numerous studies in the literature have reported a robust stress-induced hypoactivity in novel environments 24h after shock exposure. For instance, Van Dijken et al. (1992) found reduced distance and number of rearings and Belda et al. (2016) reported decreased peripheral and central ambulation and number of rearings one day after IS exposure in a novel environment (OF). The finding that hypoactivity in the HB was not as marked in our manipulation experiments as that reported in the literature could be partially explained by the fact that experimental manipulations, including prior exposure to an OF the day before, could reduce the cognitive generalisation of fear or somehow affect behaviour in another novel environment.

Concerning the specific effects of neuronal manipulation the day before, in the excitatory DREADD cohort we found no impact on horizontal or vertical activity, whereas we found reduced frequency of head-dips in stressed animals injected with CNO the day before compared to stress-vehicle animals. This suggests that re-activation of IS-responsive PL neurons after IS exposure and during the OF reduced exploratory behaviour 24h later. The effects of CNO administration on head-dipping time showed an opposite pattern in control and stressed groups: neuronal re-activation

increased head-dipping time in control animals whereas reduced it in stressed animals. These data illustrate the fact that manipulation of stress-relevant neuronal populations in the PL can have different behavioural consequences than general manipulation of PL neurons.

In the inhibitory DREADD cohort, CNO administration the day before resulted, regardless of prior stress (control or IS) exposure, in reduced distance travelled in the periphery and increased distance in the centre, accompanied by increased head-dipping time. Furthermore, the number of rearings was reduced in control-CNO compared to control-vehicle animals.

We found differences between control and stress vehicle groups from both cohorts (e.g. distance travelled or head-dipping behaviour in the HB). This could be due to different factors, such as that animals were acquired from two different batches or that experiments were performed several months apart (7-8 months). Hence, although the experimental design was the same for both cohorts (e.g. the time of the day at which the experiments were performed, the time elapsed between tests), other factors could have contributed to these inter-cohort differences.

3.4. Consequences of IS stress and PL neuronal manipulation in grooming behaviour

We assessed grooming behaviour, a common innate self-directed behaviour that is observed in response to stressful situations (e.g. van Erp et al., 1994). Whereas in our pilot experiment IS exposure significantly increased grooming frequency and time in an OF (4h later), in the manipulation experiments no main effects of stress were found on grooming behaviour in any of the two cohorts. In addition, grooming frequency and time were lower than in the pilot experiment. Furthermore, we found no effects of CNO administration in any of the two cohorts.

Factors such as interference of the manipulations that animals from the DREADDs experiments received (e.g. surgical procedures and i.p. injections before behaviour assessment) could underlie these discrepancies. In fact, there is still controversy about the functional meaning of grooming in stress, with some authors postulating that grooming might be involved in reducing stress-induced arousal (Spruijt et al., 1992; Estanislau et al., 2013). So far, little attention has been paid to the short-term impact of prior stress exposure on grooming behaviour in novel contexts. Roth and Katz (1979) found that rats previously exposed to loud noise and bright light showed higher levels of grooming when immediately exposed to an OF, whereas Van Dijken et al. (1992) reported no effects of IS on time spent grooming in an OF 4h later and reduced grooming 2, 7 and 14 days after IS. These

differences could be attributed to different intensities of the stressors used or the time elapsed between stress exposure and behavioural evaluation. It could also be that traditional quantitative measures of grooming such as the ones used in the present thesis might be insufficient for correct interpretation. Several authors support the idea that evaluation of grooming behaviour should measure alterations in grooming microstructure, including aspects such as disturbance of the general cephalocaudal progression pattern, interrupted activity and assessment of the regional distribution of grooming (Kalueff and Tuohimaa, 2005).

3.5. Consequences of IS stress and PL neuronal manipulation in coping strategies

One week after the first IS exposure, animals were re-exposed to IS to induce again viral vector expression for later neuronal manipulation. 4 h later we assessed their behaviour in the FST. In brief, in the excitatory cohort, there was a trend to reduced immobility in the stress-vehicle group compared to controls, whereas in the inhibitory cohort there were no obvious effects of stress. Most studies dealing with effects of stress on the FST have focused on chronic stress and there is little published data on the effects of acute stress exposure. Some authors have reported reduced immobility and increased mild swim in male SD rats immediately after electric tail shocks (Armario et al., 1991), which would be in line with our results in the excitatory cohort. Other authors, however, have found in mice that IS induces strain-dependent behavioural alterations in the FST in mice both immediately and 24h after, with some strains showing increased struggling whereas in others IS had no effects or even reduced active swimming (Shanks and Anisman, 1988). One key underlying factor for these inconsistencies and the differences we observed between the two cohorts could be individual or strain differences in vulnerability or resilience, a fact particularly evident regarding forced swim behaviour (Armario and Nadal, 2013; Armario, 2021).

With respect to the effects of neuronal manipulation on FST behaviour in controls, CNO administration significantly increased swim, an effect not observed in previously stressed animals. In the stress group, reactivation of stress-activated neurons increased passive coping (i.e. immobility) and tended to reduce struggling. This would indicate that the re-activation of PL stress-activated neurons during FST increases passive coping and reduces active coping, whereas neuronal inhibition did not appear to affect FST.

It is difficult to compare these findings with the literature since many studies manipulate globally the PL or mPFC areas without activity-dependent strategies, and this was done mostly in previously stress-naïve animals or

chronically stressed animals (e.g. Warden et al., 2012; Kumar et al., 2013; Fuchikami et al., 2015). Another factor to be is that we used water at 36-37°C instead of 25°C, the temperature usually employed in most studies. We do so to eliminate the physical component of the FST associated with hypothermia. The risk of hypothermia at 25°C (R. D. Porsolt et al., 1979) makes the animals more prone to be active despite they evaluate the situation as inescapable, which could confound the interpretation of the results in terms of the natural or stress-induced tendency to adopt a passive behaviour. Accordingly, our group has shown that exposure to water at 36°C resulted in higher levels of immobility than at 25°C (Rabasa et al., 2013), in accordance with results in the literature (Armario, 2021). In our case, this could have reduced the chance to detect changes in immobility after stress and masks possible differences between groups.

3.6. Consequences of PL neuronal manipulation after IS exposure in contextual fear memory

We benefited from the fact that animals had to be re-exposed 1 week after IS to induce expression of the viral vector again in order to evaluate conditioning to the IS context (indexed by freezing behaviour) during the first 2 min before shock delivery. In the excitatory DREADD cohort, neuronal re-activation of stress-activated PL neurons 4h after IS exposure resulted in reduced freezing levels when animals were re-exposed to IS context 1 week later, whereas in the inhibitory DREADD cohort all rats exhibited similar levels of freezing in response to the conditioning context. These results suggest that the re-activation of stress-activated neurons 4h after IS exposure (i.e. a time of consolidation of fear memory; Bourtochouladze et al., 1998) interferes with the consolidation of contextual fear memory, whereas the inactivation of these neurons does not. However, freezing levels of the stress-vehicle group were lower in the inhibitory DREADD cohort, which could have masked the effects of neuronal manipulation. We have previously observed in our group that fear conditioning levels vary among different cohorts (*unpublished results*). However, in both experiments there were the corresponding stress-vehicle control groups to which we compared the stress-CNO groups.

A complete understanding of the role of each mPFC subdivision in contextual fear conditioning has not been reached yet, but in general, it is reported that activity of the rodent PL is critical for the expression of learned fear, but does not seem to be involved in fear acquisition (Sierra-Mercado et al., 2011); for a comprehensive review see Giustino and Maren, 2015). For instance, temporal inactivation of PL during CFC did not alter contextual fear expression the day after (Corcoran and Quirk, 2007). Furthermore,

studies of functional magnetic resonance imaging in humans immediately after fear acquisition have shown that the amygdala-mPFC functional coupling is decreased during fear memory consolidation and that there is a negative correlation between the amygdala-mPFC functional connectivity and subjective fear ratings of the participants (Feng et al., 2014). It could be that artificially re-activating PL neurons during the CFC consolidation window interferes with the normal circuitry of fear consolidation and this underlies the decreased freezing observed one week after.

The major problem when aiming to compare our results with the literature is that most studies have been performed immediately before contextual fear acquisition instead of during the consolidation window. Moreover, usually these studies have manipulated globally the mPFC, without distinguishing between activated and non-activated neurons (e.g. Corcoran and Quirk, 2007). Other studies which have used activity-dependent manipulation strategies have focused mainly on the HF and the amygdala (e.g. Liu et al., 2012; Gore et al., 2015). The fact that re-activation of IS-associated PL neurons can affect long-term memory is a very interesting finding that can be explained by an interference of “out of context” activation of PL neurons with the association of fear with the appropriate context.

3.7. Modulation of HPA response to emotional stressors by PL neuronal manipulation

We also assessed the consequences of manipulating PL stress-activated neurons on the HPA response to emotional stressors (OF and FST). We will first discuss the effects of prior stress exposure and then the effects observed after PL neuronal activation or inhibition.

In the excitatory DREADD cohort there was no effect of prior stress exposure on the HPA response to OF and FST, whereas in the inhibitory DREADD cohort prior IS exposure reduced corticosterone response to the OF, but not to the FST. A prior history of acute stress can sensitise the HPA response to novel (heterotypic) stressors for some days (Belda et al., 2008). Importantly, there are critical characteristics that can determine whether or not sensitisation would appear, such as the intensity of the triggering (first) and challenging (second) stressors (Belda et al., 2016). Comparison with the present results is difficult because in most of the published studies the time elapsed between the triggering and the challenging stressors was at least 24h, whereas in our experiments it was only 4h due to methodological requirements. Although the levels of HPA hormones would have certainly returned to baseline at 4h after IS (Márquez et al., 2002), at this time point GC negative feedback regulatory mechanisms associated with previous exposure to IS are taking place. Thus, the resulting corticosterone response

to the heterotypic stressors would be the result of a balance between possible stress-induced sensitisation and negative GC feedback. The specific weight of each component and how these factors interact to determine the actual HPA response may be highly dependent on individual differences, which could easily explain the relative inconsistency found between the two cohorts and with the literature. Unfortunately, this topic remains poorly investigated.

Regarding the effects of PL neuronal re-activation on the corticosterone response to OF and FST, both control and previously stressed animals showed clearly reduced HPA axis response to the two stressors after CNO administration. Neuronal inhibition of PL neurons did not have any effects in the OF, but tended to enhance the HPA response to FST in both control and previously stressed animals. The results with both stimulation and inhibition experiments clearly point towards an inhibitory role of PL neurons in modulating the HPA response in response to emotional stressors. Interestingly, the effect was not dependent on prior experience with a severe acute stressor and therefore suggests a tonic role of PL neurons.

A large body of studies using lesioning, pharmacological and optogenetic approaches have also indicated that the PL plays an inhibitory role in HPA activation during acute stress exposure, as lesioning or inactivating PL cortex enhanced ACTH and CORT response to acute emotional stressors (e.g. restraint, TST) (Diorio et al., 1993; Figueiredo et al., 2003; Radley et al., 2006; Johnson et al., 2019). Other studies have employed the opposite strategy and reported reduced ACTH and CORT response to acute restraint after PL stimulation (Jones et al., 2011), which would be in line with our results, although in this case, all rats were stress-naïve and the stimulation was performed globally in the PL using the GABA antagonist bicuculline.

In contrast to all the above findings, Crane and colleagues (2003) reported that global mPFC lesions did not alter ACTH levels in response to white noise. Differences could be attributed to the fact that in this study lesions affected the whole mPFC, whereas in our experiments and most of the studies above mentioned, the manipulation was targeted specifically at the PL region. In this regard, an opposite role of PL and IL subdivisions in the regulation of the HPA response to stress has been suggested (Radley et al., 2006).

Several important aspects emerge from our results with the modulation of the HPA axis. First, viral vector expression levels in the PL of animals maintained in resting conditions before exposure to OF and FST (control groups) are sufficient to modulate the HPA axis response to stress. Second,

the CNO effect on corticosterone response is unlikely to be due to off-target effects, which have been reported in some conditions by its conversion to clozapine (e.g. MacLaren et al., 2016; Gomez et al., 2017). The supporting argument for this hypothesis is that changes in corticosterone levels go in exactly opposite directions after neuronal stimulation and neuronal inhibition, ruling out non-specific effects of CNO, which should be independent of the type of DREADD used (i.e. excitatory vs inhibitory). Third, it is important to highlight that the differential changes induced by stress and PL neuronal manipulation on behaviour versus corticosterone illustrate a clear dissociation between behaviour and HPA activation, which has been already described in other stress-related paradigms (e.g. HB test; Gagliano et al., 2008). With regard to this, we analysed the correlation between all the behavioural parameters evaluated in the OF and the FST with the corresponding corticosterone response of each animal and we found no significant correlations in any of the parameters assessed.

There are several limitations regarding the evaluation of the hormonal response in the present thesis. First, ACTH could not be measured due to unexpected technical problems. ACTH is more sensitive to the intensity of stress as the capacity of the adrenal to secrete corticosterone becomes saturated with relatively low levels of ACTH (for a comprehensive revision see Armario, 2006b). This would be relevant, particularly for the FST, which is a more severe stressor than OF. We selected a 15-min stress time for blood sampling based on reaching a compromise between ACTH and corticosterone measurement, but a longer stress exposure time could have been chosen for corticosterone only, as maximum corticosterone levels are reached usually between 30 - 60 min after the initiation of exposure when it continues for 15 min or more. Furthermore, due to the complexity of our experimental design, we do not know the effects of manipulating PL stress-activated neurons on basal levels of ACTH and corticosterone prior to the tests. Nevertheless, numerous papers have already shown that ACTH and corticosterone basal levels are not affected by either PL activation or inhibition (e.g. Diorio et al., 1993; Figueiredo et al., 2003; Jones et al., 2011).

3.8. Important considerations

Several aspects should be considered when interpreting the findings discussed above. One concern about the results of neuronal manipulation in the present thesis is the small size of samples used and another is that experiments were performed only in males. Originally it was 6 animals per group, but in some cases, this was reduced due to surgery problems or incorrect targeting of the injection. Behavioural measures, and to a lesser extent corticosterone levels showed high variability, which might have been

improved by a greater sample size. Furthermore, the consequences of stress exposure could be strongly influenced by individual differences in the response to IS and coping strategies. Given the difficulty of the experimental design and the strict temporal constraints, performing everything simultaneously with a higher number of animals would have been extremely difficult. Further testing the effects of PL manipulation in females is essential, as these findings might be greatly influenced by sex differences. Another limitation is that the tests used to evaluate the consequences of IS exposure (OF, HB and FST) have a stressful component and the behavioural and hormonal differences observed can also be affected not only by prior re-activation or inhibition of IS-activated neurons but also by the interaction of the previous exposure to stress with the new stressful situation.

Regarding the manipulation strategy, there are some concerns to bear in mind when interpreting the results. First, our strategy does not provide access to neurons inhibited by stressors or those neurons activated in a manner that does not induce *c-fos* expression, which might be also relevant to the regulation of the stress response. Second, an inherent feature of our design is that it requires exposure to stress to induce expression of the viral vector, and hence, if we aim to perform a battery of behavioural tests at a specific time after stress, we need to repeatedly expose animals to the stressor as effector expression is limited to a few hours after the experience. The neurons expressing the construct after the second exposure to IS might at least in part be different from those activated by the first IS exposure 1 week before due to homotypic adaptation, observed with *c-fos* at this same time frame in other brain areas. For instance, Vallès and Colleagues (2006) reported that exposure to IMO reduces post-stress *c-fos* mRNA levels after a the second exposure to IMO 1 week later in some stressor-processing areas such as the MeA and the LSv. An alternative approach to solve this problem would be to use one cohort for each behavioural test (and hence a unique exposure to IS), but this would imply multiplying the number of animals, implying ethical concerns and enormous efforts.

A third limitation of our strategy is that animals maintained in standard home cage conditions already had considerable viral vector expression levels. Although the levels in stressed animals were significantly higher, this non-stress-related expression in control animals could mask some of the effects of neuronal manipulation, which would explain the few effects found in the present thesis. An underlying reason for this high expression in control animals could be attributed to the fact that our approach was not inducible (e.g. doxycycline- or tamoxifen-dependent). Nevertheless, we compensated for this by reducing the half-life of the construct with the sequence PEST, which also reduced the time window for viral vector

expression. Moreover, our viral strategy bypasses the need for transgenic animals. In fact, other inducible techniques are not free from limitations either.

The Fos-tTA and Fos-CreERT2 methodologies (*see Section 5.1 of the Introduction*) are based on the use of transgenic mice. For rats, we would need to simultaneously inject two viral vectors to introduce the two constructs (e.g. Fos-tTA and TRE-receptor), which could limit infection efficiency and imply the targeting of a smaller subset of neurons. Furthermore, the Fos-tTA approach depends on 1-2 days minimum of Dox withdrawal due to the slow metabolism of Dox (Liu et al., 2012; DeNardo and Luo, 2017), which also implies a long time window for labelling Fos+ neurons and thus can result in high background expressions levels. Furthermore, Dox is usually administered to mice through the diet, but this strategy with rats would suppose a considerably higher economical cost. With the Fos-CreERT2 strategy, the time window for capturing activated neurons is shorter than with doxycycline (12-24h), although using the 4-hydroxytamoxifen form reduces the labelling window to <12h (Guenthner et al., 2013). However, this approach requires the injection of tamoxifen, which binds also to native estrogen receptors, and hence it could affect the behavioural and biochemical outcomes. Furthermore, a single tamoxifen injection typically only activates a fraction of CreER enzymes and this may result in stochastic labelling of small subsets of activated neurons (Sakurai et al., 2016). Finally, authors have reported a high frequency of recombination already under home cage conditions (Guenthner et al., 2013), given the fact that CreER-mediated recombination is irreversible, and hence, labelled cells accumulate as long as tamoxifen is present.

Hence, both with Fos-tTA and Fos-CreERT2 methodologies the targeted population is the result of activity integrated over a particular window of time determined by the stability of proteins (tTA and CreERT2) and the metabolism and excretion of the drugs used to control the system (Dox and TAM). In our case, the labelling window is much shorter, although this transient expression also has limitations with regard to the experimental design as mentioned above. Novel methodologies including synthetic activity-regulated promoters are emerging which could help to solve these drawbacks.

Finally, a major disadvantage of all IEG-based manipulation strategies is that they do not allow to mimic complex physiological responses typical of some neuronal populations (for a revision see (Gore, Schwartz, and Salamanz, 2015)). For instance, neurons that encode different information at different time points, or that integrate information about multiple different parameters. Furthermore, these strategies do not allow access to all activated

neurons due to the possible cell-type specificities of endogenous IEGs expression. In this respect, again synthetic promoters might feature broader targeting of different populations of activated neurons.

3.9. Future directions

In future experiments, it would be interesting to combine our activity-dependent manipulation strategy with the specific targeting of neurons projecting to other brain regions involved in stress processing. In this regard, the Tye lab showed that direct stimulation of mPFC neurons had no effects on behaviour in the FST, but when they targeted a specific subset of mPFC neurons defined by their specific projections (e.g. to the DRN), they found important changes in coping strategies. Broadening our studies to other PL-projecting structures might allow us to integrate the whole circuit that participates in the stress response. Moreover, it would be ideal to find other markers of neuronal activation typical of stress in the PL cortex which are not activated by other non-stress-related reasons, which would solve the problems encountered with *c-fos*. Although this is a difficult challenge, detailed transcriptomic and translational analyses could definitely help in this endeavour.

The ultimate goal of our thesis was to assess the specific role of PL neurons in regulating the behavioural and hormonal response to different emotional stressors. Unfortunately, due to technical limitations and temporal constraints, we could only target neurons activated after IS. It is well known that IMO and other emotional stressors result in different consequences than IS (e.g. animals do not develop CFC). Thus, manipulating neurons using other stressors such as IMO would allow us to study whether the behavioural and hormonal effects are similar or different from IS. Finally, it would be of great interest to extend our approach to manipulate mPFC neurons differentially activated by controllable and uncontrollable stress, as it has been also shown that the consequences greatly differ depending on whether animals have control over the stressful situation. Activity-based neuronal manipulation strategies are an interesting tool that open up exciting avenues for further research and provide many potential possibilities, although currently there are some technical limitations and methodological complexities that complicate reaching clear results. Novel and more sophisticated technological developments in the field will be a step forward and will definitely help to unravel the role of stressor-specific ensembles in the stress response.

Conclusions

1. The different parameters employed to assess neuronal activation (e.g. number of positive neurons vs total intensity of signal or intensity of signal per cell; c-fos intronic vs mature RNA; c-Fos vs pS6) can provide complementary information which could have relevant functional implications.
2. IMO and IS induce a great activation in the PL and IL cortex, with both stressors recruiting a similar number of neurons. Brief (5 min) exposure to stressors reduces the number of c-fos positive neurons in response to a subsequent stressor 25 min later, regardless of whether the stressor is the same or different, suggesting a desensitisation process.
3. The catFISH technique and our experimental design are appropriate to study stressor-specific neuronal populations after short stress exposures. The results suggest that most neurons activated by IMO and IS in the mPFC are common to the two stressors, but there is evidence for a relatively low percent of neurons that appear to be stressor-specific.
4. Phosphorylation of the ribosomal protein S6 has emerged as a useful marker of neuronal activation after exposure to emotional stressors in telencephalic regions such as the PL region. Furthermore, it exhibits a high overlap with the c-Fos marker after 1 h of IMO.
5. The PhosphoRiboTRAP methodology is appropriate to study the gene expression profile of neurons activated in response to stress, as shown by the enrichment in IEGs levels after pS6 immunoprecipitation. Furthermore, it markedly enhances the sensitivity to detect significantly upregulated and downregulated transcripts after stress exposure compared to basal conditions.
6. The comparison of the translomic profiles of activated neurons between different emotional stressors (RES, IMO and IS) reveals a great proportion of shared differentially expressed genes compared to basal conditions. A large portion of upregulated genes corresponds to well-known IEGs, whereas many other common genes have not been studied yet in the context of stress and may emerge as useful and relevant markers of stress exposure.

7. Our transcriptome analysis reveals genes that are exclusively upregulated or downregulated in the PL in response to each of the stressors compared to basal conditions. Still more important, the molecular profile of IMO and RES is strikingly similar despite being markedly different on intensity, whereas that of IS markedly differ from the latter stressors, suggesting a major contribution of the particular nature of the stressor. Whether this also applies to other brain regions warrants further investigation.
8. We have developed a viral vector strategy to manipulate stress-activated neurons which is based on the c-fos promoter driving the expression of either the excitatory or inhibitory DREADD and the degradation sequence PEST, which reduces half-life of the receptor and prevents accumulation over time. Viral vector expression is appropriately induced in PL neurons 4h after stress exposure, enabling activity-dependent labelling and manipulation of neurons after stress.
9. IS exposure induces short-term and long-term behavioural changes. Re-activation of previously activated PL neurons does not exert major behavioural effects, but when observed, it tends to increase exploration on stress-naïve animals whereas it accentuates the negative consequences of IS in stressed animals. Inhibition of IS-activated neurons results in a very modest effect on behaviour.
10. Re-activation of IS-responsive neurons 4h after IS exposure reduces long-term contextual fear memory, probably by interfering with consolidation, whereas inhibition does not alter fear memory.
11. PL neuronal re-activation clearly reduces corticosterone response to the OF and FST both in stress-naïve and previously shocked animals. Conversely, neuronal inhibition of PL neurons tended to enhance the HPA response to FST in both groups, albeit no effects are observed in the response to the OF. Together, these results point towards a tonic inhibitory role of PL neurons in modulating the HPA response to emotional stressors.
12. Notwithstanding the inherent limitations of using c-fos and pS6 as surrogate markers of neuronal activity, and some methodological considerations, the present thesis has provided useful insights into the molecular profile of stress-activated neurons and their role in the behavioural and hormonal stress response.

Bibliography

- Adell A, Casanovas JM, Artigas F (1997) Comparative study in the rat of the actions of different types of stress on the release of 5-HT in raphe nuclei and forebrain areas. *Neuropharmacology* 36:735–741.
- Aguilera G (2012) The hypothalamic-pituitary-adrenal axis and neuroendocrine responses to stress. In G. Fink, D. Pfaff, & J. Levine (Eds.), *Handbook of Neuroendocrinology* (pp. 175–196) Academic Press, Oxford UK.
- Alexander GM, Rogan SC, Abbas AI, Armbruster BN, Pei Y, Allen JA, Nonneman RJ, Hartmann J, Moy SS, Nicolelis MA, McNamara JO, Roth BL (2009) Remote control of neuronal activity in transgenic mice expressing evolved G protein-coupled receptors. *Neuron* 63:27–39.
- Alpert T, Herzel L, Neugebauer KM (2017) Perfect timing: splicing and transcription rates in living cells. *Wiley Interdiscip Rev RNA* 8:10.1002/wrna.1401.
- Anastasiades PG, Carter AG (2021) Circuit organization of the rodent medial prefrontal cortex. *Trends Neurosci* 44:550–563.
- Andrews S, Krueger F, Laura K (2012) FastQC. Babraham Inst .
- Anthony TE, Dee N, Bernard A, Lerchner W, Heintz N, Anderson DJ (2014) Control of stress-induced persistent anxiety by an extra-amygdala septohypothalamic circuit. *Cell* 156:522–536.
- Antoni FA (1986) Hypothalamic control of adrenocorticotropin secretion: Advances since the discovery of 41-residue corticotropin-releasing factor. *Endocr Rev* 7:351–378.
- Armario A (2006a) The Hypothalamic-Pituitary-Adrenal Axis: What can it Tell us About Stressors? *CNS Neurol Disord - Drug Targets* 5:485–501.
- Armario A (2006b) The contribution of Immediate Early Genes to the understanding of brain processing of stressors. In R. Pinaud & L. Tremere (Eds.), *Immediate Early Genes in sensory processing, cognitive performance and neurological disorders* (pp. 199–221) Springer Science & Business Media, LLC.
- Armario A (2021) The forced swim test: Historical, conceptual and methodological considerations and its relationship with individual behavioral traits. *Neurosci Biobehav Rev* 128:74–86.
- Armario A, Daviu N, Muñoz-Abellán C, Rabasa C, Fuentes S, Belda X, Gagliano H, Nadal R (2012) What can we know from pituitary-adrenal hormones about the nature and consequences of exposure to emotional stressors? In *Cellular and Molecular Neurobiology* (Vol. 32, Issue 5, pp. 749–758).
- Armario A, Gil M, Marti J, Pol O, Balasch J (1991) Influence of various acute stressors on the activity of adult male rats in a holeboard and in the forced swim test. *Pharmacol Biochem Behav* 39:373–377.
- Armario A, Nadal R (2013) Individual differences and the characterization of animal models of psychopathology: A strong challenge and a good opportunity. *Front Pharmacol* 4 NOV:1–13.
- Arnsten AFT (2009) Stress signalling pathways that impair prefrontal cortex structure and function. *Nat Rev Neurosci* 10:410–422.
- Arnsten AFT (2015) Stress weakens prefrontal networks: Molecular insults to higher cognition. *Nat Neurosci* 18:1376–1385.
- Arnsten AFT, Goldman-Rakic PS (1998) Noise stress impairs prefrontal cortical cognitive function in monkeys: Evidence for a hyperdopaminergic mechanism. *Arch Gen Psychiatry* 55:362–368.
- Azevedo EP, Pomeranz L, Cheng J, Schneeberger M, Vaughan R, Stern SA, Tan B, Doerig K, Greengard P, Friedman JM (2019) A Role of Drd2 Hippocampal Neurons in Context-Dependent Food Intake. *Neuron* 102:873–886.

- Azevedo EP, Tan B, Pomeranz LE, Ivan V, Fetcho R, Schneeberger M, Doerig KR, Liston C, Friedman JM, Stern SA (2020) A limbic circuit selectively links active escape to food suppression. *Elife* 9:1–23.
- Bale TL, Vale WW (2004) CRF and CRF Receptors: Role in Stress Responsivity and Other Behaviors. *Annu Rev Pharmacol Toxicol* 44:525–557.
- Barth AL, Gerkin RC, Dean KL (2004) Alteration of neuronal firing properties after in vivo experience in a FosGFP transgenic mouse. *J Neurosci* 24:6466–6475.
- Belda X, Nadal R, Armario A (2016) Critical features of acute stress-induced cross-sensitization identified through the hypothalamic-pituitary-adrenal axis output. *Sci Rep* 6:1–12.
- Belda X, Rotllant D, Fuentes S, Delgado R, Nadal R, Armario A (2008) Exposure to severe stressors causes long-lasting dysregulation of resting and stress-induced activation of the hypothalamic-pituitary-adrenal axis. *Ann N Y Acad Sci* 1148:165–173.
- Belloso E, Hernandez J, Giralt M, Kille P, Hidalgo J (1996) Effect of Stress on Mouse and Rat Brain Metallothionein I and III mRNA Levels. *Neuroendocrinology* 64:430–439.
- Benjamini Y, Hochberg Y (1995) Controlling the False Discovery Rate: A Practical and Powerful Approach to Multiple Testing. *J R Stat Soc Ser B* 57:289–300.
- Berridge CW (2008) Noradrenergic modulation of arousal. *Brain Res Rev* 58:1–17.
- Bertran-Gonzalez J, Chieng BC, Laurent V, Valjent E, Balleine BW (2012) Striatal Cholinergic Interneurons Display Activity-Related Phosphorylation of Ribosomal Protein S6. *PLoS One* 7:e53195.
- Bhatnagar S, Vining C, Denski K (2004) Regulation of chronic stress-induced changes in hypothalamic-pituitary- adrenal activity by the basolateral amygdala. *Ann N Y Acad Sci* 1032:315–319.
- Biever A, Valjent E, Puighermanal E (2015) Ribosomal protein S6 phosphorylation in the nervous system: From regulation to function. *Front Mol Neurosci* 8:75.
- Bland ST, Hargrave D, Pepin JL, Amat J, Watkins LR, Maier SF (2003) Stressor controllability modulates stress-induced dopamine and serotonin efflux and morphine-induced serotonin efflux in the medial prefrontal cortex. *Neuropsychopharmacology* 28:1589–1596.
- Bonapersona V, Schuler H, Damsteegt R, Adolfs Y, Pasterkamp RJ, van den Heuvel MP, Joëls M, Sarabdjitsingh RA (2022) The mouse brain after foot shock in four dimensions: Temporal dynamics at a single-cell resolution. *Proc Natl Acad Sci U S A* 119:1–9.
- Bossert JM, Stern AL, Theberge FRM, Cifani C, Koya E, Hope BT, Shaham Y (2011) Ventral medial prefrontal cortex neuronal ensembles mediate context-induced relapse to heroin. *Nat Neurosci* 14:420–422.
- Bottai D, Guzowski JF, Schwarz MK, Kang SH, Xiao B, Lanahan A, Worley PF, Seeburg PH (2002) Synaptic activity-induced conversion of intronic to exonic sequence in Homer 1 immediate early gene expression. *J Neurosci* 22:167–175.
- Bourtchouladze R, Abel T, Berman N, Gordon R, Lapidus K, Kandel ER (1998) Different training procedures recruit either one or two critical periods for contextual memory consolidation, each of which requires protein synthesis and PKA. *Learn Mem* 5:365–374.
- Buckner RL, Andrews-Hanna JR, Schacter DL (2008) The brain’s default network: Anatomy, function, and relevance to disease. *Ann N Y Acad Sci* 1124:1–38.
- Cai DJ, Aharoni D, Shuman T, Shobe J, Biane J, Song W, Wei B, Veshkini M, La-Vu M, Lou J, Flores SE, Kim I, Sano Y, Zhou M, Baumgaertel K, Lavi A, Kamata M, Tuszyński M, Mayford M, ... Silva AJ (2016) A shared neural ensemble links distinct contextual memories encoded close in time. *Nature* 534:115–118.

- Campeau S, Falls WA, Cullinan WE, Helmreich DL, Davis M, Watson SJ (1997) Elicitation and reduction of fear: Behavioural and neuroendocrine indices and brain induction of the immediate-early gene c-fos. *Neuroscience* 78:1087–1104.
- Campeau S, Watson SJ (1997) Neuroendocrine and Behavioral Responses and Brain Pattern of c-fos Induction Associated with Audiogenic Stress. *J Neuroendocrinol* 9:577–588.
- Canteras NS, Simerly RB, Swanson LW (1995) Organization of projections from the medial nucleus of the amygdala: A PHAL study in the rat. *J Comp Neurol* 360:213–245.
- Cassatario D, Sjulson L (2015) The Use of DREADDs (Designer Receptors Exclusively Activated by Designer Receptors) in Transgenic Mouse Behavioral Models. In G. Thiel (Ed.), *Designer Receptors Exclusively Activated by Designer Drugs, Neuromethods* (Vol. 108, pp. 95–108) Springer Science & Business Media.
- Cerqueira JJ, Mailliet F, Almeida OFX, Jay TM, Sousa N (2007) The prefrontal cortex as a key target of the maladaptive response to stress. *J Neurosci* 27:2781–2787.
- Cho J, Yu NK, Choi JH, Sim SE, Kang SJ, Kwak C, Lee SW, Kim J Il, Choi D Il, Kim VN, Kaang BK (2015) Multiple repressive mechanisms in the hippocampus during memory formation. *Science* (80-) 350:82–87.
- Choi DC, Furay AR, Evanson NK, Ostrander MM, Ulrich-Lai YM, Herman JP (2007) Bed nucleus of the stria terminalis subregions differentially regulate hypothalamic-pituitary-adrenal axis activity: Implications for the integration of limbic inputs. *J Neurosci* 27:2025–2034.
- Cifani C, Koya E, Navarre BM, Calu DJ, Baumann MH, Marchant NJ, Liu QR, Khuc T, Pickel J, Lupica CR, Shaham Y, Hope BT (2012) Medial prefrontal cortex neuronal activation and synaptic alterations after stress-induced reinstatement of palatable food seeking: A study using c-fos-GFP transgenic female rats. *J Neurosci* 32:8480–8490.
- Cook SC, Wellman CL (2004) Chronic stress alters dendritic morphology in rat medial prefrontal cortex. *J Neurobiol* 60:236–248.
- Corcoran KA, Quirk GJ (2007) Activity in prelimbic cortex is necessary for the expression of learned, but not innate, fears. *J Neurosci* 27:840–844.
- Coulon V, Chebli K, Cavalier P, Blanchard J-M (2010) A Novel Mouse c-fos Intronic Promoter That Responds to CREB and AP-1 Is Developmentally Regulated In Vivo. *PLoS One* 5:e11235.
- Crane JW, Ebner K, Day TA (2003) Medial prefrontal cortex suppression of the hypothalamic-pituitary-adrenal axis response to a physical stressor, systemic delivery of interleukin-1 β . *Eur J Neurosci* 17:1473–1481.
- Cruz FC, Javier Rubio F, Hope BT (2015) Using c-fos to study neuronal ensembles in corticostriatal circuitry of addiction. *Brain Res* 1628:157–173.
- Cruz FC, Koya E, Guez-Barber DH, Bossert JM, Lupica CR, Shaham Y, Hope BT (2013) New technologies for examining the role of neuronal ensembles in drug addiction and fear. *Nat Rev Neurosci* 14:743–754.
- Cullinan WE, Herman JP, Battaglia DF, Akil H, Watson SJ (1995) Pattern and time course of immediate early gene expression in rat brain following acute stress. *Neuroscience* 64:477–505.
- Cullinan WE, Herman JP, Watson SJ (1993) Ventral subicular interaction with the hypothalamic paraventricular nucleus: Evidence for a relay in the bed nucleus of the stria terminalis. *J Comp Neurol* 332:1–20.
- Dal-Zotto S, Martí O, Armario A (2000) Influence of single or repeated experience of rats with forced swimming on behavioural and physiological responses to the stressor. *Behav Brain Res* 114:175–181.

- Dalley JW, Cardinal RN, Robbins TW (2004) Prefrontal executive and cognitive functions in rodents: Neural and neurochemical substrates. *Neurosci Biobehav Rev* 28:771–784.
- Daviu N, Andero R, Armario A, Nadal R (2014) Sex differences in the behavioural and hypothalamic-pituitary-adrenal response to contextual fear conditioning in rats. *Horm Behav* 66:713–723.
- Daviu N, Delgado-Morales R, Nadal R, Armario A (2012) Not all stressors are equal: Behavioural and endocrine evidence for development of contextual fear conditioning after a single session of footshocks but not of immobilization. *Front Behav Neurosci* 6:1–19.
- Daviu N, Fuentes S, Nadal R, Armario A (2010) A single footshock causes long-lasting hypoactivity in unknown environments that is dependent on the development of contextual fear conditioning. *Neurobiol Learn Mem* 94:183–190.
- Dayas C V., Buller KM, Crane JW, Xu Y, Day TA (2001) Stressor categorization: Acute physical and psychological stressors elicit distinctive recruitment patterns in the amygdala and in medullary noradrenergic cell groups. *Eur J Neurosci* 14:1143–1152.
- De Kloet ER, Joëls M, Holsboer F (2005) Stress and the brain: From adaptation to disease. *Nat Rev Neurosci* 6:463–475.
- Deisseroth K (2011) Optogenetics. *Nat Methods* 8:26–29.
- DeNardo L, Luo L (2017) Genetic strategies to access activated neurons. *Curr Opin Neurobiol* 45:121–129.
- Diorio D, Viau V, Meaney MJ (1993) The role of the medial prefrontal cortex (cingulate gyrus) in the regulation of hypothalamic-pituitary-adrenal responses to stress. *J Neurosci* 13:3839–3847.
- Dobin A, Davis CA, Schlesinger F, Drenkow J, Zaleski C, Jha S, Batut P, Chaisson M, Gingeras TR (2013) STAR: ultrafast universal RNA-seq aligner. *Bioinformatics* 29:15.
- Dong HW, Swanson LW (2004) Organization of Axonal Projections from the Anterolateral Area of the Bed Nuclei of the Stria Terminalis. *J Comp Neurol* 468:277–298.
- Dragunow M, Goulding M, Faull RLM, Ralph R, Mee E, Frith R (1990) Induction of c-fos mRNA and protein in neurons and glia after traumatic brain injury: Pharmacological characterization. *Exp Neurol* 107:236–248.
- Estanislau C, Díaz-Morán S, Cañete T, Blázquez G, Tobeña A, Fernández-Teruel A (2013) Context-dependent differences in grooming behavior among the NIH heterogeneous stock and the Roman high- and low-avoidance rats. *Neurosci Res* 77:187–201.
- Fanselow MS (1986) Associative vs topographical accounts of the immediate shock-freezing deficit in rats: Implications for the response selection rules governing species-specific defensive reactions. *Learn Motiv* 17:16–39.
- Feldman S, Conforti N, Itzik A, Weidenfeld J (1994) Differential effect of amygdaloid lesions on CRF-41, ACTH and corticosterone responses following neural stimuli. *Brain Res* 658:21–26.
- Fendt M, Fanselow MS (1999) The neuroanatomical and neurochemical basis of conditioned fear. *Neurosci Biobehav Rev* 23:743–760.
- Feng P, Feng T, Chen Z, Lei X (2014) Memory consolidation of fear conditioning: Bi-stable amygdala connectivity with dorsal anterior cingulate and medial prefrontal cortex. *Soc Cogn Affect Neurosci* 9:1730–1737.
- Figueiredo HF, Bruestle A, Bodie B, Dolgas CM, Herman JP (2003) The medial prefrontal cortex differentially regulates stress-induced c-fos expression in the forebrain depending on type of stressor. *Eur J Neurosci* 18:2357–2364.
- File SE, Wardill AG (1975) Validity of head-dipping as a measure of exploration in a modified hole-board. *Psychopharmacologia* 44:53–59.

- Fivaz J, Bassi MC, Pinaud S, Mirkovitch J (2000) RNA polymerase II promoter-proximal pausing upregulates c-fos gene expression. *Gene* 255:185–194.
- Floriou-Servou A, von Ziegler L, Stalder L, Sturman O, Privitera M, Rassi A, Cremonesi A, Thöny B, Bohacek J (2018) Distinct Proteomic, Transcriptomic, and Epigenetic Stress Responses in Dorsal and Ventral Hippocampus. *Biol Psychiatry* 84:531–541.
- Floriou-Servou A, von Ziegler L, Waag R, Schläppi C, Germain PL, Bohacek J (2021) The Acute Stress Response in the Multiomic Era. *Biol Psychiatry* 89:1116–1126.
- Fontes MAP, Xavier CH, de Menezes RCA, DiMicco JA (2011) The dorsomedial hypothalamus and the central pathways involved in the cardiovascular response to emotional stress. *Neuroscience* 184:64–74.
- Fuchikami M, Thomas A, Liu R, Wohleb ES, Land BB, DiLeone RJ, Aghajanian GK, Duman RS (2015) Optogenetic stimulation of infralimbic PFC reproduces ketamine's rapid and sustained antidepressant actions. *Proc Natl Acad Sci U S A* 112:8106–8111.
- Fuster J (2008) *The prefrontal cortex* (J. Fuster (ed.); 4th ed.) Academic Press.
- Füzesi T, Daviu N, Wamsteeker Cusulin JJ, Bonin RP, Bains JS (2016) Hypothalamic CRH neurons orchestrate complex behaviours after stress. *Nat Commun* 7:1–14.
- Gabbott PLA, Warner TA, Jays PRL, Salway P, Busby SJ (2005) Prefrontal cortex in the rat: Projections to subcortical autonomic, motor, and limbic centers. *J Comp Neurol* 492:145–177.
- Gagliano H, Fuentes S, Nadal R, Armario A (2008) Previous exposure to immobilisation and repeated exposure to a novel environment demonstrate a marked dissociation between behavioral and pituitary-adrenal responses. *Behav Brain Res* 187:239–245.
- García A, Martí O, Vallès A, Dal-Zotto S, Armario A (2000) Recovery of the Hypothalamic-Pituitary-Adrenal Response to Stress. *Neuroendocrinology* 72:114–125.
- Garner AR, Rowland DC, Hwang SY, Baumgaertel K, Roth BL, Kentros C, Mayford M (2012) Generation of a synthetic memory trace. *Science* (80-) 335:1513–1516.
- Gilabert-Juan J, Castillo-Gomez E, Guirado R, Moltó MD, Nacher J (2013) Chronic stress alters inhibitory networks in the medial prefrontal cortex of adult mice. *Brain Struct Funct* 218:1591–1605.
- Gillespie M, Jassal B, Stephan R, Milacic M, Rothfels K, Senff-Ribeiro A, Griss J, Sevilla C, Matthews L, Gong C, Deng C, Varusai T, Ragueneau E, Haider Y, May B, Shamovsky V, Weiser J, Brunson T, Sanati N, ... D'Eustachio P (2022) The reactome pathway knowledgebase 2022. *Nucleic Acids Res* 50:D687–D692.
- Giustino TF, Maren S (2015) The role of the medial prefrontal cortex in the conditioning and extinction of fear. *Front Behav Neurosci* 9:298.
- Goldman-Rakic PS (1995) Cellular basis of working memory. *Neuron* 14:477–485.
- Goldwater DS, Pavlides C, Hunter RG, Bloss EB, Patrick R, McEwen BS, Morrison JH, Hof PR (2009) Following Chronic Restraint Stress and Recovery. *Neuroscience* 164:798–808.
- Gómez-Román A, Ortega-Sánchez JA, Rotllant D, Gagliano H, Belda X, Delgado-Morales R, Marín-Blasco I, Nadal R, Armario A (2016) The neuroendocrine response to stress under the effect of drugs: Negative synergy between amphetamine and stressors. *Psychoneuroendocrinology* 63:94–101.
- Gomez JL, Bonaventura J, Lesniak W, Mathews WB, Sysa-Shah P, Rodriguez LA, Ellis RJ, Richie CT, Harvey BK, Dannals RF, Pomper MG, Bonci A, Michaelides M (2017) Chemogenetics revealed: DREADD occupancy and activation via converted clozapine. *Science* (80-) 357:503–507.

- Gore F, Schwartz EC, Brangers BC, Aladi S, Stujenske JM, Likhtik E, Russo MJ, Gordon JA, Salzman CD, Axel R (2015) Neural Representations of Unconditioned Stimuli in Basolateral Amygdala Mediate Innate and Learned Responses. *Cell* 162:134–145.
- Gore F, Schwartz EC, Salzman DC (2015) Manipulating neural activity in physiologically classified neurons: Triumphs and challenges. *Philos Trans R Soc B Biol Sci* 370:.
- Groeneweg FL, Karst H, de Kloet ER, Joëls M (2012) Mineralocorticoid and glucocorticoid receptors at the neuronal membrane, regulators of nongenomic corticosteroid signalling. *Mol Cell Endocrinol* 350:299–309.
- Guenthner CJ, Miyamichi K, Yang HH, Heller HC, Luo L (2013) Permanent genetic access to transiently active neurons via TRAP: Targeted recombination in active populations. *Neuron* 78:773–784.
- Guzowski JF, McNaughton BL, Barnes CA, Worley PF (1999) Environment-specific expression of the immediate-early gene *Arc* in hippocampal neuronal ensembles. *Nature Neuroscience* 2:1120–1124.
- Guzowski JF, Miyashita T, Chawla MK, Sanderson J, Maes LI, Houston FP, Lipa P, McNaughton BL, Worley PF, Barnes CA (2006) Recent behavioral history modifies coupling between cell activity and *Arc* gene transcription in hippocampal CA1 neurons. *Proc Natl Acad Sci U S A* 103:1077–1082.
- Guzowski JF, Setlow B, Wagner EK, McGaugh JL (2001) Experience-dependent gene expression in the rat hippocampus after spatial learning: A comparison of the immediate-early genes *Arc*, *c-fos*, and *zif268*. *J Neurosci* 21:5089–5098.
- Guzowski JF, Timlin JA, Roysam B, McNaughton BL, Worley PF, Barnes CA (2005) Mapping behaviorally relevant neural circuits with immediate-early gene expression. *Curr Opin Neurobiol* 15:599–606.
- Haery L, Deverman BE, Matho KS, Cetin A, Woodard K, Cepko C, Guerin KI, Rego MA, Erasing I, Bachle SM, Kamens J, Fan M (2019) Adeno-Associated Virus Technologies and Methods for Targeted Neuronal Manipulation. *Front Neuroanat* 13:1–16.
- Hall C, Ballachey E (1932) A study of the rat's behavior in a field. A contribution to method in comparative psychology. *Univ Calif Publ Psychol* 6:1–12.
- Heidbreder CA, Groenewegen HJ (2003) The medial prefrontal cortex in the rat: Evidence for a dorso-ventral distinction based upon functional and anatomical characteristics. *Neurosci Biobehav Rev* 27:555–579.
- Heiman M, Kulicke R, Fenster RJ, Greengard P, Heintz N (2014) Cell type-specific mRNA purification by translating ribosome affinity purification (TRAP). *Nat Protoc* 9:1282–1291.
- Heinsbroek RPW, van Haaren F, van de Poll NE (1988) Sex differences in passive avoidance behavior of rats: Sex-dependent susceptibility to shock-induced behavioral depression. *Physiol Behav* 43:201–206.
- Herdegen T, Leah JD (1998) Inducible and constitutive transcription factors in the mammalian nervous system: Control of gene expression by Jun, Fos and Krox, and CREB/ATF proteins. In *Brain Research Reviews* (Vol. 28, Issue 3, pp. 370–490) Elsevier.
- Herman JP, Cullinan WE (1997) Neurocircuitry of stress: Central control of the hypothalamo-pituitary-adrenocortical axis. *Trends Neurosci* 20:78–84.
- Herman JP, Cullinan WE, Watson SJ (1994) Involvement of the Bed Nucleus of the Stria Terminalis in Tonic Regulation of Paraventricular Hypothalamic CRH and AVP mRNA Expression. *J Neuroendocrinol* 6:433–442.
- Herman JP, Dolgas CM, Carlson SL (1998) Ventral subiculum regulates hypothalamo-pituitary-adrenocortical and behavioural responses to cognitive stressors. *Neuroscience* 86:449–459.

- Herman JP, Figueiredo H, Mueller NK, Ulrich-Lai Y, Ostrander MM, Choi DC, Cullinan WE (2003) Central mechanisms of stress integration: Hierarchical circuitry controlling hypothalamo-pituitary-adrenocortical responsiveness. *Front Neuroendocrinol* 24:151–180.
- Herman JP, McKlveen JM, Ghosal S, Kopp B, Wulsin A, Makinson R, Scheimann J, Myers B (2016) Regulation of the hypothalamic-pituitary- adrenocortical stress response. *Compr Physiol* 6:603–621.
- Herman JP, Mueller NK (2006) Role of the ventral subiculum in stress integration. *Behav Brain Res* 174:215–224.
- Herman JP, Ostrander MM, Mueller NK, Figueiredo H (2005) Limbic system mechanisms of stress regulation: Hypothalamo-pituitary- adrenocortical axis. *Prog Neuro-Psychopharmacology Biol Psychiatry* 29:1201–1213.
- Hidalgo J, Campmany L, Martí O, Armario A (1991) Metallothionein-I induction by stress in specific brain areas. *Neurochem Res* 16:1145–1148.
- Hisanaga K, Sagar SM, Hicks KJ, Swanson RA, Sharp FR (1990) c-fos proto-oncogene expression in astrocytes associated with differentiation or proliferation but not depolarization. *Mol Brain Res* 8:69–75.
- Hoffman GE, Le WW, Abbud R, Lee W Sen, Susan Smith M (1994) Use of Fos-related antigens (FRAs) as markers of neuronal activity: FRA changes in dopamine neurons during proestrus, pregnancy and lactation. *Brain Res* 654:207–215.
- Hohoff C, Gorji A, Kaiser S, Willscher E, Korsching E, Ambrée O, Arolt V, Lesch KP, Sachser N, Deckert J, Lewejohann L (2013) Effect of Acute Stressor and Serotonin Transporter Genotype on Amygdala First Wave Transcriptome in Mice. *PLoS One* 8:e58880.
- Hoover WB, Vertes RP (2007) Anatomical analysis of afferent projections to the medial prefrontal cortex in the rat. *Brain Struct Funct* 212:149–179.
- Hughes P, Lawlor P, Dragunow M (1992) Basal expression of Fos, Fos-related, Jun, and Krox 24 proteins in rat hippocampus. *Mol Brain Res* 13:355–357.
- Hurley KM, Herbert H, Moga MM, Saper CB (1991) Efferent projections of the infralimbic cortex of the rat. *J Comp Neurol* 308:249–276.
- Imaki T, Shibasaki T, Chikada N, Harada S, Naruse M, Demura H (1996) Different Expression of Immediate-Early Genes in the Rat Paraventricular Nucleus Induced by Stress: Relation to Corticotropin-Releasing Factor Gene Transcription. *Endocr J* 43:629–638.
- Imaki T, Shibasaki T, Hotta M, Demura H (1992) Early induction of c-fos precedes increased expression of corticotropin-releasing factor messenger ribonucleic acid in the paraventricular nucleus after immobilization stress. *Endocrinology* 131:240–246.
- Jackson ME, Moghaddam B (2006) Distinct patterns of plasticity in prefrontal cortex neurons that encode slow and fast responses to stress. *Eur J Neurosci* 24:1702–1710.
- Jacobson L, Sapolsky R (1991) The role of the hippocampus in feedback regulation of the hypothalamic-pituitary-adrenocortical axis. *Endocr Rev* 12:118–134.
- Jankord R, Herman JP (2008) Limbic regulation of hypothalamo-pituitary-adrenocortical function during acute and chronic stress. *Ann N Y Acad Sci* 1148:64–73.
- Johnson SB, Emmons EB, Lingg RT, Anderson RM, Romig-Martin SA, Lalumiere RT, Narayanan NS, Viau V, Radley JJ (2019) Prefrontal-bed nucleus circuit modulation of a passive coping response set. *J Neurosci* 39:1405–1419.
- Jones KR, Myers B, Herman JP (2011) Stimulation of the prelimbic cortex differentially modulates neuroendocrine responses to psychogenic and systemic stressors. *Physiol Behav* 104:266–271.

- Kalueff A V., Tuohimaa P (2005) The grooming analysis algorithm discriminates between different levels of anxiety in rats: Potential utility for neurobehavioural stress research. *J Neurosci Methods* 143:169–177.
- Katz RJ, Roth KA, Carroll BJ (1981) Acute and chronic stress effects on open field activity in the rat: Implications for a model of depression. *Neurosci Biobehav Rev* 5:247–251.
- Kawashima T, Kitamura K, Suzuki K, Nonaka M, Kamijo S, Takemoto-Kimura S, Kano M, Okuno H, Ohki K, Bito H (2013) Functional labeling of neurons and their projections using the synthetic activity-dependent promoter E-SARE. *Nat Methods* 10:889–895.
- Kawashima T, Okuno H, Bito H (2014) A new era for functional labeling of neurons: Activity-dependent promoters have come of age. *Front Neural Circuits* 8:37.
- Keller-Wood ME, Dallman MF (1984) Corticosteroid inhibition of ACTH secretion. *Endocr Rev* 5:1–24.
- Knight ZA, Tan K, Birsoy K, Schmidt S, Garrison JL, Wysocki RW, Emiliano A, Ekstrand MI, Friedman JM (2012) Molecular profiling of activated neurons by phosphorylated ribosome capture. *Cell* 151:1126–1137.
- Kolde R (2019) *pheatmap: Pretty Heatmaps*. CRAN.
- Korosi A, Baram TZ (2008) The central corticotropin releasing factor system during development and adulthood. *Eur J Pharmacol* 583:204–214.
- Kovács KJ (1998) c-Fos as a transcription factor: A stressful (re)view from a functional map. *Neurochem Int* 33:287–297.
- Kovács KJ (2008) Measurement of immediate-early gene activation- c-fos and beyond. *J Neuroendocrinol* 20:665–672.
- Koya E, Golden SA, Harvey BK, Guez-Barber DH, Berkow A, Simmons DE, Bossert JM, Nair SG, Uejima JL, Marin MT, Mitchell TB, Farquhar D, Ghosh SC, Mattson BJ, Hope BT (2009) Targeted disruption of cocaine-activated nucleus accumbens neurons prevents context-specific sensitization. *Nat Neurosci* 12:1069–1073.
- Kukushkin AN, Abramova M V., Svetlikova SB, Darieva ZA, Pospelova T V., Pospelov VA (2002) Downregulation of c-fos gene transcription in cells transformed by E1A and cHa-ras oncogenes: A role of sustained activation of MAP/ERK kinase cascade and of inactive chromatin structure at c-fos promoter. *Oncogene* 21:719–730.
- Kumar S, Black SJ, Hultman R, Szabo ST, Demaio KD, Du J, Katz BM, Feng G, Covington HE, Dziras K (2013) Cortical control of affective networks. *J Neurosci* 33:1116–1129.
- Kvetnansky R, Sabban EL, Palkovits M (2009) Catecholaminergic systems in stress: Structural and molecular genetic approaches. *Physiol Rev* 89:535–606.
- Lee PR, Fields RD (2021) Activity-Dependent Gene Expression in Neurons. *Neuroscientist* 27:355–366.
- Lehnert H, Reinstein DK, Strowbridge BW, Wurtman RJ (1984) Neurochemical and behavioral consequences of acute, uncontrollable stress: Effects of dietary tyrosine. *Brain Res* 303:215–223.
- Li HY, Sawchenko PE (1998) Hypothalamic effector neurons and extended circuitries activated in “neurogenic” stress: A comparison of footshock effects exerted acutely, chronically, and in animals with controlled glucocorticoid levels. *J Comp Neurol* 393:244–266.
- Li X, Zhao X, Fang Y, Jiang X, Duong T, Fan C, Huang CC, Kain SR (1998) Generation of destabilized green fluorescent protein as a transcription reporter. *J Biol Chem* 273:34970–34975.
- Lichtman JW, Denk W (2011) The big and the small: Challenges of imaging the brain’s circuits. *Science (80-)* 334:618–623.

- Lin D, Boyle MP, Dollar P, Lee H, Lein ES, Perona P, Anderson DJ (2011a) Functional identification of an aggression locus in the mouse hypothalamus. *Nature* 470:221–227.
- Lin D, Boyle MP, Dollar P, Lee H, Lein ES, Perona P, Anderson DJ (2011b) Functional identification of an aggression locus in the mouse hypothalamus. *Nature* 470:221–227.
- Listerman I, Sapra AK, Neugebauer KM (2006) Cotranscriptional coupling of splicing factor recruitment and precursor messenger RNA splicing in mammalian cells. *Nat Struct Mol Biol* 13:815–822.
- Liston C, McEwen BS, Casey BJ (2009) Psychosocial stress reversibly disrupts prefrontal processing and attentional control. *Proc Natl Acad Sci U S A* 106:912–917.
- Liston C, Miller MM, Goldwater DS, Radley JJ, Rocher AB, Hof PR, Morrison JH, McEwen BS (2006) Stress-induced alterations in prefrontal cortical dendritic morphology predict selective impairments in perceptual attentional set-shifting. *J Neurosci* 26:7870–7874.
- Liu X, Ramirez S, Pang PT, Puryear CB, Govindarajan A, Deisseroth K, Tonegawa S (2012) Optogenetic stimulation of a hippocampal engram activates fear memory recall. *Nature* 484:381–385.
- Love MI, Huber W, Anders S (2014) Moderated estimation of fold change and dispersion for RNA-seq data with DESeq2. *Genome Biol* 15:1–21.
- Luckman SM, Dyball REJ, Leng G (1994) Induction of c-fos expression in hypothalamic magnocellular neurons requires synaptic activation and not simply increased spike activity. *J Neurosci* 14:4825–4830.
- Ludwig M, Johnstone LE, Neumann I, Landgraf R, Russell JA (1997) Direct hypertonic stimulation of the rat supraoptic nucleus increases c-fos expression in glial cells rather than magnocellular neurones. *Cell Tissue Res* 287:79–90.
- Lyons MR, West AE (2011) Mechanisms of specificity in neuronal activity-regulated gene transcription. *Prog Neurobiol* 94:259–295.
- Maaswinkel H, Gispen WH, Spruijt BM (1996) Effects of an electrolytic lesion of the prelimbic area on anxiety-related and cognitive tasks in the rat. *Behav Brain Res* 79:51–59.
- MacLaren DAA, Browne RW, Shaw JK, Radhakrishnan SK, Khare P, España RA, Clark SD (2016) Clozapine N-Oxide Administration Produces Behavioral Effects in Long-Evans Rats: Implications for Designing DREADD Experiments. *ENeuro* 3:ENEURO.0219-16.2016.
- Marín-Blasco I, Muñoz-Abellán C, Andero R, Nadal R, Armario A (2018) Neuronal Activation After Prolonged Immobilization: Do the Same or Different Neurons Respond to a Novel Stressor? *Cereb Cortex* 28:1233–1244.
- Márquez C, Belda X, Armario A (2002) Post-stress recovery of pituitary-adrenal hormones and glucose, but not the response during exposure to the stressor, is a marker of stress intensity in highly stressful situations. *Brain Res* 926:181–185.
- Martí J, Armario A (1993) Effects of diazepam and desipramine in the forced swimming test: influence of previous experience with the situation. *Eur J Pharmacol* 236:295–299.
- McCulloch C, Searle S (2001) *Generalized, linear and mixed models* Wiley.
- McKlveen JM, Myers B, Herman JP (2015) The Medial Prefrontal Cortex: Coordinator of Autonomic, Neuroendocrine and Behavioural Responses to Stress. *J Neuroendocrinol* 27:446–456.
- McReynolds JR, Christianson JP, Blacktop JM, Mantsch JR (2018) What does the Fos say? Using Fos-based approaches to understand the contribution of stress to substance use disorders. In *Neurobiology of Stress* (Vol. 9, pp. 271–285) Elsevier Inc.

- Mechti N, Piechaczyk M, Blanchard JM, Jeanteur P, Lebleu B (1991) Sequence requirements for premature transcription arrest within the first intron of the mouse c-fos gene. *Mol Cell Biol* 11:2832–2841.
- Meyuhas O (2008) Physiological Roles of Ribosomal Protein S6: One of Its Kind. *Int Rev Cell Mol Biol* 268:1–37.
- Meyuhas O (2015) Ribosomal Protein S6 Phosphorylation: Four Decades of Research. In *International Review of Cell and Molecular Biology* (Vol. 320) Elsevier Ltd.
- Misund K, Steigedal TS, Lægreid A, Thommesen L (2007) Inducible cAMP early repressor splice variants ICER I and IIy both repress transcription of c-fos and chromogranin A. *J Cell Biochem* 101:1532–1544.
- Moghaddam B (1993) Stress Preferentially Increases Extraneuronal Levels of Excitatory Amino Acids in the Prefrontal Cortex: Comparison to Hippocampus and Basal Ganglia. *J Neurochem* 60:1650–1657.
- Moghaddam B, Jackson M (2004) Effect of stress on prefrontal cortex function. *Neurotox Res* 6:73–78.
- Mueller NK, Dolgas CM, Herman JP (2004) Stressor-selective role of the ventral subiculum in regulation of neuroendocrine stress responses. *Endocrinology* 145:3763–3768.
- Munck A, Guyre PM, Holbrook NJ (1984) Physiological Functions of Glucocorticoids in Stress and Their Relation to Pharmacological Actions. *Endocr Rev* 5:25–44. <http://press.endocrine.org/doi/pdf/10.1210/edrv-5-1-25>
- Murphy BL, Arnsten AFT, Goldman-Rakic PS, Roth RH (1996) Increased dopamine turnover in the prefrontal cortex impairs spatial working memory performance in rats and monkeys. *Proc Natl Acad Sci U S A* 93:1325–1329.
- Musazzi L, Milanese M, Farisello P, Zappettini S, Tardito D, Barbiero VS, Bonifacino T, Mallei A, Baldelli P, Racagni G, Raiteri M, Benfenati F, Bonanno G, Popoli M (2010) Acute stress increases depolarization-evoked glutamate release in the rat prefrontal/frontal cortex: The dampening action of antidepressants. *PLoS One* 5:e8566.
- Myers B, Mark Dolgas C, Kasckow J, Cullinan WE, Herman JP (2014) Central stress-integrative circuits: Forebrain glutamatergic and GABAergic projections to the dorsomedial hypothalamus, medial preoptic area, and bed nucleus of the stria terminalis. *Brain Struct Funct* 219:1287–1303.
- Myers B, McKlveen JM, Herman JP (2012) Neural Regulation of the Stress Response: The Many Faces of Feedback. *Cell Mol Neurobiol* 32:.
- Myers B, McKlveen JM, Morano R, Ulrich-Lai YM, Solomon MB, Wilson SP, Herman JP (2017) Vesicular glutamate transporter 1 knockdown in infralimbic prefrontal cortex augments neuroendocrine responses to chronic stress in male rats. *Endocrinology* 158:3579–3591.
- Myers B, Scheimann JR, Franco-Villanueva A, Herman JP (2017) Ascending mechanisms of stress integration: Implications for brainstem regulation of neuroendocrine and behavioral stress responses. *Neurosci Biobehav Rev* 74:366–375.
- Nava N, Treccani G, Liebenberg N, Chen F, Popoli M, Wegener G, Nyengaard JR (2015) Chronic desipramine prevents acute stress-induced reorganization of medial prefrontal cortex architecture by blocking glutamate vesicle accumulation and excitatory synapse increase. *Int J Neuropsychopharmacol* 18:1–11.
- Nestler EJ (2015) δ fosB: A transcriptional regulator of stress and antidepressant responses. *Eur J Pharmacol* 753:66–72.
- Olver JS, Pinney M, Maruff P, Norman TR (2015) Impairments of spatial working memory and attention following acute psychosocial stress. *Stress Heal* 31:115–123.

- Ongur D, Price JL (2000) The Organization of Networks within the Orbital and Medial Prefrontal Cortex of Rats, Monkeys and Humans. *Cereb Cortex* 10:206–219.
- Ons S, Martí O, Armario A (2004) Stress-induced activation of the immediate early gene Arc (activity-regulated cytoskeleton-associated protein) is restricted to telencephalic areas in the rat brain: Relationship to c-fos mRNA. *J Neurochem* 89:1111–1118.
- Osterlund CD, Rodriguez-Santiago M, Woodruff ER, Newsom RJ, Chadayammuri AP, Spencer RL (2016) Glucocorticoid fast feedback inhibition of stress-induced ACTH secretion in the male rat: Rate independence and stress-state resistance. *Endocrinology* 157:2785–2798.
- Pacák K, Palkovits M (2001) Stressor specificity of central neuroendocrine responses: Implications for stress-related disorders. *Endocr Rev* 22:502–548.
- Pace TWW, Gaylord R, Topczewski F, Girotti M, Rubin B, Spencer RL (2005) Immediate-early gene induction in hippocampus and cortex as a result of novel experience is not directly related to the stressfulness of that experience. *Eur J Neurosci* 22:1679–1690.
- Pati S, Sood A, Mukhopadhyay S, Vaidya VA (2018) Acute pharmacogenetic activation of medial prefrontal cortex excitatory neurons regulates anxiety-like behaviour. *J Biosci* 43:85–95.
- Paxinos G, Watson C (2014) *Paxinos and Watson's the rat brain in stereotaxic coordinates* Academic.
- Perova Z, Delevich K, Li B (2015) Depression of excitatory synapses onto parvalbumin interneurons in the medial prefrontal cortex in susceptibility to stress. *J Neurosci* 35:3201–3206.
- Pfarr S, Schaaf L, Reinert JK, Paul E, Herrmannsdörfer F, Roßmanith M, Kuner T, Hansson AC, Spanagel R, Körber C, Sommer WH (2018) Choice for drug or natural reward engages largely overlapping neuronal ensembles in the infralimbic prefrontal cortex. *J Neurosci* 38:3507–3519.
- Picelli S, Faridani OR, Björklund ÅK, Winberg G, Sagasser S, Sandberg R (2014) Full-length RNA-seq from single cells using Smart-seq2. *Nat Protoc* 9:171–181.
- Pignatelli M, Beyeler A (2019) Valence coding in amygdala circuits. *Curr Opin Behav Sci* 26:97–106.
- Pinto L, Dan Y (2015) Cell-Type-Specific Activity in Prefrontal Cortex during Goal-Directed Behavior. *Neuron* 87:437–450.
- Porsolt R, Le Pichon M, Jalfre M (1977) Depression: a new animal model sensitive to antidepressant treatments. *Nature* 266:730–732.
- Porsolt RD, Deniel M, Jalfre M (1979) Forced swimming in rats: Hypothermia, immobility and the effects of imipramine. *Eur J Pharmacol* 57:431–436.
- Quintana A, Sanz E, Wang W, Storey GP, Güler AD, Wanat MJ, Roller BA, La Torre A, Amieux PS, McKnight GS, Bamford NS, Palmiter RD (2012) Lack of GPR88 enhances medium spiny neuron activity and alters motor- and cue-dependent behaviors. *Nat Neurosci* 15:1547–1555.
- R Core Team (2020). — *European Environment Agency* (n.d.). Retrieved March 21, 2022, from <https://www.eea.europa.eu/data-and-maps/indicators/oxygen-consuming-substances-in-rivers/r-development-core-team-2006>
- Rabasa C, Delgado-Morales R, Gomez-Roman A, Nadal R, Armario A (2013) Adaptation of the pituitary-adrenal axis to daily repeated forced swim exposure in rats is dependent on the temperature of water. *Stress* 16:698–705.
- Rabasa C, Gagliano H, Pastor-Ciurana J, Fuentes S, Belda X, Nadal R, Armario A (2015) Adaptation of the hypothalamus-pituitary-adrenal axis to daily repeated stress does not follow the rules of habituation: A new perspective. *Neurosci Biobehav Rev* 56:35–49.

- Radley JJ, Arias CM, Sawchenko PE (2006) Regional differentiation of the medial prefrontal cortex in regulating adaptive responses to acute emotional stress. *J Neurosci* 26:12967–12976.
- Radley JJ, Gosselink KL, Sawchenko PE (2009) A discrete GABAergic relay mediates medial prefrontal cortical inhibition of the neuroendocrine stress response. *J Neurosci* 29:7330–7340.
- Radley JJ, Rocher AB, Janssen WGM, Hof PR, McEwen BS, Morrison JH (2005) Reversibility of apical dendritic retraction in the rat medial prefrontal cortex following repeated stress. *Exp Neurol* 196:199–203.
- Radley JJ, Rocher AB, Rodriguez A, Ehlenberger DB, Dammann M, McEwen BS, Morrison JH, Wearne SL, Hof PR (2008) Repeated stress alters dendritic spine morphology in the rat medial prefrontal cortex. *J Comp Neurol* 507:1141–1150.
- Radulovic J, Kammermeier J, Spiess J (1998) Generalization of fear responses in C57BL/6N mice subjected to one- trial foreground contextual fear conditioning. *Behav Brain Res* 95:179–189.
- Raveh A, Margalioth M, Sontag ED, Tuller T (2016) A model for competition for ribosomes in the cell. *J R Soc Interface* 13:.
- Reijmers LG, Perkins BL, Matsuo N, Mayford M (2007) Localization of a stable neural correlate of associative memory. *Science* (80-) 317:1230–1233.
- Reul JMHM, De Kloet ER (1986) Anatomical resolution of two types of corticosterone receptor sites in rat brain with in vitro autoradiography and computerized image analysis. *J Steroid Biochem* 24:269–272.
- Ritchie ME, Phipson B, Wu D, Hu Y, Law CW, Shi W, Smyth GK (2015) Limma powers differential expression analyses for RNA-sequencing and microarray studies. *Nucleic Acids Res* 43:e47.
- Rivest S, Laflamme N (1995) Neuronal Activity and Neuropeptide Gene Transcription in the Brains of Immune-Challenged Rats. *J Neuroendocrinol* 7:501–525.
- Robertson LM, Kerppola TK, Vendrell M, Luk D, Smeyne RJ, Bocchiaro C, Morgan JI, Curran T (1995) Regulation of c-fos expression in transgenic mice requires multiple interdependent transcription control elements. *Neuron* 14:241–252.
- Rogan SC, Roth BL (2011) Remote control of neuronal signaling. *Pharmacol Rev* 63:291–315.
- Rogers S, Wells R, Rechsteiner M (1986) Amino acid sequences common to rapidly degraded proteins: The PEST hypothesis. *Science* (80-) 234:364–368.
- Roland BL, Sawchenko PE (1993) Local origins of some GABAergic projections to the paraventricular and supraoptic nuclei of the hypothalamus in the rat. *J Comp Neurol* 332:123–143.
- Roszkowski M, Manuella F, Von Ziegler L, Durán-Pacheco G, Moreau JL, Mansuy IM, Bohacek J (2016) Rapid stress-induced transcriptomic changes in the brain depend on beta-adrenergic signaling. *Neuropharmacology* 107:329–338.
- Roth BL (2016) DREADDs for Neuroscientists. *Neuron* 89:683–694.
- Roth KA, Katz RJ (1979) Stress, behavioral arousal, and open field activity-A reexamination of emotionality in the rat. *Neurosci Biobehav Rev* 3:247–263.
- Rotllant D, Pastor-Ciurana J, Armario A (2013) Stress-induced brain histone H3 phosphorylation: Contribution of the intensity of stressors and length of exposure. *J Neurochem* 125:599–609.
- Russell JA, Shipston M (2015) Neuroendocrinology of Stress. In J. Russell & M. Shipston (Eds.), *Neuroendocrinology of Stress* John Wiley & Sons, Ltd.

- Sakurai K, Zhao S, Takatoh J, Rodriguez E, Lu J, Leavitt AD, Fu M, Han BX, Wang F (2016) Capturing and Manipulating Activated Neuronal Ensembles with CANE Delineates a Hypothalamic Social-Fear Circuit. *Neuron* 92:739–753.
- Salgado-Pirbhoy P, Farris S, Steward O (2016) Synaptic activation of ribosomal protein S6 phosphorylation occurs locally in activated dendritic domains. *Learn Mem* 23:255–269.
- Sanacora G, Yan Z, Popoli M (2022) The stressed synapse 2.0: pathophysiological mechanisms in stress-related neuropsychiatric disorders. *Nat Rev Neurosci* 23:86–103.
- Sanz E, Quintana A, Deem JD, Steiner RA, Palmiter RD, McKnight GS (2015) Fertility-regulating kiss1 neurons arise from hypothalamic pomc-expressing progenitors. *J Neurosci* 35:5549–5556.
- Sanz E, Yang L, Su T, Morris DR, McKnight GS, Amieux PS (2009) Cell-type-specific isolation of ribosome-associated mRNA from complex tissues. *Proc Natl Acad Sci U S A* 106:13939–13944.
- Sapolsky RM, Romero LM, Munck AU (2000) How do glucocorticoids influence stress responses? Integrating permissive, suppressive, stimulatory, and preparative actions. *Endocr Rev* 21:55–89.
- Sassone-Corsi P, Sisson JC, Verma IM (1988) Transcriptional autoregulation of the proto-oncogene fos. *Nature* 334:314–319.
- Sawchenko PE, Li HY, Ericsson A (2000) Circuits and mechanisms governing hypothalamic responses to stress: A tale of two paradigms. *Prog Brain Res* 122:61–78.
- Sayers EW, Bolton EE, Brister JR, Canese K, Chan J, Comeau DC, Connor R, Funk K, Kelly C, Kim S, Madej T, Marchler-Bauer A, Lanczycki C, Lathrop S, Lu Z, Thibaud-Nissen F, Murphy T, Phan L, Skripchenko Y, ... Sherry ST (2022) Database resources of the national center for biotechnology information. *Nucleic Acids Res* 50:D20–D26.
- Schilling K, Luk D, Morgan JI, Curran T (1991) Regulation of a fos-lacZ fusion gene: A paradigm for quantitative analysis of stimulus-transcription coupling. *Proc Natl Acad Sci U S A* 88:5665–5669.
- Seamans JK, Lapish CC, Durstewitz D (2008) *Comparing the Prefrontal Cortex of Rats and Primates: Insights from Electrophysiology* 14:249–262.
- Shanks N, Anisman H (1988) Stressor-Provoked Behavioral Changes in Six Strains of Mice. *Behav Neurosci* 102:894–905.
- Shansky RM, Rubinow K, Brennan A, Arnsten AFT (2006) The effects of sex and hormonal status on restraint-stress-induced working memory impairment. *Behav Brain Funct* 2:8.
- Sheng M, Greenberg ME (1990) The regulation and function of c-fos and other immediate early genes in the nervous system. *Neuron* 4:477–485.
- Shyu AB, Greenberg ME, Belasco JG (1989) The c-fos transcript is targeted for rapid decay by two distinct mRNA degradation pathways. *Genes Dev* 3:60–72.
- Sierra-Mercado D, Padilla-Coreano N, Quirk GJ (2011) Dissociable roles of prelimbic and infralimbic cortices, ventral hippocampus, and basolateral amygdala in the expression and extinction of conditioned fear. *Neuropsychopharmacology* 36:529–538.
- Simmons DM, Arriza JL, Swanson LW (1989) A complete protocol for in situ hybridization of messenger RNAs in brain and other tissues with radiolabeled single-stranded RNA probes. *J Histochemol* 12:169–181.
- Singewald GM, Rjabokon A, Singewald N, Ebner K (2011) The modulatory role of the lateral septum on neuroendocrine and behavioral stress responses. *Neuropsychopharmacology* 36:793–804.

- Smeyne RJ, Curran T, Morgan JI (1992) Temporal and spatial expression of a fos-lacZ transgene in the developing nervous system. *Mol Brain Res* 16:158–162.
- Smith ML, Li J, Cote DM, Ryabinin AE (2016) Effects of isoflurane and ethanol administration on c-Fos immunoreactivity in mice. *Neuroscience* 316:337–343.
- Somogyi P, Tamás G, Lujan R, Buhl EH (1998) Salient features of synaptic organisation in the cerebral cortex. *Brain Res Rev* 26:113–135.
- Son H, Baek JH, Go BS, Jung D hyuk, Sontakke SB, Chung HJ, Lee DH, Roh GS, Kang SS, Cho GJ, Choi WS, Lee DK, Kim HJ (2018) Glutamine has antidepressive effects through increments of glutamate and glutamine levels and glutamatergic activity in the medial prefrontal cortex. *Neuropharmacology* 143:143–152.
- Sørensen AT, Cooper YA, Baratta M V., Weng FJ, Zhang Y, Ramamoorthi K, Fropf R, Laverriere E, Xue J, Young A, Schneider C, Göttsche CR, Hemberg M, Yin JCP, Maier SF, Lin Y (2016) A robust activity marking system for exploring active neuronal ensembles. *Elife* 5:e13918.
- Soumier A, Sibille E (2014) Opposing effects of acute versus chronic blockade of frontal cortex somatostatin-positive inhibitory neurons on behavioral emotionality in mice. *Neuropsychopharmacology* 39:2252–2262.
- Spencer SJ, Buller KM, Day TA (2005) Medial prefrontal cortex control of the paraventricular hypothalamic nucleus response to psychological stress: Possible role of the bed nucleus of the stria terminalis. *J Comp Neurol* 481:363–376.
- Spencer SJ, Day TA (2004) Role of catecholaminergic inputs to the medial prefrontal cortex in local and subcortical expression of Fos after psychological stress. *J Neurosci Res* 78:279–288.
- Spruijt BM, Van Hooff JARAM, Gispen WH (1992) Ethology and neurobiology of grooming behavior. *Physiol Rev* 72:825–852.
- Sullivan RM, Gratton A (1999) Lateralized effects of medial prefrontal cortex lesions on neuroendocrine and autonomic stress responses in rats. *J Neurosci* 19:2834–2840.
- Swanson LW, Sawchenko PE (1983) Hypothalamic Integration: Organization of the Paraventricular and Supraoptic Nuclei. *Annu Rev Neurosci* 6:269–324.
- Tan CL, Cooke EK, Leib DE, Lin YC, Daly GE, Zimmerman CA, Knight ZA (2016) Warm-Sensitive Neurons that Control Body Temperature. *Cell* 167:47–59.
- Tanimura SM, Sanchez-Watts G, Watts AG, Phil D (1998) *Peptide Gene Activation, Secretion, and Steroid Feedback during Stimulation of Rat Neuroendocrine Corticotropin-Releasing Hormone Neurons**. <https://academic.oup.com/endo/article-abstract/139/9/3822/2987074>
- Trněčková L, Rotllant D, Klenarová V, Hynie S, Armario A (2007a) Dynamics of immediate early gene and neuropeptide gene response to prolonged immobilization stress: Evidence against a critical role of the termination of exposure to the stressor. *J Neurochem* 100:905–914.
- Tsolakidou A, Trümbach D, Panhuysen M, Pütz B, Deussing J, Wurst W, Sillaber I, Holsboer F, Rein T (2008) Acute stress regulation of neuroplasticity genes in mouse hippocampus CA3 area - Possible novel signalling pathways. *Mol Cell Neurosci* 38:444–452.
- Tyssowski KM, DeStefino NR, Cho JH, Dunn CJ, Poston RG, Carty CE, Jones RD, Chang SM, Romeo P, Wurzelmann MK, Ward JM, Andermann ML, Saha RN, Dudek SM, Gray JM (2018) Different Neuronal Activity Patterns Induce Different Gene Expression Programs. *Neuron* 98:530–546.e11.
- Úbeda-Contreras J, Marín-Blasco I, Nadal R, Armario A (2018) Brain c-fos expression patterns induced by emotional stressors differing in nature and intensity. *Brain Struct Funct* 223:2213–2227.
- Ulrich-Lai YM, Herman JP (2009) Neural regulation of endocrine and autonomic stress responses. *Nat Rev Neurosci* 10:397–409.

- Urban DJ, Roth BL (2015) DREADDs (designer receptors exclusively activated by designer drugs): Chemogenetic tools with therapeutic utility. *Annu Rev Pharmacol Toxicol* 55:399–417.
- Usenko T, Kukushkin A, Pospelova T, Pospelov V (2003) Transient expression of E1A and Ras oncogenes causes downregulation of c-fos gene transcription in nontransformed REF52 cells. *Oncogene* 22:7661–7666.
- Uylings HBM, Groenewegen HJ, Kolb B (2003) Do rats have a prefrontal cortex? *Behav Brain Res* 146:3–17.
- Vallès A, Martí O, Armario A (2006) Long-term effects of a single exposure to immobilization: A C-fos mRNA study of the response to the homotypic stressor in the rat brain. *J Neurobiol* 66:591–602.
- Van Aerde KI, Feldmeyer D (2015) Morphological and physiological characterization of pyramidal neuron subtypes in rat medial prefrontal cortex. *Cereb Cortex* 25:788–805.
- Van Dijken HH, Van Der Heyden JAM, Mos J, Tilders FJH (1992) Inescapable footshocks induce progressive and long-lasting behavioural changes in male rats. *Physiol Behav* 51:787–794.
- van Erp AMM, Kruk MR, Meelis W, Willekens-Bramer DC (1994) Effect of environmental stressors on time course, variability and form of self-grooming in the rat: Handling, social contact, defeat, novelty, restraint and fur moistening. *Behav Brain Res* 65:47–55.
- Vazdarjanova A, McNaughton BL, Barnes CA, Worley PF, Guzowski JF (2002) Experience-dependent coincident expression of the effector immediate-early genes Arc and Homer 1a in hippocampal and neocortical neuronal networks. *J Neurosci* 22:10067–10071.
- Vertes RP (2004) Differential Projections of the Infralimbic and Prelimbic Cortex in the Rat. *Synapse* 51:32–58.
- Warden MR, Selimbeyoglu A, Mirzabekov JJ, Lo M, Thompson KR, Kim SY, Adhikari A, Tye KM, Frank LM, Deisseroth K (2012) A prefrontal cortex-brainstem neuronal projection that controls response to behavioural challenge. *Nature* 492:428–432.
- Watts AG (2005) Glucocorticoid regulation of peptide genes in neuroendocrine CRH neurons: A complexity beyond negative feedback. *Front Neuroendocrinol* 26:109–130.
- Weyers P, Bower DB, Vogel WH (1989) Relationships of plasma catecholamines to open-field behavior after inescapable shock. *Neuropsychobiology* 22:108–116.
- Wickham H, Averick M, Bryan J, Chang W, D' L, McGowan A, François R, Grolemond G, Hayes A, Henry L, Hester J, Kuhn M, Lin Pedersen T, Miller E, Bache SM, Müller K, Ooms J, Robinson D, Seidel DP, ... Yutani H (2019) Welcome to the Tidyverse. *J Open Source Softw* 4:1686.
- Woods SC, Seeley RJ, Porte D, Schwartz MW (1998) Signals that regulate food intake and energy homeostasis. *Science* (80-) 280:1378–1383.
- Xiu J, Zhang Q, Zhou T, Zhou TT, Chen Y, Hu H (2014) Visualizing an emotional valence map in the limbic forebrain by TAI-FISH. *Nat Neurosci* 17:1552–1559.
- Xu Y, Day TA, Buller KM (1999) The central amygdala modulates hypothalamic-pituitary-adrenal axis responses to systemic interleukin-1 β administration. *Neuroscience* 94:175–183.
- Yang L, Ton H, Zhao R, Geron E, Li M, Dong Y, Zhang Y, Yu B, Yang G, Xie Z (2020) Sevoflurane induces neuronal activation and behavioral hyperactivity in young mice. *Sci Rep* 10:1–14.
- Yap EL, Greenberg ME (2018) Activity-Regulated Transcription: Bridging the Gap between Neural Activity and Behavior. *Neuron* 100:330–348.
- Ye L, Allen WE, Thompson KR, Tian Q, Hsueh B, Ramakrishnan C, Wang AC, Jennings JH, Adhikari A, Halpern CH, Witten IB, Barth AL, Luo L, McNab JA, Deisseroth K (2016) Wiring and Molecular Features of Prefrontal Ensembles Representing Distinct Experiences. *Cell*

165:1776–1788.

- Yuen EY, Liu W, Karatsoreos IN, Feng J, McEwen BS, Yan Z (2009) Acute stress enhances glutamatergic transmission in prefrontal cortex and facilitates working memory. *Proc Natl Acad Sci U S A* 106:14075–14079.
- Yuen EY, Liu W, Karatsoreos IN, Ren Y, Feng J, McEwen BS, Yan Z (2011) Mechanisms for acute stress-induced enhancement of glutamatergic transmission and working memory. *Mol Psychiatry* 16:156–170.
- Yuen EY, Wei J, Liu W, Zhong P, Li X, Yan Z (2012) Repeated Stress Causes Cognitive Impairment by Suppressing Glutamate Receptor Expression and Function in Prefrontal Cortex. *Neuron* 73:962–977.
- Zander G, Krebber H (2017) Quick or quality? How mRNA escapes nuclear quality control during stress. *RNA Biol* 14:1642–1648.
- Zhang S, Chen Y, Wang Y, Zhang P, Chen G, Zhou Y (2020) Insights Into Translatomics in the Nervous System. *Front Genet* 11:1–17.

